Università
Ca'Foscari
Venezia

Scuola Dottorale di Ateneo
Graduate School

Dottorato di ricerca
in Scienze Chimiche
Ciclo XXV
Anno di discussione 2013

NEW DIRECTIONS ON PHOTOCHEMICAL AND SUPRAMOLECULAR CONTROL OF HOMOGENEOUS CATALYSIS

SETTORE SCIENTIFICO DISCIPLINARE DI AFFERENZA: CHIM/04
Tesi di Dottorato di Giulio Bianchini, matricola 796184

Coordinatore del Dottorato	**Tutore del Dottorando**
Prof. Maurizio Selva	**Prof. Giorgio Strukul**

TABLE OF CONTENTS

INTRODUCTION

Dreaming enzymes perfection

The word "catalysis" comes from the greek verb *καταλύειν*, which means "*to dissolve*". The first using this term was the Swedish chemist Jöns Jacob Berzelius in 1835 who tried to explain processes such as bodies' decomposition and starch to sugar conversion in the presence of strong acids. He didn't know how these processes were working but he was sure that a kind of force or power was acting on the reaction.[1]

A catalyst in modern chemistry is a substance used to enhance both reaction's rate and selectivity, furthermore the catalyst does not enter in the reaction's mass balance so, theoretically it could be reused indefinitely.

The catalysts involved in the biochemical transformations are called enzymes; this word comes from Greek's preposition *en* + *zyme* (in + yeast) and it was first used by Fredrich Wilhelm Küne in 1878 to underline the fermentation improvement due to yeast usage. A few years later, Emil Fisher discovered in 1894 that enzymes were able to choose between stereoisomers and this surprising ability was the direct evidence of substrate-enzyme complementarity. The "*lock and key*" concept had been created and it is still now the better qualitative explanation for enzymes activity and selectivity. Eduard Buchner obtained sixteen years later a cell extract that was able to synthesize ethanol from glucose, confirming the catalytic ability of these substances whose nature was still mysterious. It was only in 1926 that James Summer collected the first enzyme's crystals and proposed that enzymes were made of proteins. His thesis was confirmed few years later by John Northrop and Moses Kunitz and finally in 1963 the first amino acid sequence determined for bovine pancreatic ribonuclease A. Only two years later, the complete X-ray structure of egg album lysozyme was solved for the first time.[2]

Enzymes are globular proteins involved in important bio-chemical transformations such as foodstuff metabolism, DNA replication, and so on. Like proteins, they are characterized by different amino acid sequences (primary structure) different arrangements like α *helix and* β *sheet* (secondary structure) and different three-dimensional spatial arrangements (tertiary structure). If the enzyme is composed of more than one peptidic sequence, there is also a quaternary structure which explains how different sequences are reciprocally arranged.[2]

Enzymes are characterized by the presence of a pocket called enzyme active site where the catalytic event occurs. Weak intermolecular forces like hydrogen bonding, hydrophobic interactions, ion-dipole interaction, π stacking and many others are responsible of the structure of the enzyme and of its affinity for the substrate and the transition state of the reaction.[2]

Generally the enzyme active site shows shape complementary with the substrate (geometric complementary) and the amino acid moieties, present within the cavity, create precise

favourable electrostatic interactions with the substrate (electrostatic complementary) allowing its chemical activation. In most cases an induced adjustment always takes place after cavity-substrate binding. [2]

The activity of an enzyme is often subordinated to the presence of other species called co-factors. The latter could be part of the protein, or may bind it reversibly.

As could be easy understood the organism catalytic activity must be regulated. This is not only to ensure better matching between the various metabolic pathways, but also to be available to react as a consequence of a modification of the environment.

Two different strategies may be undertaken: *i)* regulation of the amount of the enzyme, or *ii)* regulation of the enzyme activity. The first one is performed by the cell through different mechanisms while the latter is related to the affinity between enzyme and substrate. The *feedback inhibition* (retro-regulation) is a clear and common example of regulation where the amount of enzyme at the begging of a metabolic pathway is regulated by the concentration of the products formed at the end of the metabolic pathway. The feedback regulation of aspartate transcarbamylase (ATC) (Scheme 1) is reported as a representative example.[2]

ATC binds in a positive and cooperative way both to carbamyl phosphate and to aspartate yielding *N*-carbamyl aspartate, an important building block in the biosynthesis of pyrimidines. ATC is heterotropically inhibited by cytidine triphosphate (CTP), a pyrimidine nucleotide, and heterotropically activated by adenosine triphosphate (ATP), a purinic nucleotide. As suggest before, CTP is not only a product of pyrimidine's biosynthesis but also precursor of nucleic acids; CTP's concentration is extremely reduced after an intense nucleic acids biosynthesis and, due to a mass effect, CTP is released by ATC and activity of the enzyme restored. When CTP production rate exceeds its intake one, CTP binds again ATC and the enzyme becomes inactive again.[2]

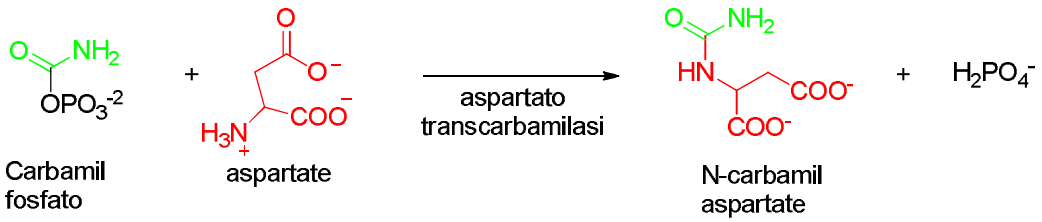

Scheme 1 The feedback regulation of aspartate transcarbamylase.

Allosteric models

Globular proteins are not to be considered rigid objects and they not only contain an active site where the substrate could bind but also other sites are available which can be occupied by other species such as inhibitors. Why and how they work is a frequently asked question. Allosteric effects come from protein-ligand (substrate) interactions which may be affected by pre-existing protein-ligand (effector) interactions; when the ligands involved are all of the same type than the allosteric effect is called homotropic, otherwise it is called heterotropic. These effects could be positive or negative depending on whether they increase or decrease enzyme activity.[2]

Generally speaking, the interactions between oligomeric proteic subunits are responsible of allosterism; Aldair's equation, originally made to explain oxygen-haemoglobin interactions, describes the bond between protein and a ligand but it does not give any explanation about the variation of the dissociation constants. In order to get a better understanding, two models were proposed in the last fifty years: the symmetric model, also called Monod- Wyman-Changeux (MWC) model, and the sequential model proposed by Koshland. The MWC model basic rules are: *i)* allosteric proteins are considered as oligomeric aggregates of protomers which are symmetrically correlated; *ii)* every protomer may exist in two different conformations, R (relaxed) or T (tensed), and these two forms are in equilibrium independently from the presence of ligands; *iii)* ligand binds the protomer in both configurations but their affinity is affected only by variation of the configuration; *iv)* retention of protein molecular symmetry occurs during the configuration variation, meaning that configuration with both T and R conformation are not possible (Figure 1).[2]

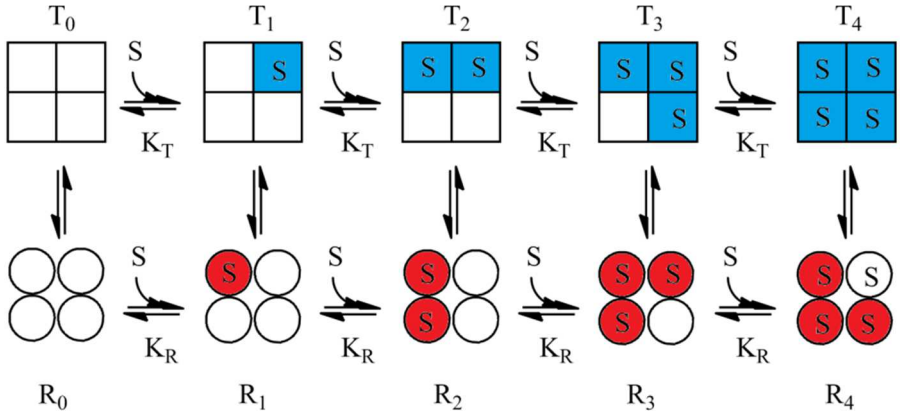

Figure 1. Oversimplification of symmetric model (MWC); the squares and the circles represent the oligomeric proteic subunits respectively in tensed (T) and relaxed (R) conformation. S stays for substrate (ligand) and K_R and K_T are the binding constants with substrate respectively for the relaxed and tensed conformations.

The symmetric model gives explanation of both homotropic and heterotropic interactions but it is very difficult to accept protein molecular symmetry retention discarding any $R_{n-2}T_2$ hybrid conformations.

Koshland's model offers another way for describing the allosteric effects and the key-assumption considers the *self-induced adaptation* of the subunits as consequence of ligands binding. More precisely when ligand-subunit binding occurs, it results in improved or decreased ability in ligand-protein binding of neighbouring subunits leading to a dynamic system (Figure 2).

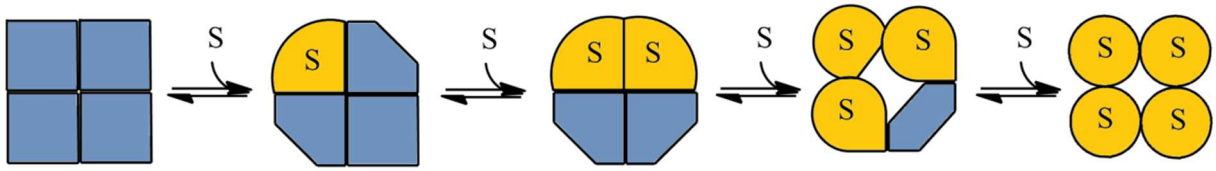

Figure 2. Oversimplification of Koshland model for the self-adaptation; the blue squares represent the original subunits constituting the enzyme. After binding substrate (ligand, S), binding to one subunit imposes modification on the neighbouring subunits yielding increased or decreased binding for later subunit-substrate interactions.

Independently on which model offers the best explanation for the allosteric effects, both MWC and Koshland models suggest that the catalytic performance is affected by conformational or structural variations that can be obtained by coordination of convenient species (*effectors*). In conclusion understanding biological systems offers a strategy for the emulation of enzymes and one more time Nature is an unrivalled source of inspiration.

STATE OF THE ART-Supramolecular Coordination Chemistry

Mankind has always been attempting to emulate the magnificence and perfection of Nature. Enzyme mimics began to be a chemical challenge in the last decades and since then different approaches have been proposed. The present and the next two chapters will deal with the presentation of the most important achievements obtained in the development of synthetic catalysts, selected with the aim of focusing on those that better mimic the activity of enzymes with emphasis on the regulation of such activity.

Supramolecular coordination chemistry approaches

Chad A. Mirkin and co-workers recently reported a review titled *"Enzyme mimics based upon supramolecular coordination chemistry"* showing how supramolecular coordination chemistry could be an effective tool for the construction of artificial enzymes.[3] The authors classified catalysts mimetic of enzymes into three structural classes: *i)* assemblies that mimic the pocket (active site) of an enzyme; *ii)* assemblies that mimic the allosteric regulation of an enzyme; *iii)* assemblies that mimic the non-symmetric nature of enzymes active site, which is often an important element for the substrate activation and consequently for enzymes activity. Many of these assemblies are prepared by convergent, modular, and high-yield multicomponent supramolecular coordination approaches such as the directional bonding approach (DBA), the symmetric-interaction approach (SIA), and the weak-link approach (WLA).

(DBA) The directional bonding approach, also called molecular library approach, is based on transition metal complexes characterized by the presence of blocking ligands (ligand that strongly coordinate to the metal) and weakly coordinating ligands. The latter could be replaced by rigid multitopic ligands and thanks to the precise molecular geometry imposed by the blocking ligands, new multi-metallic shapes could be achieved, such as molecular squares and molecular triangles (Figure 3).[4]

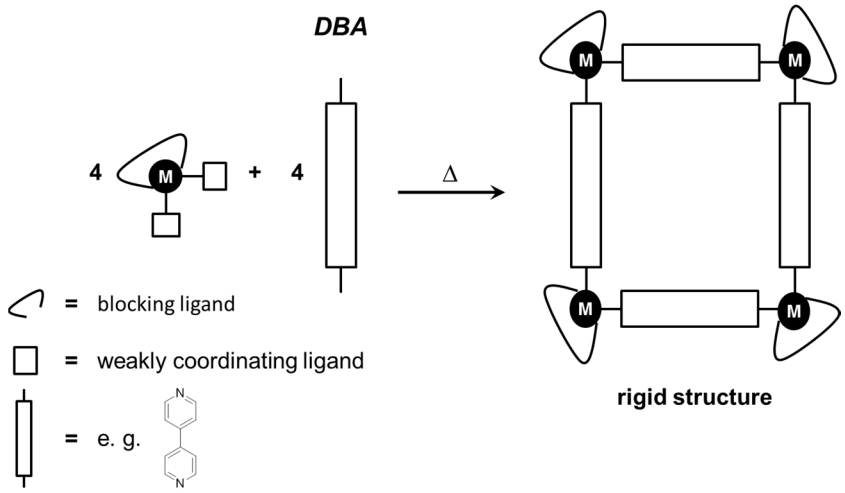

Figure 3. The weakly coordinated ligands could be easily replaced by rigid multitopic ligands yielding precise molecular geometry. The new geometries are imposed by the combination of the chosen metal center and blocking units.

(SIA) Symmetric interaction approach consist of rigid multitopic ligands coordinating metal centers in higher ordered multi-metallic structures fashion, in the absence of any blocking and directing ligand. The assemblies obtained from both the SIA and the DBA are structurally rigid macrocyclic systems due to design and virtue of the rigid linkers (Figure 4).[5]

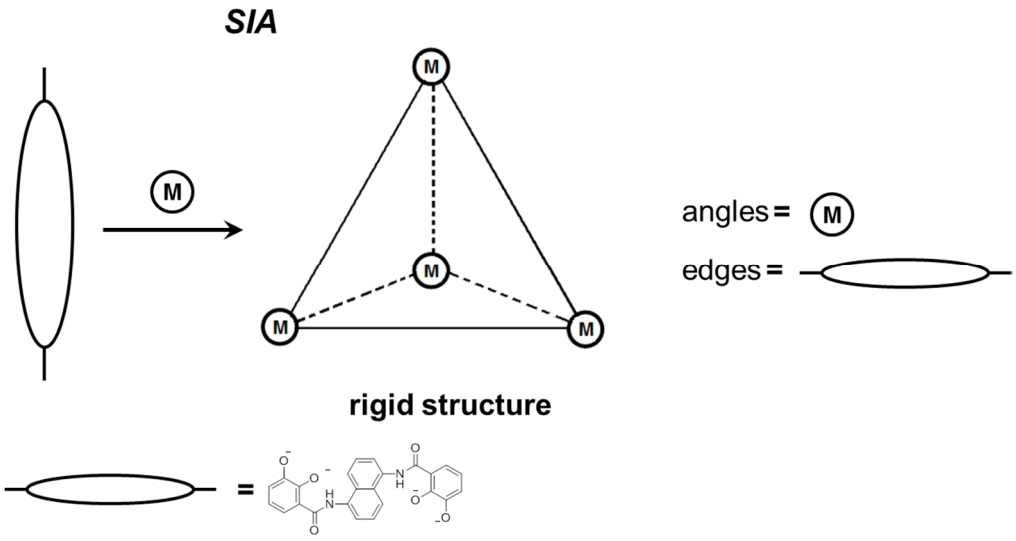

Figure 4. Symmetric interactions between rigid multitopic ligands and metal centers in high ordered multi-metallic structures.

(WLA) The weak-link approach is made using flexible hemilable ligands and metal ions which are arranged in condensed chelate bi- or multi-metallic complexes. The flexible hemilable ligand is characterized by a strongly coordinating donor, usually a trivalent phosphorous atom, and a weakly coordinating one, such as nitrogen (III) sulphur (II) oxygen (II). The weaker bond could be easily cleaved by addition of competing ligands such as inorganic ions or small molecules (CO) while the stronger metal-phosphorous bond remains intact, leading to an expansion of the multimetallic complex, a variation of its charge and an improvement of its flexibility (Figure 5).[6]

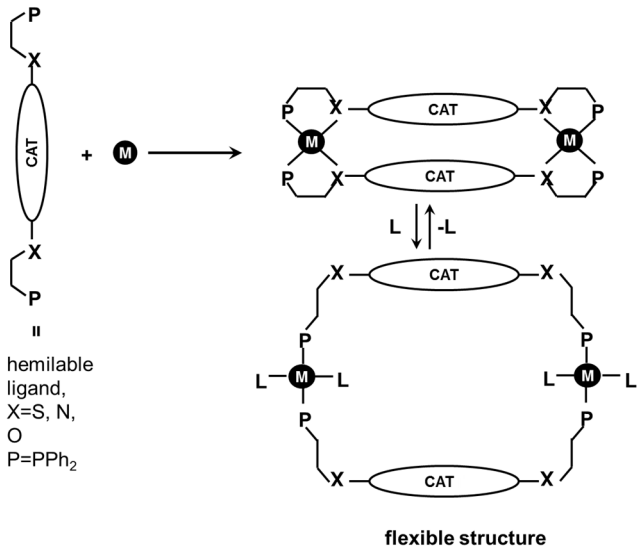

Figure 5. Hemilable ligands set up in sandwich-like structures where the successive coordination of effectors (L) allows cleavage of the weak X-M bonds yielding new molecular species characterized by different charge, flexibility and shape.

Macrostructures and improved catalytic systems obtained through DBA and SIA

Supramolecular coordination chemistry, and especially DBA, has been widely used for the realization of molecular cage complexes containing a catalytic moiety, where the cage affects the outcome of the reaction influencing the interaction between catalyst and substrate. Hupp and Nguyen groups, following this strategy, prepared different systems such as an artificial cytochrome P450 system,[7] a molecular square,[8] and a molecular rectangular box[9]. In all cases the authors observed an increased lifetime of the catalytic moieties for the assembled systems and in certain cases enhanced values of selectivity were obtained by virtue of new steric demanding environment surrounding the catalytic moiety.

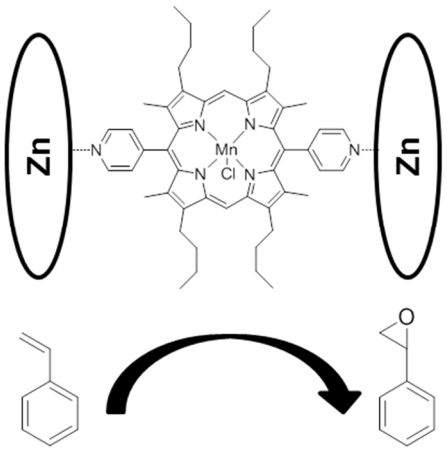

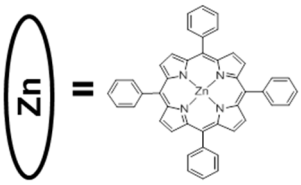

Catalyst (Mn)	TON	Lifetime (min)
Deassembled	59	10
Assembled	140	45

Figure 6. Comparison of the catalytic performances between (Mn)-porphyrin oxidation catalyst as itself and the multimetallic system obtained through DBA; from reference 7.

Taking advantage of supramolecular coordination chemistry the Raymond and Bergman groups aimed to trap catalysts within supramolecular structures. Following SIA, Raymond synthesized a supramolecular tetrahedral-cage which was composed by four gallium ions as vertices and by bis-catechol units as edges (Figure 7). The M_4L_6 cluster has been obtained as a racemic mixture of homochiral complexes, referred to the metal centers which have all the same symmetry *Δ,Δ,Δ,Δ* or *Λ,Λ,Λ,Λ*. [10] The clusters may be resolved by addition of a chiral cations such as (S)-N-methylnicotinium, which selectively precipitates the *Δ,Δ,Δ,Δ* enantiomer.[11] The tetrahedral cluster is highly water soluble by virtue of its high negative charge (12), while its internal cavity is hydrophobic and has been shown to host not only cationic organic species but also metallorganic compounds.[12]

The ability to host a metallorganic species pushed the authors to perform the encapsulation of transition metal complexes which display catalytic activity. Two different sets of Rh((I) complexes were successfully encapsulated and the discriminating ability of the tetrahedron cluster was examined using the allylic alcohols or ethers isomerization as test reaction[13] The cage, if compared to the free catalyst, showed substrate selectivity allowing only to 2-propen-1-ol and 3-methoxy-1-propene to reach the catalyst within the cage while the branched substrates did not. The shape and size selectivity imposed by the cluster are so restrictive that 3-ethoxy-1-propene did not react even if it was just one carbon longer than the methoxy analog.

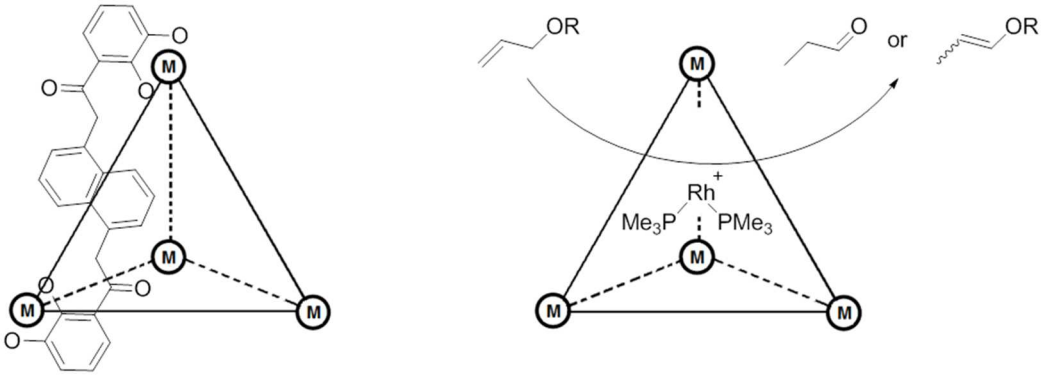

Figure 7. (left) Raymond's tetrahedral-cage: M=gallium ion, edges= bis-catechol unit; **(right)** The tetrahedral-cage incorporating a Rh(I) complex active in ethers isomerization reaction: the supramolecular cage shows substrate's selectivity allowing only to linear and short allylic substrates to reach the catalyst.

Both SIA and DBA have been also used for the preparation of molecular cages without any catalytic moiety where the catalytic benefit comes from the pre-orientation and or compartmentalization imposed by the cavity.

Raymond's nanoclusters showed to be useful nanoreactors also without incorporating any organic or metallorganic catalytic moiety. Infact they effectively catalysed several reactions such as aza-Cope rearrangement,[14] and acetals,[15] and orthoformates[16] hydrolysis. In the former reaction 850-fold rate improvement was observed, probably due to the correct pre-orientation of the substrate within the cavity. Catalyst turnover was afforded by the prompt aldehyde product replacement with fresh *aza*-substrate which, due to its cationic nature, was a better guest for the anionic cluster. The above mentione hydrolysis reactions were a further goal for the tetrahedral cage because they occurred in mild basic conditions while acidic ones are commonly required. In all cases, shape and size selectivity were observed and in the orthoformates hydrolysis 3900-fold rate improvement, for some substrates, was achieved only by addition of 5 % cluster catalyst. In both reactions the catalytic activity was explained presuming the anionic cluster plays a stabilizing effect on the cationic protonated substrate form which is the activated one. Another and probably the best example concerning enzyme mimic obtained with Raymond's tetrahedral cage was reported in 2010. The authors observed rate enhancements up to $2 \cdot 10^6$ fold when the Nazarov cyclization of 1,4-pentadien-3-ols were performed in the presence of the nanocluster with respect to the uncatalyzed reaction.[17] These surprising improvements were ascribed to preorganization of the reactant and stabilization of the transition state by constrictive binding as well as an increase in basicity of the alcohol group within the cage.

Fujita group synthesized various cage structures via DBA and showed that they are able to encapsulate a wide variety of molecules.[18] One of those capsules being used as catalyst is a complex of octahedron shape where tridentate ligands, based on a triazine core, (2,4,6 –tris(4-pyridil)-1,3,5-triazine), cover half faces of the octahedron and are blocked at the vertices by Pd^{II} or Pt^{II} *cis*-square planar complexes (Figure 8A).[18a] Changing the tridentate ligand into a new one where pyridine moieties are linked in meta position (2,4,6-tris(3-pyridil)-1,3,5-triazine), a square pyramidal cage (Figure 8B) characterized by an open side was synthesized.[18c]

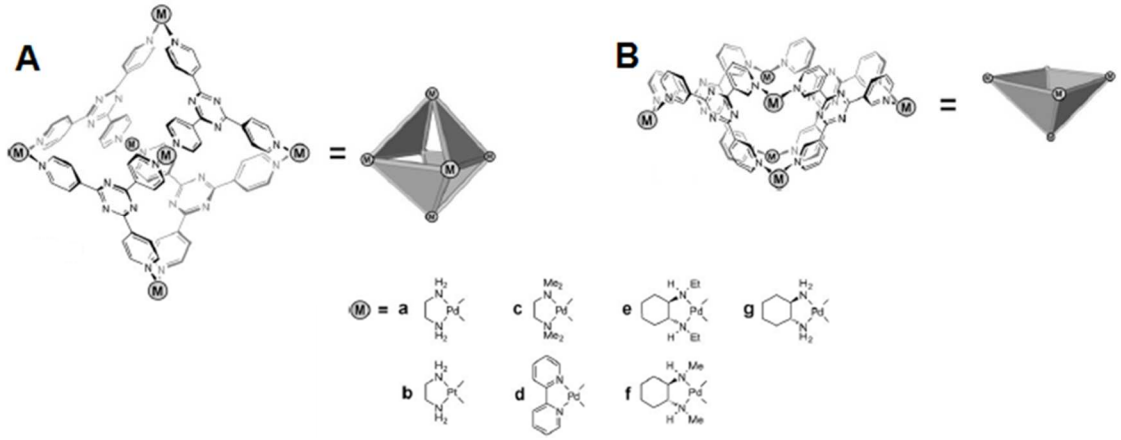

Figure 8. A) Fujita's nano-cage; **B)** Fujita nano-square pyramidal cage; in both structures the corners are constituted by Pd(II) or Pt(II) square planar complexes while surface are tridentate ligands based on a triazine core.

These supramolecular complexes showed the ability to catalyse reactions, such as Wacker oxidations[19] and both thermal,[20] and photochemical,[21] pericyclic reactions without the presence of any catalyst but just by virtue of compartmentalization effects played by their cavities. For example, the rate of Diels-Alder reaction between naphthoquinone and 1,3-cyclohexadiene was increased by about 21 times in the presence of the octahedron capsule and more surprisingly, the reaction rate showed better improvement when acyclic dienes were tested, as demonstrated by the 113-fold enhancement in the reaction rate of naphthoquinone and 2-methyl-1,3-butadiene cycloaddition. This rate enhancement has been attributed not only to the compartmentalization of the substrates within the cage but also to the cavity ability in substrates pre-orientation.

The main problem in performing catalysis within nanocages is that they are required in at least stoichiometric amounts because often the products show better binding for the capsule then the reactants and, especially for Diels Alder reactions, the encapsulation of both reactants is entropically disfavoured instead of the single product molecule.

Nano-vase complexes, such as the square pyramidal cage (Figure 8B), showed catalytic activity too. When used in 10 % mol amount in the Diels Alder reaction between anthracene and maleimide derivatives, quantitative conversions were achieved after 5 hours with products characterized by the typical 9, 10-regioselctivity. Catalytic turnover was attributed to the lower strength of the pile-stacking interactions between the products and bowl with respect to those between anthracene and bowl.[22]

Another important goal in enzyme's mimic obtained with DBA consists in strategies for the design of supramolecular ligands.
Van Leeuwen and Reek have proposed since 2001 new ligands structures that take advantage from supramolecular coordination chemistry.[23] The core of these new ligands, in their very first version, was made using a *tris*-pyridilphosphine where the phosphorous atom binds the catalytically active metal center while the pyridines moieties bind, through Lewis acid/ Lewis-base interactions, other complexes such as Zn(II)-salphen or Zn(II)-porphyrin. The latter complexes are then responsible of a second coordination sphere which may play a discriminating role on the catalyst performance.

More recently the same authors proposed a slightly different way to use DBA, instead of using Zn(II)-porphyrins as blocking group they used them as structure directing agent achieving bidentate chelating ligands starting from monodentate ones. [2425] Indeed switching ligand topicity is known to affect the performance of the catalyst as confirmed by the increased selectivity obtained in the asymmetric hydrogenation,[26] and in hydroformylation reactions when switching is performed from monodentate to bidentate chelating ligands.[27] Furthermore, when chiral ligands are involved, this modification resulted useful for increasing *ee* values.[28] Scheme 2 reports, a remarkable example of the startegies proposed by Van Leeuwen and Reek, i.e. the switching from monodentate to bidentate chelating ligand systems and the catalytic performance obtained with these systems in the hydroformylation of 1-octene.

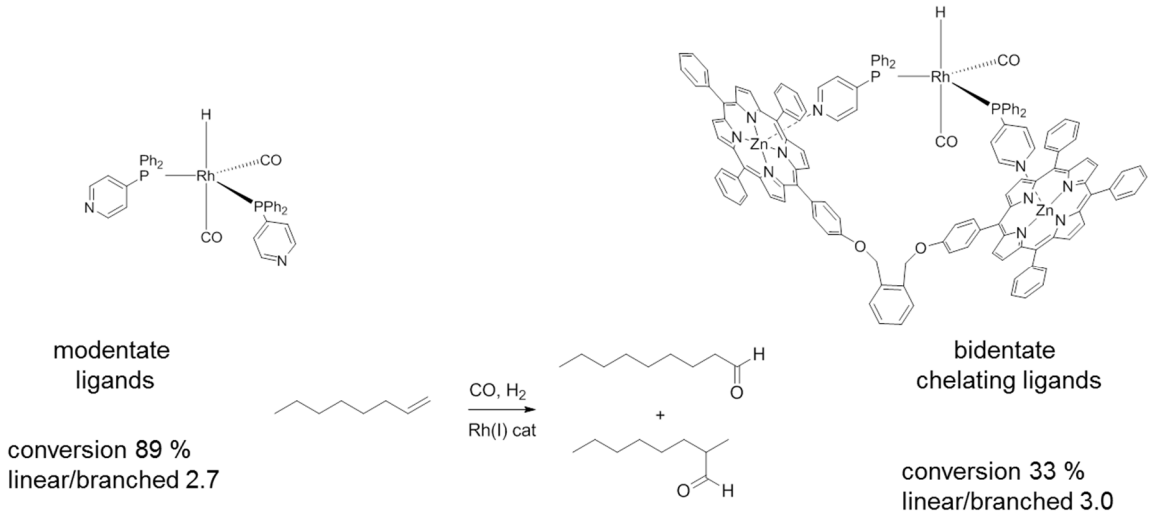

Scheme 2. Effects obtained in the hydroformylation reaction of 1-octene when the ligands are switched from monodentate to bidentate chelating ones. From ref. 25b.

Systems showing regulation phenomena. The Weak link approach (WLA)

All the above presented supramolecular structures are characterized by rigid structures and despite the impressive results observed in terms of substrate selectivity, rate enhancement and product chemo/regio/stereoselectivity, they did not show any sort regulation phenomena.

The weak link approach (WLA) allows the synthesis of flexible structures which may show regulation properties mimicking these important features typical of enzymes. The goal in using WLA was the preparation of structures where two sites are present, such as the active site and the regulation site of an enzyme. The regulation site may be influenced by an external *stimulus*, such as a neutral molecule or an ion, and as a direct consequence the catalytic behaviour could be tuned. Pioneering contribution to the field were made by Krämer and co-workers who prepared ligands bearing a tetradentate regulatory site which binds strongly metals such as Cu^{II}, Ni^{II}, Pd^{II}, Pt^{II}, $Co^{II/III}$ (M^a in Figure 9) in close proximity to extra binding sites which may be useful to coordinate one or two metal ions (M^b in Figure 9) deputed to promote the catalytic event.[29]

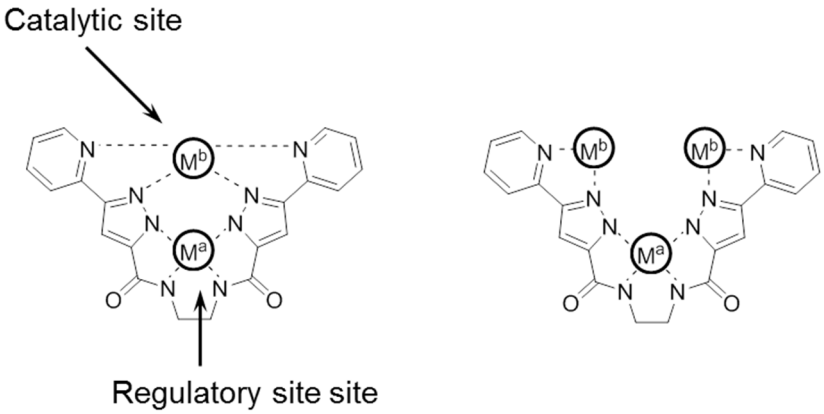

Figure 9. Krämer's catalyst showing separated catalytic and regulatory sites.

In one remarkable example it was observed that using Pd(II) as regulation metal, two Cu(II) ions can be complexed while using Pt(II) as regulation ion just one Cu(II) ion coordinates the active site. These different coordination behaviours were translated in different catalytic activities in the phosphodiester cleavage of RNA that is known to proceed in a bimetallic catalysis. More precisely it was observed no reactivity when Pt(II) was used as structural metal whereas a pseudo-first order reaction's rate was observed for Pd(II) as regulatory metal.[30]

A more complex multi-metallic catalytic system was reported by Scarso and co-workers where the regulatory site was based on a tripodal *tris*(2-aminoethyl)amine (*tren*) ligand covalently linked to three chelating cyclic triazacyclononane (*tacn*) macrocyclic ligands which acted as catalytic moieties (Scheme 3).[31] The regulating *tren* site preferentially binds Zn(II) cations that act as a template leading to closer positioning of the *tacn* moieties. All *tacn* moieties showed chelating ability towards extra Zn(II) cations added to the system and their arrangement favoured the phosphodiester cleavage of RNA analogues used as test substrates. The Zn_4- *tcn/tren* structure showed a 30-fold increase in activity compared to the unassembled and separated Zn-*tcn* and Zn-*tren* molecules.[32]

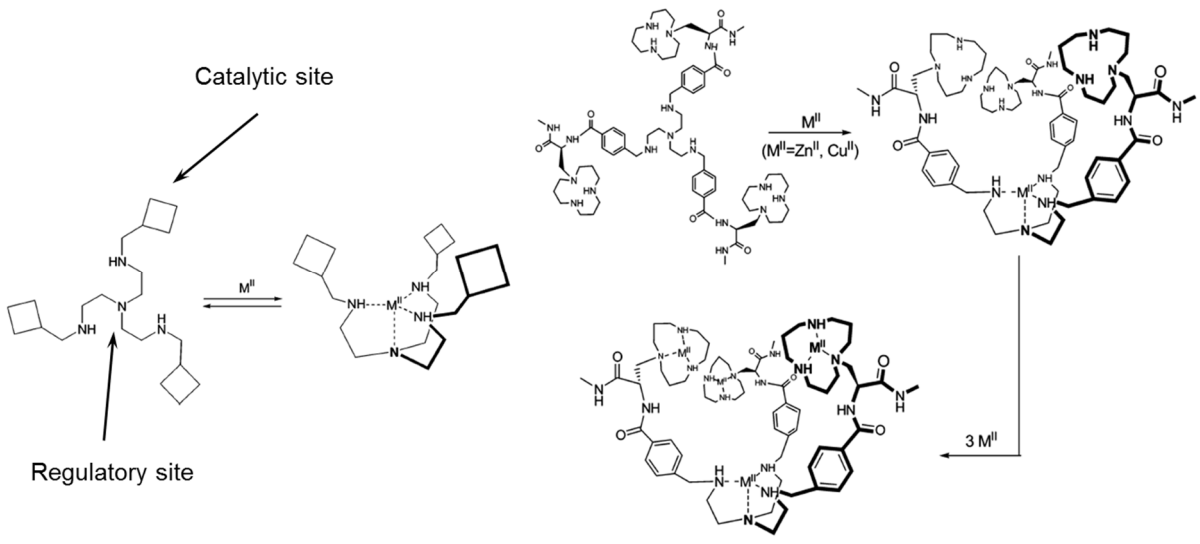

Scheme 3. Tripodal enzyme mimic. Zn(II) coordination at the *tren* moiety caused the Zn-*tacn* moieties to be closer in space and as a consequence the rate of phosphodiester cleavage resulted enhanced.

Mirkin macrocycles

The WLA allows not only to synthesize structures that show *one way* regulation, but also to prepare others where the regulation is reversible, which is what better emulates an allosteric enzyme. Mirkin and co-workers prepared through WLA various macrocycles where two catalytic units are symmetrically superimposed and connected through two extra coordination compounds in a sandwich fashion (Figure 10). More in detail, the catalytic units are M-salen/porphyrin/pyridine-*bis*-imine complexes and the regulation sites are Rh(I) complexes whose phosphorous-based ligands are covalently bonded to the catalytic units.

The Rh(I) metal centers coordinate via two strong metal-phosphorous bonds and two weak metal-sulphur bonds assuming a square planar geometry. When stronger donors, such as chloride ions or CO, are added to the system, the Rh-S bonds are cleaved and this causes the expansion of the macrocyclic structure. As a consequence, the two metal centers implemented in the catalytic units are placed at longer reciprocal distance and, more importantly, due to the increased space in between, substrate molecules are allowed to reach the catalytic metal centers inside the macrocycle. The two forms of the catalyst are called CLOSED and OPEN. Reversible switching among the two is achieved by removing CO in vacuum or by purging nitrogen followed by further cloride anion or CO addition. The authors applied this class of allosteric catalysts to several reactions where both selectivity and activity were reversibly switched by proper addition of chemical effectors. Rate difference of 25-fold was observed from the open (ON) and closed (OFF) state when Zn(II)-salen (Figure 10B) was used as catalytic unit in the acyl transfer reaction between 4-pyridilcarbinol and acetic anhydride.[33] This rate difference has been attributed, at least partially, to on/off switching between a monometallic Lewis acid catalysed reaction pathway operating in the closed state to a bimetallic pathway operating in the open state.

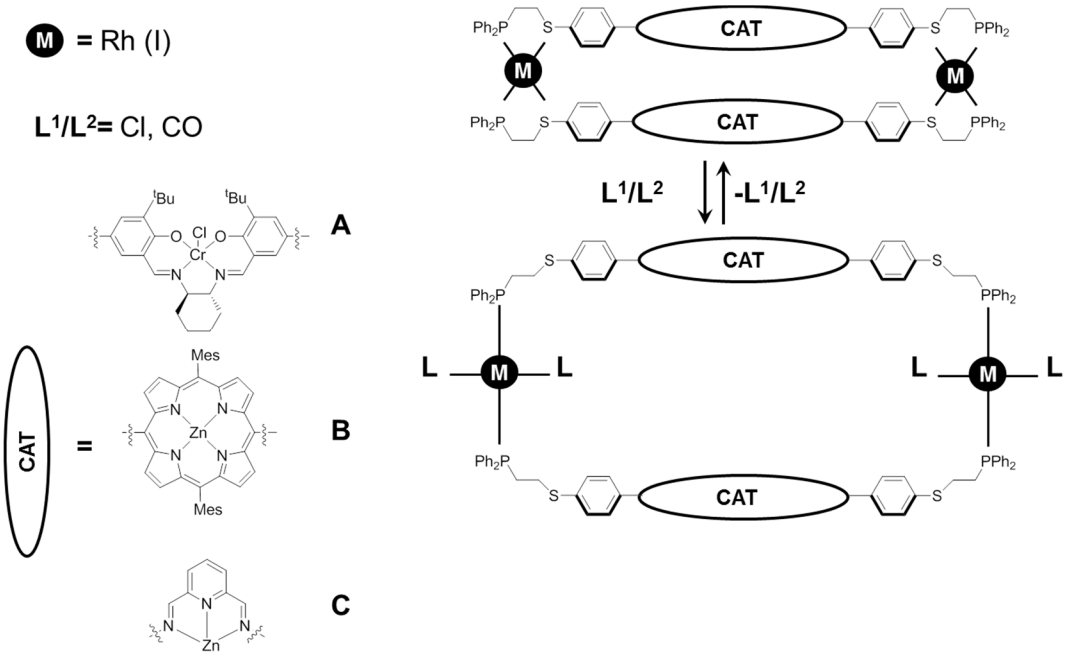

Figure 10. Mirkin's macrocycles; two catalytic units (of different types **A**, **B** or **C**) are symmetrically superimposed and connected through two extra coordination compounds in a sandwich fashion.

Recently Mirkin and co-workers improved their allosteric systems proposing a supramolecular allosteric triple-layer catalyst,[34] extending their repertoire from allosteric bimetallic catalysts to monometallic ones endowed with two tuneable shields positioned on both sides of the flat catalytic metal unity. The synthesized triple-layer-catalyst (TLC) was composed of two transition metal nodes, two chemically inert blocking exterior layers and a single catalytically active interior Al(III)-salen complex, which acts as catalyst in the ring-opening polymerization of ε-caprolactone (ε-CL) (Scheme 4).

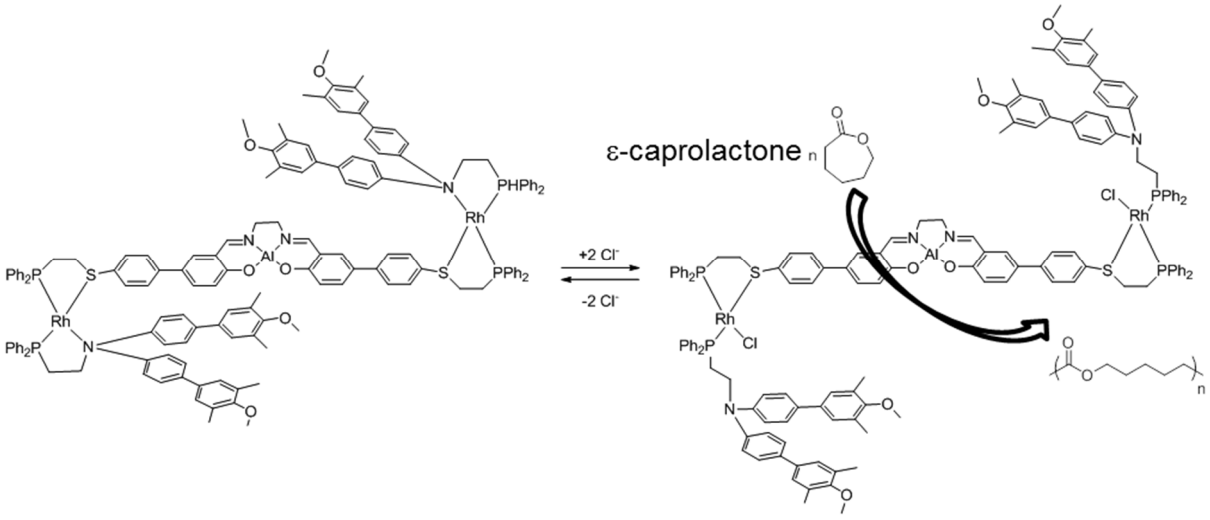

Scheme 4. Mirkin allosteric triple layer catalyst. Cleavage of Rh-N bond allowed switching from closed to semi-open structures and as consequence the reactants could reach the Al catalytic site.

Halide addition induces ligand rearrangement that allows assembling or disassembling of the trilayer structure. In this molecule the chloride ions bind to the Rh(I) regulation sites and can be easily removed by reaction with Na^+ or Li^+BARF^- (BARF=*tetrakis*[(3,5-bis(trifluoromethyl)phenyl]borate)) allowing the structure to switch from semi-open and active to closed and inactive. When these supramolecular complexes were tested in the ε-CL ring-opening polymerization no activity was detected for the closed form (only 7% conversion was observed after 100 hours due to catalyst degradation) while, the open form not only showed a much higher activity, but also a living polymerization catalyst character. The catalytic activity can be interrupted just by adding a stoichiometric amount of chloride abstracting agent and can be further restored by addition of acetonitrile. The molecular weight of the polymers was increased after the reactivation as confirmation of the living nature of the polymerization.

STATE OF THE ART-Metal free Supramolecular Chemistry

Metal free supramolecular chemistry offers the possibility to build new elaborate structures without using any metal as templating or scaffolding agent.

Weak intermolecular forces such as van der Waals, hydrogen bonding and hydrophobic interactions among certain molecular species allow the build-up of highly ordered self-assembled structures or inclusion complexes that may be used as hosts for catalysts or they can display intrinsic catalytic activity. Due to *host-guest* interactions, the hosted species experience a different environment with respect to the bulk solvent, analogously to a substrate hosted in the active site of an enzyme.

Metal free Supramolecular Chemistry-Cyclodextrin

Cyclodextrins (CD), also called cycloamyloses, are cyclic oligosaccharides composed of 5 or more α-D-glucopyranoside units linked between each other in positions 1 and 4 such as in amylose. Cyclodextrins have truncated cone shape and may be composed by 6 (α-CD), 7 (β-CD) or 8 (γ-CD) glucose rings; in addition the hydroxyl groups are oriented to the external surface while the alkyl and ethereal fragments are oriented at the inner surface. Figure 11 reports the molecular structure, the length and the internal diameter values for α,β,γ-CDs.

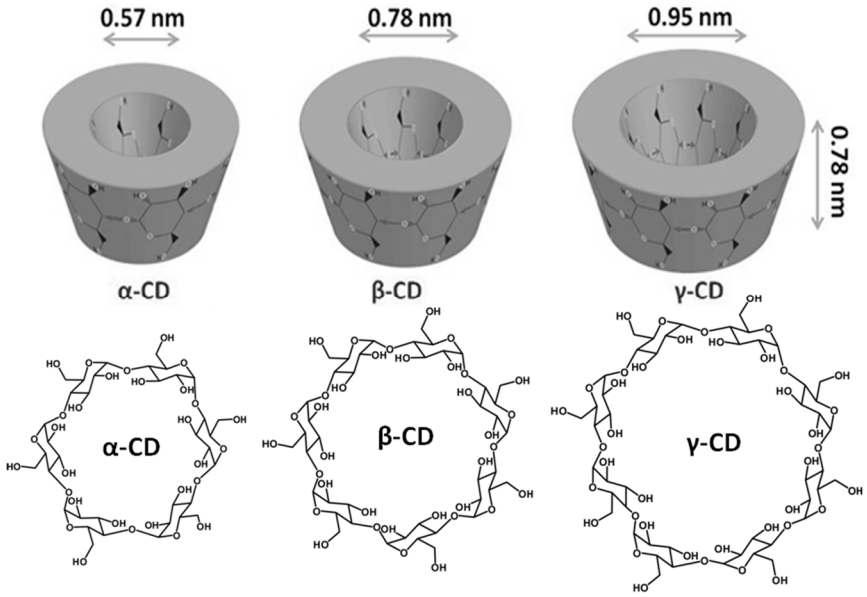

Figure 11. $\alpha, \beta; \gamma$ CDs and their truncated cone representation.

The hydrophobicity of CD's cavity allows *host-guest* interactions with organic molecules, via inclusion complexes, while the hydrophilicity of their outer surface assures water solubility; due to these properties CDs are used as solubilizing agents. Nowadays cyclodextrins are currently used in pharmaceutical and environment protection applications, in food industry as molecular carriers, as building block material for the preparation of chiral HPLC columns and as supramolecular catalysts.

Catalysis within cyclodextrin's cavity

Cyclodextrins catalyse a plenty of organic reactions.[35] The acyl transfer reaction of different phenyl acetates to the proximal hydroxyl group of the cyclodextrin was one of the first reactions studied. Rate enhancement of 100 fold was achieved in the acyl transfer from *m*-nitrophenylacetate to a secondary side hydroxyl group of a β-CD if compared to the ester hydrolysis in the absence of β-CD.[36] The presence of substituents in *meta* position forces the substrate to partially exit the cavity when the tetrahedral transition state is reached and this does not allow higher rate improvements whereas, when *p*-nitrophenyl ferrocenyl acrylate esters were used rate improvements of 5900000-fold were achieved.[37] These rate differences, even if not involved in any catalytic reaction, suggest that correct binding within the CD's cavity for both reactant and transition state is fundamental to get the best results from this *host-guest* systems.

Breslow and co-workers were the first to report a reaction being catalysed from cyclodextrins; the reaction was the selective chlorination of anisole in presence of an excess of α-CD.[38] Anisole chlorination with hypochlorous acid has been shown to be not regioselective but when anisole is included into α-CD the hypochlorous acid transfer a chlorine atom to a hydroxyl group of CD and the reaction proceeds with 100% selectivity to the *p*-substituted product.

Subsequently CDs were widely used in catalysis to improve either the reaction rate or the product selectivity.[35b] Pericyclic reaction between small diene and dienophile, such as cyclopentadiene and acrylonitrile, has been shown to be catalysed by β-CD.[39] The α-CD inhibits the DA reaction because it encapsulates only the diene, avoiding the transition state formation and it has been shown that β-CD can be also an inhibitor if large dienes are used. Houk and co-workers in 2002 highlighted β-CD catalysis on the reaction between cyclopentadiene and diethyl fumarate. After a qualitative computational study, the authors found that β-CD stabilizes better the CD-transition state complex than the CD-reactants one essentially because the former is bimolecular whereas the latter is termolecular. For this reason they used the expression "*entropy trap*" for the description of the catalytic effect obtained from the usage of cyclodextrin in those Diels Alder reactions. [40]

Finally remembering the product inhibition already seen for nanocapsules, the low binding constants between cycloaddition products and the β-CD has been used as an explanation for turnover effects.

Modulation of the solvatation sphere by encapsulation within cyclodextrin cavity

Encapsulation of known ligands or homogeneous catalysts within the CD cavity has been used to achieve second-sphere coordination.[41] The supramolecular ligand obtained from the encapsulation of triphenylphosphine tris-sulfonated within β-CD has been tested in the hydroformylation reaction but, it resulted in a decrease of the reaction regioselectivity.[42] It has been also reported that encapsulation of ligands within β-CD allows to obtain low-coordinate Rh phosphine species which showed different selectivity and improved activity.[43]

Leclercq and Schmitzer reported in 2010 the hydroformylation reaction of allylic alcohols and 1-octene mediated by $Rh(acac)(DABP)_2$ in presence of methylated-βCDs in both homogeneous or biphasic media (Figure 12).[44]

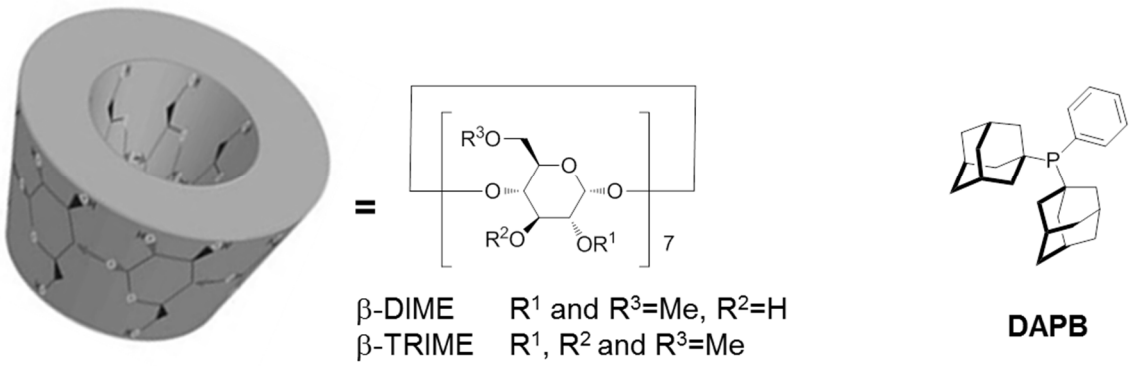

Figure 12. Modification of catalyst's performances by encapsulation of ligand's moieties within bis and tri-methylated cyclodextrins. From ref. 44.

Bis-methylated (DIME-CD) and *tris*-methylated (TRIME-CD) CDs were used as supramolecular host; the former affords better solubility in aqueous media while the second in organic media. First of all the rhodium phosphine complex was tested in absence of any CD either in water (allylic alcohol substrate) and dichloromethane (1-octene substrate) showing almost no catalytic activity (<1% conversion) in both cases. After CD addition, with an optimal CD/Rh ratio of 2 for both β-DIME-CD and β-TRIME-CD, catalyst activation was observed. Of course it was found that β-DIME-CD affords better results than β-TRIME-CD in aqueous media (76% conversion *vs.* 23%), and the contrary in dichloromethane (15 % *vs.* 59%). The activation effect was attributed to the removal of a DABP ligand from the metal coordination sphere due to the formation of an inclusion complex between DABP and CD. When the supramolecular assemblies were tested in biphasic media, it was found 57% conversion of 1-octene with the water friendly β-DIME-CD while, hydroformylation of allylic alcohol in presence of the lipophilic β-TRIME-CD affords 79 % conversion.

This study shows how the correct CD choice not only permits catalyst activation although it is strategic to place the catalyst, reactants and products in different phases without dramatic loss of activity and selectivity and yielding easier separation processes.

Cyclodextrins may be conveniently modified by different reactions.[45] Thanks to these modifications, cyclodextrins *host-guest* properties are not only preserved but they are coupled with the specificity of the introduced moiety. Improved catalysts, specific recognition and photomodulable *host-guest* systems have been developed just following this strategy.

Metal free supramolecular chemistry-Cavitands and capsules

Following the cyclodextrins examples there are other organic molecules such as cucurbiturils, crown ethers and calixarenes that may act as a *host-guest* systems useful to complex reactants or catalysts.

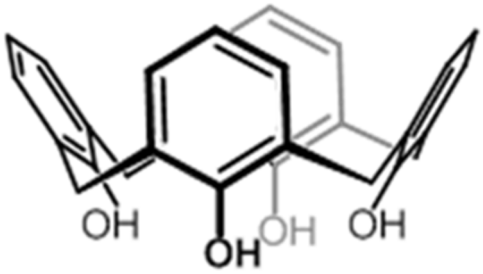

Figure 13. Calix[4]arene obtained from hydroxyl alkylation between phenol and formaldehyde.

Calixarenes have been first synthesized by Adolf von Baeyer in 1872 but until Zinke experiments to improve their yield they were considered only an exotic side product. These molecules are now efficiently obtained by cyclic hydroxyl-alkylation between phenols and aldehydes and are characterized by a typical calix shape. John Conforth realized the potential of their cavity as enzymes' pocket analogue in 1955 introducing their use in supramolecular chemistry. Indeed they could act as catalysts and mimic enzymes due to the possible substrate activation and catalyst complexation within their cavity.

As in cyclodextrins the artificial cavitands have been covalently functionalized with catalytic moieties to afford improved catalysts.[46] One remarkable example is constituted by the resorcin[4]arene derived octamide cavitand reported by J. Rebek and coworkers in 2007. [47] This molecule was used as catalyst in Diels Alder reaction between 9-methanolanthracene and N-cyclooctyl maleimide; the authors observed that while the maleimide bounds the cavity with the hydrophobic cyclooctyl moiety, leaving the dienophile fragment out of the capsule, the hydroxyl group takes the anthracene close to the capsule thanks to hydrogen bond network. The result was a 57-fold reaction rate enhancement and the turnover was allowed by the low binding constant between cycloadduct and cavitand.

Cavitands have recently shown to be able to host as inclusion complex not only organic molecules but also organometallic species which may be used as catalysts. [48] Ballester and co-workers reported in 2010 the modification of a Rh complex catalytic performance due to its supramolecular encapsulation within Rebek's calixarene-based cavitand self-folding host.[49] The encapsulation of $[Rh(norbornadiene)_2]BF_4$ was followed by partial norbornadiene dissociation and solvent (CH_2Cl_2) saturation. When the system was treated with molecular hydrogen (1 bar) the catalyst did not decompose to Rh(0) and after further addition of norbornadiene, hydrogenation of the latter with unusual product distribution was observed. Instead of the expected dimer, which is the common product, a mixture of dimers, norbornane and norbornene was achieved. Authors argued that the transition state for the dimer formation is too large to fit conveniently the *host* cavity and therefore other reaction pathways become competitive.

Despite the mechanism is still not clear, this system clearly shows how cavitands could be used to achieve non-covalent catalyst functionalization which allows control of the catalytic performance.

Supramolecular catalysis in organic medium within hydrogen bonded structures

We all know that 70-75% of our body is made of water while the remaining part is constituted by both small and large molecules assembled in a supramolecular fashion. Strong covalent bonds (~100 kcal/mol) are involved in biomolecules whose reciprocal organization occurs through weak interactions such as H-bonding (5-10 kcal/mol), Wan der Waals interactions, electrostatic interactions and the hydrophobic effect. The α-helix, β-sheet, tertiary and quaternary structures of proteins are the result of these interactions.

In the recent past artificial self-assembled structures have been proposed by different authors. One of the top authors in this field is J. Rebek famous for his ball like systems where supramolecular assembly was provided by different H-bonding donors and H-bonding acceptors interactions. The first system proposed, the so called *tennis-ball*, consisted in the dimerization process of two diphenyl-glycouril units linked by a durene spacer, and it was used to successfully encapsulate small guests, such as methane, ethane, argon and xenon (Scheme 5). [50] The two units are held together by eight H-bond and the dimerization process took place in low polarity organic solvents, such as chloroform and benzene. Solvent choice is of remarkable importance for developing such supramolecular systems: the more apolar the medium the stronger the hydrogen bond interactions.

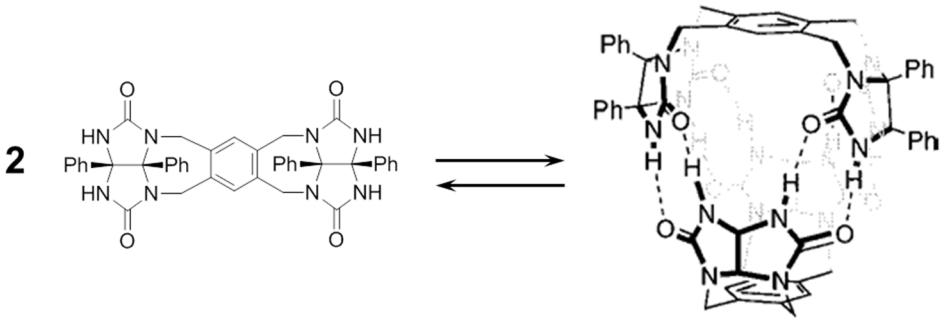

Scheme 5. Self-assembly in the so called *tennis-ball* of two diphenyl-glycouril units linked by a durene spacer.

Following the same synthetic strategy, but improving the spacer length, the same author proposed larger versions of the same capsule which were called *soft-balls*.

Soft-balls showed to be able to form both homodimeric and heterodimeric capsules,[51] and due to their higher volume, the encapsulation of large organic molecules could be performed. 1-adamantanecarboxylic acid (K_d=1.3 mM), 1-ferrocenecarboxylic acid (K_d=3.6 mM), camphor derivatives and two benzene molecules were successfully encapsulated.[52] These systems were then used as nanoreactors for the Diels-Alder reaction between 1,3-cyclohexadiene and *p*-quinone aiming to improve the reactivity due to the compartmentalization of the reactants and

transition state stabilization within the cavity. The *soft-ball* afforded a 20-fold rate enhancement but suffered from product inhibition due to a better product-capsule binding emphasizing the importance of the entropy contribution, as the reactants-capsule adduct is termolecular while the product-capsule adduct is bimolecular.[53]

This problem is limited to reaction products showing high affinity for the cavity; changing the diene from 1,3-cyclohexadiene to 2,5-dimethylthiophene dioxide allowed to obtain a true catalytic system where 10% soft-ball loading allowed 55% and 75% conversions after two and four days, respectively. The same reactions in the absence of capsule showed 10% and 17% conversions, respectively.[54]

Supramolecular control of homogeneous catalyst through encapsulation within a self-assembled cage

While organometallic complexes have been successfully bound in a supramolecular fashion inside cavitands, there are only a few examples of supramolecular adducts between organometallic and self-assembled capsules. Two main reasons may be considered:

- the polar groups in the capsule monomers necessary to achieve self-assembly may act as ligands toward metal center, making DBA or SIA assemblies more likely than self-assembly;
- the internal volume available is not enough to host the complex.

The largest known hydrogen bonded capsule is based on the self-assembly of resorcin[4]arene providing a hexameric pseudo-spherical capsule first characterized in the solid state by McGillivray and Atwood in 1997.[55] The structure was shown to exist also in organic solvents like chloroform or benzene where the assembly is held together by a seam of sixty hydrogen bonds involving six resorcin[4]arene units and eight water molecules.[56] The internal volume of the cavity is about 1375 $Å^3$ and such space is usually filled by six to eight solvent molecules. The inner electron rich surface well complements cations, such as ammonium and phosphonium as well as cationic metal complexes with weakly coordinating anions, which may be efficiently encapsulated with or without residual extra solvent molecules.[57]

Organometallic catalysis carried out within the resorcin[4]arene hexamer was accomplished in 2011 when Scarso and Strukul's group successfully encapsulated a NHC-Au(I)(OTf) catalyst (NHC *N*-heterocyclic carbene) characterized by a pseudo-spherical shape and occupying approximately one third of the total volume, leaving enough space to accommodate solvent or reactant molecules. Complex encapsulation was confirmed by ^{1}H-NMR and ^{1}H-NOESY and DOSY experiments and the system was tested in the hydration reaction of 4-phenyl-1-butyne (Figure 14).[58]

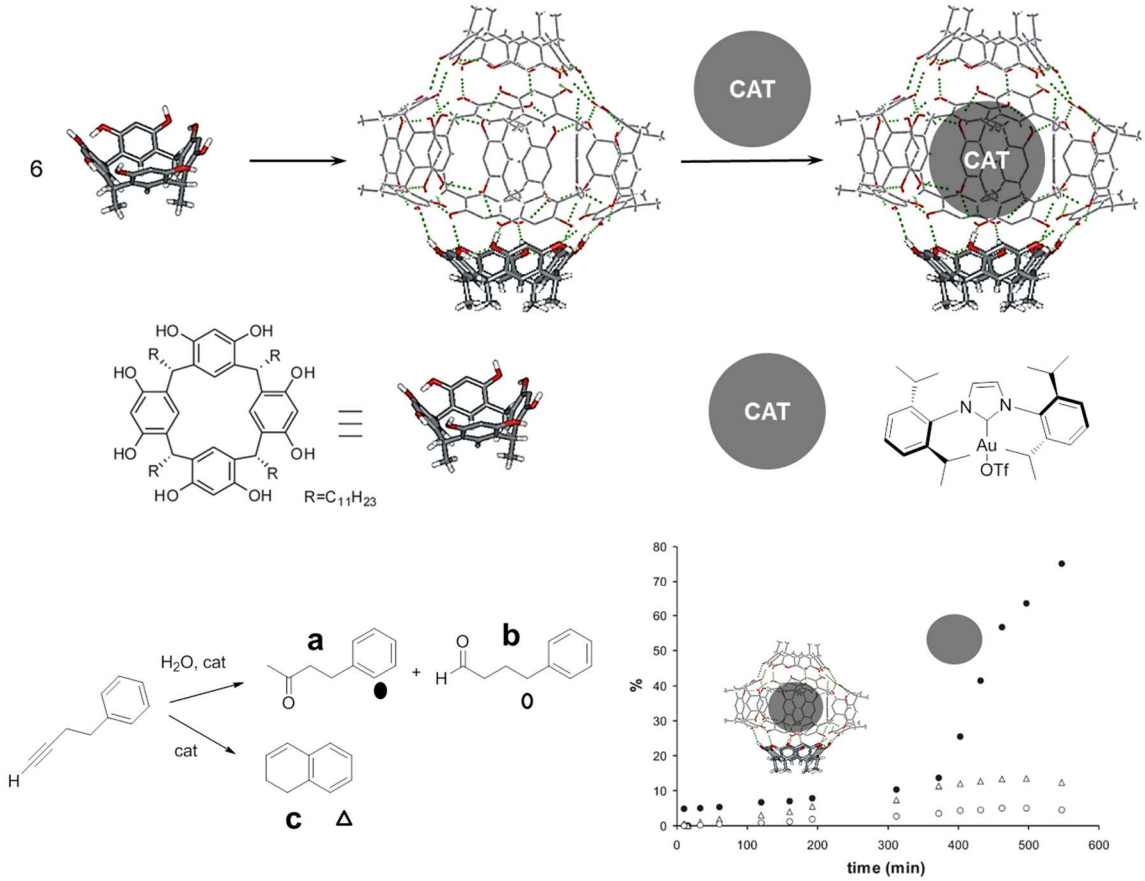

Figure 14. Modification of the solvatation sphere of an organometallic catalyst by encapsulation within a supramolecular cage obtained by self-assembly of 6 resorcin[4]arene units. Encapsulation of the catalyst allowed modulation of the catalytic performances. When, after 400 min a competitive guest for the supramolecular cage (tetraethylammonium triflate) was added, instantaneous recover of the typical performance of the catalyst was observed.

The authors observed that while the reaction rate was depressed by the trapped catalyst, unexpected products selectivity was observed. Comparable amounts of hydration products **a** and intramolecular cyclization product **c** and considerable amounts of hydration product **b** were achieved representing an absolute novelty for this kind of catalysts. The authors suggested that steric hindrance performed by the capsule on the catalyst is responsible for the unexpected regioselectivity while, the different chemoselectivity was attributed to two possible reasons: *i) the* capsule lowers the water income slowing the hydration pathway and making the ring-closing pathway competitive; *ii)* steric hindrance imposes to the coordinated alkyne an arrangement which is particularly effective for the ring closing reaction. Finally as proof of reversibility, the traditional catalytic performance and products distribution were restored by means of catalyst expulsion from the hexamer by addition of a competitive *gues*t (tetraethylammonium).

The regulation of the catalytic performance offered by encapsulating the catalyst within the supramolecular cage coupled with the possibility to neutralize such effects by addition of competitive *guests* constitutes the basis for a supramolecular allosteric strategy which could be used with success in enzyme mimic.

STATE OF THE ART-Light as effector

We have always been told that *"water is the most important substance for life "*. Light is very important too. Think about photosynthesis occurring in the vegetable kingdom which allows storing sunlight energy in the form of covalent bonds allowing plants to grow and reproduce; fossil fuels are another example of sunlight energy stored millions of years ago and then converted into hydrocarbons.

Another example of the use of light in living system is bioluminescence. Many children love to trap fireflies during summer nights and even without knowing how this luminescence is generated they correctly understand its meaning, which is *"I'm here"*. When in the firefly's abdomen region the oxyluciferin, obtained from the reaction between the pigment luciferin and oxygen, meets the enzyme luciferase, the chemical reaction energy is released as light.[59] Many others living systems use bioluminescence to perform important life needs, such as communication and defence against predators.

Photocontrolled catalytic systems

All the above mentioned strategies may allow enzyme mimic and, in certain cases, allosteric control by selective addition and removal of a chemical entity that plays the role of effector. However, differently from living organisms where ingress and egress of effectors are efficiently regulated by the cell, man-made systems suffer from rudimental separation techniques. Conversely, electromagnetic radiation is known to induce chemical processes with minimal modification of the sample and without requiring any kind of product removal or external integration. Moreover light can be considered the most advantageous stimulus (*effector),* especially thanks to the advent of modern light sources and optics.

In 2010 R. S. Stoll and S. Hecht reported a review where they pointed out the state of the art of light-gated systems.[60] The use of light in this area is classified in two categories: *i)* photocatalysis and *ii)* photocontrolled thermal catalysis. In the former the excited state of the catalyst, after light absorption, has catalytic activity whereas the ground-state has not and participates in the catalytic cycle in most cases in virtue of an electron transfer event. In photocontrolled thermal catalysis light promotes the activation of the ground-state of a given catalyst and, after the catalyst promotion no light irradiation is required.

These light-gated systems may be divided in two further classes: *i)* the *"caged"* ones, where the masked dormant catalyst system is irreversibly activated by light once, and *ii)* the *"switchable"* ones, where reversible photoreactions are possible, enabling repetitive triggering of the catalyst between active and inactive forms.

Photocatalytic systems

Photocatalysis may be based on electron transfer or energy transfer systems. The former are characterized by electron transfer between the photo active compound (the photocatalyst) in its excited state and a reactant species and by virtue of this a redox mediator is needed for the restoration of the catalyst. In energy transfer systems the excited state of the photo active molecule transfers energy to a second catalytic species which display catalytic activity only in this energized form.

Successful examples of mononuclear photocatalysis include oxygenation of alkenes with water,[61] photocatalytic reduction of CO_2 to CO[62] and photochemical epoxidation of alkenes in the P-450 enzyme like systems[63] were reported during the past twenty years. Many of the developed systems take advantage of the peculiar properties of $[Ru(bpy)_3]^{2+}$ that was recognized as a useful photosensitizer since 1970s.[64] Its main properties are:

i. Intense visible absorption (λ_{max}=450 nm; ε= $1.5x10^4$ $M^{-1}cm^{-1}$);

ii. Very efficient and fast Intersystem crossing (rate constant=10^{12} s^{-1}), almost unitary quantum yield; longer lifetime of the triplet excited state (~1μs) compared to the timescale of a chemical reaction (ns-μs);

Thanks to its intense visible light absorption and its energy transfer features *tris*-bipyridil ruthenium (II) has been used as a prototype catalyst in the photo-oxidation of water. Recently it has shown to be an effective sensitizer in [2+2] photocycloaddition.[65] In addition to that, it has been conjugated with common organic and metallorganic catalysts providing bimetallic systems with the aim of obtaining light-regulated allosteric catalysts.

Inagaki and M. Akita proposed a new intramolecular bimetallic system where both electron and energy transfer could be tailored. Their bimetallic system was composed by a $Ru(bpy)_2^{2+}$ core which presented also a bipyrimidine (*bpm*) ligand that, with the other two N atoms, coordinates a Pd^+ metal center (Figure 15).[66]

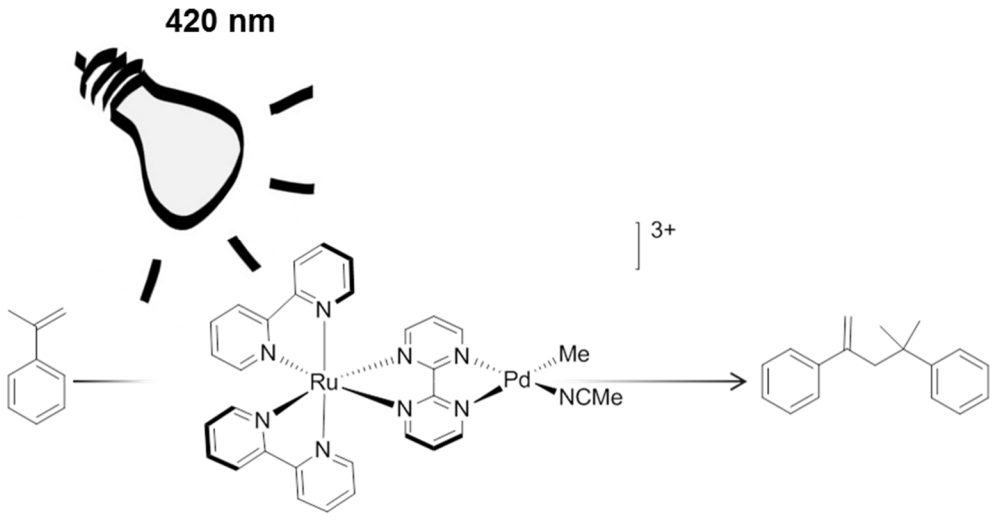

Figure 15. Akita's bimetallic photocatalyst. α-methyl styrene dimerization is allowed only when irradiation of the complex at 420 nm is performed.

The main feature of such systems was the bridging ligand between the two metal centers; indeed for efficient electron/energy transfer, effective overlap of wave functions of the two components is of crucial importance. When *bpm* is used as ligand, the two metals are directly connected by the planar π-conjugated ligand and this turns into strong interaction between them and the arrangement of the two metals is also appropriate for the energy transfer. The authors argued that efficient MLCT[a] from the occupied Ru orbital to the vacant *bpm* orbital (LUMO) in place of the vacant *bpy* orbital, could promote catalysis on the Pd site. Thanks to an accurate DFT study on *bpm* and *bpy*'s substituents they found that introduction of electron-withdrawing substituents onto the *bpm* and electron-releasing substituents on *bpy* allows to perform MLCT selectively towards *bpm*. The proposed system was successfully tested in the dimerization of *α*-methylstirene, observing dimers and trimers formation exclusively under light exposition. From control tests, the author confirmed that no electron transfer occurred and the presence of the bimetallic system was essential to perform the reaction ($[Pd(bpy)]^{2+}$ was inactive). When the reaction was performed in the dark, no conversion was achieved and this allowed ON-OFF control on the catalytic activity simply by turning ON-OFF the irradiation with proper light.

Photocaged systems-Irreversible activation of the catalyst

Photocaged systems may be prepared by several approaches. Activation of the catalyst may occur as a consequence of the irreversible photo-transformation of a molecular species which acts as an effector being able to coordinate and activate the catalyst only in its photoreacted form. Similarly, inhibitors can be photocleaved from the catalyst enabling its activity. In a slight variation of this concept, the catalyst can be de-shielded from an encapsulating/protecting system and its activity restored after photo-cleaving the system which does not allow the catalyst-substrate interaction. Otherwise, in a more complicated fashion, an inhibitor species hampering the correct catalyst-substrate pre-organization can be irreversibly removed by light stimuli. Finally a photoreaction can lead to a modulation of the electronic communication between an activating or deactivating substituent and the catalytically active site.

Photoexcitation of certain transition metal complexes leads to population of anti-bonding orbitals and this facilitates discharge of a bound ligand with consequent generation of a vacant site at the metal center. Pioneering studies in the field made by Asinger and co-workers in early 1960s and later by Wrighton on photoexcitation of iron carbonyl complexes, led to improved catalytic performance in reaction such as olefin isomerization, hydrogenation and hydrosilylation.[60] These results were attributed to CO dissociation from $[Fe(CO)_5]$ or $[Fe_3(CO)_{13}]$ with consequent formation of the more active $[Fe(CO)_4]$ which acted as a thermally driven catalyst (Figure 16A).[60] This strategy was subsequently applied to other CO containing metal complexes; improved catalyst's performance, after light promoted CO dissociation, in [2+2+2] cycloaddition was successfully accomplished by Vollhardt and co-

a MLCT: metal to ligand charge transfer.

workers with [$CpCo(CO)_2$] complex,[67] while tungsten and molybdenum hexacarbonyl compounds were used to effectively catalyse acetylene polymerization.[60]

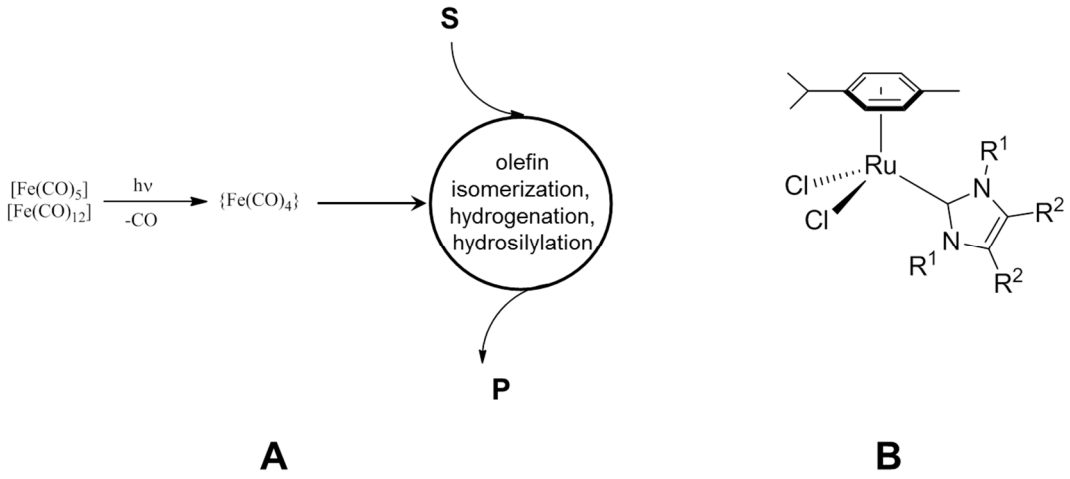

Figure 16. A) Scematic representation for the activation of $Fe(CO)_n$ catalysts by light promoted dissociation of CO ligand. **B)** Noels and co-workers used light to enhance the catalytic performances in the polymerization of cyclooctene for the reported Ru NHC catalyst.

In the field of polymerization in particular ring opening metathesis polymerization (ROMPs), many research groups reported innovative approaches to photoinitiate *"quenched"* thermal catalysts. One of the most recent and relevant contribution was provided by Noels and co-workers who effectively used a known *N*-heterocyclic carbene (NHC) ruthenium complex as a photocaged catalyst in the polymerization of cyclooctene (Figure 16B).[68] The proposed Ru NHC catalyst showed thermally induced activity without any photoactivation step; polymerization tests performed in the dark afforded 22% monomer conversion, averaged molecular weight (M_w) of ≈ 21000 amu, polydispersity (PDI) of 1.53 and *cis*-olefin content of 36%. When the catalyst was irradiated with an ordinary 40 W "cold-white" fluorescent tube or light bulb, almost quantitative monomer conversion was achieved, leading to polymers with M_w of ≈ 500000 amu, narrower polydispersity (PDI=1.33) and *cis*-olefin content of 20%. The higher activity and, as a consequence, the better M_w, PDI and *cis*-olefin content was attributed to the light promoted dissociation of the η^6 bound *p*-cymene substituent which leads to a more reactive unsaturated ruthenium species. Furthermore the use of mild irradiation wavelength, at a variance with the high energy ones used for CO dissociation in the previous systems, was permitted by the substitution pattern of the ruthenium complex.

While photocaged organometallic catalysts were studied since the second half of the past century, the advent of photocaged-organocatalysts occurred only very recently. Since many chemical reactions are catalysed by the presence of acid or base, the photo-generation of these catalysts could be strategic for the development of photocaged systems. PGAs (photo-generated acids) and PGBs (photo-generated bases) are Brønsted acid and base produced by light promoted irreversible rearrangements and their main application field is constituted by photolithography processes.[60]

The first and, to the best of our knowledge, only photocaged organocatalyst able to promote polymerization was developed by Wang and co-workers in 2008. The authors reported an

adduct between 1,5,7-triaza-bicyclo-[4.4.0]dec-5-ene (TBD) and tetraphenylboric acid that upon UV irradiation (254 nm, quantum yield 18%) liberates TBD, which in turn catalyse the living ring-opening polymerization of ε-caprolactone. It was confirmed that the salt did not exhibit any catalytic performance and it was also found that the choice of tetraphenylborate as counterion was of fundamental importance to achieve photoactivation.[69]

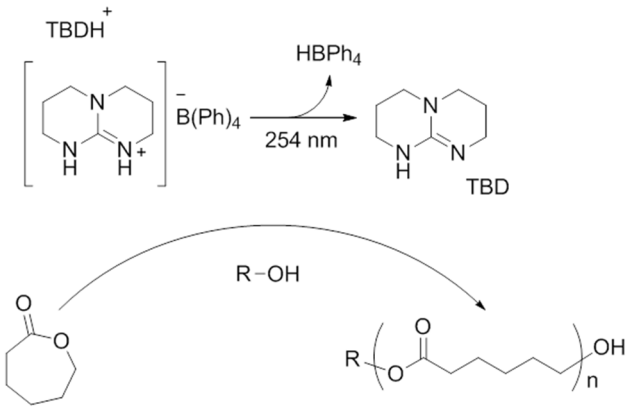

Scheme 6. Light promotes dissociation of tetraphenylboric acid from $TBDH^+B(Ph)_4^-$ yielding TBD species which shows catalytic activity in the living ring opening polymerization of ε-caprolactone.

PGAs and PGBs could be also used as effectors for the activation of dormant catalytic species, as reported by Grubbs group in 2009. The authors merged a known metathesis inactive Ru-alkylidene complex bearing an acetylacetonate (*acac*) ligand with PGA chemistry thus obtaining a dormant complex that can be activated after protonation and displacement of weakly coordinated *acac* ligand providing an active metathesis system.[70] Protons produced by irradiation of PGA effectively protonated acac ligand producing a reactive Ru-alkylidene species active for both RCM and ROMP. The authors observed that the PAG counterion played a fundamental role in developing an active system; indeed switching from a more nucleophilic chloride to the non-nucleophilic nonaflate[b] caused inactivation of the complex.

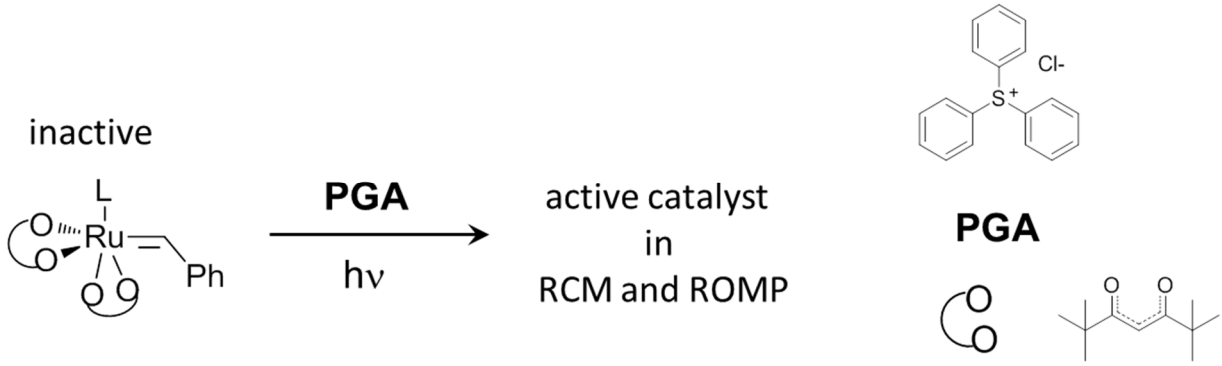

Scheme 7. The Brønsted acidity obtained from irradiation of PGA is responsible of protonation of the *acac* moieties. By virtue of this ligands (*acac*) dissociate from the Ru center yielding an active catalyst.

b Nonaflate: $CF_3(CF_2)_3SO_3^-$

Photocaged systems-Reversible activation of the catalyst

The term "photochromism" was proposed by Yehuda Hirshberg of the Weizmann Institute of Science in Israel,[71] and means the reversible transformation of chemical species between two forms characterized by different absorption spectra as a consequence of the absorption of electromagnetic radiation. One of the recent applications of photochromic materials are the plastic photochromic lenses showing reversible darkening effect. That effect is achieved thanks to the presence in the lens matrix of photochromic molecules such as oxazines and naphthopyrens that absorb the visible light changing their colour to dark.
The difference in the absorption spectra displayed by the two species under photochromic equilibrium is a consequence of their different electronic properties; conjugation of photochromic moieties into a catalyst would allow the development of new reaction mediators endowed with photomodulable catalytic skills. Three well-known molecular structures showing photochromism are spirooxazines, diarylethenes and alkenes showing *E-Z* photoisomerism.

In photoswitchable systems light is used to trigger a reversible photoreaction. Due to this scope photochromic moieties must be incorporated into the catalyst system. The more active system is usually referred as ON state and the less active as OFF state. These two states are better characterized by k_{rel}, which is the ratio between the ON and OFF rate constants.

$$k_{rel} = \frac{k_{ON}}{k_{OFF}}$$

To achieve high k_{rel} values these following requisites have to be followed:

- high attainable photostationary states for the forward and backward photochemical reactions with fast and quantitative switching in both directions;
- the photochromic moiety should shows photochemical stability and the excitation should be localized on the photochromic part, thus prohibiting competing dissipation process (energy and electron transfer to or from the catalyst).
- the photoreaction has to produce strong geometric and electronic variations on the photochrome in order to produce significant variation in catalytic performances

The photochromes can be divided in *P*-type and *T*-type ones. The former requires two different wavelengths to perform catalyst switching while in the latter a thermal-back reaction takes place, adding another possible means to gate the catalyst systems besides photochemical switching. If the half-life of the less thermodynamically stable isomer is sufficiently long, both the thermal and photochemical deactivation of the catalyst is possible.

Generally, the E-Z isomerization reactions of alkenes and azobenzene compounds may be useful to obtain large structural change while the electrocyclic ring-closing/ring-opening reactions of 1,3,5-triene systems such as spiropyranes/spirooxazines, diarylethenes and fulgides yield new structures with substantially different electronic properties.

Systems based on E→Z isomerization

When photolyzation of olefins is performed, both both S_1 and T_1 species have in many cases a perpendicular rather than a planar geometry, so E-Z isomerism disappears upon excitation. [72] This twisted geometry was expected to minimize electron-electron repulsion; derived potential energy diagram for the electronic states of ethylene indicated that the twisted singlet could produce either the *Z* or *E* olefin by internal conversion and that intersystem crossing from the twisted triplet could likewise produce either olefin. Basically, direct irradiation of alkenes will likely produce ($\pi^2_S+\pi^2_S$) cycloaddition in competition with the desired isomerization.[73]
Both isomers may be achieved when the molecule drops to the S_0 state but the *E/Z* ratio achieved is strongly related to the olefin's nature. Compounds such as azobenzene show selective isomerization to *Z* or *E* form as function of the light source chosen.

Azobenzene is a chemical compound bearing two phenyl rings linked by nitrogen-nitrogen double bond whose main photochemical property is the selective photoisomerization between the *E* and *Z* diastereoisomers (Scheme 8). The *E* isomer is more stable by about 12 kcal/mol with respect the *Z* isomer and the energy gap for the isomerization reaction is 23 kcal/mol, therefore *E* is the predominant isomer at room temperature in the dark. *E→Z* isomerization could be achieved upon irradiation by ultraviolet light (320-350 nm), corresponding to π-π^* excitation (S_2 state). The less stable *Z*-isomer will relax to the more stable *E* isomer via both thermal and photochemical pathway. *Z→E* photochemical isomerization could be achieved by irradiation at longer wavelength (blue light, 400-450 nm), which corresponds to n-π^* excitation (S_1 state).[74] The isomerization process involves a decrease of distance between the carbon atoms in positions 4 and 4' on the two phenyl groups, from ~ 9.0 Å in the *E*-form to the ~ 5.5 Å in the *Z*-form.

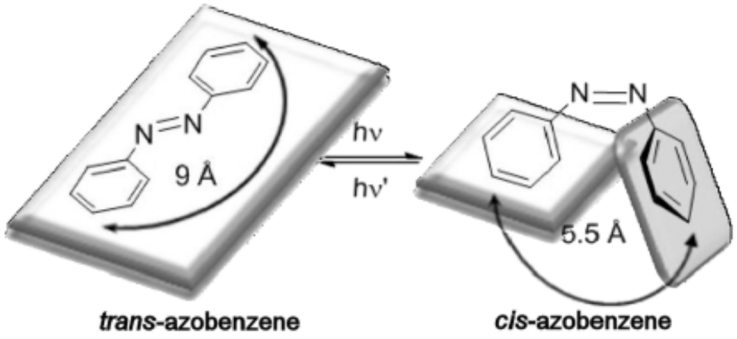

Scheme 8. *E* (left) and *Z* (right) forms of azobenzene

E-azobenzene is almost flat and shows no dipole moment while the *Z* isomer presents an angular geometry and a dipole moment of 3.0 D. In the latter, one of the rings rotates to avoid steric repulsion due to facing the second one π-clouds; this effect is well-displayed by the high field resonance in ^{1}HNMR spectroscopy of the aromatic protons which are affected by an anisotropic effect of the π's cloud of the aromatic ring.[74]

Photoswitchable systems based on azobenzene moieties

E-Z isomerization of azobenzene moieties is probably the most used approach for the development of photoresponsive molecules and materials. As previously explained they are particularly useful in designing systems where two catalytic units connected at the extremities of the azobenzene chromophore may be placed in close proximity in the *Z* isomer or far away if they are placed far away in the *E* isomer. Analogously, systems characterized by photomodulable steric encumbrance could be achieved as well with this chromophore.

Switching the host-guest abilities of supramolecular catalysts

The earliest example of this approach dates back 1980 when Ueno and co-workers decided to join together the *host-guest* features of a *β*-cyclodextrin (*β*-CD) and the *E-Z* photoisomerization skills of 4-carboxyazobenzene. The key concept was to switch the *β*-CD encapsulation properties through the selective self-inclusion of *E* pseudo-linear azobenzene isomer while the kinked *Z*-isomer cannot fit into the cavity of the host.[75] The authors tested their supramolecular light-switchable *host-guest* system in the acyl transfer reaction of *p*-nitrophenylacetate and found that the linear *E*-4-carbossyazobenzene was a much more effective competitor with respect to the *Z*–azobenzene for the *β*-CD cavity hampering the encapsulation of the ester substrate. As a consequence, higher rate in the acyl transfer reaction was observed in presence of the *Z* inhibitor.

This photoswitchable *host-guest* system was further improved by derivatization of the CD. In one remarkable example the same research group developed a *β*-CD bearing both imidazole and azobenzene moieties bound to the same carbon atom on the narrow rim of the CD (Scheme 9). The obtained catalyst displayed no *host-guest* properties and no catalytic functions when the azobenzene moiety was in *E* form due to its self-inclusion within the cavity. Conversely, when the catalytic system was photoisomerized to the *Z* isomer, the azobenzene moiety left the cavity enabling binding of activated esters that were rapidly cleaved thanks to its inclusion into the cavity in close proximity to the imidazole catalytic moiety.[76]

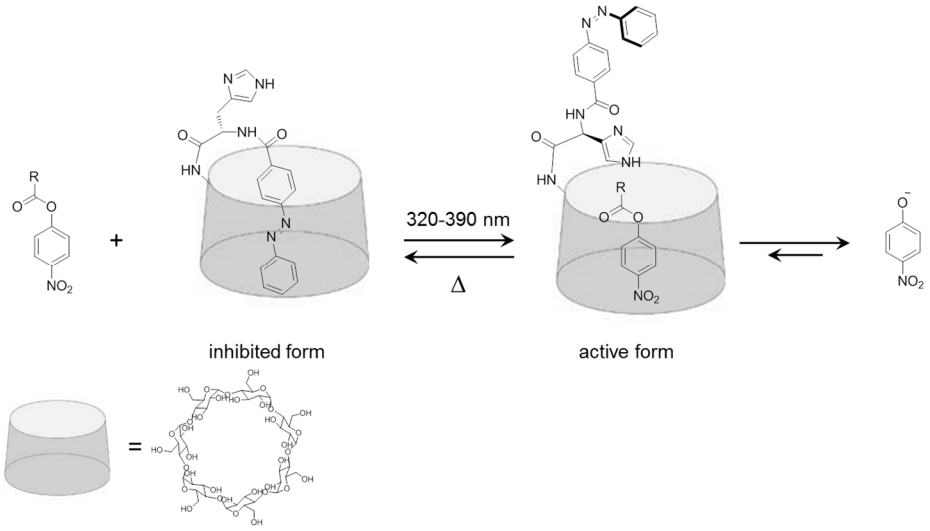

Scheme 9. *E*→*Z* photoisomerization of the azobenzene moiety allows substrate encapsulation within the cavity of the CD and correct orientation of the imidazole catalytic moiety.

Modulation of the reciprocal distance between catalytic units

As suggested above, photoisomerization of azobenzene can be exploited to modulate the reciprocal distance between two catalytic units covalently connected at the extremities of the photochromic moiety. Two catalytic systems sharing the same strategy were reported by R. Cacciapaglia's and J. Rebek's research groups. The latter proposed in 1995 a system composed by two carbazole-based receptors derived from Kemp's triacid, which is known to efficiently bind adenine moieties, reciprocally connected through an azobenzene fragment.[77] The complementarity between the reactants and the Kemp's acid containing moieties allowed an effective binding and, due to the presence of the azobenzene unit, the amide bond formation was triggered by light. The authors observed that higher activity was possible with the Z isomer (50-fold after extrapolation) due to the favourable orientation and confinement of the reactants. The observed value was deduced from the concentration of the *Z*-isomer and by binding constants determination. It was observed that after irradiation at 366 nm (UV, *Z*→*E* isomerization) only 50% of the azobenzene supramolecular catalyst was in the desired *Z* geometry, in contrast to the expected photostationary state (PSS) composition for the azobenzene moiety. The authors argued that strong light adsorption by the carbazole units hampered the formation of higher amounts of the *Z*-isomer enriched PSS. The system suffered for background activity in the absence of catalyst as well as product inhibition thus not displaying turnover ability and reducing the difference in the activity of the two diastereoisomers.

Cacciapaglia's system consisted in two alkaline-earth metal crown ether based catalytic moieties connected by an azobenzene spacer.[78]. Above mentioned metal species are known to be efficient catalysts for the ethanolysis of acetanilides under basic conditions and the presence of two contiguous alkaline metal centers enables substrate activation by ditopic binding.

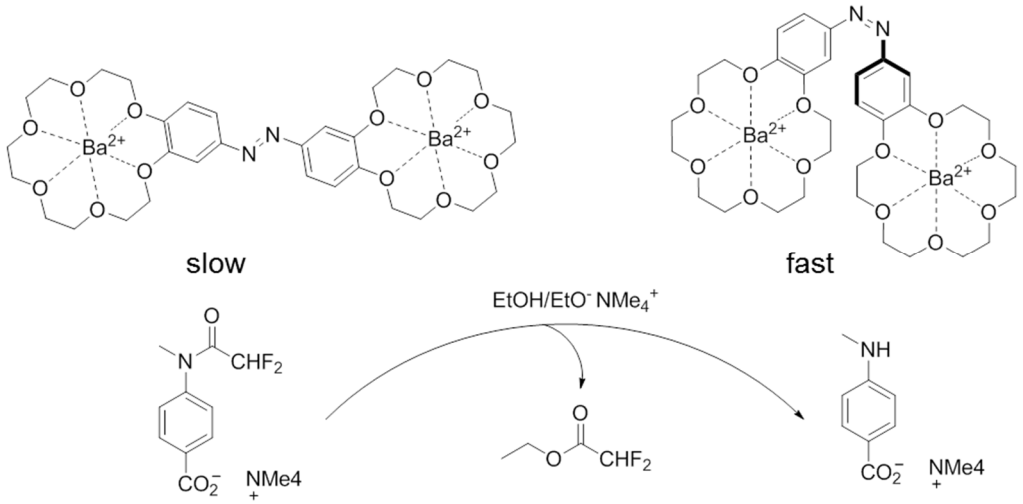

Scheme 10. The *Z* form of the azobenzene moiety allows proper preorganization of the substrate and, as a consequence, enhanced reaction rate.

The latter system allowed to obtain *Z*-enriched (95%) PSS(1) upon irradiation with UV light, while photochemical *Z*→*E* switching was performed with near visible-light irradiation leading to *E*-enriched (81%) PSS(2). The ratio between the catalytic activity of the ON (*Z*-isomer) and OFF (*E*-isomer) reached the value of 3 and this allowed to reversibly switch

several times the catalytic activity leading to an alternating activity profile. Again, the system showed product inhibition at high conversions and, as a consequence, equimolar amounts of catalyst needed to be used to afford efficient catalysis.

E-Z isomerization as active site steric encumbrance effector

Inoue and co-workers reported in 1999 an Al-porphyrin complex whose catalytic activity was regulated by light. Al-porphyrins bearing an axial nitrogen-based ligand are known to be effective catalysts promoting efficient carbonation of alkenes. The authors combined the activation ability of a nitrogen-based ligand endowed to the *E*-*Z* interconversion ability of a stilbazole derivative.[79] Due to its particular design, the stilbazole moiety in the *E*-form (ON state) efficiently binds the Al metal center turning ON the catalytic activity, while *Z*-isomer (OFF state) of the stilbazole could not coordinate to the metal center due to steric hindrance thus turning OFF the catalytic activity. The ratio observed between ON/OFF states was 10 and the system showed the ability to be efficiently switched from one state to the other without losing efficiency.

Following the same strategy Hecht and Stoll reported in 2008 the first photoswitchable basic catalyst. A piperidine moiety acted as a basic organocatalytic function that was covalently bonded to a stilbene or azobenzene moiety through a spiro rigid derivative. The new system, comprising both a photoisomerizable and a catalytic moiety, showed a rigid and orthogonal shape and due to this particular design, lower steric encumbrance is expected for the *Z*-isomer (Scheme 11).[80] The nucleophilicity and basicity of the piperidine moiety in both *Z* and *E* isomers was determined by titration experiments which gave pk_a of 15.9 and 16.7, respectively. This large change in basicity was exploited employing the organocatalyst in the nitroaldol (Henry reaction) addition of nitroethane to 4-nitrobenzaldheyde observing a difference of 35 between the ON/OFF states. The system showed high *E*→*Z* isomerization (90:10) upon irradiation with UV light and a remarkable thermal stability of the *Z* isomer. Despite the well-arranged molecular design, the low activity of the catalyst required high catalyst loading, which affected the photoisomerization due to the strong absorbance of the concentrated solution. To overcome this issue the authors bound the piperidine photoswitchable catalyst to a heterogeneous support providing a new catalytic system showing much better performance.[81]

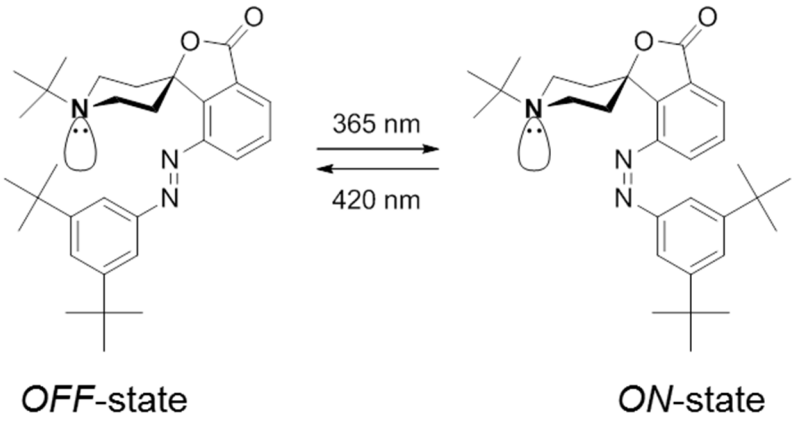

Scheme 11. Photoswitchable azobenzene-based piperidine as light controlled general base catalysts where light triggers reversible steric shielding of the basic/nucleophilic site.

Photocycloadditions

Other interesting, and theoretically reversible, photochemical reactions that lead to consistent modification of both molecular shape/size and electronic properties are photocycloadditions. This class of reactions could be achieved both in an intramolecular and intermolecular fashion. An intermolecular based approach could lead to reversible photocrosslinking of the catalyst to heterogeneous support yielding heterogeneous catalyst possessing the typical features of homogeneous ones. Otherwise different catalytic units may be joined in superior catalyst affording unexpected catalytic performance. Intramolecular photocycloaddition could afford consistent geometrical rearrangements and may be used to regulate access to the catalytic moiety.

Light absorption by an olefin promotes an electron from HOMO to LUMO orbital and this enables [2+2] cycloaddition between two olefins.[72] The excited state can take several relaxation mechanisms such as light emission (fluorescence between excited and ground state with the same spin multiplicity and phosphorescence between states with different multiplicity), electron/energy transfer, non radiative relaxation and the previously mentioned *E-Z* isomerization. Fortunately $E \rightarrow Z$ isomerization could be avoided in solution by using cyclic alkenes where the ring geometry constrains the olefin in a *Z*-fashion, also in the excited state; intersystem crossing could be sensitized and it may be useful to obtain a longer lived excited state.

Photocyclodimers formation upon irradiation at a proper wavelength is observed for many molecules, such as anthracene, thymine, cycloalkenones and especially coumarin.
Coumarin (1-benzopyran-2-one) is an α,β-unsaturated lactone enclosing an aromatic ring and its structure is widely present in nature especially in apiacae's plant family. Umbelliferone is a natural substance comprising a coumarin moiety with an hydroxyl group that finds employment as light filter in suntan lotions and creams.

Photodimerization of coumarin leads to loss of the α,β-unsaturation and formation of a cyclobutane ring between the two coumarin molecules. Four dimers are possible depending on the position of the carbonyl fragment: *head-to-head* dimers (HH) show carbonyls on the same side of the cyclobutane ring in 1-2 positions, while *head-to-tail* dimers (HT) show carbonyl on opposite 1-3 positions. Both HH and HT dimers exist into two possible stereoisomers *syn* or *anti* depending on the presence of substituents on the same side or on opposite sides of the cyclobutane planar structure, respectively.

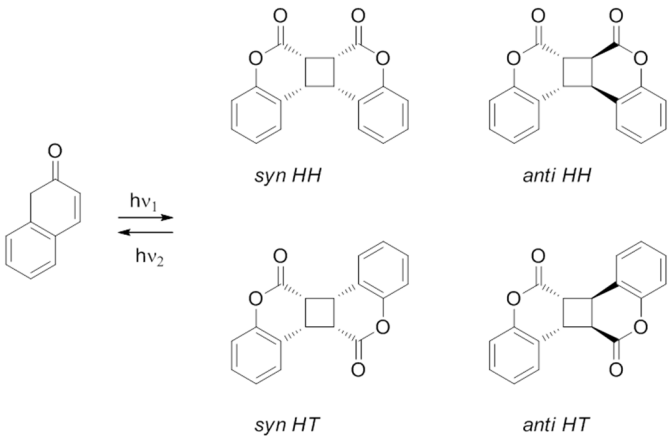

Scheme 12. Coumarin and coumarin's dimers chemical structures.

H. Morrison and A. A. Lamola studied the coumarin photodimerization process since 1960s investigating in detail the effect of the solvent on the reaction and the correspondence between excited state and product distribution of the possible dimers.[82] Summarizing the authors' work, direct irradiation of coumarin in polar solvents produces the *HH-syn* dimer via a singlet excimer (^{1}CC*), whose formation is known to be favoured by a high dielectric medium. Conversely, irradiation in the presence of a triplet sensitizer, such as benzophenone, leads to the *HH-anti* adduct in both polar and apolar solvents. *HT-anti* dimers are found in trace amounts during sensitized irradiation while the *HT-syn* isomers are found in small amounts during irradiation in apolar solvents. HH-*anti* dimers formation is favoured also by the so called *"heavy atom"* effect. It was found that the quantum efficiency for *HH-anti* formation ($\Phi_{HH\text{-}anti}$) was essentially independent of solvent polarity since high polarity is a requirement for *HH-syn* adducts formation, while the enhanced $\Phi_{HH\text{-}anti}$ values found in halocarbon confirm their sensitization effect. Formation of *HH-syn* dimers is quite inefficient ($\Phi = 4.4\cdot10^{-4}$ in acetonitrile) and, since intersystem crossing is minimal ($\phi_{ic} = 8.8\cdot10^{-3}$ in acetonitrile), the overwhelmingly dominant process for the excited coumarin singlet state is the decay to the ground state. H. Morrison and co-workers explained the *"heavy atom"* effect as follow: the excited coumarin in triplet state reacts with a ground state coumarin yielding a 1, 4 diradical ($^3C_2$*), which in turns could partially undergo bond closure to form dimer via an intersystem crossing step. Such closure step has to compete with rotation about the new formed bond (1,4) and since the rotated diradical is geometrically unable to close and complete dimerization, it could only undergo cleavage to give back two coumarin molecules. Since closure is essentially an intersystem crossing process, external heavy atoms might facilitate bond formation and increase the efficiency of the product forming step ($\Phi_{HH\text{-}anti} = 35\cdot10^{-4}$ in carbon tetrachloride).[82e]

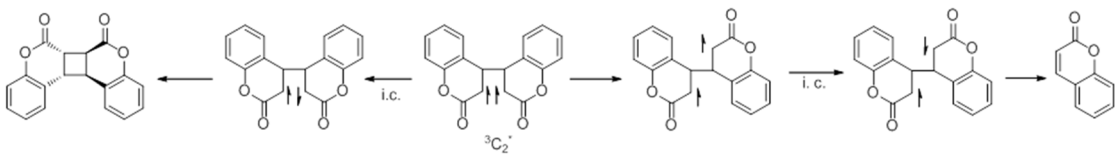

Scheme 13. The *heavy atom* effect proposed by Morrison and co-workers for the *HH-anti* dimer formation mechanism. The 1,4diradical ($^3C_2$*) may form successfully the dimer after intersystem crossing (*i.c.*) process (left) while rotation about the new formed bond (1,4) lead to unproductive excited molecules that undergo bond cleavage yielding back two coumarin molecules (right).

Due to the presence of a competing non-reactive self-quenching process, the dimerization quantum yield of coumarin is rather low, requiring in most cases long irradiation time (>24 h) as well as high sample concentration and powerful light source.

As previously mentioned, the dimerization process could be reversed by irradiation at shorter wavelength. Commonly coumarin dimer cleavage is performed with UV-C light source under 280 nm which could be achieved by low pressure mercury lamp.

Systems exploiting [2+2] photocycloadditions

[2+2] photocycloaddition found wide application in organic chemistry, especially for the synthesis of structurally complex and bicyclic compounds.[83] Recently coumarin and thymine based systems have been successfully used in development of light-responsive luminescence probes, drugs and non-drugs delivery systems,[84] block copolymer micelles,[85] data storage systems,[86] and several other functionalized materials.[87] Nevertheless, despite this wide applicability range, to the best of our knowledge, no examples of coumarin based photomodulable catalytic system are known in the literature while a photoswitchable catalytic system exploiting the [2+2] cycloaddition of thymine has been reported by Nozaki and collaborators in 1997.[88]

Their system was based on a *β*-cyclodextrin equipped with two thymine moieties mounted on the same rim of the *β*-CD (Scheme 14). The intramolecular cycloaddition of those moieties provided a shield to the narrower opening of the *β*-CD, partially undermining the hosting capacity of the CD but providing a deeper hydrophobic cavity. The proposed light-modulable CD showed reversible photodimerization skills allowing three closing-opening cycles without any loss of efficiency; the *host-guest* abilities of the two open and closed forms were evaluated using the acyl transfer reaction of *p*-nitrophenylacetate (PNPA) as a test reaction.

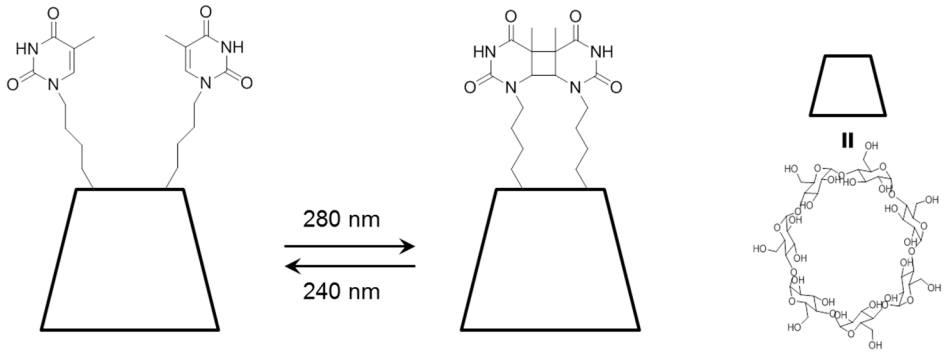

Scheme 14. *β*-CD equipped with two thymine moieties mounted on the same rim of the β-CD. After photocycloaddition between the thymine fragments a more deep hydrophobic cavity is obtained.

The catalytic efficiencies of the new supramolecular *host* before and after the cycloaddition process, expressed as the ratio $[(k_{cat})/(k_{diss})]$,[c] were determined and compared to the analogous properties of an unfunctionalized *β*-CD. It was observed that the functionalized open derivative was more active than the unfunctionalized *β*-CD and that after dimerization the activity was boosted from $[(k_{cat})/(k_{diss})]$ values of 42 to 162 thanks to the presence of a more

c The ratio between the rate constant under catalytic conditions (k_{cat}) and the rate constant for the dissociation of PNPA from the cyclodextrin cavity (k_{diss}) could be used as an expression of the catalytic effect yielded by the CD.

deep and hydrophobic cavity that more deeply and tightly hosts the substrate leading to a substantial decrease of k_{diss}.

Spirooxazines as light-switchable devices with marked variation of electronic properties

Spirooxazines are constituted by different aromatic units bearing an oxazine heterocyclic moiety bound in spiro fashion that prevents the π-conjugation between the two rings, as reported in Scheme 15. The closed neutral spirooxazines (SO) isomer is transparent to the visible light while, the open merocyanine isomer (MC), obtained upon ultraviolet light irradiation, leads to ring opening of the oxazoline ring with formation of a switterionic structure characterized by π-conjunction between the two connected aromatic units, which usually corresponds to intense visible light absorption.

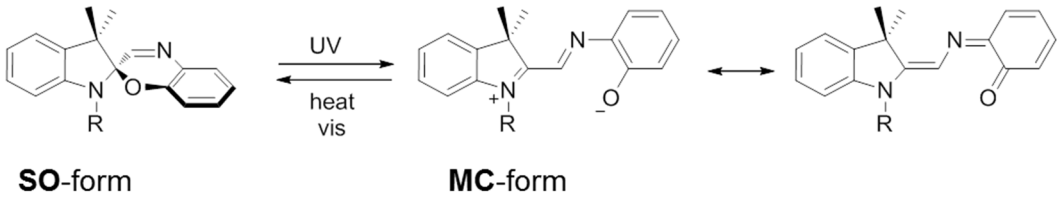

Scheme 15. The two photochromic forms for the spiroxazine; in the SO isomer no π-conjugation is observed between the two aromatic rings whereas they are conjugated in MC form. By virtue of this the former is transparent to the visible light while the latter shows intense light absorption in the visible region. SO→MC switching is performed by UV irradiation while the MC could be returned to SO both in photochemically and thermally fashion.

MC form is less stable than the SP form and gradually converts to the ring closed isomer with a rate that is influenced by temperature, solvent polarity, light and by the presence of certain substituents in the aromatic rings.[89] It is known that the presence of aromatic derivatives on the oxazine moiety shifts the equilibrium toward the SO form while[90] the presence of electron-donating groups in the indoline moiety shifts it towards the MC form.[91] The light driven conversion SO→MC allows not only to prepare catalytic moieties with different electronic properties due to the extended π-conjunction of the MC form, but also the marked difference observed in the solubility and coordination ability may be exploited.

Spirooxazines, and more generally spiropyranes, have been widely studied due to their potential applicability in molecular devices such as optoelectronic components,[92] data storage devices,[93] liquid crystals,[94] and so on.[95] Several examples of metal complexes bearing spirooxazine moieties have been reported[96] and in one remarkable example a photoswitchable catalyst has been proposed where light was used to reversibly recycle the catalyst. G. Liu and J. Wang described in 2010 a ruthenium catalyst active in the ring closing metathesis whose solubility may be triggered by light.[97] The authors linked the spirooxazine moiety to the Hoveyda-Grubbs boomerang-shaped ruthenium-carbene complex obtaining a catalyst active in the ring-closing metathesis (RCM) reaction and that shows the typical spirooxazine/merocyanine (SO/MC) interconversion feature.

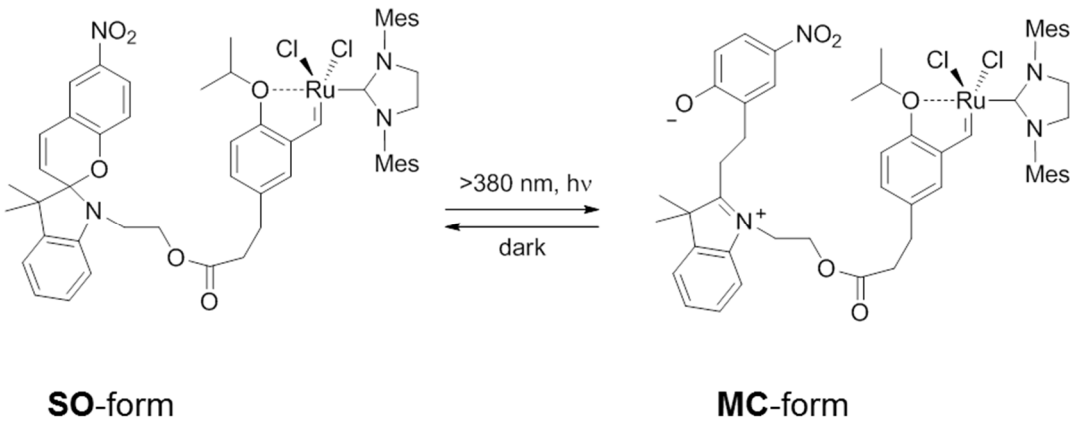

Scheme 16. Light promoted SO→MC switching yielded large variation of the solubility properties of the catalyst allowing phase transfer and consequently recover of the catalytic complex.

Switching from the neutral SO to the zwitterionic MC drastically alters the polarity of the catalyst. The SO form of the catalyst showed good solubility in cyclohexane while MC showed to be easily solubilized in polar media such as glycol/methanol mixtures. RCM reaction tests were carried out in biphasic systems (cyclohexane/glycol/methanol, 3:2:1 v:v:v). SO-catalyst and reactants were solubilized in the apolar cyclohexane phase where reaction occurred until complete conversion. Thereafter the biphasic mixture was irradiated with UV light causing the transfer of the catalyst on the apolar phase due to MC form, confirmed by coloration of the alcoholic phase. This catalyst separation strategy allowed firstly easy collection of products and, upon addition of fresh apolar solvent and after visible light irradiation (or by thermal ring-closing in dark) the SO-complex was formed back again available for further cycles.

Diarylethenes as light-switchable devices with marked variation of electronic properties

Diarylethenes are 1,3,5-hexatrienes derivatives showing interesting photochromic properties. Due to their particular molecular structure, which could be exemplified considering the *E* and *Z* stilbene isomers, they undergo both *E-Z* photoisomerization and photocycloisomerization. An oxidative re-aromatization process could follow the cycloisomerization leading to more stable products, as pictured in Scheme 17

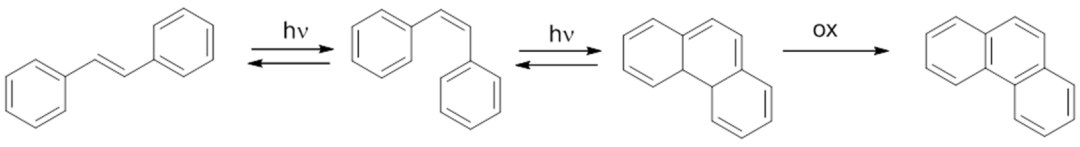

Scheme 17. Stilbene *E*→*Z* photoisomerization, photocycloisomerization of the *Z* isomer and its oxidation to phenanthrene.

Since *E-Z* isomerism is not possible in constrained cyclic olefin, 1,3,5-hexatrienes based on cyclic olefin bearing two aromatic rings linked to the olefin have been reported. Photocyclized isomers showing higher stability toward oxidative re-aromatization could be achieved exchanging the ortho-hydrogen atoms on the aromatic rings with other substituents

such as methyl groups. According with Woodward-Hoffmann rule (*principle of conservation of orbital symmetry*), cyclization of 1,3,5-hexatriene is allowed in the conrotatory fashion only in the photoexcited state; suddenly the closed ring isomers are less stable than the open ones due to loss of aromaticity and this normally limits achievement of thermally stable closed isomers. Irie ad co-workers carried out a theoretical study on the photochromic reaction of 1,3,5-hexatriene to cyclohexadiene in order to gain access to guiding principle for thermally irreversible photochromic molecules synthesis.[d98] Cycloreversion in the ground state has to overcome an energy barrier, and the required energy amount correlates with the energy differences at the ground state between the open and closed isomers: *i)* large energy difference, the energy barrier becomes small and thermal reversion is allowed; *ii)* low energy differences, the energy barrier becomes large and thermal reversion is avoided.

Table 1. Relative ground state energy differences between the open and closed-ring forms.

1, 2-diarylethene	**ΔE Kca/mol**
1, 2-diphenylethene	27.3
1, 2-di(3-pyrrolyl)ethene	15.3
1, 2-di(3-furyl)ethene	9.2
1, 2-di(3-thienyl)ethene	-3.3

Both the open and the closed forms become thermally more stable when the ground state energy of the closed-ring isomer is closer in energy to the open one. As could be understood by the stabilization energies due to aromaticity reported in Figure 17 and from the energies differences between the ground state of the two isomers reported in Table 1, the higher is the aromatic stabilization energy and the lower is the thermal stability of the closed isomer.

Aromatic ring	Energy kcal/mol
phenyl	27.7
pyrrolyl	13.8
furyl	9.1
thienyl	4.7

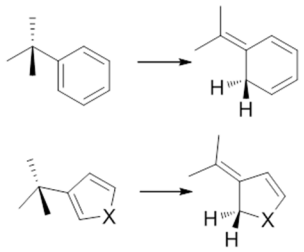

Figure 17. Aromatic stabilization energies for the different aromatic rings.

d Calculation was carried out at the semi empirical level (MNDO).

Due to its properties, the thienyl moiety is the most used in the synthesis of diarylethenes showing thermal stable closed ring and high quantum yield for the cycloisomerization process. When 1,2-*bis*(2-methylthiophen-3-yl)ethenes are irradiated, two possible conformers may be involved in the cycloisomerization: one presents the thienyl rings in a parallel C_2 symmetry orientation or *anti*-parallel orientation with a plane of symmetry.[99] Such conformers are in dynamic equilibrium and their interconversion rate is estimated to be much slower than the lifetime of the photoexcited states. This means that each conformer is excited independently (no conformational change in the excited state). Because of this, the maximum cyclization quantum yield is 0.5.[100]

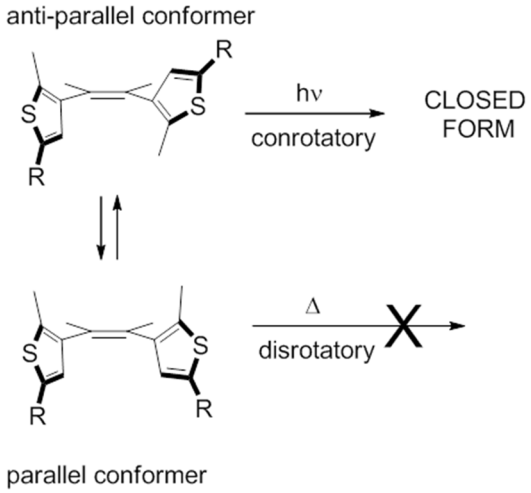

Scheme 18. The two conformers of a dithinylethene moiety. Photoisomerization is allowed only in conrotatory fashion from the anti-parallel conformer.

The ring open isomers of dithienylethenes are usually colourless due to the electronic isolation of the thiophene rings while the closed isomer, which is practically flat, present and extended π-system along the molecular backbone. Thanks to the small shape variation cycloisomerization could be achieved both in solution and in solid matrix enhancing their applicability. Cycloisomerization alters their light absorption properties redox potentials, dielectric constants, refractive indices and several other physicochemical properties as well. It has been found that the presence of electron-donating groups in positions *5, 5'* of the thiophene ring decreases the ring-opening quantum yield while the presence of electron-withdrawing or push-pull substituents provides less thermal stable ring-closed isomers.[101] Thiophenes without any substituent in position 4 are recommended to discard any steric hindrance between this position and the allylic group in the cyclic olefin bearing the two aromatic rings.

The reverse ring-opening reaction could be performed both under thermal and photochemical conditions. Some ring-closed isomers show high thermal stability and in these cases ring-opening is efficiently performed simply by irradiation. The photocleavage of the new formed bond is commonly achieved by irradiation in the visible region, where the π-extended system shows strong absorption.

The electronic differences between the open and the closed dithienylethenes coupled with their excellent ring-closing ring-opening quantum yields and unprecedented photofatigue

(1000 ring open cycles)[102] make this molecular structure extremely interesting in the manufacture of photomodulable enzyme mimics.

Photoswitchable systems exploiting the diarylethene moiety

Diarylethenes have been implemented in the construction of several molecular devices with reversible properties like photochromic complexes,[103] photomodulable mixed valence systems,[104] photocontrolled paralysis in biological systems,[105] data storage systems,[106] synthetic materials and many others.[107] Recently the diarylethene moiety has been employed to introduce light control on chemical reactivity,[108] spurring the preparation of new molecules incorporating this moiety aiming at the development of photomodulable detectors,[109] ligands, complexes and eventually catalysts.

One of the top authors in this field of research is N. R. Branda who studied deeply the different reactivity of diarylethene moiety in both photochromic isomeric forms. He argued that it is possible to exploit the large differences in electronic properties existing between the two isomers obtained by photoisomerization to modulate catalytic activity in homogeneous catalysts. The presence of certain functional groups installed on one of the two aromatic units connected to the thiophene moieties may affect the substituent on the other side only when the open highly π-conjugated isomer is present.

One remarkable example of this strategy is based on the molecule reported in Scheme 19 that aims at mimicking pyridoxal 5'-phosphate (PLP), the B6 vitamin active form where the electrophilicity of the aldehyde moiety present in one thiophene residue is drastically enhanced by the presence of an electron withdrawing group, such as the pyridinium cation installed on the other thiophene unit. The PLP mimicking molecule was tested in the racemization of L-alanine aiming at the evaluation of the different catalytic abilities of the two photochromic forms.

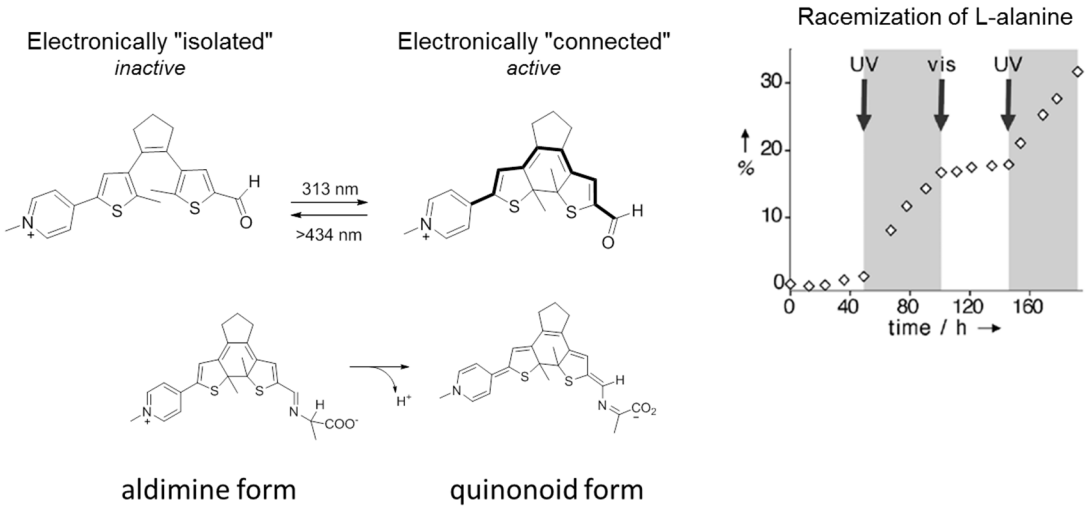

Scheme 19. UV and visible light toggles the dithienylethene structure between its "inactive" ring-open and "active" ring-closed forms. Deprotonation of the aldimine adduct, obtained from reaction with l-alanine, to the quinonoid adduct is allowed only with the closed form.

When the dithienylethene is in its open form there is no π-conjugation between the two aromatic rings and racemization of L-alanine does not proceed. Conversely, when the molecule is subjected to UV irradiation the closed isomer is formed, which is characterized by higher level of conjugation, and as a consequence the racemiztion of L-alanine is observed. This OFF/ON effect could be explained considering that deprotonation of the aldimine adduct is allowed only with the closed isomer by virtue of the large electron withdrawing effect played by the conjugated pyridinium ion. Conversely, the same process is not possible when the thiophene rings are isolates as like as in the open form. Deprotonation of the aldimine is followed by the formation of the quinonoid form that after reaction with water yields a racemic mixture of alanine.

The PLP mimicking molecule showed how the substitution pattern in one of the two thiophene rings affects the chemical properties of the second thiophene rings only in the closed form by virtue of the electronic connection between the two fragments.

As showed by Branda and co-workers the electronic properties of the bridging unity installed between the thiophene rings is affected by the photoisomerization process as well. As reported in Scheme 20, the authors realized a diarylethene system incorporating a phenylborate moiety, where the boron atom is involved in the resonance with the bridging unit. In the open isomer the boron atom is part of a dioxaborole aromatic system (-O-B-O-C=C-, 6 π electrons) and this makes it a weak Lewis acid since the empty *p* orbital of the boron atom is filled with the electrons of the aromatic system.

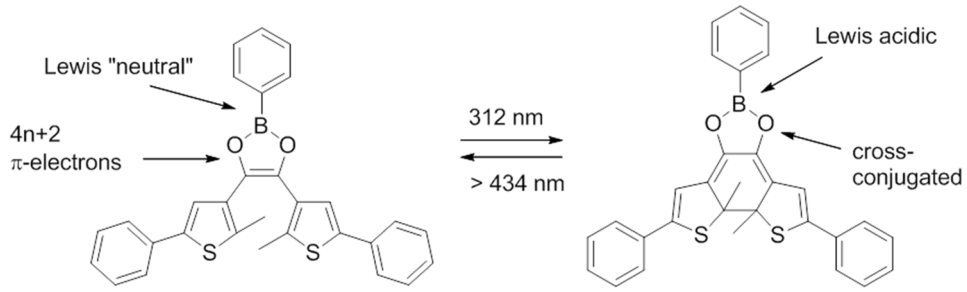

Scheme 20. UV and visible light toggles the dithienylethene structure between the ring-open and ring-closed forms. The boron atom in the former one is part of an aromatic system and by virtue of this it does not show the expected Lewis acidity. Such effect is completely reversed and the Lewis acidity restored after photoisomerization to the ring-closed form.

When the molecule is irradiated with UV light (312 nm) the closed isomer is formed and this restores the expected Lewis acid character of the B atom since in the new isomeric structure it is not involved anymore in an aromatic system. The authors confirmed this performing pyridine binding experiments that showed no significant changes in the ^{1}H-NMR spectrum of the open isomer after addition of 10 eq. pyridine, while remarkable chemical shift changes were detected for the closed isomer supporting the higher Lewis acid.

Very recently, Bielawski and co-workers prepared a photomodulable dithienyl derivative bearing a carbenes moiety in the central backbone to be used as ligand for metal centers. The electron-donor properties of the photomodulable carbene were obtained through preparation the corresponding NHC-chalcogen (X=O, S) and Ir-NHC carbonyl derivatives.[110] The authors found that switching from the open isomer to the closed one entailed a shift of 28 cm^{-1} shift to higher frequencies (ν_{CO}) for the carbonyl moiety in the IR spectrum. This means that the CO

bond was reinforced by the photoisomerization. This phenomenon was explained by considering the delocalization of the N lone pair that was delocalized on the π system after the cyclization, while it was not at the beginning. The Ir-NHC carbonyl complex was then used for Tolman Electronic Parameters determination (TEPs), finding a TEP value of 2049 cm^{-1} for the open isomer typical for NHC ligand, while the closed isomer showed a TEP value of 2055 cm^{-1} typical for phosphines.

In a related study the same research group used an analogous dithienylethene-based NHC carbene as photomodulable catalyst for the transesterification reaction of vinyl acetate (Scheme 21).[111] When a hexafluorophosphate photomodulable carbene salt was used in catalytic amounts (1 mol%) it was found that the open isomer led to the formation of the elongated ester, while the closed turned out to be almost inacitve. The open/closed interconversion was not prevented and ON/OFF triggering of catalytic activity was achieved just irradiating the catalyst with the proper wavelength. The activity differences between the two photochromic forms were explained taking into account that the disruption of the endocyclic double bond after the ring closing process significant changes in the nucleophilic character of the carbene since losing the C=C unsaturation in the carbene backbone leads to lower catalytic performance. [112]

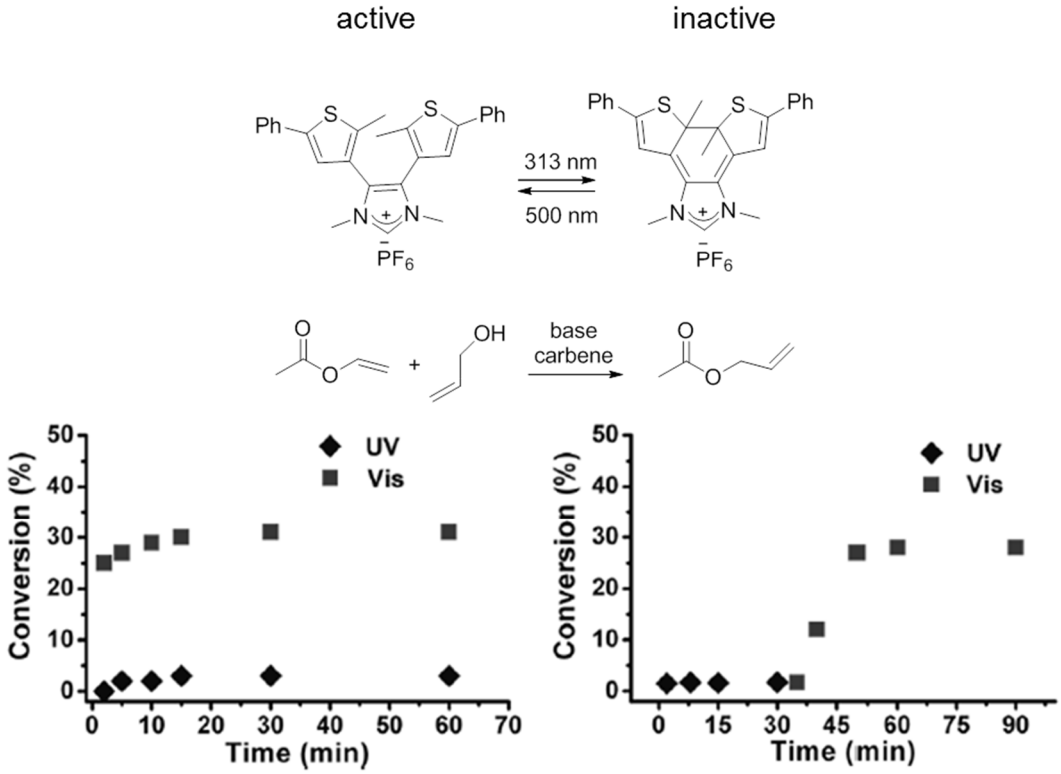

Scheme 21. Switching from the open "active" to the closed "inactive" forms caused dramatic variation of the electronic properties of the diarylethene based carbene that is an active catalyst for the transesterification of vinyl esters only in the open photochromic form.

Another important class of ligands, probably the most used in catalysis, are phosphines. Until now only one example of phosphine incorporating a diarylethene moiety has been reported. Branda's research group in 2005 succeeded in the synthesis of a diarylethene bearing two diphenyl moieties in the side arms and investigated the σ-donation properties of the

photoisomers (Scheme 22).[113] The symmetric bisphosphine selenide derivatives were prepared and showed marked differences in the $J^{31}{}_{P}{}^{77}{}_{Se}$ coupling constants between the open and the closed isomers. The authors reported that switching from one form to the other was as effective as changing a phenyl substituent with a methyl in terms of σ-donor properties of the phosphorous atom. The closed isomer showed enhanced σ-donation ability confirming that the electron density on a metal center might be tuned by light irradiation when a diarylethene moiety is incorporated in the ligand.

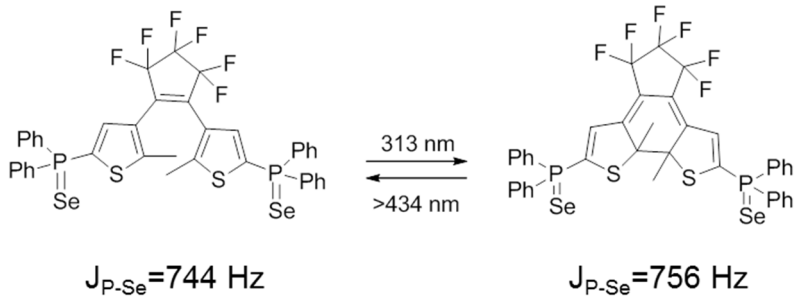

Scheme 22. UV and visible light toggles the dithienylethene structure between its ring-open and ring-closed forms. By virtue of the new formed π extended system, the electronic properties of the two phosphines are different. As showed by the selenium-phosphorous coupling constants of the corresponding selenides, the σ-donation ability resulted enhanced in the closed isomer with respect to the open form.

Finally the photochemical switch of dithienyl moieties has been exploited to prepare ligands whose geometry and coordination ability can be heavily modulated while maintaining almost unaffected their electronic properties. Branda and co-workers reported an example where the diarylethene photoisomerization is a powerful tool to switch the enantioselectivity of an asymmetric reaction.[114] The dithienylethene scaffold was modified comprising two chiral enantiopure oxazoline moieties in the side arms (Scheme 23). The obtained ligand was tested in the copper catalysed enantioselective cyclopropanation of styrene with ethyl diazoacetate observing that the open isomer led to the formation of the chiral cyclopropane derivative in 30% and 50% *ee* for *trans* and *cis* products, respectively, while the open isomer afforded only 5 % *ee* for both products.

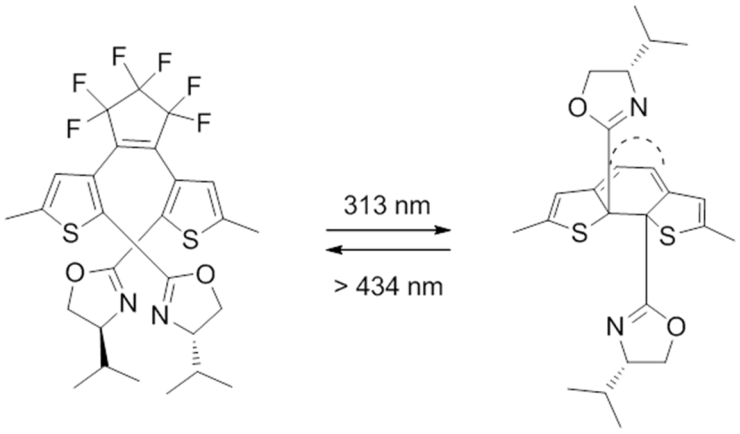

Scheme 23. The two photochromic forms of the dithienylethene scaffold equipped with two chiral enantiopure oxazoline moieties used in the copper catalysed enantioselective cyclopropanation of styrene with diazoacetate.

AIM OF THE THESIS

This thesis aims to develop and study new strategies for achieving control in homogeneous catalysis according to three strategies:

i. Through geometrical and electronic modulation of the coordination environment surrounding metal complexes obtained as an effect of photochemical reactions.

ii. Another strategy takes advantage from the photochemical interconversion of a guest molecule which acts as inhibitor towards supramolecular catalysts.

iii. Finally supramolecular modification of the solvatation sphere surrounding a metal complex is considered to develop controllable photocatalysts.

The first developed system consists in the introduction of a photo-reactive moiety within a common phosphorous based ligand. More precisely a coumarin moiety, which is known to be active towards *[2+2]* photocycloadditions, has been introduced and its photochemical behaviour in square planar bisphosphines Pt(II) complexes established (Scheme 24). The photo reacted and un-reacted forms of these Pt(II) complexes were used in catalytic reactions aiming to understand which activity differences were to be ascribed to the photochemical transformation.

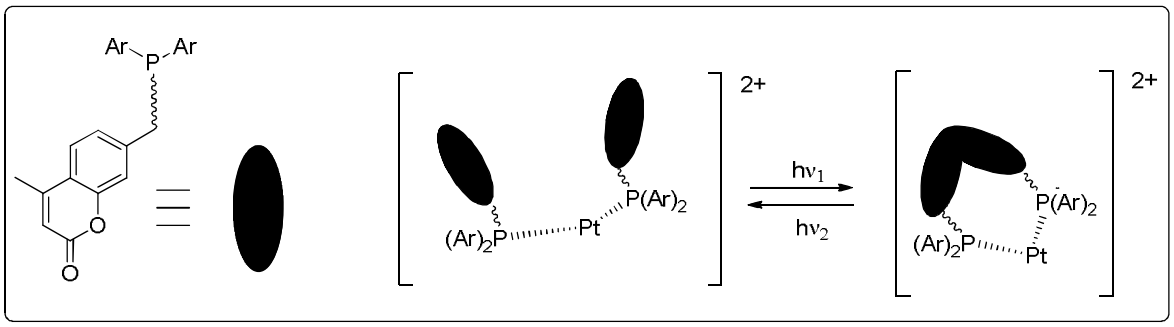

Scheme 24. Geometrical modification of the coordination sphere by intramolecular photocyclodimerization of coumarin-based ligands.

A second study involves the introduction of a diarylethene moiety, a known chromophore, within a phosphorous based ligand. The chosen chromophore has two photochromic forms which are interested by different electronic distribution and by virtue of this, different electronic properties are expected in coordination chemistry for the two photochromic forms. More precisely the open form shows the two thiophene rings electronically isolated while in the closed form they are connected, showing a more extended π-system (Scheme 25). The different electronic properties of the two photochromic forms have been studied synthesizing the corresponding selenides of each phosphine and by the synthesis of the corresponding Rh(I) Vaska type complexes.

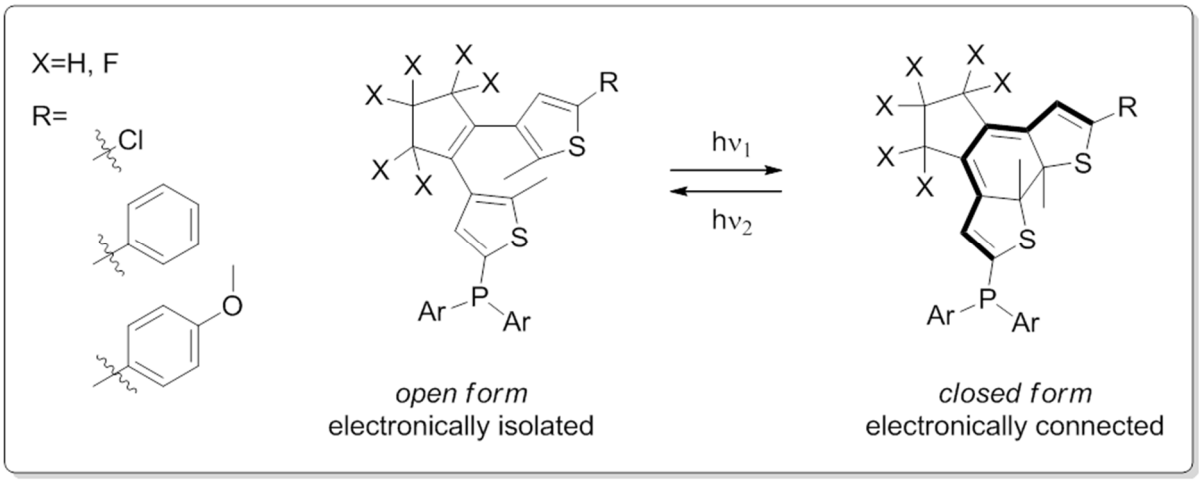

Scheme 25. Modulation of the electronic properties of dithienylethene-based phosphines.

The second strategy involves the synthesis of a photo-switchable inhibitor for supramolecular catalysts through incorporation of the dithienylethene moiety within a *bis*-pyridinium cation. The different photochromic forms may interact in different manners with supramolecular catalysts by virtue of their different electronic distribution and molecular flexibility.

The first *host-guest* system concerns catalysis in organic media and was constituted by the hexamer obtained by self-assembly of six resorcin[4]arene molecules which acts both as host and catalyst while the guest inhibitor was constituted by a dithienylethene based bis-pyridinium (Scheme 26). The second photo-switchable *host-guest* system was composed by *β*-cyclodextrin and by the dithienylethene previously tested and considers water as more environment friendly reaction media.

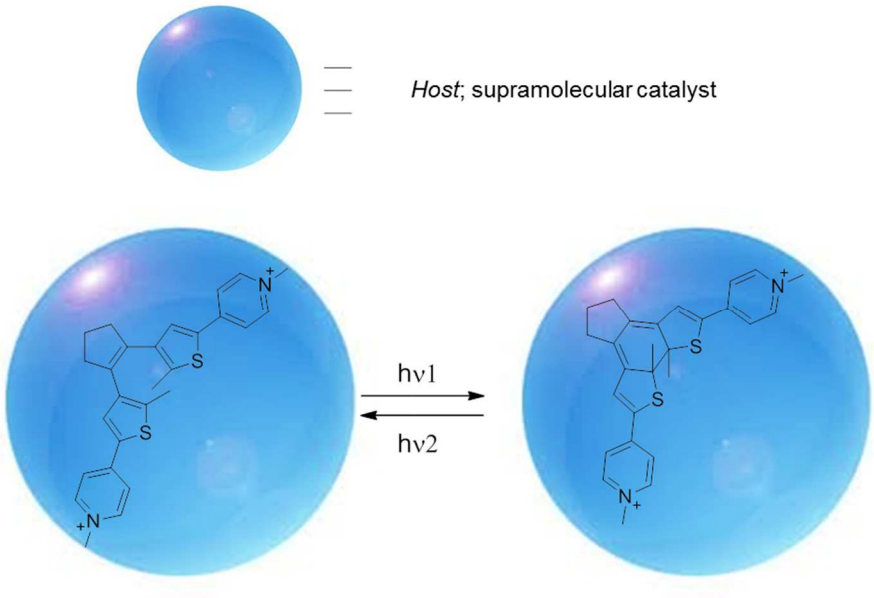

Scheme 26. Photoswitchable inhibitors for supramolecular catalysts.

Finally, we studied the sequestration effect of a supramolecular cavity towards a photoredox catalyst. Since we were interested in introducing a second level of control in a photochemical

catalyst, where the first level is the presence or the absence of light, we argued that modification of the solvatation sphere of the catalyst could be crucial for the regulation of the catalyst activity. Again the host system was constituted by the hexamer obtained by self-assembly of resorcin[4]arene while $[Ru(bpy)_3]^{2+}$ was used as the photocatalyst. After evaluation of the supramolecular interactions we came along with catalysis using as test reaction the aerobical oxidation of sulphides (Scheme 27).

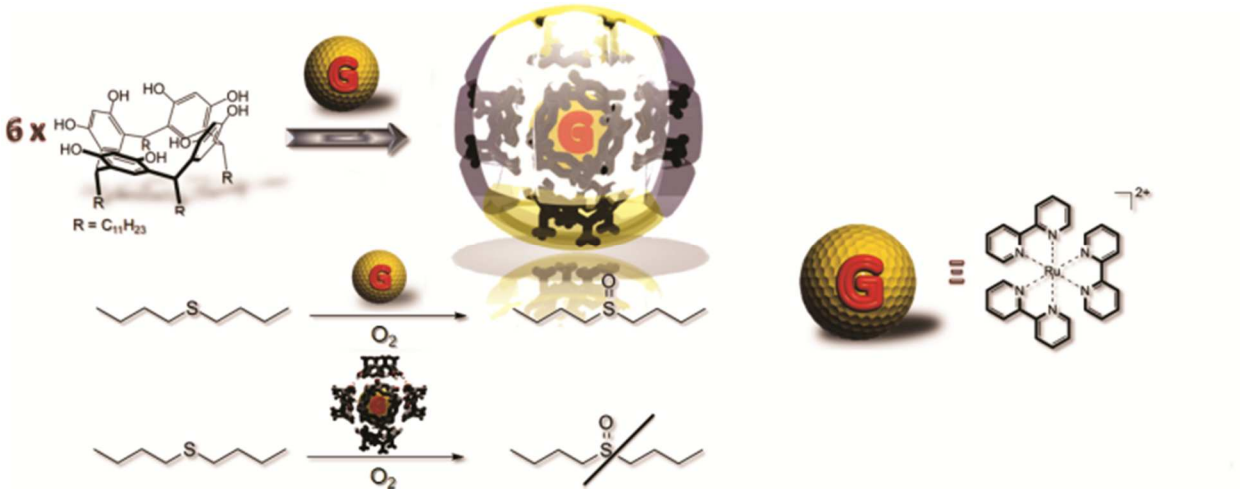

Scheme 27. Modulation of the solvatation sphere of a photoredox catalyst by encapsulation within a supramolecular cage.

PHOTOMODULATION OF THE GEOMETRICAL ENVIRONMENT SURROUNDING A METAL CENTER

Coumarin moiety shows, as previously described, the ability to reversibly form dimers upon UV irradiation due to [2+2] photocycloaddition reaction. By virtue of this, two molecular fragments may be jointed together yielding new molecular species characterized by different shapes. We argued that the introduction of a coumarin moiety into a common phosphorous-based compound may be interesting for the development of light-dimerizable ligands and cross-linkable units. Indeed, using light as effector to promote the dimerization of two monodentate ligands into a bidentate one may allow different catalytic performance for the complex bearing such species.

Herein we report the synthesis of a new phosphorous ligand constituted by a diphenylphosphine moiety equipped with a 4-methylcoumarin fragment. The new phosphine was then coordinated to a Pt(II) center affording the corresponding *bis*-phosphine *bis*-chloride square planar complex whose photochemical behaviour was investigated. Upon chloride ion removal, new *bis*-cationic platinum species can be obtained for catalytic purpose and its photochemical behaviour was studied in different solvents. Finally the *bis*-cationic complexes in their light reacted and un-reacted forms were tested in different reaction, such as the Diels-Alder reaction, alkenes isomerization and dimerization.

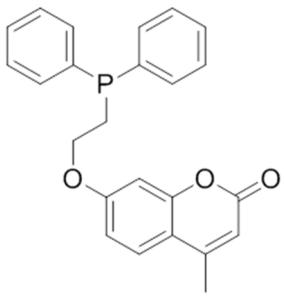

3

Figure 18. The proposed monophosphine bearing two penyl rings and a 4-methylcoumarin moiety.

Monophosphine synthesis

The retrosynthetic approach, reported in Scheme 28, considers the synthesis of the 4-methyl-7-hydroxycoumarin from the low cost resorcinol, followed by addition of a two carbon atom long spacer which provides more flexibility to the structure, and finally the introduction of a diphenyl moiety leading to the desired coumarin-based ligand.

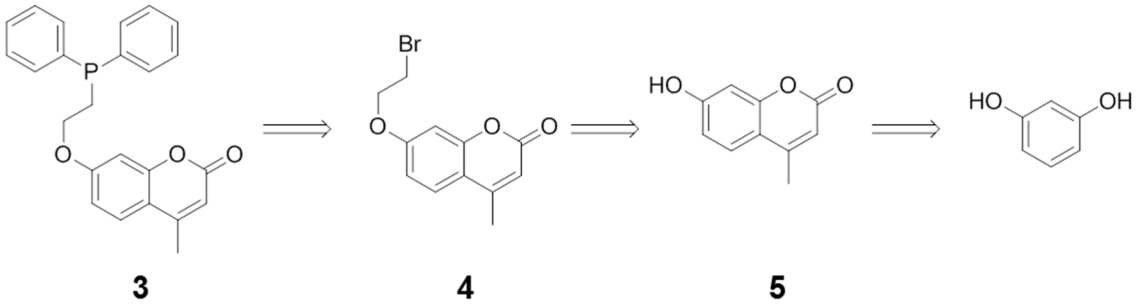

3 **4** **5**

Scheme 28. Retrosynthetic approach for the coumarin-based phosphine ligand synthesis.

*4-methyl-7-hydroxy-coumarin (**5**)*

Coumarin moieties are readily available from different chemical suppliers or could be easily synthetized in laboratory by Perkin's reaction between salicylic aldehyde and acetic anhydride or by Pechmann condensation between hydroxyarenes and acetoacetates.[115] Many reactions have been recently proposed as useful synthetic pathways to achieve coumarins with different substitution patterns, such as: Friedel-Crafts alkenylations of aromatic compounds,[116] Knoevenagel condensation of aldehyde or ketones with active methylenes,[117] hydroarylation of arylpropiolic esters bearing MOM[e]-protected *orto*-hydroxyl group with boronic acids,[118] ring-closing methatesis,[119] Horner-Wadsworth-Emmons olefination[120] and Wittig reaction.[121]

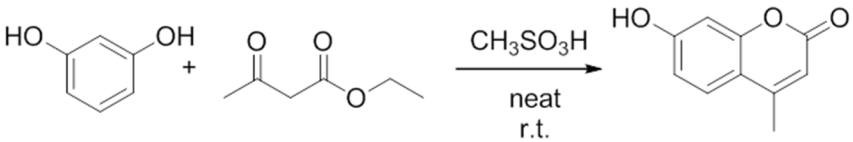

5

Scheme 29. Methanesulfonic acid catalysed Pechmann's condensation between resorcinol and ethyl acetoacetate.

As reported in Scheme 29, the Pechmann condensation between resorcinol and ethyl acetoacetate was catalysed by ~5 equivalents of methanesulfonic acid. The product was isolated simply pouring the crude mixture in crushed ice under stirring followed by filtration of the yellowish solid formed. The crude product achieved in 88-90% yield, but still containing impurities, was re-crystallized from hot water-ethanol solution (2:3) yielding a white solid in 68% yield.

The molecular structure was confirmed by ^{1}H-NMR, ^{13}C-NMR, GC-MS and UV-Vis analysis. The UV-Vis spectrum is characterized by intense absorption band at ~320 nm which is due to absorption by the enone moiety of the coumarin molecule. Since the dimerization of coumarin causes the loss of the enone moiety, the disappearance of its absorption band could be used to follow the progress of the dimerization. Similarly, the ^{1}H-NMR signals of the coumarin moiety could be used to follow the dimerization progress; indeed the shift of the aromatic protons and especially the shift of the proton and the methyl linked to the α,β-unsaturated moiety after the dimerization are easy to monitor and allow to understand which

e MOM=Methoxymethyl ether

isomeric photo-dimer is formed upon irradiation. Figure 19 reports the ^{1}H-NMR spectrum of 4-methylcoumarin as well as the signal attribution.

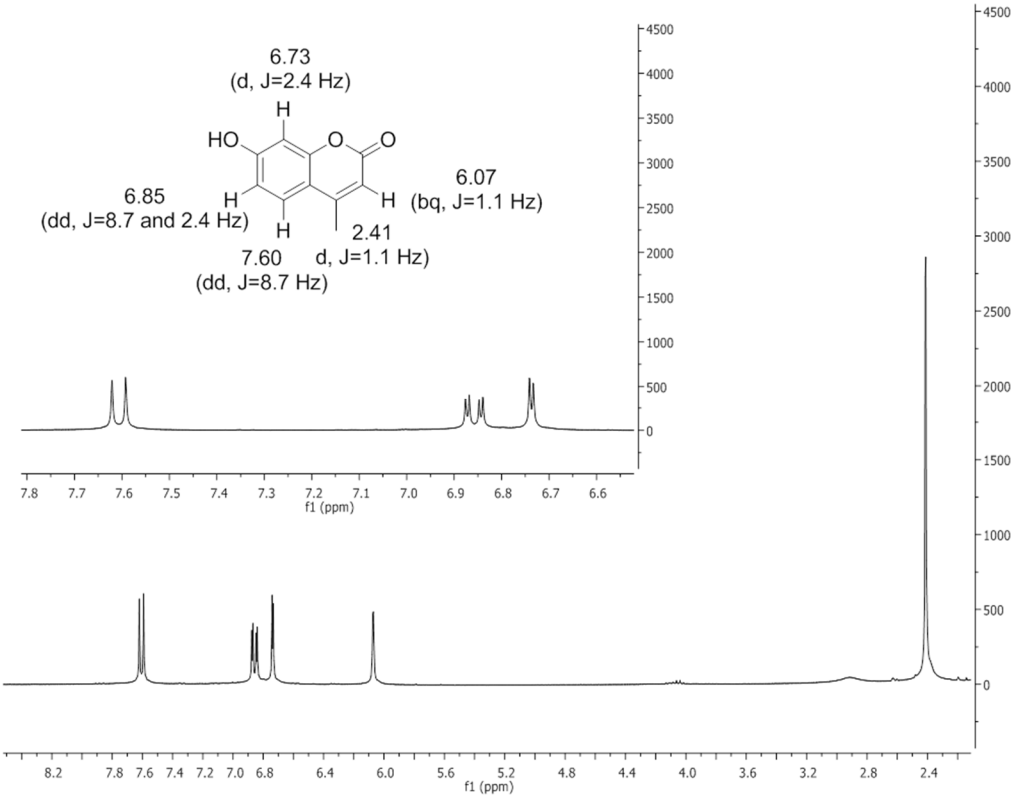

Figure 19. ^{1}H-NMR spectrum of 4-methylcoumarin in acetone-d.

*7-(2-bromoethoxy)-4-methylcoumarin(**4**)*

The product previously obtained was reacted with 1, 2-dibromoethane, aiming to introduce a spacer between the phosphorous ligand moiety and the photo-reactive coumarin fragment. The reaction, reported in Scheme 30, consisted in the nucleophilic substitution of bromide ion in the halo-alkane by attack of the conjugated base of the hydroxyl coumarin.

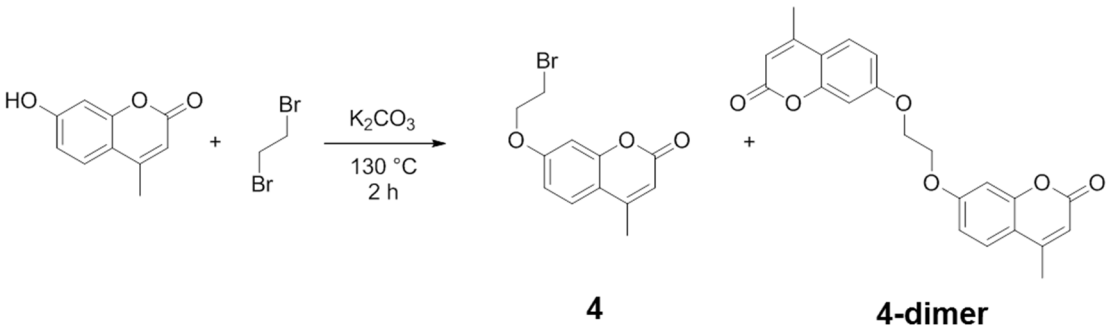

Scheme 30. Synthesis of 4-methylcoumarin bearing a two carbon atoms long spacer.

The reaction was carried out using 1,2-dibromoethane as both reactant and solvent while potassium carbonate was used as base. The heterogeneous crude reaction mixture contained poorly soluble carbonate and coumarin at room temperature, while the latter almost dissolved at high temperature (130 °C). Complete substrate conversion was achieved but analysis of the crude reaction mixture showed the presence of both *mono*-substituted (**4**) and the undesired *bis*-substituted (**4-dimer**) products. The latter product arises by reaction between the mono-substituted product and the coumarin reagent leading to consumption of both reactant and the desired product. The by-product formation is probably favoured by the higher solubility of the mono-substituted product in the reaction media. The use of larger amounts of 1,2-dibromoethane (50 eq.) and an ammonium ion as phase transfer agent did not allow any improvement of the selectivity of the reaction. The desired product was isolated in 58 % yield as a white solid by flash chromatography, using an hexane-ethylacetate mixture (75:25) as eluent. All the spectroscopic analyses confirmed the proposed molecular structure of the product.

*7-(2-(diphenylphosphino)ethoxy)-4-methylcoumarin (**3**)*

The phosphine moiety was introduced in the coumarin fragment by nucleophilic substitution of the bromine atom in the product obtained by the previous step with diphenylphosphide anion. The reaction is reported in Scheme 31, and was performed by addition of a potassium diphenyl phosphide THF-solution to a THF-solution of **4** at room temperature. Anhydrous and deoxygenated reaction conditions are of vital importance to avoid degradation of the phosphide and minimize by-products formation.

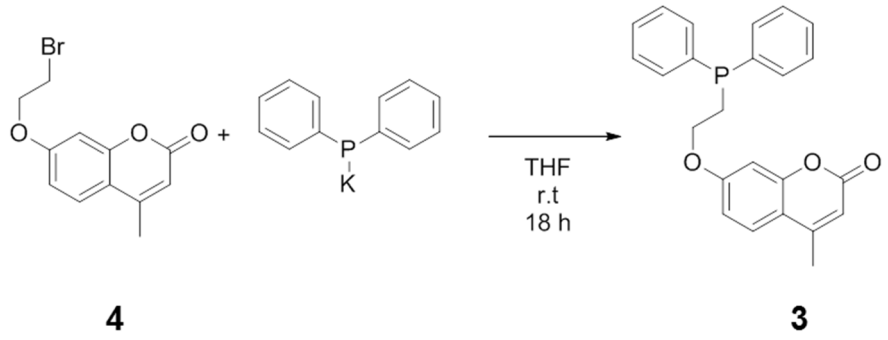

4 **3**

Scheme 31. Introduction of the coumarinic moiety within a diphenyl phosphine fragment**.**

After potassium diphenyl phosphide addition the reaction mixture was allowed to react overnight, then the product was isolated by flash chromatography (eluent hexane/ethylacetate 75:25). The fractions containing the product were quickly concentrated in vacuum and the obtained ligand was stored under nitrogen. The ligand (**3**) was obtained as a white solid in 67% yield and showed easy and rapid oxidation if exposed to the air; as a consequence, after quick characterization the ligand was promptly reacted with the Pt(II) precursor yielding an air and moisture stable compound.

The ligand was characterized by ^{1}H-NMR, ^{31}P-NMR and UV-Vis analysis. The UV-Vis spectrum showed the typical coumarin absorption band at ~320 nm and two relative maxima at 292 and 280 nm, as reported inFigure 20.

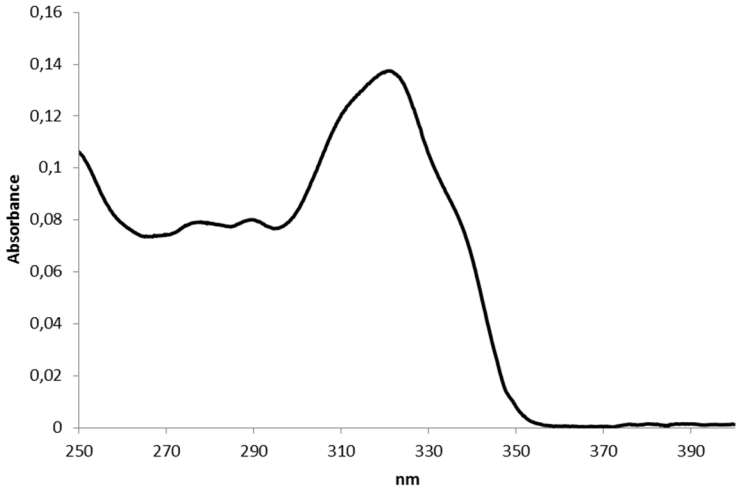

Figure 20. [3] = 10^{-5} M in dichloromethane.

The ^{1}H-NMR spectrum showed the typical resonances of the coumarin moiety as showed in Figure 21; the ^{31}P-NMR resonance was found at -23.92 ppm which is a reasonable value for a diphenyl-alkyl phosphine. The ^{31}P-NMR phosphine oxide resonance was detected at 38 ppm.

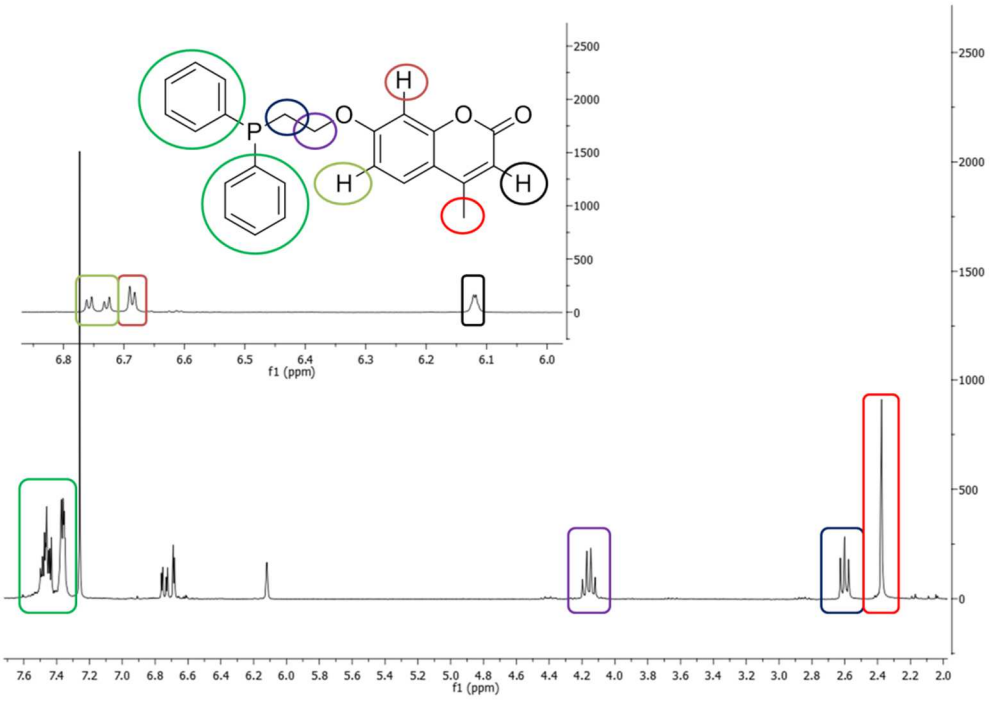

Figure 21. ^{1}H-NMR spectrum of **3** in chloroform-d.

Synthesis of the bis-monophosphine square planar Pt(II) complexes

Since it is known that several reactions like hydroformylation and others are sensitive to the topicity of the ligand, leading different catalytic performance upon switching from monodentate to bidentate chelating ligands,[26,27] we decided to prepare a square planar Pt(II) complex as model compound to understand the photodimerization ability of the newly

synthesized coumarin based ligand. This complex was further studied in different catalytic reactions. Pt(II) complexes bearing *bis*-phosphine ligands are well known soft Lewis acids that have been widely used as catalyst in different reactions such as: B.V. oxidation, alkene epoxydation, sulfoxidation, alkenes isomerization and many others.[129]

In Scheme 32 the retrosynthetic approach for the synthesis of the above mentioned square planar complex is reported which was directly obtained by reaction of the coumarin-based phosphine and a suitable Pt(II) precursor; the catalytically active version of this complex was obtained after chloride ligand substitution with the less coordinating triflate.

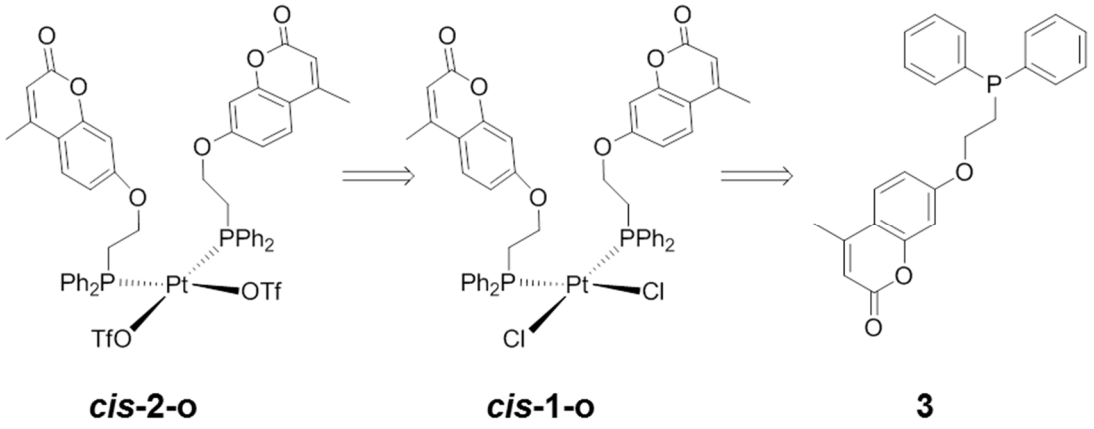

Scheme 32. Retrosynthetic approach for the synthesis of square planar Pt(II) complexes.

Cis dichloro complex

The monodentate coumarin-based ligand **3** was reacted with [Pt(COD)Cl_2], (COD= 1,5-cyclooctadiene) as Pt(II) source, yielding the corresponding Pt(II) square planar complex ***cis*-1-o** in the kinetically favoured *cis* configuration. The complex was easily precipitated with *n*-pentane from a dichloromethane solution and characterized by ^{1}HNMR, ^{13}C-NMR, ^{31}P-NMR and UV-Vis spectroscopy.

The ^{31}P-NMR spectrum shows a resonance at 3.16 ppm and a typical value of 3629 Hz for the phosphorous-platinum coupling constant ($^{1}J^{31}_{P-}{}^{195}_{Pt}$) typical for a *cis* P ligands geometry.[122] ^{1}H-NMR spectrum confirmed the presence of the coumarin moieties since the spectrum showed clearly two out of three coumarin aromatic protons at 6.74 ppm (dd, J=8.8 and J=2.5 Hz) and 6.57 (d, J=2.5 Hz). The vinyl and methyl protons were detected respectively at 6.08 (bq, J=1.2 Hz) and 2.36 ppm (d, J=1.2 Hz). The remaining coumarin aromatic proton and the phenyl ring resonances were detected as two sets of multiplets in the range 7.20-7.30 and 7.38-7.58 ppm. The UV-Vis analysis confirmed the presence of the coumarin moieties. In fact, an intense absorption band was observed between 350 and 300 nm which is typical for the coumarin fragment (λ_{max}=323 nm) together with two relative maxima at 292 and 280 nm, while absorption observed for λ< 260 nm was attributed to the phenyl rings.

Chloride-triflate ligand substitution

The abstraction of the chloride ligands from ***cis*-1-o** was performed by metathesis reaction with silver triflate. The precipitated silver chloride was remover by filtration and the desired complex ***cis*-2-o** was obtained by precipitation with diethylether from an acetone/dichloromethane (1:1) solution. The new compound was characterized by ^{1}HNMR, ^{31}PNMR, and UV-Vis spectroscopy.

The ^{31}P-NMR spectrum showed a slight upfield shift of the resonance at -3.26 ppm with a typical value of 3997 Hz for the $^{1}J^{31}_{P\text{-}}{}^{195}_{Pt}$ coupling constant. The increased value found for the coupling constant is considered a reliable indication of the presence of a more weakly bound ligand such as triflate in *trans* position with respect to P. The ^{1}H-NMR and ^{31}P-NMR spectra revealed very broad signals as reported in Figure 22. The UV-Vis spectra showed the typical coumarin absorption band between 350 and 300 nm with an absorption maximum at 320 nm while the absorption observed at $\lambda < 260$ nm was attributed also in this case to the phenyl rings.

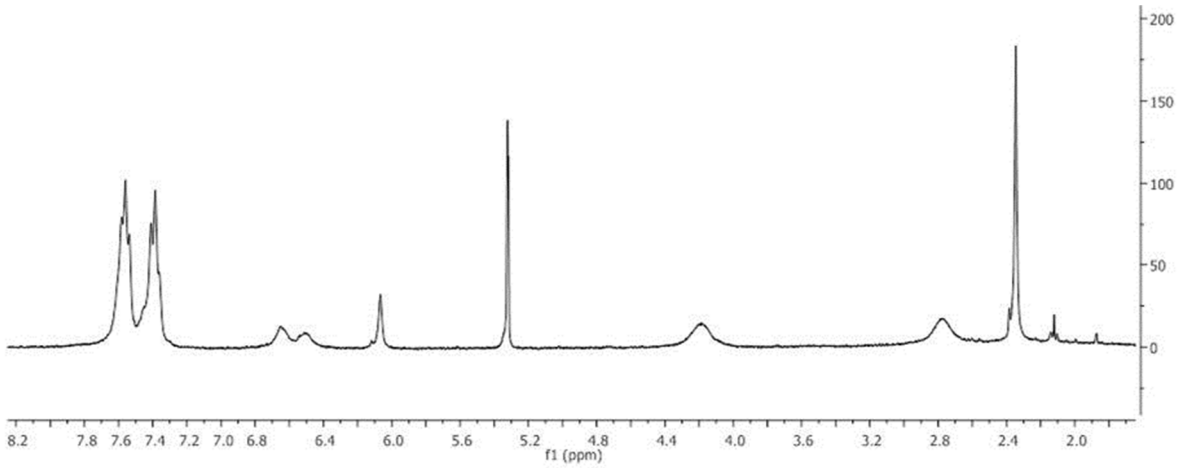

Figure 22. ^{1}H-NMR spectrum of ***cis*-2-o** in dichloromethane-d.

Photochemical behaviour of the dichlorocomplex

The Pt(II) dichloro complex ***cis*-1-o** showed good solubility in chlorinated solvents. Spectra acquired in dichloromethane can be recorded down to 245 nm without interference provided by the solvent itself.[123] This cut-off value allows, theoretically, to perform both the dimerization and the inverse cleavage of the dimer reactions. Conversely, the low polarity of these solvents may decrease the dimerization quantum yield while the presence of chlorine atoms in the solvents may enhance the *HH-anti* dimer formation due to the "*heavy atom*" effect.[82e]

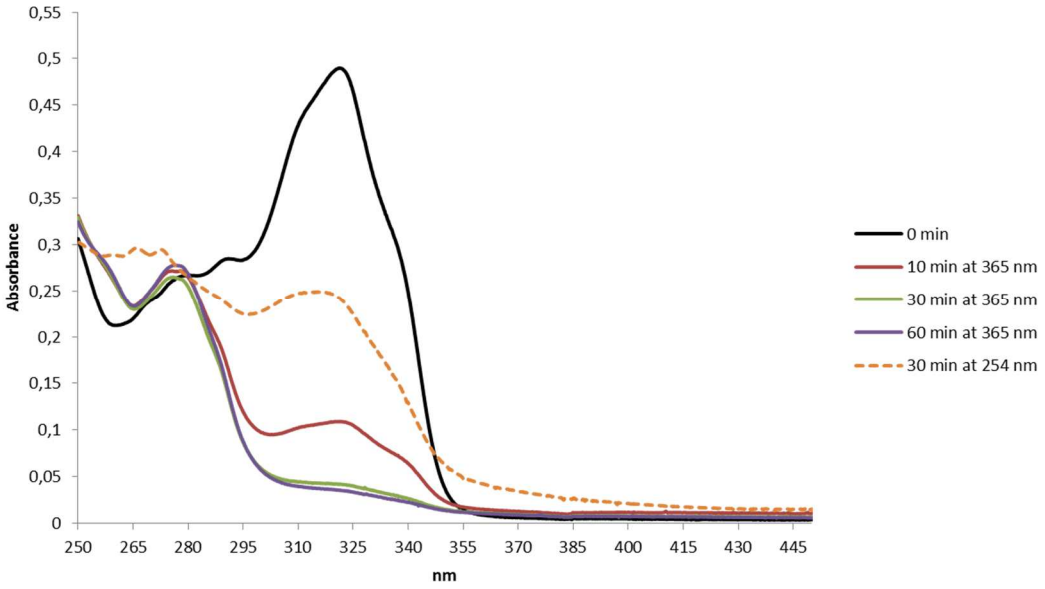

Figure 23. UV-Vis spectra of ***cis*-1-o** in chloroform 1.6 $\cdot 10^{-5}$ M solutions after different irradiation times at different wavelength.

The dimerization process was firstly studied by UV-Vis spectroscopy as reported in Figure 23. The intense absorption between 350 and 300 nm decreased after irradiation with UV light at 365 nm and after 30 minutes the phtostationary state (PSS) was reached. Dimerization of the coumarin moieties is characterized by loss of the unsaturation and concomitant formation of the cyclobutane moiety. Dimers could be formed both in an intermolecular or intramolecular fashion but considering the low concentration employed (10^{-5} M) and the low dimerization quantum yields for the coumarin moieties we argued that the dimerization process occurs intramolecularly between coumarin fragments belonging to the same molecule.

The complex was consequently irradiated at 254 nm to promote dimer cleavage; after 30 min of irradiation the new collected spectrum showed a different profile with respect to the starting material together with a modification of the sample concentration. As expected, the absorption at ~320 nm was increased but the relative maxima at 292 and 280 nm were shifted respectively to 275 and 267 nm showing that the species formed after the photo-cleavage was different from the starting one. In order to shed light on the observed phenomenon and to achieve a better interpretation of the dimerization process, we studied the same reaction by ^{1}H-NMR and ^{31}P-NMR spectroscopy.

Due to its intrinsic lower sensibility, NMR experiments were performed on much more concentrated samples (~ 1 mM). The chemical shift of the proton and methyl bound to the bridging cyclobutane ring could be used to understand which types of dimers are formed by photo-irradiation. Typical values for the above mentioned resonances are 3.4 and 1.2-1.35 ppm for the *anti*-dimers, while 3.6 and 1.6-1.7 ppm are common values observed for *syn* dimers (Figure 24). [124]

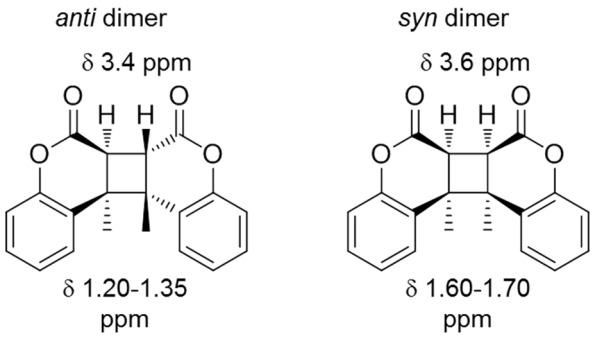

Figure 24. Typical 1H-NMR resonances value for *anti* (left) and *syn* (right) dimers.

As long as the irradiated complex is concerned, it was observed that in order to achieve good conversions into the dimerized products, long irradiation times or strong irradiation equipments were required. After irradiation with UV light at 365 nm for one hour, in the same conditions previously reported, a mixture of products was obtained, as confirmed by the ^{1}H-NMR spectrum reported in Figure 25.

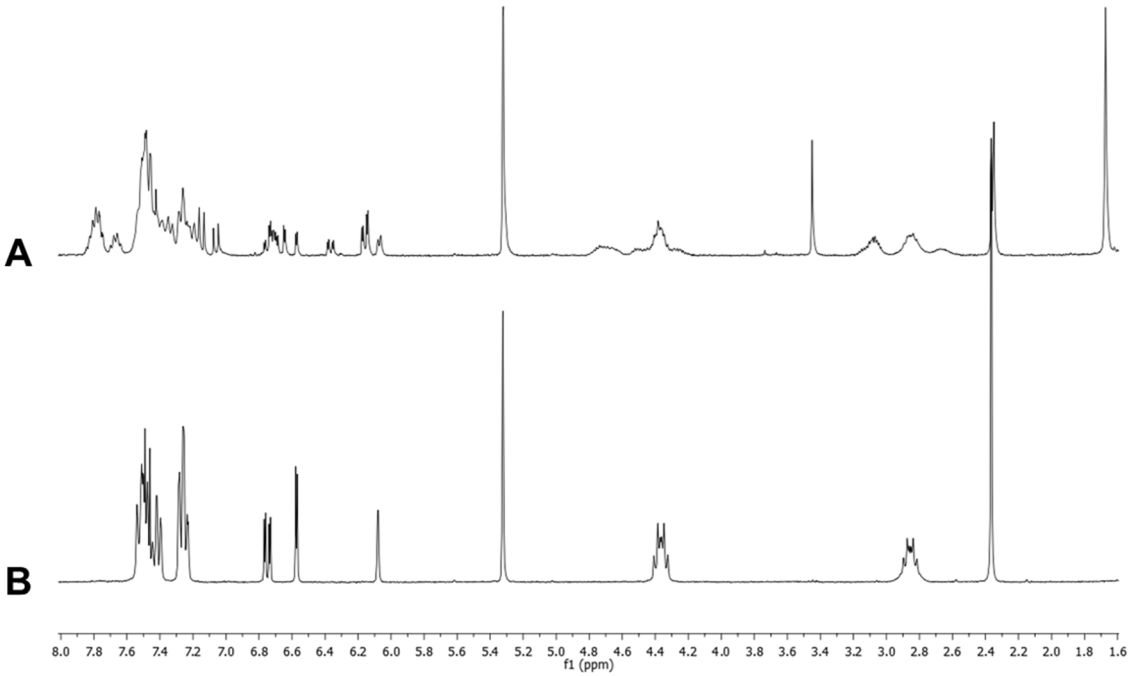

Figure 25. A) *cis*-1-o after 1 hour irradiation at 365 nm in dichloromethane-d; **B) *cis-1-o*** before irradiation in dichloromethane-d.

At the beginning of the irradiation process, a *cis*→*trans* isomerization was observed as already reported in the literature for this class of Pt complexes;[125] the *trans* isomer (***trans*-1-o**) is characterized by a ^{31}P-NMR resonance at 7.48 ppm ($J^{31}_{P-}{}^{195}_{Pt}$=2561 Hz) and by the new ^{1}H-NMR resonances for the coumarin protons. The methyl and the proton of the enone moiety resonate respectively at 2.34 (d, J=0.9 Hz) and 6.06 (bd, J=0.9 Hz) and the two detectable aromatic coumarin protons at 6.69 (dd, J= 8.7 and 2.4 Hz) and 6.57 (d, J=2.4 Hz), respectively. After prolonged irradiation (16 hours), two different photocycloaddition products were found in 1.6:1 ratio corresponding to two closed species (Scheme 33)

respectively characterized by the ^{31}P-NMR resonances at 8.68 ppm ($J^{31}_{P-}{}^{195}_{Pt}$=3621 Hz) for the more abundant species (***cis*-1-c**), and 12.32 ppm ($J^{31}_{P-}{}^{195}_{Pt}$=2577 Hz) for the less abundant species (***trans*-1-c**). All the coumarin aromatic protons were shifted upfield and were detected at 7.14 ppm (d, J= 8.4 Hz), 6.71 ppm (dd, J= 8.40 and 2.40 Hz), 6.14 (d, J=2.4 Hz) for ***cis*-1-c** and at 7.06 ppm (d, J=8.70 Hz), 6.40 (dd, J=8.70 and 2.70 Hz), 6.17 (d, J=2.7 Hz) for ***trans*-1-c**. As to the proton and the methyl group linked to the cyclobutane ring, their resonances were respectively detected at 1.67 (s) and 3.45 (s) ppm for both products; while the former value is typical of *syn* coumarin adducts the latter is typical for *anti*-dimers. Because of this, we were not able to unequivocally assign a precise configuration, but from the P-Pt coupling constants and from the analysis of the sample at different times we understood that irradiation of the complexes induces first a *cis→trans* photoisomerization of the starting material which is followed by dimerization process. After dimer formation another *trans→cis* photoisomerization process occurs yielding the *cis*-closed Pt(II) complex. Scheme 33 reports the above mentioned isomerization-dimerization process above mentioned.

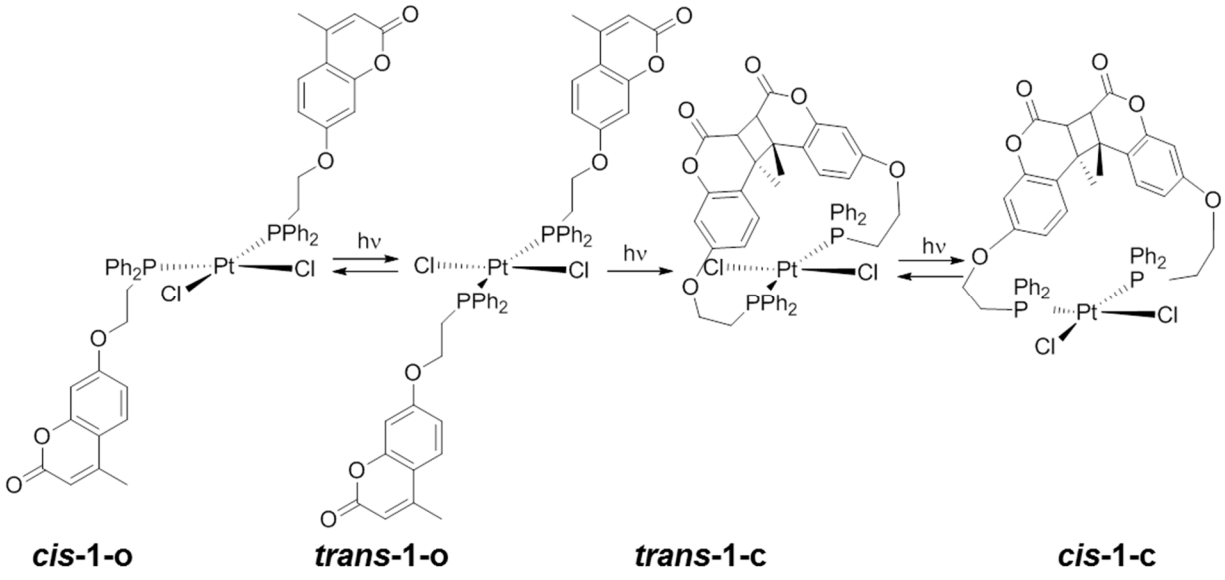

Scheme 33. Proposed photochemical behaviour of ***cis*-1-o** upon UV light irradiation.

Dimerization studies carried out in other chlorinated solvents such as chloroform and 1,2-dichloroethane revealed the same trend. The use of more coordinating and more polar solvents, such as dimethyl sulfoxide, allowed obtaining a dimerization mixture which is characterized by the presence in lower amounts of the above described products in lower amounts and by a new complex due to cycloaddition between the phosphines in a *cis* geometry. The latter is characterized by ^{31}P-NMR resonance at 6.48 ppm ($J^{31}_{P-}{}^{195}_{Pt}$=3613 Hz) and by ^{1}H-NMR resonances of the aromatic coumarin protons at 7.08 ppm (d, J=8.70 Hz), 6.82 ppm (dd, J=8.40 and 2.40 Hz), 6,17 ppm (d, J=2.40 Hz). The resonances of proton and methyl linked to the cyclobutane ring of this stereoisomer were detected at 3.66 and 1.65 ppm. The high chemical shift observed for such H atoms suggested a *syn* geometry for the photo-irradiated complex, which is also the expected one for the dimerization of single coumarin molecules in such a solvent.

Photochemical behaviour of the Pt(II) bis-triflate complex

The *bis*-triflate Pt(II) complex ***cis*-2-o** showed good solubility in chlorinated solvents such as chloroform, dichloromethane and 1,2-dichloroethane. Photoirradiation in such solvents was studied by ^{1}H-NMR and ^{31}P-NMR spectroscopy and by UV-Vis spectroscopy. Irradiation of the starting complex in chloroform with a Wood lamp (365 nm) revealed decreasing of the absorption band at ~320 nm as a consequence of the dimerization reaction (Figure 26). The PSS state was reached after 60 minutes and was followed by irradiation at 254 nm seeking for dimer cleavage. The spectrum registered after 30' of irradiation at 254 nm (low pressure mercury lamp 12 W) revealed also in this case different values for the relative maxima which were now detected respectively at 275 and 266 nm.

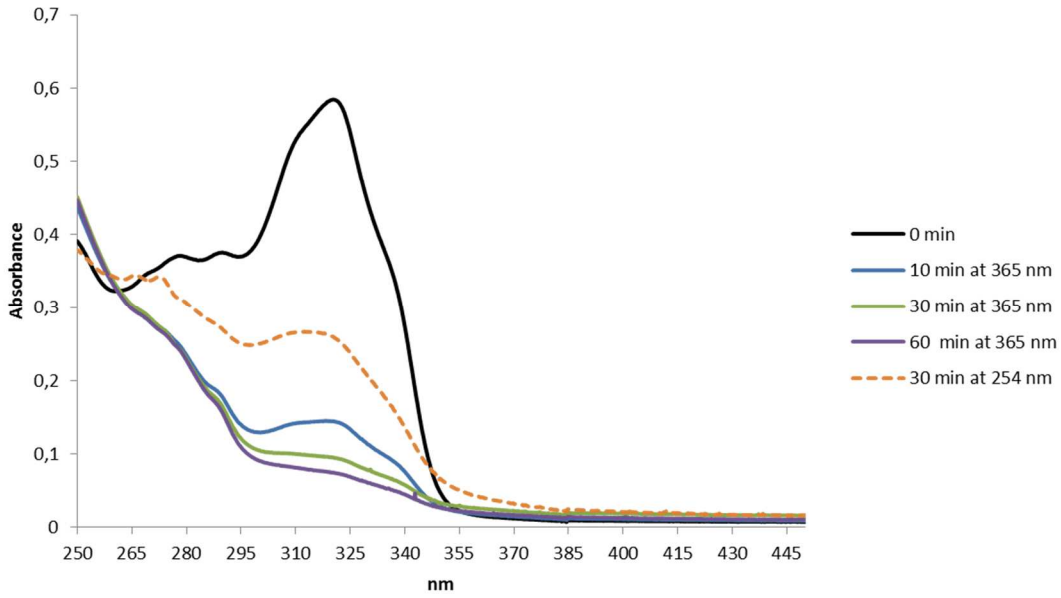

Figure 26. UV-Vis spectra of ***cis*-2-o** in chloroform 1.6 $\cdot 10^{-5}$ M solutions after different irradiation times at different wavelength.

^{1}H-NMR and ^{31}P-NMR analysis revealed that long irradiation times were required to achieve good yield in dimer formation. Indeed, only 20% conversion of the starting material was observed after 2 hours of irradiation. The dimerization product was characterized by *cis* geometry (***cis*-2-c**), confirmed by the ^{31}P-NMR resonance and coupling constant at -0.268 ($J^{31}_{P-}{}^{195}_{Pt}$=3959 Hz), while the ^{1}H-NMR spectra reported the aromatic coumarin protons at 7.18 ppm (d, J=8.4 Hz), 6.83 ppm (dd, J=8.4 and 2.4 Hz), 6.16 (d, J=2.4 Hz) and the proton and the methyl group bound to the cyclobutane moiety respectively at 1.67 and 3.46 ppm respectively. From the latter values and from the stereoisomer expected from dimerization in chlorinated solvents it was established that the ligands were cross-linked in an *anti* fashion. Curiously with respect to what observed for ***cis*-2-o**, the ^{1}H-NMR resonances of the ***cis*-2-c** are well resolved. Figure 27 reports the ^{1}H-NMR spectra of the non-irradiated (Figure 27B) and irradiated (Figure 27A) ***cis*-2-o** complex. Longer irradiation times caused degradation of the complex; indeed after one day of irradiation, the solution became yellowish and a grey precipitate was observed.

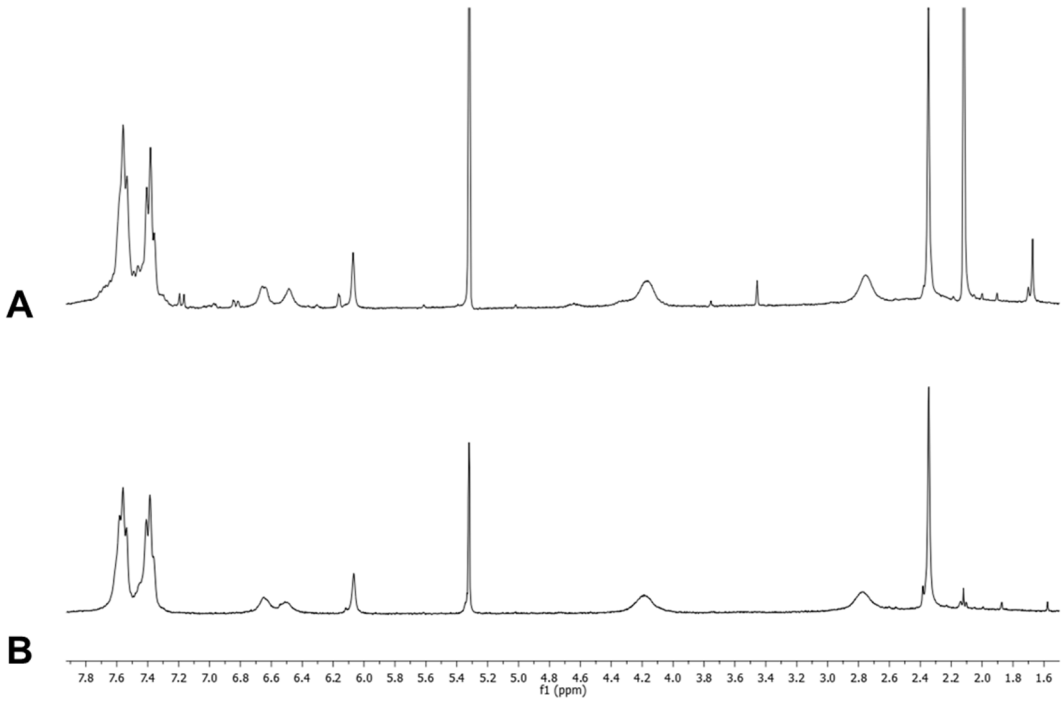

Figure 27. A) *cis*-2-o after 1 hour irradiation at 365 nm in dichloromethane-d; **B) *cis-2-o*** before irradiation in dichloromethane-d.

We studied the irradiation process also in other more polar solvents, such as dimethyl sulfoxide. Also in this case the dimerization yielded a *cis* adduct characterized by ^{31}P-NMR resonances at -2.73 ppm ($J^{31}_{P-}{}^{195}_{Pt}$.=3936 Hz) and by the resonances of the coumarin aromatic protons at 7.11 ppm (d, J=8.4 Hz), 6.90 ppm (dd, J=8.4 and 2.4 Hz), 6.31 ppm (d, J=2.4 Hz). The resonances of the methyl and proton linked to the bridging cyclobutane ring were found at 1.66 and 3.88 ppm, respectively, clearly indicating the formation of a *syn* dimer. Also in this solvent, long irradiation times are required (quantitative conversions was achieved in 10 hours)[f] and an appreciable degradation of the complex was observed. As demonstrated by the photodimerization tests in dimethyl sulfoxide, irradiation in highly polar solvents yields selective and quantitative dimerization in *syn* fashion in shorter times.

Analogously, the irradiation of the complex was performed in methanol analyzing the products by UV-Vis and by ^{1}H-NMR and ^{31}P-NMR. Irradiation with a UV light source at 365 nm caused a decrease of the band at ~320 nm and reaching of the PSS after just 10 minutes (Figure 28). Photo-cleavage of the dimers, performed by irradiation for 30 minutes at 254 nm yielded an increased absorption at 320 nm confirming the reversibility of the [2+2] photocycloaddition. Analysis of the latter spectrum revealed growth of the concentration of the sample, increased absorption at longer wavelength and disappearance of one of the two relative maxima. The maximum at 276 nm was preserved while the one at 287 nm disappeared.

f With a Wood lamp, omnilux 25 W, irradiance at 365 nm 10 W/m^2

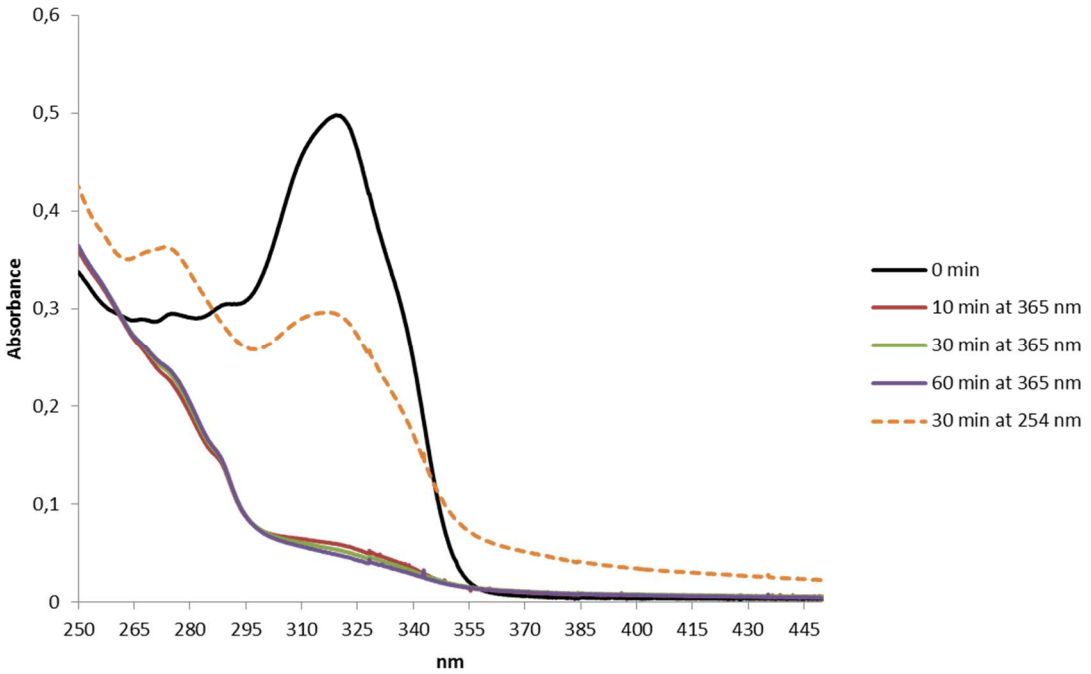

Figure 28. UV-Vis spectra of ***cis*-2-o** in methanol 1.6 $\cdot 10^{-5}$ M solutions after different irradiation times at different wavelength.

The ^{1}H-NMR spectrum of the starting material was characterized by sharp signals like two detectable coumarin aromatic protons at 6.60 ppm (dd, J=8.7 and 2.4 Hz), 6.55 ppm (d, J=2.4 Hz) while the proton and the methyl group of the enone moiety was found at 6.10 ppm (bq, J=1.2 Hz) and 2.36 ppm (d, J=1.2 Hz), respectively. Also the signals of the ethyl spacer were well-resolved and appeared as two multiplets at 4.40 and 3.20 ppm, respectively. The ^{31}P-NMR spectrum showed resonance at 23.16 ppm ($J^{31}_{P-}{}^{195}_{Pt}$.=2928Hz) which is reasonable for a *trans* square planar Pt(II) *bis*-phosphino *bis*-triflate complex (***trans*-2-o**). The isomerization of such complex could be considered as a substitution reaction where two mechanisms may occur: the associative mechanism and the dissociative/solvolysis mechanism. The former is more frequent with d^8 ML_4 complexes and normally is characterized by negative entropy of activation and by retention of configuration; the substitution rate is influenced by: *i)* the nature of the leaving group; *ii)* the incoming ligand; *iii)* the metal center; *iv)* the *cis* and *trans* ligands to the leaving group (*trans* effect).[g,126]

The dissociative mechanism is more common with coordinatively saturated 18 electron complexes since they can more readily form a 16 electron complex rather than a 20 electron complex. The main factors influencing the substitution rate are: *i)* transition series; *ii)* electronic configuration; *iii)* steric encumbrance of the ligand.[h] Since we did not observe retention of configuration and since phosphines are not good leaving groups, we discarded the associative mechanism. We suggest that when the ***cis*-2-o** is solubilized in methanol,

g Incoming ligand series: PR_3>pyridine>NH_3, Cl^->H_2O>OH^-; leaving group series: NO_3^->H_2O>Cl^->Br^->I^->N_3^->CN^-; metal center series: M^{2+}=Ni>Pd>>Pt; *trans* effect for a given ligand consists in its influence on the rate of exchange of the ligand in *trans* position to it. An experimental series for the *trans* effect is: F^-<H_2O<OH^-<NH_3<amines<piridines< Cl^-<Br^-<SCN^-<I^-<NO_2^-<$C_6H_5^-$<CH_3^-<phosphines<arsines<H-<olefins<CN-<CO<NO.

h Transition series: 2nd row> 3rd row> 1st row; electronic configuration series: d^8>d^{10}>>d^6; the larger the Tolman cone angle, the larger the dissociation constant.

replacement of the weakly coordinated triflate ions by a solvent molecule occurs leading to a solvento species (dissociation/ solvolysis step). After that, *cis→trans* isomerization takes place leading to the Pt(II) complex ***trans*-2-o** with the sterically hindered coumarin-based ligands in *trans* geometry. The dissociation or solvolysis step is supported by the high *trans* effect of the phosphine and by the low coordinating ability of the triflate ion (good leaving group). Scheme 34 shows the proposed mechanism for the isomerization process. A similar isomerization process has been described for other Pt(II) complexes, such as $[PtX(C_6H_5)(PEt_3)_2]$ (X=Br, Cl).[127]

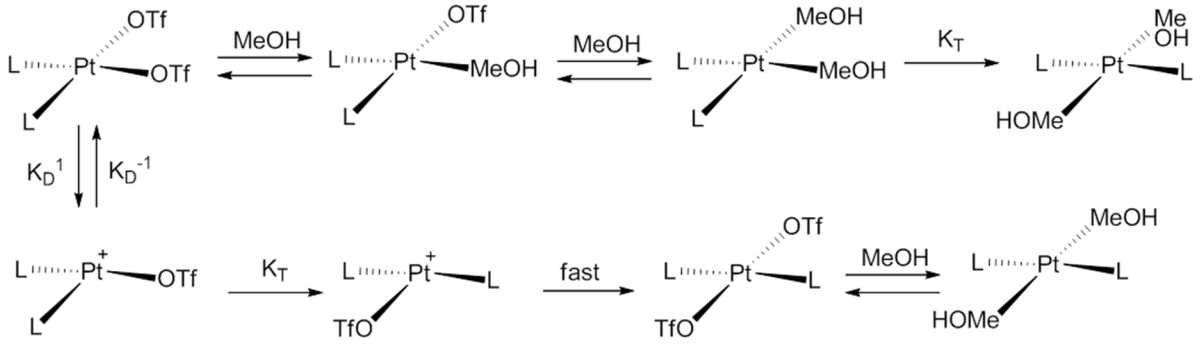

Scheme 34. Proposed *cis→trans* isomerization mechanism for the ***cis*-2-o**.

Quantitative dimerization products were observed after 1.5 h of irradiation or less, depending on the concentration and the irradiation equipment used. Two products (***trans*-2-c_s**) were detected in a ~5:1 ratio. The more abundant species showed a ^{31}P-NMR resonances at 26.18 ppm ($J^{31}_{P-}{}^{195}_{Pt}$=2925 Hz) which confirms a retained *trans* geometry while the ^{1}H-NMR showed the coumarin aromatic protons at 6.93 ppm (d, J=8.7 Hz), 6.08 ppm (dd, J=8.7 and 2.4 Hz), 5.92 ppm (d, J=2.4 Hz) and the proton and the methyl group bound to the cyclobutane moiety at 1.60 and 3.52 ppm, respectively. The less abundant species showed ^{31}P-NMR resonance at 23.94 ppm (the coupling could not be detected due to low resolution) and its distinctive ^{1}H-NMR signals were found at 6.76 ppm (d, J=8.7 Hz), 6.31 ppm (dd, J=8.7 and 2.4 Hz) for the two detectable aromatic coumarin protons, 3.80 and 1.63 ppm respectively for the proton and the methyl group bound to the cyclobutane ring. Due to the known photochemical behaviour of 4-methyl coumarin in methanol and to the observed chemical shift of the diagnostic cyclobutane proton resonances, we argued that the coumarin moieties dimerized in a *syn* fashion. Figure 29 reports the superimposed spectra of both the non-irradiated (Figure 29B) and irradiated (Figure 29A) complexes in methanol.

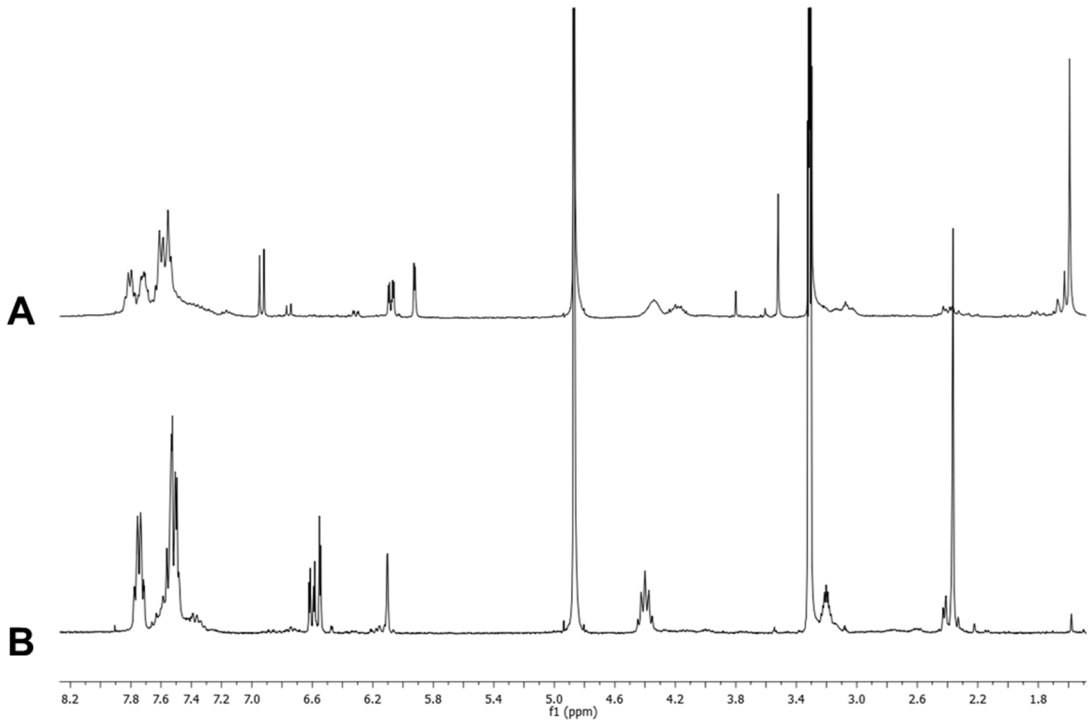

Figure 29. A) ***trans*****-2-o** after 1.5 hour irradiation at 365 nm in methanol-d; **B)** ***trans-2-o*** before irradiation in methanol-d.

Cleavage of the coumarin dimers at 254 nm in methanol did not quantitatively yield back the starting *trans* complex.[i] The mixture appeared yellowish and a grey precipitate was found, suggesting that complex degradation occurs in such a solvent upon irradiation with low wavelength light.

General considerations on the photodimerization process

From the above mentioned studies it was clear that effective dimerization of the coumarin ligand could be achieved in polar and nucleophilic solvents such as methanol. High polarity is probably involved in positive solvation/stabilization of the excimers formed during excitation ($S^0 \rightarrow S^1$), while, the nucleophilic character of the solvent plays a fundamental role in promoting *cis* to *trans* isomerization of ***cis*****-2-o** that can undergo faster dimerization more easily.

The shape of the NMR signals of the open and closed complexes deserves a separate discussion. The signals of both the *cis* and *trans* complexes in their open forms appeared broad in non-coordinating solvents such as chloroform and dichloromethane. When the spectra are recorded in the more polar dimethyl sulfoxide the signals appear much more resolved but still partially broad. The spectra collected in the polar and nucleophilic methanol revealed perfectly sharp signals, such as those recorded for the Pt(II) dichloro complex. In contrast, the NMR signals of the closed isomers were all sharp in all the solvents tested. Figure 30 reports the ^{1}H-NMR spectra for the both the open and closed *trans* complexes in different solvents.

[i] Methanol cut off wavelength is around 240 nm.

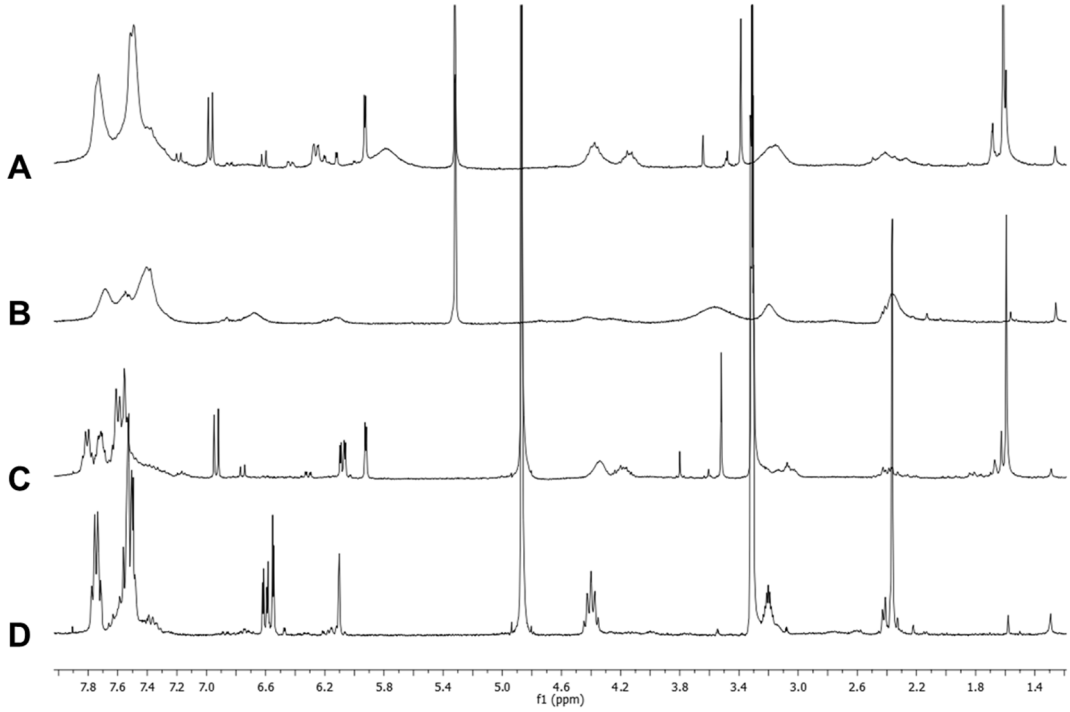

Figure 30. A) ***trans*****-2-c$_S$** in dichloromethane-d; **B)** ***trans*****-2-o** in dichloromethane-d; **C)** ***trans*****-2-c$_S$** in methanol-d; **D)** ***trans*****-2-o** in methanol-d.

We suggest that the oxygen atoms present in the coumarin moiety and in the ethyl spacer, may act as weakly coordinating units allowing the monophosphine ligand **3** to act as a P-O chelating species. Due to the weakness of such interaction, the *bis*-monodentate and the chelate species exchange with each other at a rate that is comparable with the NMR time scale and, because of this, the spectra show broad averaged signals (Figure 30B). In Scheme 35 the equilibria involved in the reversible bidentate/monodentate exchange involving the coumarin monophosphine ligands are depicted. In the presence of more coordinating solvents, the latter compete for the available coordination site on the metal and this shifts the equilibria described in Scheme 35 to the right.

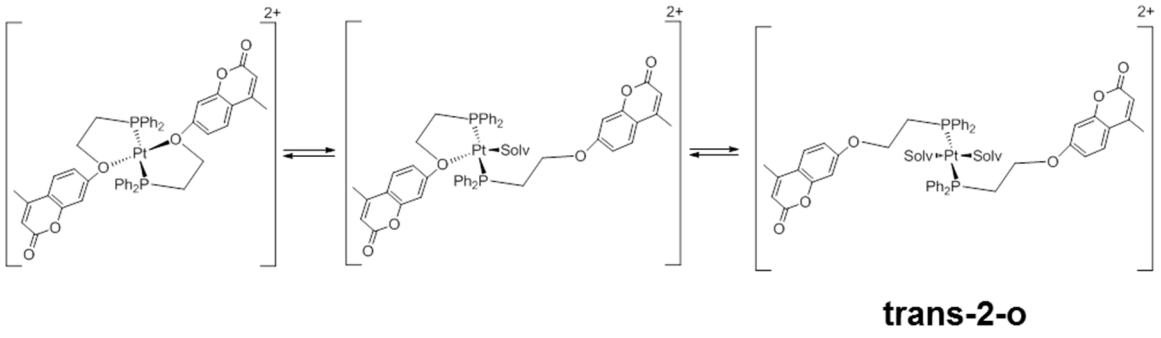

Scheme 35. Possible exchange processing operating in non coordinating solvents and involving different Pt(II) species comprising different ligand topicity from bis P-O bidentate up to bis P monodentate fashion.

The sharp signals observed in the closed complexes (Figure 30A) are probably due to the more rigid structure of the closed isomers for which self-coordination is prevented by steric and geometric requirements.

All the above observations suggest some considerations on the potential catalytic applications of these Pt(II) complexes. It is likely that the coordination sites available for catalysis on the closed *trans* complexes are more accessible than the corresponding ones on the open *trans* complex. Because of this a higher catalytic activity of the closed complex is expected. Competition for the coordination site on the metal center is expected to favour coordination of a substrate with better coordination ability with respect to the oxygens present on the ligand. Pt(II) complexes are soft Lewis acids and better coordination is observed with soft Lewis bases such as alkenes while oxygenated ligands are weaker ligands. As a consequence, it is expected that the coumarin based Pt(II) complexes would be more sensitive to alkene substrates able to coordinate to the metal center rather than to oxygenated substrates whose coordination to Pt(II) is in competition with self-coordination by the coumarin based phosphine ligand.

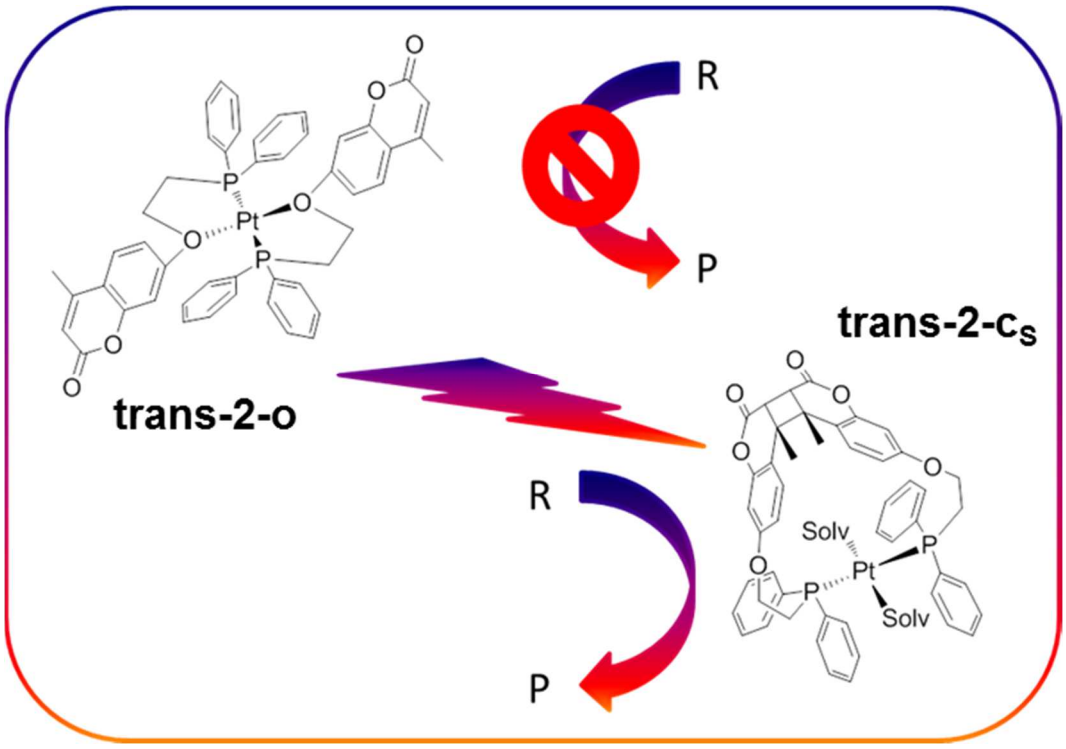

Figure 31. Photoswitching of the Pt(II) complex from non dimerized chelating ligands to a dimerized-ligands complex where chelation of the oxygen moieties is inhibited by the more rigid structure.

To prove this consideration we tested the open and the closed form of the *trans* complex in three different catalytic reactions, two with alkene substrates like the isomerization reaction of allylbenzene to give internal alkenes and the dimerization of α-methyl styrene and one with a carbonyl compound like the Diels Alder reaction between 1, 3-cyclohexadiene and acrolein.

Catalytic tests with Pt(II) complexes

Allylbenzene isomerization

Recently Strukul and co-workers reported an efficient isomerization method for the conversion of terminal alkenes into internal alkenes mediated by *mono*-cationic and *bis*-cationic Pt(II) species.[128] The reaction turned out to be sensitive to the steric hindrance and bite angle provided by the *cis*-bidentated phosphine ligand employed and this suggested that the same reaction could evidence different catalytic features for the open and closed *trans* Pt(II) complex.

The isomerization tests were carried out on allylbenzene as a model substrate at 30°C, employing chloroform as solvent and a catalyst loading of 1% mol with respect to the substrate following the progress of the reaction by GC. The isomerization yields a mixture of *Z* and *E-trans*-3-phenyl-2-propene where the more stable *trans* isomer is predominant (Scheme 36).

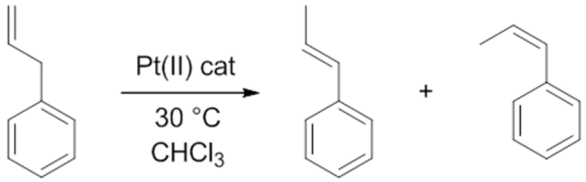

Scheme 36. Catalytic isomerization of allylbenzene mediated by Pt(II) species.

In order to obtain reproducible procedures and reliable data the open and closed complexes were prepared as follows: ***cis*-2-o** was charged in a Schlenk tube and isomerized to ***trans*-2-o** simply by solubilisation in methanol. Then, two equal amounts of solution were loaded in separate vials via a microsyringe. One vial was irradiated for 60 minutes with a Wood lamp to prepare the *trans* closed species and subsequently both vials were dried under vacuum. Finally an allylbenzene chloroform solution was added in equal amount to each thermostatted vial following the progress of the reaction by direct sampling the reaction mixture at given times. The catalytic performances of ***trans*-2-o** and ***trans*-2-c_S** were compared to the ***cis-2-o*** and to other *bis*-triflate complexes such as $[Pt(dppe)](OTf)_2$, $[Pt(dppb)](OTf)_2$ and $[Pt(PPh_3)_2](OTf)_2$. The obtained results are reported in Table 2 and the kinetic profiles for the isomerization reaction with open and closed complex are reported in Figure 32.

Table 2. Catalytic isomerization of allylbenzene mediated by Pt(II) species.

Complex	Internal alkenes (%)[a]
$[Pt(dppe)](OTf)_2$	0
$[Pt(dppb)](OTf)_2$	9
$[Pt(PPh_3)_2](OTf)_2$	22
***trans*-2-o**	66
***trans*-2-c_S**	80
cis-2-o	15

Experimental conditions: [allylbenzene]=0.157 M, **[Pt(II)catalyst]**=1.57 mM ; T= 30 °C; solvent chloroform (0.6 mL); conversion determined by GC analysis. a) 24 h.

First of all it was observed that *trans* complexes showed higher activity with respect those with *cis* geometry. Time course of the isomerization reaction showed that ***trans*-2-o** and ***trans*-2c$_s$** are characterized by similar activity up to 480 min, while the closed complex remained active for longer times even at higher substrate conversions. This divergence is likely due to the fact that at higher conversion the remaining terminal alkene competes with the oxygen in the coumarin moiety in binding the metal center and the latter process is more likely to occur with the open complex than the closed one (Figure 31).

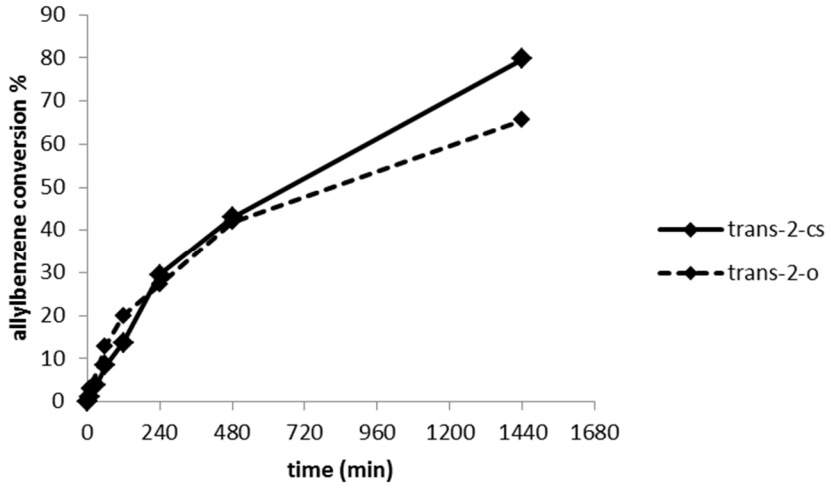

Figure 32. Kinetic profiles for catalytic isomerization of allylbenzene mediated by ***trans*-2-o** and ***trans*-2-c. Experimental conditions: [allylbenzene]=**0.157 M, **[Pt(II)catalyst]=**1.57 mM ; T= 30 °C; solvent chloroform (0.6 mL); conversion determined by GC analysis.

α-methyl styrene isomerization

Subsequently the new photomodulable Pt(II) catalysts were tested in a catalytic C-C bond forming reaction involving alkenes. In order to avoid double bond migration, α-methylstirene was selected as model substrate as it provides (Scheme 37) a dimer derived by nucleophilic attack of a free α-methyl styrene molecule on a coordinated (activated) α-methyl styrene molecule yielding 1,1'-(4-methylpent-1-ene-2,4-diyl)dibenzene. The latter presents a terminal C=C double bond that can be isomerized to the internal alkene 1,1'-[(2E)-4-methylpent-2-ene-2,4-diyl]dibenzene.

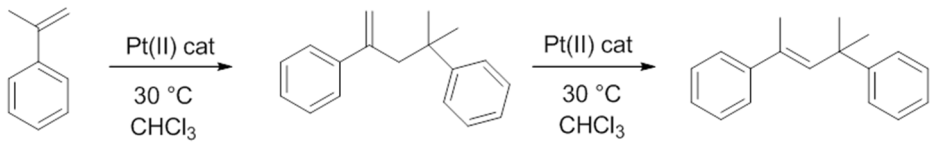

Scheme 37. Pt(II) catalysed dimerization of α-methylstyrene and subsequent internal alkene isomerization.

The samples of open and closed *trans* Pt(II) catalysts were prepared as described above for the isomerization reaction and, also in this case, the catalytic performances of the open and the closed *trans* complexes were compared to other known Pt(II) catalysts as reported in Table 3. The *cis*-complexes showed to be completely inactive under the experimental

conditions employed. This could be somehow expected because of the strong *trans* effect of phosphines that would enhance the exchange rate for olefin/oxygen coordination in *cis* complexes. The same argument favors *trans* complexes where the potential olefin binding sites are *cis* to P donors and even more so closed complexes where binding by the oxygen donors present on the ligand is far less likely (Figure 31).

Table 3. Pt(II) catalysed dimerization of α-methylstyrene.

Complex	**dimers (%)[a]**
$[Pt(dppe)](OTf)_2$	0
$[Pt(dppb)](OTf)_2$	0
$[Pt(PPh_3)_2](OTf)_2$	0
***trans*-2-o**	50
***trans*-2-c_S**	56
***cis*-2-o**	3

Experimental conditions: [α-methylstyrene] =0.157 M, **[Pt(II) catalyst]**=1.57 mM; T=30°C; solvent chloroform (0.6 mL); conversions determined by GC analysis. a) 24h.

This view is confirmed by the kinetic profile of the reactions, reported in Figure 33 and in Figure 34 for the open and closed complexes, respectively, where it is evident that in both systems the isomerization rate is higher than the dimerization rate which is therefore the rate determining step. Also in this case the open complex seems to suffer more than the closed one from the competition on the catalytic sites among substrate, products and ligand side chains. This consideration is particularly evident if the different amounts of dimerization product for both open and closed complexes are examined after 4 and 24 hours. While ***trans*-2-o** shows 8% and 16% dimer after 4 and 24 hours respectively, in the case of ***trans*-2-c_S** dimer formation changes very little over the same time (12 % and 15% respectively). This observation supports the evidence that the closed isomer is more active than the open one in the consecutive isomerization reaction, as confirmed by the higher overall conversions reached in agreement with what previously observed in the allylbenzene isomerization tests.

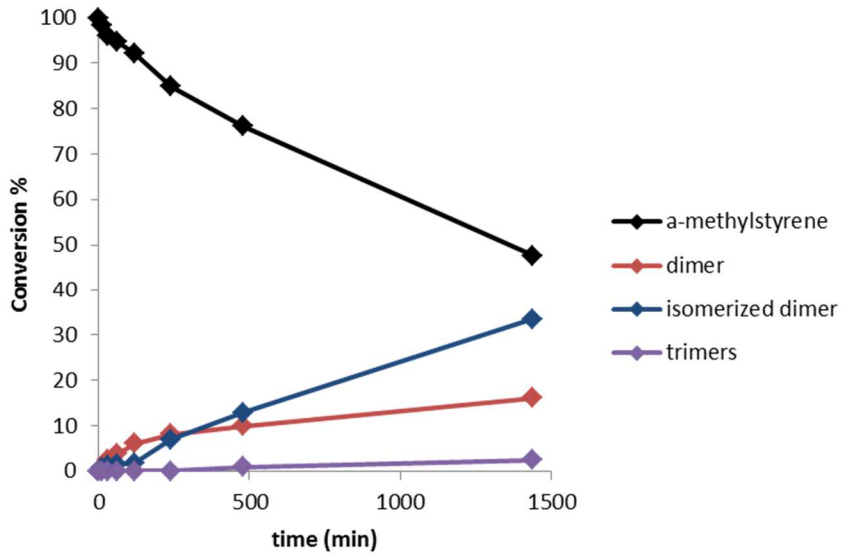

Figure 33. Kinetic profile for α-methylstyrene dimerization mediated by Pt(II) catalyst. **Experimental conditions: [α-methylstyrene]** =0.157 M, **[*trans*-2-o]**=1.57 mM; T=30°C; solvent chloroform (0.6 mL); conversions determined by GC analysis.

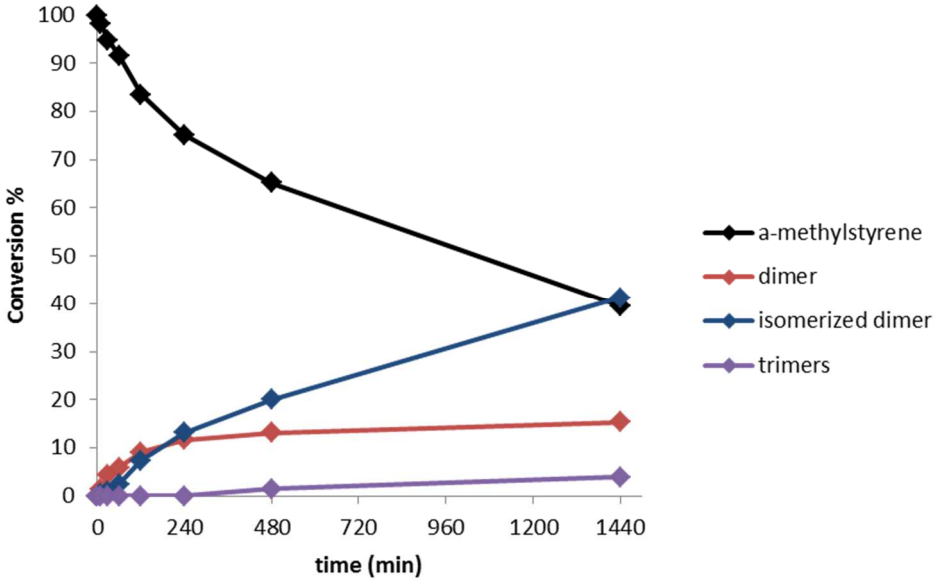

Figure 34. Kinetic profile for α-methylstyrene dimerization mediated by Pt(II) catalyst. **Experimental conditions: [α-methylstyrene]** =0.157 M, **[*trans*-2-c_S]**=1.57 mM; T=30°C; solvent chloroform (0.6 mL); conversions determined by GC analysis.

Both the isomerization and dimerization tests confirmed the enhanced affinity of the closed Pt(II) isomer for alkenes as initially argued. The difference of activity between open and closed catalysts is expected to widen when employing more weakly coordinating substrates and, in general, hard Lewis bases rather than soft Lewis bases.

Diels-Alder reaction

In the Diels-Alder reactions it is known that lowering the energy difference between the HOMO (LUMO) of the diene and LUMO (HOMO) of the dienophile enhances the reaction rate. Electron donating substituents on the diene increase the activity while electron withdrawing ones reduce its reactivity. The contrary applies to dienophiles which are activated by the presence of electron withdrawing groups, such as CO and CN.[72] When the electron withdrawing group in the dienophile is CO or CN, as in unsaturated aldehydes or in acrylonitriles, Lewis acid activation is particularly effective because the heteroatom coordinates the Lewis acid metal catalyst contributing to lowering the energy of the LUMO orbital.

Pt(II) bisphosphine complexes bearing triflate counter-ions are well known soft Lewis acids[129] and have been used in the past as useful homogeneous catalysts for the Diels Alder reaction between *α,β*-unsaturated aldehydes and various dienes.[130] Since acrolein is the simplest *α,β*-unsaturated aldehyde and since its activating carbonyl group could effectively compete with the coordination sites with the oxygenated moieties of the coumarin-ligand, we decided to use such reagent in combination with 1,3-cyclohexadiene to test the different catalytic performance between the *trans-open* ant *trans-closed* complexes (Scheme 38).

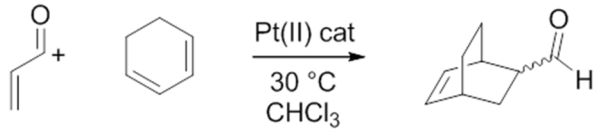

Scheme 38. Diels-Alder reaction between acrolein and 1,3-cyclohexadiene mediated by photomodulable Pt(II) catalysts.

***trans*-2-o** and ***trans*-2-c$_S$** were prepared in the same manner used for the isomerization and dimerization tests and the reaction progress was monitored for 4 hours by GC analysis. As in the previous studies on isomerization the catalytic performance of our catalysts was compared with other Pt(II) complexes. Such results are reported in Table 4.

Table 4. Conversion values obtained from Diels-Alder reaction between acrolein and 1,3-cyclohexadiene mediated by Pt(II) catalysts.

Complex	Conversion (%)[a]
[Pt(dppe)](OTf)$_2$	2
[Pt(dppb)](OTf)$_2$	71
[Pt(PPh$_3$)$_2$](OTf)$_2$	65
***trans*-2-o**	67
***trans*-2-c$_S$**	76
cis-2-o	54

Experimental conditions: [acrolein] =0.157 M, **[1,3-cyclohexadiene]** =0.157 M, **[Pt(II)catalyst]**=1.57 mM; T=30°C; solvent chloroform (0.6 mL); conversions determined by GC analysis. a) 4h.

With the exception of [Pt(dppe)](OTf)$_2$, all the Pt(II) complexes showed high conversions and as observed for the isomerization and dimerization of alkenes the closed complex showed higher activity compared to the open one. Looking at the kinetic profiles reported in Figure 35, at low conversions the differences in catalytic performance between the open and the closed complex are even higher. Indeed, after ten minutes the activity difference between the two systems is about 5-fold and slightly decreases during the progress of the reaction.

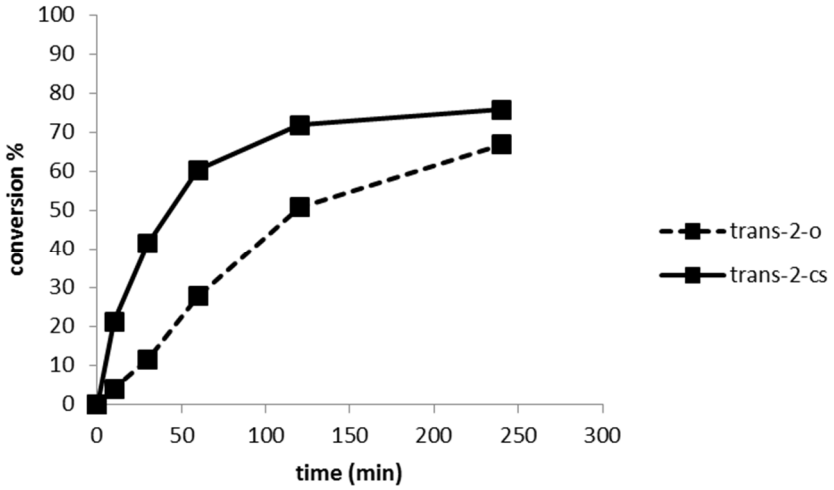

Figure 35. Kinetic profile for Diels Alder reaction between 1,3-cyclohexadiene and acrolein mediated by Pt(II) species. **Experimental conditions: [acrolein**] =0.157 M, **[1,3-cyclohexadiene]** =0.157 M, **[Pt(II)catalyst]** =1.57 mM; T=30°C; conversions determined by GC analysis**.**

These experimental observations confirm our hypothesis concerning the different level of competition provided by the ligand **3** to the Pt(II) coordination sites. The rigid ***trans*-2-c$_S$**

isomers do not suffer from the intramolecular competition by the coumarin based ligands, while the more flexible ***trans*-2-o** isomer does. Another confirmation about the "self-quenching" or "self competitive inhibition" given by the coumarin ligand on the Pt(II) active sites comes from the data obtained from ***cis*-2-o** isomer, which shows the lowest activity with respect to all the other active Pt(II) complexes. Confirmation of this came from ^{1}H-NMR and ^{31}P-NMR spectra of such Pt(II) complex in non-coordinating solvents as reported in Figure 22. In apolar non competitive solvents, broad spectra for the open species mean catalytically more inert complex due to self-inhibition, while sharp spectra for the closed species means more accessible metal catalyst.

Since we have not yet found the best conditions to obtain *cis*-closed dimers (***cis*-2-c**) in high yield with negligible complex degradation, we could not establish if the *cis*-closed complex is more or less sensitive to self-quenching–due to the coordination of the oxygens of the coumarin moieties.

Conclusions

Coumarin moiety was effectively incorporated into a phosphine ligand with a three steps synthetic approach. Synthesis of the corresponding Pt(II) bisphosphino complexes allowed to understand the intramolecular photochemical behaviour of such ligands, showing in particular the strong dependence of the photocycloaddition behaviour from the solvent used to perform the process. The newly developed coumarin based phosphine ligand demonstrated fast photodimerization properties in methanol allowing effective switching from a monophosphinic to a bidentate bis-phosphinic ligand. Moreover it was found that the coumarin oxygenated moiety or that of the spacer may act as weak intramolecular chelating donor that can compete with incoming substrates for the catalytic sites of the Pt(II) *bis*-triflate complex. Such competition was found to be stronger for the non-dimerized open system that for the same reason led to broad NMR spectra, while enhanced catalytic activity and more resolved NMR spectra were found for the closed species. Indeed it was found that the closed complex was able to achieve better conversion compared to the open isomer in the dimerization and isomerization of alkenes. Such difference in activity increased when a less coordinating substrate like an *α,β*-unsaturated aldehyde was employed for Diels Alder reaction because of its similar chemical nature with respect to the coumarin moiety that partially self-quenches the open catalyst.

As an outlook on this project it is advisable that the preparation of similar ligands, where the ethyl spacer bears a tio-ether function instead a normal ether, would yield metal complexes where the equilibrium is shifted toward the chelated species and by virtue of this the differences in catalytic activity between the open (chelated complex) and the closed (non-chelated complex) might be increased.

G. Bianchini, A. Scarso, G. Strukul *A Coumarin Based Photo-Modulable Allosteric Metal Catalyst*, manuscript in preparation.

Experimental

^{1}H-NMR, ^{13}C{^{1}H}-NMR and ^{31}P{^{1}H}-NMR were recorded at 298 K with a BRUKER AVANCE spectrometer operating respectively at 300.15, 75 and 121.5 MHz and with a BRUKER AC200 operating at 200, 50 and 80.7 MHz, respectively.

GC analysis were performed on HP SERIES II 5890 equipped with a HP5 column (30 m, I. D. 0.25 m, film 0.25 μm) using He as gas carrier and FID. GC-MS analyses were performed on a GC Trace GC 2000 equipped with a HP5-MS column (30 m, I.D. 0.25 mm, film 0.25 μm) using He gas carrier and coupled with a quadrupole MS Thermo Finnigan Trace MS with *Full Scan* method. Identification of the products was accomplished by reference samples or by comparison with samples obtained as described in literature.

TLC analysis were performed on TLC Polygram ® Sil G/UV254 of 0.25 mm thickness and flash-chromatography separations were performed on silica gel Merk 60, 230-400 mesh as reported by W. C. Still, M. Khan, A. Mitra *J. Org. Chem.* **1978**, *43*, 2923.

Solvents and reactants were used as purchased; otherwise they were purified as reported in D. D. Perrin, W. L. F. Armarego *Purification of Laboratory Chemicals*, 3rd Ed., **1988**, Pergamon Press Ltd., Oxford OX3 0BW, England.

Irradiation at 365 nm was performed with a Wood lamp, omnilux 25 W, irradiance at 365 nm 10 W/m^2 (10 cm) while irradiation at 254 nm was performed with the low pressure Hg lamp commonly used for the visualization of TLC plates (12 W).

*Synthesis of 7-hydroxy-4-methylcoumarin (**5**)*

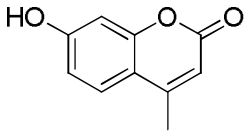

In a two necks round bottom flask, equipped with a calcium chloride cap and a dropping funnel, were loaded resorcinol (1.50 g, 13.6 mmol) and ethyl acetoacetate (2 mL, 2.05 g, 15.8 mmol). The mixture was stirred at room temperature and methansulfonic acid (4.40 mL, 6.53 g, 68 mmol) was added dropwise. The reaction mixture became yellowish with concomitant heat release. Thereafter the system was left under vigorous stirring for 16 hours. The crude reaction mixture was poured into ice and the yellowish precipitate filtered and washed with cold water. After re-crystallization from a water/ethanol (4:6) solution, the product was isolated in the form of colorless crystals (1.65 g, 68%).

^{1}H NMR (300,15 MHz, CD_3COCD_3): δ 7.60 (d, J=8.7 Hz, 1H), 6.85 (dd, J=8.7 and 2.4 Hz, 1H), 6.73 (d, J=2.4 Hz, 1H), 6.07 (bq, J=1.1 Hz, 1H), 2.41 (d, J=1.1 Hz, 3H).
^{13}C NMR (75 MHz, CD_3COCD_3): δ 160.95, 160.08, 155.47, 152.87, 126.36, 112.76, 110.92, 102.42.
GC-MS (m/z): 176 (M^+), 148 (M^+-CO).

*Synthesis of 7-(2-bromoetoxy)-4-methylcoumarin (**4**)*

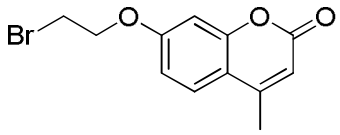

In a round bottom flask equipped with a condenser were charged 7-hydroxy-4-methylcoumarin (0.500 g, 2.8 mmol), potassium carbonate (1.100 g, 7.9 mmol) and 1,2-dibromoethane (4.5 mL, 9.81 g, 52 mmol) and the obtained mixture was heated at 130°C for 2 hours. Afterward the crude reaction mixture was slowly cooled to room temperature, filtered and the solid residue washed with dichloromethane (3x20 mL). The organic phases were then dried with $MgSO_4$ and concentrated under reduced pressure giving a brown oil. The product was isolated as a white solid (0.46 g, 58%) by means of flash chromatography using n-hexane/ethylacetate (75:25) as eluent.

^{1}H NMR (300,15 MHz, $CDCl_3$): δ 7.60 (d, J=8.8 Hz, 1H), 6.88 (dd, J=8.8 and 1.8 Hz, 1H), 6.80 (d, J=1.8 Hz, 1H), 6.14 (s, 1H), 4.34 (t, J=6.0 Hz, 2H), 3.66 (t, J=6.0 Hz, 2H), 2.39 (s, 3H).
^{13}C NMR (75 MHz, $CDCl_3$): δ 161.07, 161.01, 155.16, 152.41, 125.74, 114.13, 112.51, 112.34, 101.70, 68.17, 28.47, 18.65.
GC-MS (m/z)=282 (M^+), 175 (M^+-CH_2CH_2Br).

*Synthesis of 7-(2-(diphenylphosphino)ethoxy)-4-methylcoumarin (**3**)*

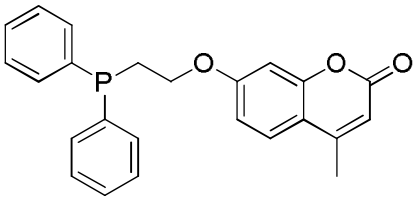

In a flame dried two necks round bottom flask 7-(2-bromoetoxy)-4-methylcoumarin (0.44 g, 1.56 mmol) were charged and three vacuum/nitrogen cycles were performed. Subsequently freshly distilled dry THF (15 mL) was charged via syringe and, under vigorous stirring, potassium diphenylphosphide (3.2 mL, 0.5 M, 1.6 mmol) was added dropwise via syringe. The pale orange solution was left under stirring overnight. The reaction mixture was then concentrated to reduced volume and directly loaded on a column for flash-chromatographic separation using hexane/ethyl acetate (75:25) as eluent. The product was isolated as a white solid (0.406 g, 67%).

^{1}H NMR (300.15 MHz, $CDCl_3$): δ 7.59-7.29 (bs, 11H), 6.74 (dd, J=8.8 and 1.5 Hz, 1H), 6.69 (d, J=2.4 Hz, 1H), 6.12 (bq, J=1.1 Hz, 1H), 4.16 (m, 2H), 2.60 (m, 2H), 2.38 (d, J=1.1 Hz, 3H).
^{31}P NMR (121.5 MHz, $CDCl_3$): δ -23.92.
GC-MS (m/z): 387 (M^+-H), 185 (M+-$C_{12}H_{11}O_3$).

*Synthesis of dichloro Pt(II) complex bearing 7-(2-(diphenylphosphino)ethoxy)-4-methylcoumarin (**cis-1-o**)*

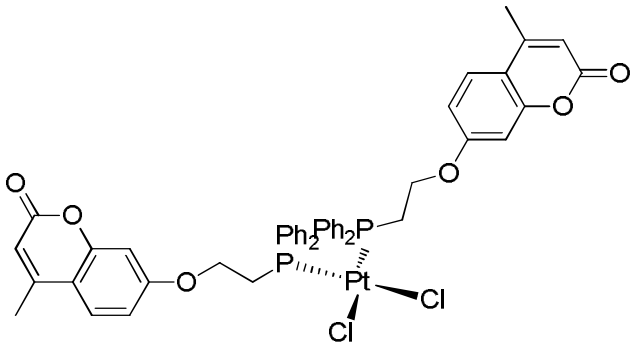

In a round bottom flask were charged 7-(2-(diphenylphosphino)ethoxy)-4-methylcoumarin (0.315 g, 0.81 mmol), chloroform (50 mL) and [Pt(COD)Cl_2] (0.150 g, 0.40 mmol). The solution was left under stirring for 3 hours, afterward the crude reaction mixture was concentrated under reduced pressure and the product was isolated by means of precipitation from a dichloromethane solution with pentane addition. The product was obtained as a white solid in (0.371 g, 89%).

^{1}H NMR (300.15 MHz, $CDCl_3$): δ 7.56 – 7.33 (m, 14H), 7.25 – 7.15 (m, 8H), 6.76 (dd, J=8.8 and 2.3 Hz, 2H), 6.49 (d, J=2.3 Hz, 2H), 6.11 (s, 2H), 4.50 – 4.17 (m, 4H), 2.90 (dt, J=10.5 and 6.8 Hz, 4H), 2.37 (s, 6H).
^{13}C NMR (75 MHz, $CDCl_3$): δ 18.97, 30.32 (d, J_{C-P}=43.9 Hz), 65.23, 102.45, 112.16, 112.63, 14.56, 126.36, 128.90 (d, J=2.3 Hz), 129.14 (dd, J=11.5 and 5.9 Hz), 129.77 (d, J=2.3 Hz), 131.97, 133.48-133.24 (m), 153.12, 155.56, 161.25, 161.32.
^{31}P NMR (121.5 MHz, $CDCl_3$): δ 3.16 (J_{P-Pt} = 3629 Hz).

*Synthesis of bis-triflate Pt(II) complex (**cis-2-o**)*

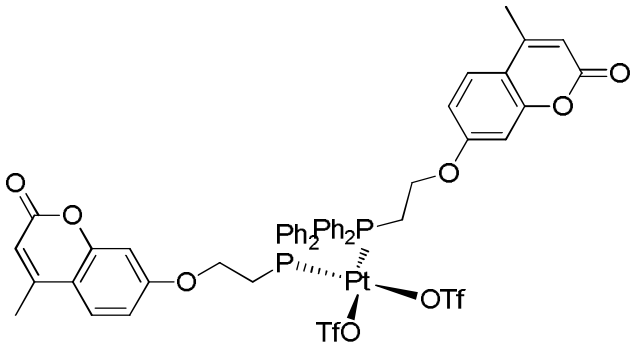

In a round bottom flask were charged ***cis-1-o*** (0.1897 g, 0.18 mmol), dichloromethane (20 mL) and acetone (5 mL). Such solution was vigorously stirred at room temperature and a silver triflate solution in acetone (1.86 mL, 0.0968 M, 0.18 mmol) was added dropwise. After 2 hours, the silver chloride precipitated was removed by filtration and the solvents were removed under vacuum yielding yellowish oil. The oil was solubilized with a (1:1)

dichlormethane:acetone solution and the desired product precipitated by addition of diethyl ether. The bis-triflate complex was obtained as a white solid in 74% yield.

^{1}H NMR (300.15 MHz, CD_2Cl_2): δ 7.70 – 7.25 (bs, 22H), 6.66 (bs, 2H), 6.52 (bs, 2H), 6.08 (bs, 2H), 4.20 (bs, 4H), 2.79 (bs, 4H), 2.36 (bs, 6H).
^{31}P NMR (121.5 MHz, CD_2Cl_2): δ - 3.26 ($J_{P\text{-}Pt}$ = 3997 Hz).

Cis→trans isomerization of bis-triflate Pt(II) complex

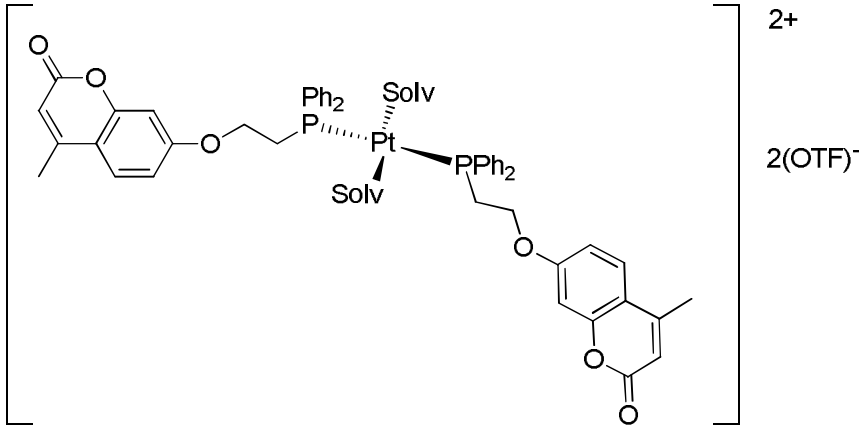

In a Schlenk reactor ***cis-2-o*** (4.0 mg, $3.15 \cdot 10^{-3}$ mmol) was charged followed by 3.15 mL of methanol. The solution was stirred for 30 minutes and subsequently the solvent was removed under reduced pressure yielding the ***trans-2-o*** isomer in quantitative yield.

^{1}H NMR (300.15 MHz, MeOD): δ 7.82-7.740 (bs, 22 H), 6.60 (dd, J=8.7 and 2.4 Hz, 2H), 6.55 (d, J=2.4 Hz, 2H), 6.10 (bq, J=1.2 Hz, 2H), 4.48-4.35 (m, 4H), 3.26-3.17 (m, 4H), 2.36 (d, J=1.2 Hz, 6H).
^{31}P NMR (121.5 MHz, MeOD): δ 23.16 ($J_{P\text{-}Pt}$=2928 Hz).

Typical procedure for irradiation tests

Three vacuum/nitrogen cycles were performed on a Schlenk reactor (pyrex glass) containing ***cis-2-o*** (4.0 mg, $3.15 \cdot 10^{-3}$ mmol). Subsequently, 3.15 mL of the desired deoxygenated solvent were added via syringe and the reactor was irradiated with a Wood Lamp (8 W) at 10 cm distance for the desired time. When the solvent employed was methanol, irradiation was lasted for 60 minutes.

Typical procedure for allylbenzene isomerization mediated by Pt(II) catalysts

The catalyst was *cis→trans* isomerized as previously described. Subsequently 0.942 mL of the solution containing the Pt(II) complex was transferred in a vial and the solvent removed under vacuum. Another sample (0.942 mL) of the isomerized Pt(II) complex was transferred in a new vial which was irradiated with a Wood Lamp (8 W) at 10 cm distance for 60 minutes. The solvent was then removed from the second vial under reduced pressure. The two vials containing respectively the open and the closed complexes were thermostatted at 30°C and charged with 0.600 mL of an allylbenzene solution in dry chloroform (10^{-3}M). The

reaction mixture was stirred at 500 rpm, following the progress of the reaction by GC analysis.

Typical procedure for α-methylstyrene dimerization mediated by Pt(II) catalysts

The catalyst was *cis→trans* isomerized as previously described. Subsequently 0.942 mL of the solution containing the Pt(II) complex was transferred in a vial and the solvent removed under vacuum. Another sample (0.942 mL) of the isomerized Pt(II) complex was transferred in a new vial which was irradiated with a Wood Lamp (8 W) at 10 cm distance for 60 minutes. The solvent was then removed from the second vial under reduced pressure. The two vials containing respectively the open and the closed complexes were thermostatted at 30°C and charged with 0.600 mL of an α-methylstyrene solution in dry chloroform (10^{-3}M). The reaction mixture was stirred at 500 rpm, following the progress of the reaction by GC analysis.

Typical procedure for Diels Alder reaction between acrolein and cyclohexadiene mediated by Pt(II) catalysts

The catalyst was *cis→trans* isomerized as previously described. Subsequently 0.942 mL of the solution containing the Pt(II) complex was transferred in a vial and the solvent removed under vacuum. Another sample (0.942 mL) of the isomerized Pt(II) complex was transferred in a new vial which was irradiated with a Wood Lamp (8 W) at 10 cm distance for 60 minutes. After irradiation process the solvent was removed from the second vial under reduced pressure. The two vials containing respectively the open and the closed complexes were thermostatted at 30°C and charged with 0.600 mL of a dry chloroform solution containing both acrolein and 1,3-cyclohexadiene at the concentration of 10^{-3}M. The reaction mixture was stirred at 500 rpm, following the progress of the reaction by GC analysis.

PHOTOSWITCHING THE ELECTRONIC PROPERTIES OF PHOSPHINIC LIGANDS

Branda and co-workers demonstrated that incorporation of photomodulable moieties such as the diarylethene fragment in a common phosphine based ligand may change its σ-donation ability.[113] Here we report an extension of this pioneering study paying particular attention to the influence of the substituents present on the diarylethene moiety.

Our study encompasses the synthesis of six different diphenyl-diarylethene phosphines, whose main difference is constituted by the substitution pattern on the dithienylethene fragment. As can be seen in Chart 1, the proposed ligands may be divided in two categories: *i)* ligands bearing cyclopentene bridging unit and *ii)* ligands bearing a fluorinated cyclopentene bridging unit. Within each category, three different substituents have been proposed: *i)* an electron withdrawing group, such as a chlorine; *ii)* an electron donating group, such as phenyl moiety bearing a methoxy group in *p*-position with respect to the dithienylethene fragment and *iii)* the phenyl group which shows intermediate electronic properties between the above mentioned substituents.

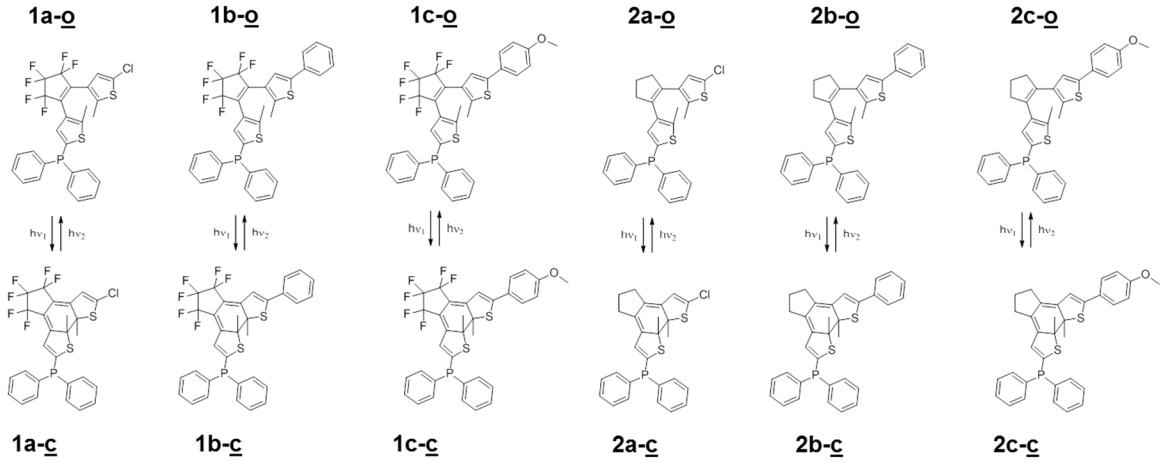

Chart 1. Dithienylethene-based phosphines object of the present study.

Synthesis of the ligands

The synthesis of the ligands reported in Chart 1 involved different synthetic steps. Scheme 39 reports the retrosynthetic approaches followed. Regarding the synthesis of phosphines containing a cyclopentene bridging unit, the first step involved the selective chlorination of 2-methylthiophene that was subsequently acylated with glutaryl chloride leading to the formation of a *bis*-ketone derivative. The latter was subjected to McMurry condensation yielding the fundamental building block used for the synthesis of all three differently substituted ligands belonging to this category. Direct halogen-metal exchange of the chlorine residue followed by quenching with diphenylphosphine chloride yielded the desired chlorine-substituted phosphine, while quenching with *tris*-*n*-butylborate yielded a suitable intermediate species further employed for the Suzuki cross coupling with different bromo-aryl derivatives.

After connection to the desired aromatic moiety by cross coupling reaction, another halogen-metal exchange followed by quenching with diphenylchlorophosphine afforded the other substituted phosphines (Scheme 39A).

As long as the synthesis of phosphines containing a perfluorocyclopentene bridging unit is concerned, 2-chloro-5-methylthiophene was firstly brominated and subsequent selective halogen-metal exchange yielded a nucleophile suitable for the nucleophilic substitution on perfluorocyclopentene. After this double substitution reaction, 1,2-*bis*-[2-methyl-5-chloro-3-thienyl]hexafluorocyclopentene (**5**) was obtained and the synthesis of the chloro substituted and the aryl substituted phosphines was performed as previously described for the non-fluorinated analogues (Scheme 39B).

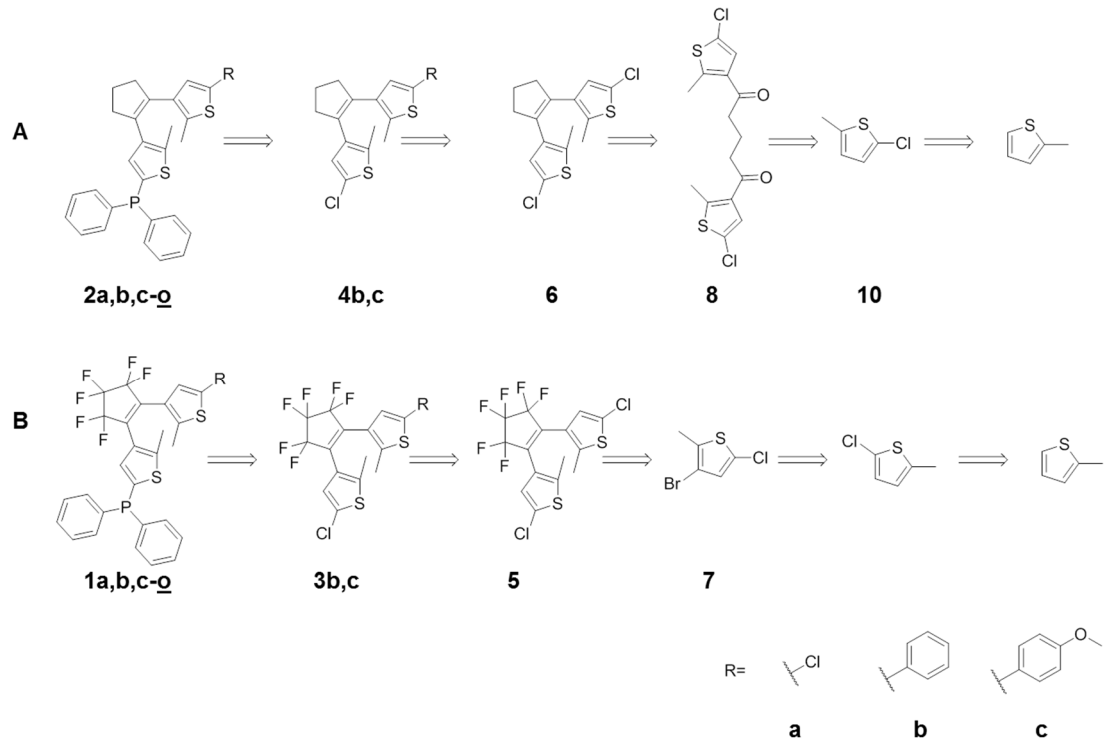

Scheme 39. Retrosynthetic approaches. **A)** retrosynthesis of diarylethene-based ligands containing a cyclopentene bridging unit; **B)** retrosynthesis of diarylethene-based ligands containing a perfluorocyclopentene bridging unit.

Photochromic phosphines with perfluorinated cyclopentene bridging unit

*Synthesis of 2-chloro-5-methylthiophene (**10**)*

The most active positions for the electrophilic aromatic substitution on the thiophene ring are positions 2 and 5 being more close to the sulphur atom. For 2-methyl tiophene only position 5 is accessible and the chlorination of 2-methylthiophene can be performed refluxing it with *N*-chlorosuccimide in a benzene/acetic acid (1:1) mixture.[131] Following the reported procedure, after chlorination, the reaction mixture is conveniently neutralized with a sodium hydroxide solution (3 M), the organic phase dried, the solvent removed and the product separated by distillation at reduced pressure. Since benzene is a recognized carcinogenic substance, we decided to replace such solvent and, both toluene and cyclohexane demonstrated to be

suitable alternative media. The latter revealed to be particularly interesting due to its relative low b.p. (80 °C, 1 atm) which is significantly different from that of 2-chloro-5-methylthiophene (155-156 °C, 1 atm) allowing simple solvent removal thus minimizing product loss (Scheme 40).

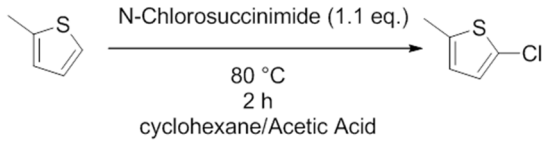

Scheme 40. Synthesis of 2-chlorothiophene.

After refluxing 2-methylthiophene in cyclohexane/acetic acid (1:1) mixture for 2 hours at 78°C with *N*-chlorosuccinimide, quantitative conversion of the thiophene ring was reached. Neutralization of the reaction mixture and solvent removal under reduced pressure allowed to obtain the desired product with 92% purity (by GC analysis) in 96% yield; pure product was obtained by distillation at reduced pressure (38-32°C, 12-8 torr) in 58% yield. The molecular structure was confirmed by ^{1}H-NMR, ^{13}C-NMR and GC-MS analysis, which were consistent with data reported in the literature.[131]

*Synthesis of 2-methyl-3-bromo-5-chlorothiophene (**7**)*

Bromination in position 4 of **10** yields a thiophene species substituted with two different halogen atoms that showed different activities towards halogen-metal exchange reaction. In particular, bromine-lithium exchange is much easier than chlorine-lithium exchange.

Bromination of the thiophene ring could be performed with different brominating agent such as *N*-bromosuccinimide, elemental bromine or by different red-ox pairs such as bromidric acid and hydrogen peroxide. For our scope and for the laboratory scale, molecular bromine was a suitable choice (Scheme 41).

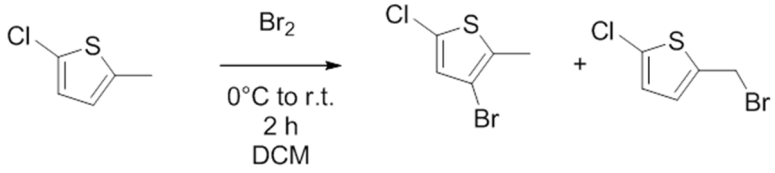

Scheme 41. Synthesis of **7**.

The reaction consisted in the slow addition of a dichloromethane solution of bromine to an ice cooled solution of 2-chloro-5-methylthiophene in dichloromethane. Afterward, the crude reaction mixture was warmed to room temperature and stirred for two hours. Substrate conversion was monitored by GC or ^{1}H-NMR analysis; when complete conversion of the substrate was reached the reaction media was poured into water and the product extracted with diethyl ether. We observed the formation of a side product due to the bromination of the thiophene in benzylic position derived by a radical bromination mechanism. It was found that simple addition of stabilizers or more easily the employment of commercial dichloromethane stabilised with ethanol (0.1-0.4%) allowed minimization of the formation of such by-product.

This side pathway was already known and the use of stabilizers was recommended.[134] Nevertheless, many synthetic procedures found in literature did not report it. The crude reaction mixture was dried, the solvent removed and the product obtained as a colourless oil in 78% yield after distillation under reduced pressure. ^{1}H-NMR, ^{13}C-NMR and GC-MS analysis of the obtained product confirmer the molecular structure and were consistent with the data reported in the literature.[131]

*Synthesis of 3,3'-(perfluorocyclopent-1-ene-1,2-diyl)bis(5-chloro-2-methylthiophene) (**5**)*

Selective halogen-lithium exchange could be performed on **7** at low temperature using *n*-butillithium. The corresponding obtained lithium-thiophene acted as a nucleophile towards the perfluorinated cyclopentene and, after disubstitution on the latter, a dithienylethene derivative useful for the synthesis of different photochromic phosphines was obtained (Scheme 42).

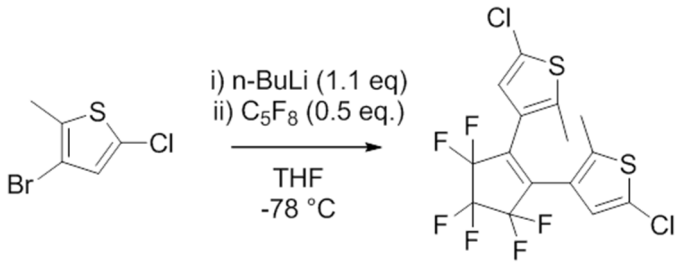

Scheme 42. Synthesis of a suitable dithienylethene moiety containing perfluorinated cyclopentene bridging unit **5**.

The thiophene ring bearing a lithium atom, i.e. a negative charge, on positions 3 or 4 are unstable molecules, known to be stable only at low temperature (we observed decomposition above -40°C). When perfluorocyclopentene was added via syringe to the cold solution of the above mentioned lithium-thiophene, the colourless solution became firstly grey then brownish and finally dark brown. Such colour change is an indication of the ongoing decomposition of the anion. After addition, the reaction mixture was stirred at the same temperature for 30 minutes and then allowed to reach the room temperature. Subsequently the reaction media was quenched by addition of an acid water solution (HCl, 1N), extracted with diethyl ether, the organic phase dried and the solvent removed. Flash chromatography using petroleum ether (40/60°C) as eluent yielded the desired product still containing impurities. Pure product was obtained as colourless crystals after crystallization in the same solvent used for the chromatography.

Under these conditions and using just two equivalents of the thiophene molecule with respect to the perfluoroalkene, yields ranging from 37% to 45% were obtained. These values are comparable with those found in the literature; better yields are possible using excess of the thiophene molecule, [132] and just in one case yield over 90 % wasreported.[133] We tried to improve the reaction yield by addition of an *n*-hexane solution containing the electrophile thermostatted at -78°C and performing the addition dropwise via cannula but even this technique allowed only minimal yield improvements. Better results were obtained with a

different strategy. Halogen-lithium exchange reaction rate is known to be solvent dependent, indeed the reaction is faster in THF with respect to diethyl ether and it is quite negligible in *n*-hexane. However, the exchange reaction could be performed in the latter solvent if small amounts of THF or diethyl ether are present. According to the literature, quite stable 3 or 4 lithium substituted thiophene could be obtained by such solutions.

Following this strategy an *n*-hexane solution of 2-methyl-3-bromo-5-chlorothiophene was first cooled at -78 °C and treated with n-BuLi. No reaction occurred unless low amounts of THF were added, yielding a white precipitate which was attributed to the insoluble lithium-thiophene. At this point a THF solution of the electrophile was added via cannula as previously described followed by another portion of cold THF added dropwise. This addition was crucial to solubilize the precipitated lithium-thiophene. After THF addition the system was left under stirring at -78°C for 1 hour and subsequently left free to reach the room temperature overnight. The crude reaction mixture with this procedure was light brown and the product was isolated by chromatography in 67% yield.

*Selective halogen-metal exchange on 3,3'-(perfluorocyclopent-1-ene-1,2-diyl)bis(5-chloro-2-methylthiophene) (**5**)*

Non symmetric dithienylethenes bearing the phosphine moiety in one thiophene ring and different substituents in the other could be obtained using the previously synthesized symmetric product **5**. Chlorine-lithium exchange could be performed in diethyl ether by reaction with either *n*-butyllithium or with the stronger *t*-butyllithium. The former is effective at room temperature while the latter can be used also at lower temperature such as at -78°C. The exchange reaction is normally affected by different side reactions such as acid-base exchange and nucleophilic substitution with the resulting halo-alkane formed. Since chlorine is less reactive than bromine and iodine, such reaction could be performed in thiophene ring lacking the presence of hydrogen atoms on positions 2.[134] Another problem affecting this reaction concerns the selective substitution of just one of the two chlorine atoms carried by the **5**; indeed the two thiophene rings are electronically isolated in the open isomer and, by virtue of this, their reactivity towards the organo-lithium reagent could be considered independent such as in two different but identical molecules.

Feringa and co-workers reported one of the first procedures concerning the synthesis of non-symmetrical diarylethenes using the selective chlorine substitution reaction as a crucial step.[135] In their study the *mono* and *bis*-lithium substituted molecules were reacted with tris-*n*-butylborate obtaining a precursor for the Suzuki cross coupling that was subsequently coupled with different aromatic halides.

We firstly reproduced the synthetic conditions reported by the authors where a THF solution of the dithienylethene precursor was treated with *n*-BuLi (1 eq.) at room temperature. After complete addition the reaction mixture became dark grey and ^{1}H-NMR analysis of the crude reaction mixture, quenched with an acidic aqueous solution, showed the presence of large amounts of the di-substituted product, a similar quantity of the unreacted dithienylethene and

just little amount of the desired *mono*-substituted product. The products were individuated by their characteristic ^{1}H-NMR resonances; indeed the mono-substituted product (**5m)** showed two different singlets for the two different methyl protons at 1.79 and 1.97 ppm, respectively, and similarly the aromatic protons of the thiophene ring led to two different signals: a broad singlet at 6.90 ppm for the proton bound to the un-reacted thiophene ring and two different doublets at 7.04 (d, J=6.0 Hz) and 7.18 ppm (d, J=6.0 Hz) for the two protons in the reacted thiophene ring, respectively. The double-substituted products (**5d**) showed clearly just one singlet at 1.87 ppm for the methyl protons and two doublets respectively at 7.06 (d, J=6.0 Hz), and 7.16 ppm (d, J=6.0 Hz) for the aromatic protons of the reacted thiophene rings (Figure 36).

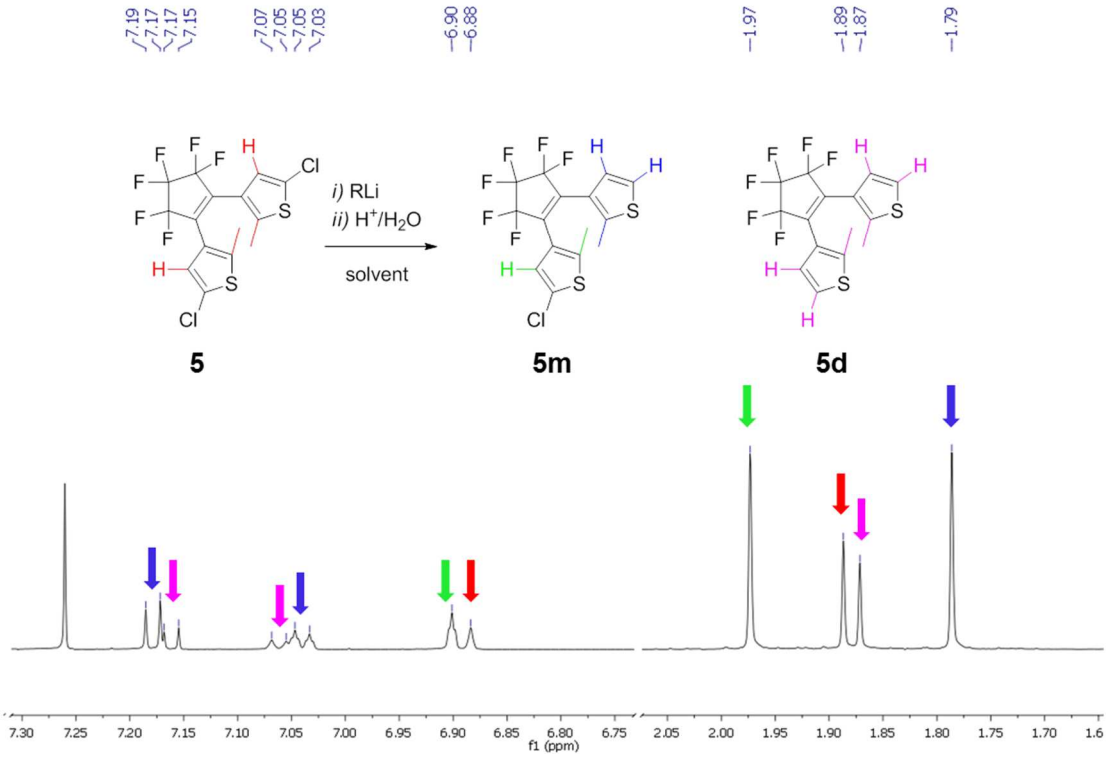

Figure 36. ^{1}H-NMR in chloroform-d of crude reaction mixture obtained after aqueous quenching of an halogen-lithium exchange test on **5**.

It was observed that the reaction was too fast in THF at room temperature and test reactions were repeated at lower temperature such as 0°C and -78°C. At the lower temperature the reaction showed to be too slow while at 0°C no selectivity improvement was obtained. A more recent procedure presented by the same authors reports that switching of the solvent from THF to diethyl ether allowed selectivity increasing towards the mono-substituted intermediate.[136] Such selectivity improvement was a proof of evidence of the lower activity of the organolithium compound in diethyl ether with respect to THF and as a consequence of this consideration we argued that usage of mixture of hexane and diethyl ether as solvent could be crucial to ensure lower reaction rates and hopefully better selectivity.

When *n*-BuLi was used, mixtures of hexane and diethyl ether showed negligible reaction rates while mixture of hexane and THF showed rates comparable to those observed with pure diethyl ether with similar to improved selectivity. Table 5 reports the most significant tests;

the best solvents to perform the halogen-metal exchange using *n*-BuLi were found to be either: i) diethyl ether at room temperature or ii) hexane containing THF (10%) at 0°C.

Table 5. Selective halogen-metal exchange on **5** with different organolithium compounds in different media.

RLi	Hexane (mL)	Et_2O (mL)	THF (mL)	Conversion %[a]	5m (%)[a]	5d (%)[a]
t-BuLi	5	-	-	-	-	-
t-BuLi	5	-	0.5	44	4	40
t-BuLi	5	0.5	-	85	71	14
n-BuLi	5	-	-	-	-	-
n-BuLi	5	0.5	-		-	-
n-BuLi	-	5	-	93	74	19
n-BuLi	-	-	5	46	4	42
n-BuLi	5	-	0.5	80	68	12
n-BuLi[b]	5	-	0.5	88	76	12

Experimental conditions: 5 0.050 g ($1.14 \cdot 10^{-4}$ mol), **RLi** (1 eq.) added via syringe at room temperature , a) determined by ^{1}H-NMR analysis; b) reaction performed at 0°C.

*Synthesis of (4-(2-(5-chloro-2-methylthiophen-3-yl)-3,3,4,4,5,5-hexafluorocyclopent-1-en-1-yl)-5-methylthiophen-2-yl)diphenylphosphine (**1a-o**)*

The first photochromic ligand bearing a chlorine atom in opposite position with respect to the phosphine moiety was obtained by replacing the acidic water solution used in the above reported synthesis with chlorodiphenylphophine (2 eq.), as reported in Scheme 43.

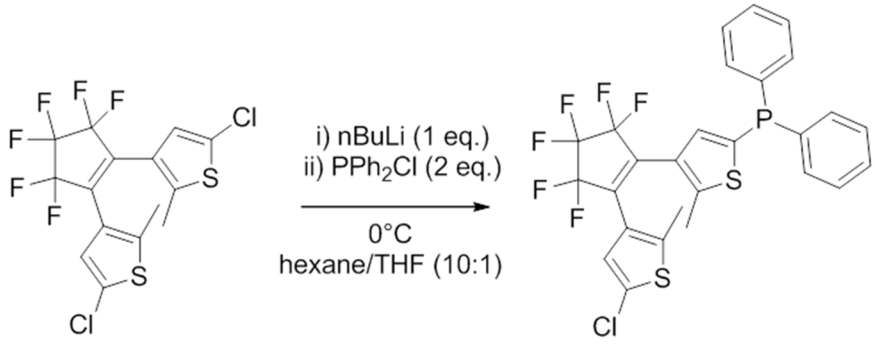

Scheme 43. Synthesis of **1a-o**.

After addition of the phosphine electrophile, the crude reaction mixture was left free to reach room temperature and stirred overnight. After solvent removal under reduced pressure, dichloromethane was added and the mixture was loaded on silica gel (230-400 mesh) and the solvent removed again under reduced pressure. The silica gel containing the crude phosphine was subsequently loaded on top of a chromatography column. Elution with a mixture of petroleum ether/dichloromethane (9:1) yielded **1a-o** as an oily white solid in 42% yield.

The product was characterized by ^{1}H-NMR, ^{13}C-NMR, ^{31}P-NMR, ^{19}F-NMR, ESI mass spectroscopy and UV-Vis analysis. It was found that the ^{31}P-NMR resonance was at -18.9

ppm which is consistent with the chemical shift reported by Branda and collaborators for their dithienylethene based phosphine.[113] The UV-Vis spectrum showed increasing absorbance close to 250 nm but an appreciable light absorption below 340 nm suggesting the use of light sources characterized by emission spectra between the above mentioned range for the ring closing photoreaction.

*Synthesis of (4-(3,3,4,4,5,5-hexafluoro-2-(2-methyl-5-phenylthiophen-3-yl)cyclopent-1-en-1-yl)-5-methylthiophen-2-yl)diphenylphosphine (**1b-o**)*

The synthesis of this photochromic ligand consists in different consecutive reactions which involve: *i)* selective chlorine-lithium exchange on **5**; *ii)* quenching of the lithium-thiophene with *tris-n*-butylborate; *iii)* Suzuki cross coupling between the obtained boron-derivate and bromobenzene; *iv)* chlorine-lithium exchange of the remaining chlorine atom at -78°C and quenching of the formed lithium-thiophene with diphenylchlorophosphine (Scheme 44).

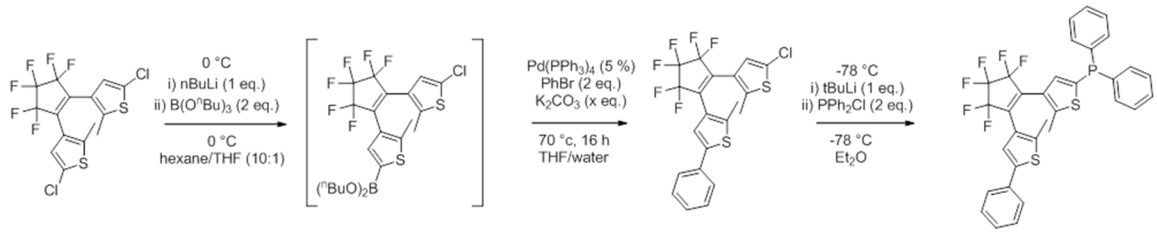

Scheme 44. Synthesis of **1b-o**.

As reported in the literature, the isolation of the corresponding boronic acid bearing the dithienyl moiety is not possible since the C-B bond undergoes rapid cleavage in the presence of water.[131,135] Because of this, the un-purified boron-derivative was firstly dried under reduced pressure then re-solubilized in THF and finally added dropwise to a refluxing THF/water solution containing the catalyst and the reactants for the cross-coupling reaction. We observed the formation of an unprecedent side product whose amount became prevalent when the boron-derivate THF solution was added by a dropping funnel which did not allow its fast dilution in the reaction mixture. The structure of this side product was revealed by ^{1}H-NMR, ^{19}F-NMR and ESI mass spectroscopy analysis and is reported in Scheme 45. The structure of the product reminds the homo-condensation of the aryl boronic acid which is not a frequent reaction, reported in the literature only once.[137]

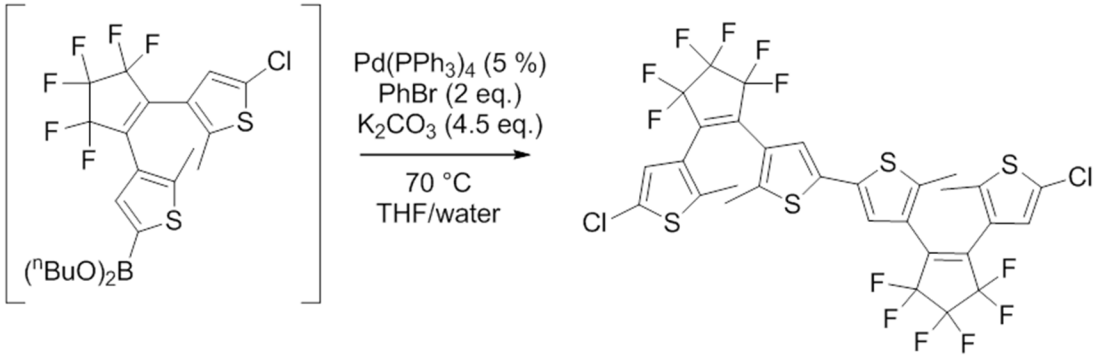

Scheme 45. Unprecedent side product formed during the synthesis of **1b-o**.

Even though the side product obtained could be extremely interesting due to the presence of two dithienyl moieties opening the way for un-precedent photochromic and electrochemical properties, in the present work the aim was to minimize its amount as much as possible. Fortunately we observed that such product could be minimized by dropping the THF solution of the boron-derivate via syringe on a well stirred solution containing the cross coupling reactants. In this way, the cross coupling reaction was refluxed for 16 hours then the product was extracted with diethyl ether, the ethereal solution dried ($MgSO_4$) and the solvent removed under reduced pressure. The product **3b** was isolated as an oily solid in 57% yield by flash chromatography using petroleum ether as eluent. The chemical structure was confirmed by ^{1}H-NMR and ^{19}F-NMR analysis which was consistent with the data reported in literature.[136]

At this point metallation in diethyl ether with *t*-BuLi at -78°C of the remaining chlorine atom in **3b** yielded a lithium-thiophene intermediate which was subsequently reacted at the same temperature with diphenylchlorophosphine. After electrophile addition, the reaction mixture was left free to reach to room temperature and stirring was continued for further 16 hours. The new photochromic ligand **1b-o** was isolated as for **1a-o** obtaining an oily white solid in 62% yield. The product was characterized by ^{1}H-NMR, ^{13}C-NMR, ^{31}P-NMR, ^{19}F-NMR, ESI mass spectroscopy (HMRS) and by UV-VIS analysis. Typical values were found for the ^{31}P-NMR resonances of the open isomer at –18.92 ppm. The UV-Vis spectrum revealed two maxima at 270 and 250 nm and an appreciable light absorption up to 365 nm. In this case it was found that a lamp with an emission spectrum between 365-250 nm was suitable for the ring closing photoreaction.

*Synthesis of (4-(3,3,4,4,5,5-hexafluoro-2-(5-(4-methoxyphenyl)-2-methylthiophen-3-yl)cyclopent-1-en-1-yl)-5-methylthiophen-2-yl)diphenylphosphine (**1c-o**)*

1c-o was obtained and isolated with an identical procedure used for the previous product, just replacing bromobenzene with 4-bromoanisole. The intermediate product **3c** obtained after Suzuki cross coupling was isolated in 60% yield with the same procedure used for **3b** and its structure was confirmed by ^{1}H-NMR analysis which was consistent with data reported in literature.[138]

The phosphine **1c-o** was obtained as an oily solid in 60% yield and its structure was confirmed and characterized by ^{1}H-NMR, ^{13}C-NMR, ^{31}P-NMR, ^{19}F-NMR, ESI mass spectroscopy (accurate-mass analysis) and by UV-Vis spectroscopy. Typical values for the ^{31}P-NMR resonances of the open isomer were found at –18.92 ppm. The UV-Vis spectrum revealed two maxima at 277 and 250 nm and appreciable light absorption up to 370 nm. As for the previous phosphine, a similar lamp with an emission spectrum between 365-250 nm represents a suitable choice for the photoisomerization reaction.

Photochromic phosphines with cyclopentene bridging unit

The main difference between the synthetic approaches undertaken for the preparation of the photochromic phosphines bearing a non perfluorinated cyclopentene bridging unit consists in the preparation of **6** as a different starting dithienylethene species.

*Synthesis of 1,5-bis(5-chloro-2-methylthiophen-3-yl)pentane-1,5-dione (**8**)*

This product was obtained by electrophilic aromatic substitution between glutaryl chloride and 2-chloro-5-methylthiophene in the presence of an excess of aluminium trichloride as reported in Scheme 46.

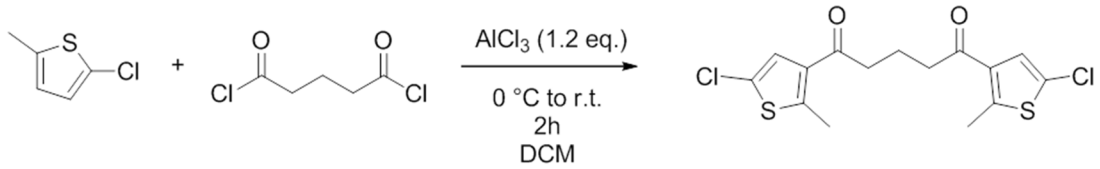

Scheme 46. Synthesis of **8**.

Aluminium trichloride (1.2 eq) was added in portions to a cold (0°C) dichloromethane solution of glutaryl chloride (0.5 eq.) and 2-chloro-5-methylthiophene. During the addition, the reaction mixture became reddish and after 2 hours the conversion of the starting thiophene rings was complete; the reaction crude was then carefully quenched with water and the product extracted with chloroform. After removal of the moisture and the solvents, a brownish solid containing the product in quantitative yield was obtained. As already reported, such impure product could be used without further purifications. The structure of **8** was confirmed by ^{1}H-NMR and ^{13}C-NMR analysis and the data obtained were consistent with those reported in the literature.[135]

*Synthesis of 1,2-bis(5-chloro-2-methylthiophen-3-yl)cyclopent-1-ene (**6**)*

The *bis*-ketone **6** was then treated with a Ti^{3+} source in THF in the McMurry condensation as reported in Scheme 47.

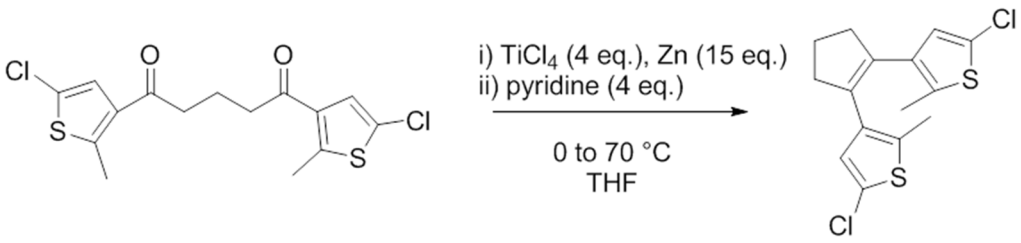

Scheme 47. Synthesis of **6**.

The Ti^{3+} source was prepared *in situ* by refluxing zinc powder with $Ti(THF)_2Cl_4$ in THF for one hour with consequent colour shift from yellow (Ti^{4+}) to dark blue (Ti^{3+}). Subsequently, the mixture was cooled to room temperature, pyridine was added followed by the *bis*-ketone

further refluxed for 2 hours.[139] Once complete substrate conversion was observed, the reaction mixture was cooled to room temperature, treated with water, filtered and the solid formed was washed with an hot (50°C) hexane:ethyl acetate 1:1 mixture. The combined organic layers yielded after evaporation of solvents a crude product which was then subjected to flash chromatography using petroleum ether as eluent. The product was obtained as a white oily solid in 62% yield. The product was fully characterized by ^{1}H-NMR and ^{13}C-NMR analysis and the obtained data were consistent with those reported in the literature.[135]

*Synthesis of the photochromic phosphines (**2a,b,c-o**)*

The phosphines **2a,b,c-o** were obtained following the same reaction and purification procedures previously reported for the **1a,b,c-o**. The intermediates obtained after the cross-coupling step (**4b,c**) were synthesized using the same procedures and their ^{1}H-NMR signals were consistent with those reported in the literature.[138] The structure of the phosphines were confirmed by ^{1}H-NMR, ^{13}C-NMR, ^{31}P-NMR and UV-Vis analysis; the most significant data of such products are reported in Table 6.

Table 6. Typical data for phosphines **2a,b,c-o.**

phosphine	δ (^{31}P-NMR, ppm)[a]	Suggested irradiation range (nm)[b]
2a-o	-20.94	340-250
2b-o	-20.91	365-280
2c-o	-20.92	365-283

a) ^{31}P-NMR spectra collected in chloroform-d; b) UV-Vis spectra of a $2 \cdot 10^{-5}$ M chloroform solution of the phosphine.

Photochemical behaviour of the synthesized phosphines

The photochemical behaviour and the evaluation of the spectroscopic differences between the corresponding open and closed forms and the effects the different substituents present on the phosphines were investigated by UV-Vis and ^{31}P-NMR spectroscopy. In Scheme 48 are reported the photo-isomerization reactions and the structures of both the open and the closed isomers of the prepared phosphines.

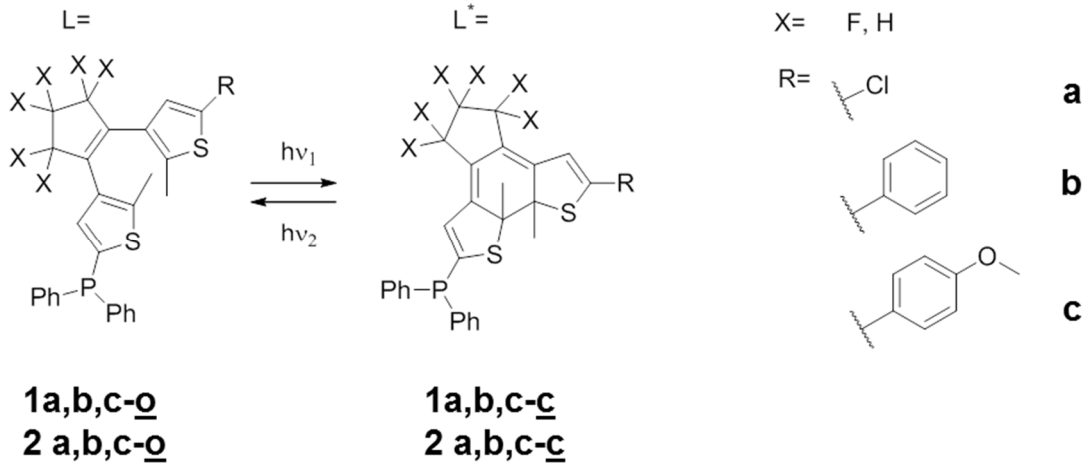

Scheme 48. Photochemical reversible ring-closing reaction of the synthesized phosphines.

All the synthesized phosphines demonstrated to be quite stable towards oxidation when stored as solids at -10°C in the fridge (no phosphine oxide formation after 3 months). The oxidation was faster in solution (deuterated chloroform or dichloromethane) due to the presence of dissolved oxygen and this undesired side reaction was boosted during the irradiation tests.[j]

The spectra of the open and irradiated phosphines belonging to both perfluorinated and traditional classes of ligands are reported in Figure 37 and Figure 38, respectively. Due to the above mentioned oxidation side reaction occurring in solution, the UV-Vis spectra of the irradiated phosphines reported are to be considered only for qualitative evaluation.

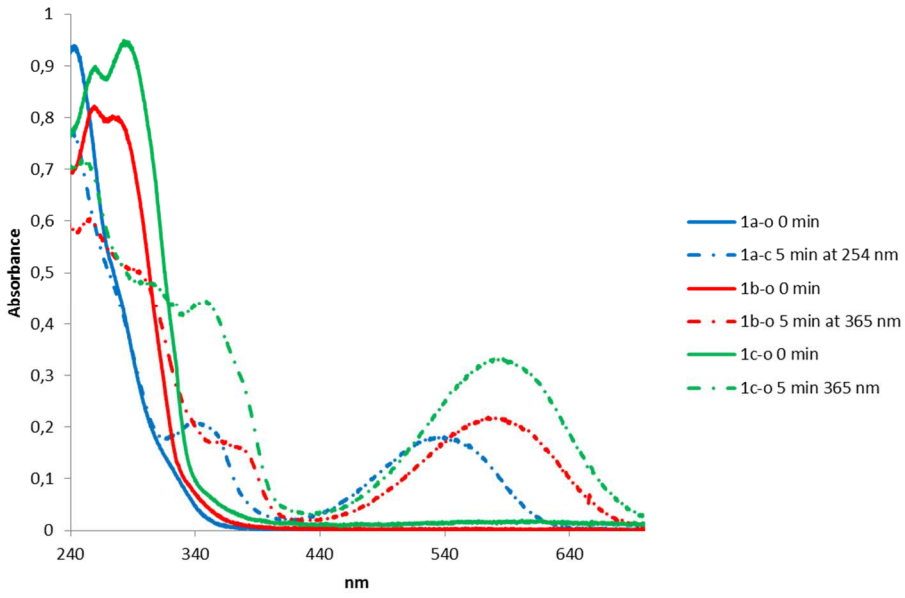

Figure 37. UV-Vis spectra of a $2 \cdot 10^{-5}$ M chloroform solution of **1a,b,c-o**. Irradiation of the samples was performed at 365 or 254 nm.

j $[O_2]$=2.4 mmol/l

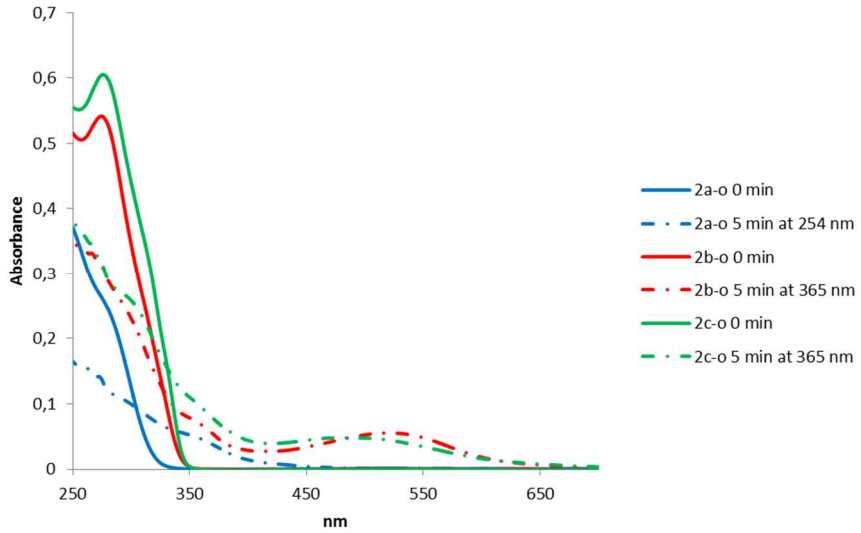

Figure 38. UV-Vis spectra of a $2 \cdot 10^{-5}$ M chloroform solution of **2a,b,c-o**. Irradiation of the samples was performed at 365 or 254 nm.

It was found that the phosphines bearing hexafluorocyclopentene as bridging unit showed higher absorbance, i.e. higher molar extinction coefficient, as already observed in other dithienylcyclopentene.[135] Upon irradiation, the perfluoro-phosphines showed new maxima at higher wavelength due to the formation of the closed isomers; the values found for **1a-c**, **1b-c** and **1c-c** were 577, 572 and 535 nm, respectively. As a real evidence formation of the new closed isomers, the former phosphine turned crimson while the latter became blue upon irradiation. Concerning the phosphines bearing the hexahydrocyclopentene unit, it was observed a down shift of the new maxima with respect with the previous ligands. The new values were detected at 529 nm for **2b-c** and 500 nm for **2c-c** with red-crimson coloured sample, while **2a-c** did not show any new maximum but increased absorbance between 450-300 nm providing a yellow-orange coloured sample.

Despite the ^{1}H-NMR spectra of the phosphines after irradiation were too complex to undertake a reliable attribution of the signals, the ^{31}P-NMR spectra were less complicated and the phosphorous resonances of the closed isomers were clearly detected. A comparison between the ^{31}P-NMR chemical shifts of the resonances for the open and closed isomer is reported in Table 7.

Table 7. ^{31}P-NMR chemical shifts for the open and closed isomers of the synthesized phosphines.

Ligand	δ_{open} (^{31}P) ppm[a]	δ_{closed} (^{31}P) ppm[a]
1a	-18.94	-8.48
1b	-18.92	-8.63
1c	-18.92	-8.88
2a	-20.94	-12.37
2b	-20.91	-12.87
2c	-20.92	-13.05

a) ^{31}P-NMR analysis in chloroform-d.

As expected the phosphines showed all similar ^{31}P resonances for the open isomer, indicating that all the phosphorous atoms are influenced by the presence of two phenyl and one

thiophene rings as substituents. The presence of the perfluorinated cyclopentene ring in **2a,b,c** affects the ^{31}P resonances by ca. 2 ppm with respect to **1a,b,c** bearing the non perfluorinated cyclopentene ring. Despite it is not easy to find a trend between the ^{31}P-NMR chemical shift and the electron donating/withdrawing properties of the substituents,[k] in this case it is possible to affirm that the presence of the electron withdrawing perfluorinated moiety decreases the chemical shift of the P atoms.

When the phosphines are irradiated, all their ^{31}P resonances are shifted downfield, with a $\Delta\delta$ of about -8.6 ppm for the perfluoroalkene containing phosphines and around -12.6 ppm for the others. This could be attributed to the loss of aromaticity of the thiophene ring and, as a consequence, to the presence of a more extended π system. Secondly, the difference of chemical shift between **1a,b,c** and **2a,b,c** increased from 2 ppm in the open form to 4 ppm in the closed one, showing that the presence of the perfluorinated bridging unit affects the electronic nature of the system more strongly in the closed isomer with respect to the open one. Finally, the chemical shifts of the closed isomers do not seem to be influenced by the presence of different substituents on the second thiophene unit, both in the open and closed forms.

From the chemical shifts values of the open and closed isomer of the photochromic phosphines the following considerations can be drawn:

- ✓ a considerable variation of the electronic properties between the two photochromic isomers could be expected as showed by the appreciable variation of the ^{31}P-NMR resonances;
- ✓ different substituents with different electron donating or withdrawing abilities in the second thiophene ring do not produce appreciable differences in terms of ^{31}P-NMR resonances;
- ✓ the most important substituent affecting the electronic properties of the closed isomers is the bridging unit: the more electron withdrawing is this moiety and the higher is the difference between the photochromic forms.

These preliminary data and the relative considerations encouraged a more detailed study concerning the net electronic properties of the new synthesized phosphines in both photochromic forms.

k Not always it is true that the more electron withdrawing the substituents and the higher are the values of the ^{31}P-NMR chemical shifts (or *vice versa*). For examples see: R. Bosque, J. Sales, *J. Chem. Inf. Comput. Sci.* **2001**, *41*, 225-232.

Net electronic properties of phosphines

In conventional descriptions of transition metal-phosphine (M-P) bonding, the electronic interaction is considered having σ and π contributions. The former involves donation of electrons from the ligand lone pair to an empty orbital, of σ pseudo-symmetry, of the metal while the latter involves back-donation from filled metal orbitals of π pseudo-symmetry to empty orbitals of the same symmetry on the phosphine ligand.[140] *Ab initio* calculations revealed that the phosphine LUMOs orbitals are a doubly degenerated pair of orbitals with π symmetry, which have P-R σ^* as well as phosphorous 3d character.[141] Such P-R σ^* molecular orbitals, corresponding to the P-R σ interaction involving $3p_x$ and $3p_y$, mix with the 3d orbital of the phosphorous yielding hybridized π-acceptor orbitals. The degree of re-hybridization depends on the relative energies of σ^* and P-3d orbitals and on the distribution of the σ^* orbital. From the perturbation theory it is expected that the lower the energy and the greater the concentration of the σ^* orbitals on the phosphorous, the more effective will be the σ^*-P-3d mixing and the resulting π-acceptor function. Regarding the substituents on the phosphorous atom, the more electronegative the substituent and the more 3p character there is in the σ^* orbital and lower it is in energy.[140,l]

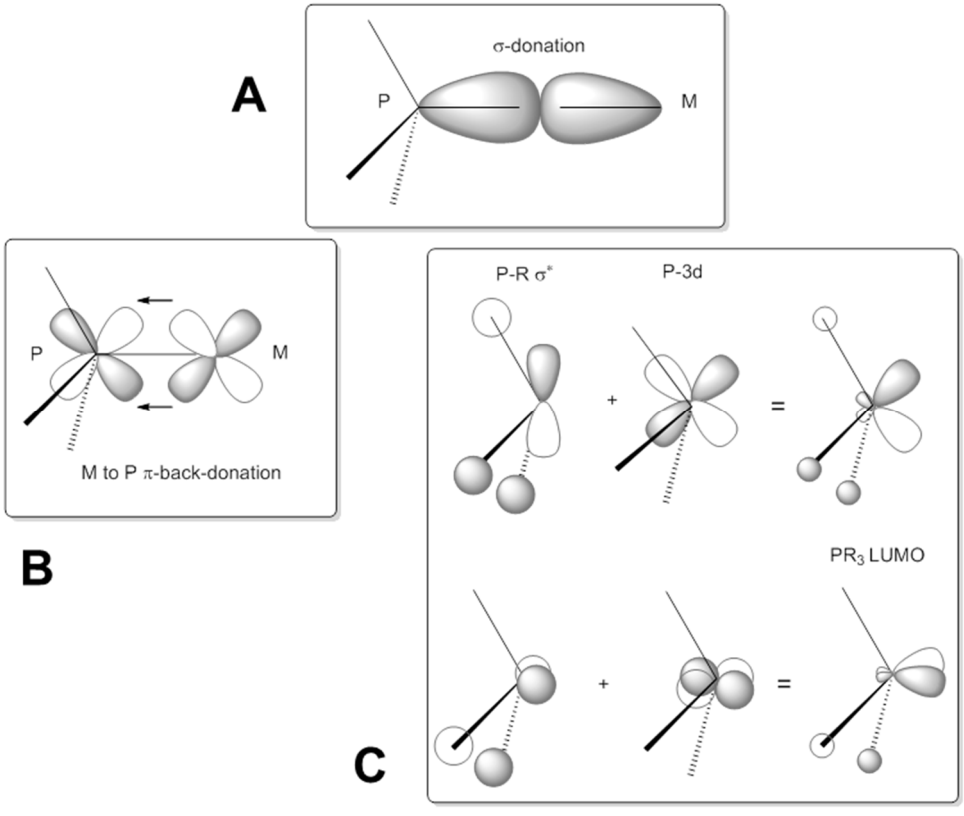

Figure 39. A) P→M σ-donation scheme; **B)** traditional M→P π-back-donation scheme; **C)** hybridization of P-R σ^* orbitals with P-3d orbitals yielding PR_3 LUMOs with π-symmetry available for M→P π-back-donation.

It is widely believed that the bonding between CO and a metal is a combination between σ- and π-bonding. Delocalization of the d electrons of the metal with π-symmetry into the π^* CO orbital gives rise to π-backbonding while overlap of σ symmetry orbitals of the metal and CO

l π-acceptor ability sequence: $PR_3 < PAr_3 < P(OR)_3 < P(Oar)_3 < PF_3$ (Ar=aryl; R=alkyl)

yields a strong σ-interaction.[142] Due to the donation of electron density from the metal centre, the CO bond may be weakened and the νCO bands in the IR spectrum shifted towards lower wavenumbers. If a CO ligand is replaced by a phosphine, the latter will act both as σ-donor and π-acceptor. Generally speaking the phosphines are better σ-donor than CO and such substitution will increase the electron density on the metal centre enhancing the π-donation ability of the metal centre; the extent of this back-bonding is dependent on the π-acceptor strength of the various ligand. If only the phosphine is altered and the other substituents remain constant, the νCO band in the IR spectrum can be used to evaluate the electronic properties of a series of phosphine ligands.[143] Commonly, shift of the νCO bands towards higher wavenumber means good π-acceptor properties.[144]

C.A. Tolman proposed an equation correlating tertiary phosphines to a specific series of transition metal complexes; indeed the equation linearly correlates the νCO frequency with the substituents in the phosphorous atom.[m] After his pioneering work, other authors proposed equations to correlate the νCO bands of carbonyl complexes of different metals to TEP (Tolman electronic parameter) and thanks to their work nowadays it is possible to evaluate the TEP of a particular phosphine from practically all carbonyl complexes. The TEP describes the net donating ability of tertiary phosphine and it is an acceptable expression of the π-acceptor features only when the σ-donation abilities of the compared phosphines are limited.

Another way to evaluate the electronic properties of tertiary phosphine comes from the analysis of the NMR coupling constants between phosphorous and selenium in phosphine selenides. It is well known that coupling constants between directly bonded atoms arise predominately from the Fermi contact interaction between nuclear moments and electron spins in *s* orbitals,[145a] and there have been a number of suggested approaches in the literature that there is a correlation between the magnitude of such coupling constants and the lengths of the bonds between adjacent atoms.[145] The magnitude of $^{1}J(^{31}P\text{-}^{77}Se)$ is related to the nature of the organic groups bound to phosphorous with the following trend: the more electron withdrawing is the substituent and the larger is the coupling constant.

Since the selenium phosphorous bond has low $P_{\pi\text{-}3d}\text{-}Se_{\pi\text{-}4d}$ character, the effects of the substituent present on phosphorous on the coupling constants value may be referred as the *s* character of the lone pair of the phosphorous. Electron withdrawing groups result in an increase in *s* character of the lone pair, whereas electron donating groups result in decrease of the *s* character; as a consequence phosphine selenides of phosphines bearing electron donating substituents are characterized by lower values of $^{1}J(^{31}P\text{-}^{77}Se)$ coupling constants than analogous phosphines bearing electron-withdrawing substituents. Since the magnitude of the coupling constant is referred in particular to the *s* character of the phosphorus' lone pair, its value could be used as a qualitative expression of the σ-donation ability of the corresponding phosphine.[145]

m Tolman's equation: $\nu CO_{Ni}=2056.1+\Sigma\,\chi_i$ where νCO_{Ni} refers to A_1 band in the IR spectra of $[Ni(CO)_3L]$ ($L=PR^1R^2R^3$), 2056.1 is the A_1 band of $[Ni(CO)_3(PBu^t_3)]$ which was set as reference; χ_i is the effect of the substituent R_i . χ_i is 0 for PBu^t_3 for definition; the latter phosphine was chosen as reference because it was the most basic one and due to this the best σ-donor and the worst π-acceptor.

The evaluation of the different electronic properties of the open and the closed isomers of the ligands bearing the diarylethene moiety was therefore performed synthesizing the phosphine-selenide and the Vaska type Rh(I) complexes.

Synthesis of the Vaska type Rh(I) complexes

All the Vaska type Rh(I) complexes were synthesized using a known procedure consisting in the reaction between the new phosphine with the Rh(I) precursor $[Rh(CO)_2]_2Cl_2$ as reported in Scheme 49.[146]

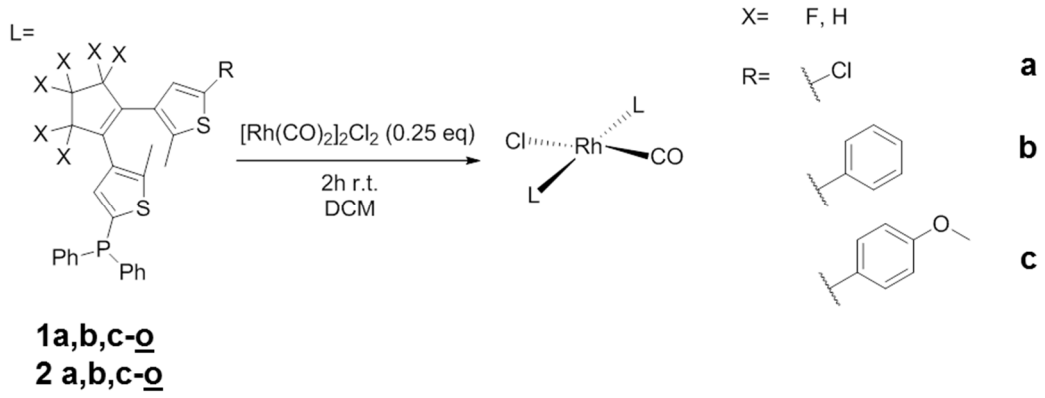

Scheme 49. Synthesis of the Rh(I) Vaska type complexes bearing the photochromic phosphines **1a,b,c-o** and **2a,b,c-o**.

The products were all obtained in quantitative yield as yellow powders by removal of the solvents under vacuum. No further purifications were performed and the complexes were all characterized by ^{1}H-NMR, ^{31}P-NMR and IR spectroscopy. In certain cases ^{19}F-NMR analysis was performed as well.

The obtained characteristic data for the open isomers, reported in Table 8, were consistent with the already known *trans*-$[Rh(CO)Cl(L)_2]$ complexes and the net electronic properties was found to be included between the ones typical for PPh_3 (1979 cm^{-1}) and P(*p*-F-Ph)$_3$ (1983 cm^{-1}).[147] Also in this case the hexafluorocyclopentene moiety acts as an electron withdrawing group.

Table 8. ^{31}P-NMR and IR data for the obtained Rh(I) Vaska type complexes containing the photochromic ligands **1a,b,c-o** and **2a,b,c-o**.

Complex	νCO[b] (cm^{-1})	δ (^{31}P) ppm[a]	^{1}J(P-Rh) Hz
***trans*-[Rh(CO)Cl(1a-o)$_2$]**	1983	19.36	127
***trans*-[Rh(CO)Cl(1b-o)$_2$]**	1983	19.29	133
***trans*-[Rh(CO)Cl(1c-o)$_2$]**	1983	bs	-
***trans*-[Rh(CO)Cl(2a-o)$_2$]**	1981	16.41	127
***trans*-[Rh(CO)Cl(2b-o)$_2$]**	1981	16.42	127
***trans*-[Rh(CO)Cl(2c-o)$_2$]**	1981	16.40	126

a) ^{31}P-NMR analysis in dichloromethane-d; b) IR analysis in dichloromethane solution.

Synthesis of the phosphine selenides

All the phosphine selenides were synthesized using a known procedure consisting in refluxing the starting phosphine with an excess of selenium in chloroform for two hours, as reported in Scheme 50.

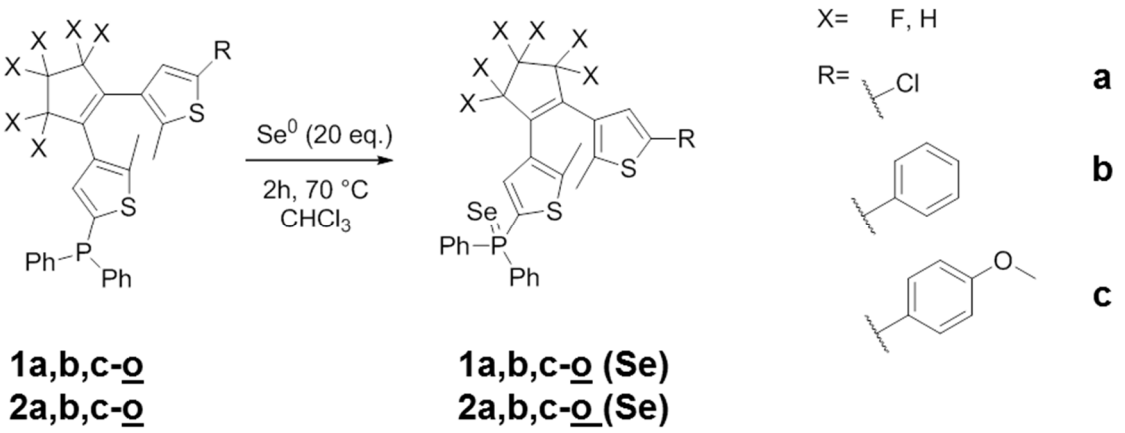

Scheme 50. Synthesis of the phosphine selenides corresponding to **1a,b,c-o** and **2a,b,c-o**.

The desired selenides were obtained in quantitative yield by removal of the selenium excess and of the solvent. The products were then characterized by ^{1}H-NMR, ^{31}P-NMR, and in certain cases ^{19}F-NMR analysis. Table 9 reports the phosphorous resonances and $^{1}J(^{31}P\text{-}^{77}Se)$ coupling constants of the synthesized compounds and other known selenides.

Table 9. Selenides' data.

Phosphine selenide	**δ (^{31}P) ppm[a]**	**$^{1}J(^{31}P\text{-}^{77}Se)$ Hz**
$PR^1{}_2R^2$, $R^1=R^2=Ph$	35.9[b]	732
$PR^1{}_2R^2$, R^1 =Ph, R^2=2-thienyl	20.6[b]	743
$PR^1{}_2R^2$, R^1 =2-thienyl, R^2= Ph	9.3[b]	752
$PR^1{}_2R^2$, R^1 =R^2=2-thienyl	-4.2[b]	757
1a-o (Se)	22.05	745
1b-o (Se)	22.08	744
1c-o (Se)	21.95	743
2a-o (Se)	20.32	737
2b-o (Se)	20.17	740
2c-o (Se)	20.14	737

a) The ^{31}P-NMR resonances were collected in dichloromethane-d; b) data from ref. 145b.

All the obtained values are similar to those reported for diphenyl(thiophene-2-yl)phosphine selenide and also to those reported by Branda and co-workers for their dithienylethene-based bisphosphine.[113]

Photochemical behaviour of the Rh(I) complexes

Irradiation of the synthesized complexes in deuterated dichloromethane at the proper wavelength was followed by intense coloration in the visible region confirming the shift from the open to the closed forms of the photochromic ligands. Similarly, irradiation of the complexes with visible light produced an appreciable discoloration proving the reversibility of the photochemical reaction. Such observation suggests that the excited states of the dithienyl moiety is localized on the ligands, in other words it is not transferred to the metal center. In the literature it is reported a case where the ring closing of a dithienylethene-bridged iron complexes is inhibited by the metal center due to the localization of the excited state on the metal center.[148]

In the case at hand, ^{1}H-NMR and especially ^{31}P-NMR analysis revealed the formation of a mixture of products which was not ascribable to Vaska type Rh(I) complexes. We presume that the original complex eliminates the CO ligand upon irradiation, which is likely to occur and already reported for this class of compounds.[125] As a consequence, the unsaturation degree increases. Under this reaction conditions transfer of phosphinic ligands between different complexes could not be excluded and since the irradiation did not produce intelligible Rh(I) carbonyl molecular species, we decided not to continue investigating the Rh(I) Vaska type complexes for the evaluation of the net electronic properties of the new synthesized phosphines.

Photochemical behaviour of the selenides

As already reported by Branda and co-workers, the obtained selenides are stable towards the irradiation and could be effectively used to evaluate the electronic properties of both the photochromic forms of the new ligands.[113] The selenides were irradiated at the proper wavelength using Pyrex or quartz NMR tubes as reactors and deuterated dichloromethane as solvent. Since the closed form of the dithienylethene is characterized by high molar extinction coefficient, high photoconversions were reached only with dilute solutions which require time consuming ^{31}P-NMR analysis or synthesis of the selenides with an enriched ^{77}Se source. For our purposes, a quantitative evaluation of the UV-Vis spectral features was not relevant and as a consequence we performed the irradiation of concentrated solutions until the desired chemical shifts and coupling constants were recordable with routinely NMR time experiments.

Table 10. Data obtained for the open and closed forms of the phosphine selenides object of this study.

Selenide	**open**		**closed**		**$\Delta J_{C/O}$ (Hz)**
	δ (^{31}P) ppm[a]	$J^{31}{}_{P\text{-}}{}^{77}{}_{Se}$ (Hz)	δ (^{31}P) ppm	$^{1}J(^{31}P\text{-}^{77}Se)$ Hz	
1a (Se)	22.05	742	26.76	757	15
1b (Se)	22.05	744	26.72	756	12
1c (Se)	21.97	744	26.60	756	12
2a (Se)	20.31	737	24.35	747	10
2b (Se)	20.18	740	24.20	746	6
2c (Se)	20.14	737	24.15	742	5

Branda bisphos[b]	22.4	744	27.0	756	12

a) ^{31}P-NMR resonances collected in dichloromethane-d; b) from ref. 113 (spectra collected in chloroform-d).

Firstly the phosphines bearing the hexafluorocyclopentene unit showed similar resonances and coupling constants of the *bis*-phosphine synthesized by Branda and co-workers, meaning that there are no appreciable differences due to different substitution pattern on the thiophene rings. Regarding the phosphines equipped with the hexahydrocyclopentene moiety, it seems that both the open and closed forms of the selenide resonate at higher field and the difference in terms of coupling constants decreased with respect the previous one. We argued that both the reduced values of chemical shift and the decreased difference between the coupling constants of the closed and open form are direct consequence of the presence of the more electron withdrawing perfluorinated ring. Data obtained from **2a,b,c (Se)** suggest another important consideration concerning the effect played by the substituent in the second thiophene ring. A trend which reminds the relative electron withdrawing series of the substituents was observed and more precisely it was found that the difference between the coupling constants of **2a-o (Se)** and **2a-c (Se)**, equipped with the more electron attracting chlorine atom, is larger (10 Hz) than that between **2b-o (Se)** and **2b-c (Se)**, the latter being quite larger than that measured for **2c-o (Se)** and **2c-c (Se)**. This empirical observation strengthens the assumption of the great importance played by the bridging unit between the thiophene moieties in determining the electronic properties of the closed isomers of the phosphines. It is therefore reasonable to conclude that the electronic nature of the substituents in the second thiophene ring becomes important in the determination of the electronic properties of the closed isomers only in the absence of a strong electron donating bridging unit such as the hexafluorocyclopentene unit.

Conclusions

From this study on the synthesis and characterization of dithienylethene-based phosphines the following considerations can be drawn:

- ✓ the open and the closed forms of these photo-modulable ligands show appreciable differences in terms of σ-donation ability, more precisely the closed isomers show enhanced σ-donation ability
- ✓ the most important substituent affecting the electronic properties of the closed isomers is the bridging unit: the more electron withdrawing is the moiety and the more enhanced is the difference between the photochromic forms
- ✓ different substituents with different electron donating or withdrawing abilities in the second thiophene ring do not produce appreciable electronic differences as long as a strong electron withdrawing bridging unit is present in the structure. Conversely, the effects imparted by those substituents become important in its absence of an electron withdrawing bridging unit

G. Bianchini, D. F. Wass, A. Scarso, G. Strukul *Photoswitching the electronic properties of phosphinc ligands containing the dithienylethene moiety*, manuscript in preparation.

Experimental

^{1}H-NMR, ^{13}C{^{1}H}-NMR and were recorded at 298 K with a BRUKER AVANCE spectrometer operating respectively at 300.15, 75 and 121.5 MHz and with a BRUKER AC200 operating at 200, 50 and 80.7 MHz, respectively. Other spectrometers were used for recording ^{1}H-NMR and ^{13}C{^{1}H}-NMR, ^{31}P{^{1}H}-NMR and ^{19}F-NMR: Joel ECP 400 operating at 400 and 101 MHz respectively and Joel ECP 300 operating at 300 and 75 MHz respectively were used for ^{1}H-NMR and ^{13}C{^{1}H}-NMR while only the latter was used for ^{31}P{^{1}H}-NMR (120 MHz) and ^{19}F-NMR (283 MHz) analyses.

GC analysis were performed on HP SERIES II 5890 equipped with a HP5 column (30 m, I. D. 0.25 m, film 0.25 μm) using He as gas carrier and FID. GC-MS analyses were performed on a GC Trace GC 2000 equipped with a HP5-MS column (30 m, I.D. 0.25 mm, film 0.25 μm) using He gas carrier and coupled with a quadrupole MS Thermo Finnigan Trace MS with *Full Scan* method. HMRS analyses were performed on Apex 4e 7.0T FT-MS Bruker Daltonics (FT-ICR-MS) using ESI. Identification of the products was accomplished by reference samples or by comparison with samples obtained as described in literature.

TLC analysis were performed on TLC Polygram ® Sil G/UV254 of 0.25 mm thickness and flash-chromatography separations were performed on silica gel Merk 60, 230-400 mesh as reported by W. C. Still, M. Khan, A. Mitra *J. Org. Chem.* **1978**, *43*, 2923.

Solvents and reactants were used purchased; otherwise they were purified as reported in D. D. Perrin, W. L. F. Armarego *Purification of Laboratory Chemicals*, 3rd Ed., **1988**, Pergamon Press Ltd., Oxford OX3 0BW, England.

Irradiation at 365 nm was performed with a Wood lamp, omnilux 25 W, irradiance at 365 nm 10 W/m^2 (10 cm) while irradiation at 254 nm was performed with the low pressure Hg lamp commonly used for the visualization of TLC plates (12 W).

*Synthesis of 2-chloro-5-methylthiophene(**10**)*

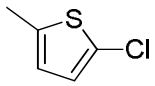

In a round bottom flask equipped with a condenser, 2-methylthiophene (15 mL, 15.04 g, 0.155 mol) and *N*-chlorosuccinimide (22.55 g, 0.169 mol) were added to a stirred 1:1 solution of cyclohexane and acetic acid (120 mL). The suspension was stirred at room temperature for 30 min, further refluxed for 2 h and subsequently cooled to room temperature and poured into a NaOH solution (3M, 45 mL). The organic phase was washed with the NaOH solution (3x45 mL), dried over $MgSO_4$, filtered and the solvent removed under reduced pressure. The product was isolated as yellowish oil in 96% yield (GC purity 92%). Further purification by vacuum distillation (12-8 torr, 38-32 °C) yielded a colorless liquid in 58% yield.

^{1}H-NMR (300.15 MHz, $CDCl_3$, TMS): δ 2.43 (d, J=0.9 Hz, 3H), 6.52 (dq, J=6.6 and 0.9 Hz, 1H), 6.83 (d, J=3.6 Hz, 1H).
^{13}C-NMR (75 MHz, $CDCl_3$, TMS): δ 15.6, 108.7, 125.6, 129.7, 141.5.

GC-MS (*m/z*): 132 (M^+), 97 (M^+-Cl).

*Synthesis of 2-methyl-3-bromo-5-chlorothiophene (**7**)*

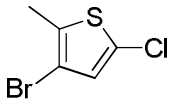

In a two necks round bottom flask, equipped with a dripping funnel, were charged **10** (10 g, 0.075 mol) and dichloromethane (70 mL containing 0.1-0.4% of EtOH as stabilizer). The solution was cooled with an ice bath and through the dropping funnel a dichloromethane (20 mL) solution of bromine (11.986 g, 3.86 mL, 0.075 mol) was slowly added under vigorous stirring. When the addition was complete the system was left under stirring at room temperature for 2h and subsequently poured in water (150 mL). The water layer was extracted with dichloromethane (3x50 mL), the combined organic phases dried over $MgSO_4$, filtered and the solvent removed under reduced pressure. Distillation at reduced pressure (34-30°C, 1.0-0.5 torr) yielded colorless oil in 78% yield.

^{1}H-NMR (400 MHz, $CDCl_3$, TMS): δ 2.33 (s. 3H), 6.73 (s, 1H).
^{13}C-NMR (101 MHz, $CDCl_3$, TMS): δ 14.8, 107.7, 126.9, 128.5, 133.3.
GC-MS (*m/z*): 212 (M^+), 131 (M^+-Br).

*Synthesis of 1,5-bis(5-chloro-2-methylthiophen-3-yl)pentane-1,5-dione (**8**)*

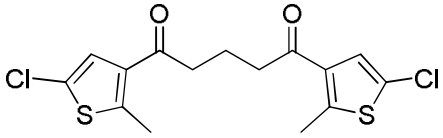

A two necks round bottom flask connected to a vacuum/nitrogen line was flame dried and three vacuum/nitrogen cycles were performed. Subsequently dry dichloromethane (100 mL), **10** (8.08 mL, 10.00 g, 0.075 mol), and glutaryl chloride (4.79 mL, 6. 34 g, 0.0375 mol) were added under nitrogen atmosphere. The solution was stirred and cooled at 0°C through an ice bath and subsequently $AlCl_3$ (12.00 g, 0.09 mol) was added in portions. During the addition the mixture turned red. Stirring was continued at 0°C for 15 min and at room temperature for 2h. Subsequently the reaction mixture was carefully quenched with ice-cooled water (100 mL), the aqueous layer separated and extracted with diethyl ether (2x50 mL). The combined organic phase was dried over $MgSO_4$, filtered and the solvent removed under reduced pressure yielding the product in quantitative yield. The obtained product was directly employed for the next step without further purification.

^{1}H-NMR (300.15 MHz, $CDCl_3$): δ 2.05 (q, J=6.7 Hz, 2H), 2.65 (s, 3H), 2.85 (t, J=6.7 Hz, 4H), 7.17 (s, 2H).
^{13}C-NMR (75 MHz, $CDCl_3$): δ 16.03, 18.14, 45.51, 125.30, 126.81, 134.87, 194.87.

*Synthesis of 3,3'-(perfluorocyclopent-1-ene-1,2-diyl)bis(5-chloro-2-methylthiophene) (**5**)*

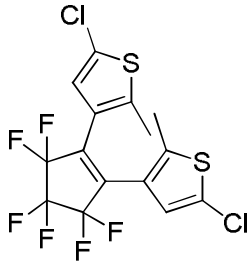

Traditional procedure

A two necks round bottom flask connected to a nitrogen/vacuum line was flame dried and 3 vacuum/nitrogen cycles were performed; subsequently dry THF (30 mL) and **7** (1.00 g, 0.0048 mol) were added via syringe under N_2 atmosphere. The reaction mixture was cooled at -78°C through an acetone/$CO_{2(s)}$ bath and then *n*-BuLi (1.6 M in hexane, 3.2 mL, 0.0051 mol) was added dropwise with a syringe. The mixture was stirred for 10 min at the same temperature and perfluorocyclopentene (0.32 mL, 0.51 g, 0.0024 mol) was slowly added while maintaining the solution under stirring for further 30 min. Then the solution was allowed to warm up to room temperature and consequently quenched with aqueous HCl (1N, 20 mL). The product was extracted with diethyl ether (3x20 mL) and the combined organic phases dried over $MgSO_4$. The solvent was removed under reduced pressure and flash chromatography (petroleum ether 40/60°C as eluent) of the crude mixture yielded an impure amount of product. Pure product was obtained as colorless crystals after crystallization from petroleum ether in 45% yield.

^{1}H-NMR (400 MHz, $CDCl_3$, TMS): δ 1.88 (s, 6H), 6.89 (s, 2H).
^{19}F-NMR (283 MHz, $CDCl_3$, CCl_3F): δ -110.20 (t, J=5.3 Hz, 4F), -131.79 (q, J=5.3 Hz), 2F).
GC-MS (*m/z*): 436 (M^+), 401 (M^+-Cl), 367 (M^+-2Cl).

Improved procedure

A two necks round bottom flask and a Schlenk reactor, connected to a nitrogen/vacuum line and to the flask via cannula, were flame dried and 3 vacuum/nitrogen cycles performed. Under nitrogen atmosphere dry *n*-hexane (30 mL) and **7** (1.00 g, 0.0048 mol) were added via syringe to the first reactor and the whole reaction mixture was cooled to -78°C with an acetone/$CO_{2(s)}$ bath. A *n*-BuLi solution (1.6 M in hexane, 3.2 mL, 0.0051 mol) was then added via syringe to the reaction mixture and after that, dry THF (3 mL) was added dropwise with a syringe observing the concomitant formation of a white precipitate which was attributed to the insoluble lithium-thiophene anion. The mixture was stirred at the same temperature for 30 min and during this time in the cooled Schlenk reactor were placed THF (4 mL) and perfluorocylopentene (0.32 mL, 0.51 g, 0.0024 mol). The latter solution was then slowly added dropwise via cannula to the lithium-thiophene mixture, further cold THF (5 mL) was added and the system stirred for 30 min. The solution was then allowed to warm up to room temperature and consequently quenched with aqueous HCl (1N, 20 mL). The product was extracted with diethyl ether (3x20 mL) and the combined organic phases dried over $MgSO_4$. The solvent was removed under reduced pressure and flash chromatography

(petroleum ether 40/60°C as eluent) of the crude mixture yielded an impure amount of product. Pure product was obtained as colorless crystals after crystallization from petroleum ether in 67% yield. The product synthesized with this procedure showed exactly the same characterization data of the product obtained following the above reported traditional procedure.

*Synthesis of 1,2-bis(5-chloro-2-methylthiophen-3-yl)cyclopent-1-ene (**6**)*

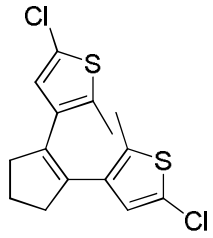

A two necks round bottom flask equipped with a condenser and connected to a vacuum/nitrogen line was flame dried and three vacuum/nitrogen cycles were performed. Subsequently zinc (13.573 g, 0.208 mol) and dry THF (120 mL) were added under nitrogen atmosphere. The mixture was vigorously stirred and cooled at 0°C using an ice bath; after that $TiCl_4$ (5.88 mL, 10.148 g, 0.055 mol) was slowly added via syringe. During the addition $Ti(THF)_2Cl_4$ was formed and the mixture became yellowish. Subsequently the system was refluxed for 1h obtaining a blue mixture containing Ti^{3+} species and subsequently the system was cooled to room temperature. Pyridine (4.9 mL, 4.38 g, 0.055 mol) and **8** (5.00 g, 0.014 mol) were added and the system refluxed for 2h; after that the system was cooled to room temperature and water (10 mL) was added. The mixture was filtered through a silica pad, washed with an hot (50 °C) hexane:ethylacetate mixture (1:1), the combined organic phase dried over $MgSO_4$ and the solvents removed under reduced pressure. Flash chromatography of the crude mixture with petroleum ether as eluent yielded the product in 62% yield as a white oily solid which solidified on standing.

^{1}H-NMR (300.15 MHz, $CDCl_3$): δ 1.89 (s, 6H), 2.02 (q, J=7.5 Hz, 2H), 2.72 (t, J=7.5 Hz, 4H), 5.58 (s, 2H).
^{13}C-NMR (75 MHz, $CDCl_3$): δ 14.30, 22.96, 38.47, 125.33, 126.82, 133.43, 134.57, 134.97.

*Synthesis of 5-chloro-3-(3,3,4,4,5,5-hexafluoro-2-(2-methyl-5-phenylthiophen-3-yl)cyclopent-1-en-1-yl)-2-methylthiophene (**3b**)*

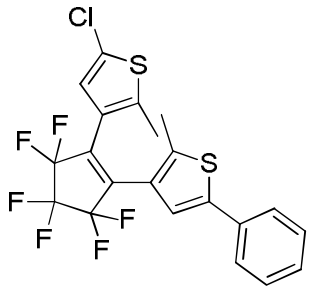

The synthesis of this product is divided in two parts. *Part A* concerns the preparation of THF solution of a thiophene-borate reactant bearing the dithyenilethene moiety suitable for the Suzuki cross coupling. *Part B* describes the cross-coupling reaction.

Part A. A two necks round bottom flask equipped with rubber septum and linked to a vacuum/nitrogen line was flame dried and 3 vacuum/nitrogen cycles performed, subsequently under nitrogen atmosphere **5** (0.5 g, 0.0011 mol), dry THF (1 mL), dry *n*-hexane (10 mL) were added and the resulting mixture stirred until complete dissolution of the reactant. When the solution was perfectly homogeneous it was cooled to 0°C with an ice bath and *n*-BuLi (1.6 M in hexane, 0.69 mL, 0.0011 mol) was slowly added dropwise. The solution became dark and after 15 min under stirring at the same temperature and *tris*-*n*-butylborate (0.6 mL, 0.51 g, 0.0022 mol) was added in one portion with a syringe. The solution became clear and it was left under stirring for 10 min at 0°C and 1h at room temperature. The solvent was removed under reduced pressure and dry THF (10 mL) was added.

Part B. To a two necks round bottom flask equipped with a condenser THF (20 mL), $Pd(PPh_3)_4$ (0.064 g, $5.5 \cdot 10^{-5}$ mol) and bromobenzene (0.23 mL, 0.345 g, 0.0022 mol) were added and the resulting solution was heated to 70°C. After 15 min at this temperature aqueous K_2CO_3 (2 M, 2.50 mL, 0.005 mol) and ethylene glycol (10 drops) were added and to the well stirred solution at the same temperature the THF solution containing the borate prepared in *Part A* was slowly added via syringe. The mixture was left at 70°C for 16h and then cooled to room temperature. Water (20 mL) was then added and the product extracted with diethyl ether (3x25 mL). The combined organic phases were dried over $MgSO_4$ and concentrated under reduced pressure. The product was obtained as white oily solid in 57% yield after flash chromatography using petroleum ether as eluent.

^{1}H-NMR (400 MHz, $CDCl_3$): δ 1.90 (s, 3H), 1.99 (s, 3H), 6.95 (s, 1H), 7.26 (s, 1H), 7.35-7.26 (m, 1H), 7.43-7.35 (m, 2H), 7.61-7.49 (m, 2H).

4,4'-bis(2-(5-chloro-2-methylthiophen-3-yl)-3,3,4,4,5,5-hexafluorocyclopent-1-en-1-yl)-5,5'-dimethyl-2,2'-bithiophene

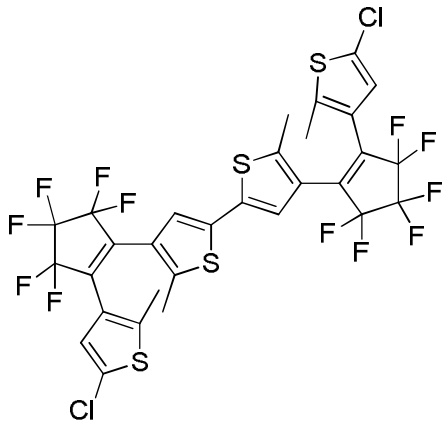

This molecule was obtauined as side-product from the Suzuki cross-coupling reactions used for the synthesis of both **3b** and **3c** and it was isolated by flash chromatography as a violet solid.

^{1}H-NMR (400 MHz, $CDCl_3$): δ 1.91 (s, 3H), 1.96 (3, 3H), 6.90 (s, 1H), 7.03 (s, 1H).
^{19}F- NMR (283 MHz, $CDCl_3$): δ -110.19 (bs, 2F), -110.28 (bs, 2F), -131.91 (m, 2F)
MS (ESI) (*m/z*)= 784.93 (M^+).

*Synthesis of 5-chloro-3-(3,3,4,4,5,5-hexafluoro-2-(5-(4-methoxyphenyl)-2-methylthiophen-3-yl)cyclopent-1-en-1-yl)-2-methylthiophene (**3c**)*

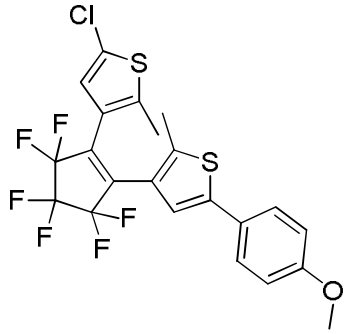

This product was synthesized and isolated following the same procedure used for the synthesis of **3b** employing 4-bromoanisole instead of bromobenzene. The product was isolated as a white oily solid in 55% yield.

^{1}H-NMR (400 MHz, CDCl3) δ 1.89 (s, 3H), 1.96 (s, 3H), 3.84(s, 3H), 6.92 (d, J=8.8 Hz, 3H), 7.12(s, 1H), 7.49 (d, J=8.8 Hz, 2H).

*Synthesis of 5-chloro-2-methyl-3-(2-(2-methyl-5-phenylthiophen-3-yl)cyclopent-1-en-1-yl)thiophene (**4b**)*

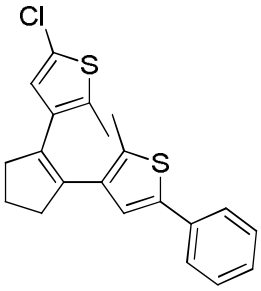

This product was synthesized and isolated following the same procedure used for the synthesis of **3b** employing **6** instead of **5**. The product was isolated as a white oily solid in 55% yield.

1H-NMR (300 MHz, $CDCl_3$): δ 1.94 (s, 3H), 2.05 (s, 3H), 2.08-2.16 (m, 2H), 2.75-2.88 (m, 4H), 6.68 (s, 1H), 7.05 (s, 1H), 7.30-7.45 (m, 5H).

*Synthesis of 5-chloro-3-(2-(5-(4-methoxyphenyl)-2-methylthiophen-3-yl)cyclopent-1-en-1-yl)-2-methylthiophene (**4c**)*

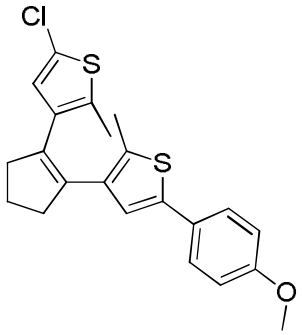

This product was synthesized and isolated following the same procedure used for the synthesis of **3b** employing 4-bromoanisole instead of bromobenzene and **6** instead of **5**. The product was isolated as a white oily solid in 55% yield.

^{1}H-NMR (400 MHz, CDCl3) δ 1.92 (s, 3H), 2.01 (s, 3H), 2.03-2.11 (m, 2H), 2.74-2.85 (m, 4H), 3.83 (s, 3H), 6.66 (s, 1H), 6.90 (s, 1H), 6.91 (d, J=8.8 Hz, 2H), 7.45 (d, J=8.79 Hz, 2H).

*Synthesis of (4-(2-(5-chloro-2-methylthiophen-3-yl)-3,3,4,4,5,5-hexafluorocyclopent-1-en-1-yl)-5-methylthiophen-2-yl)diphenylphosphine (**1a-o**)*

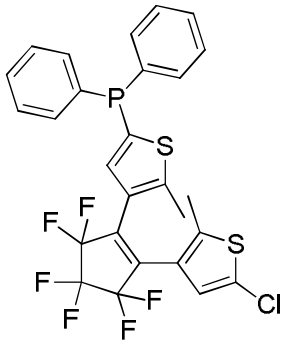

A two necks round bottom flask equipped with a rubber septum and connected to a vacuum/nitrogen line was flame dried and 3 vacuum/nitrogen cycles performed. Subsequently under nitrogen atmosphere ***5*** (0.5 g, 0.0011 mol), dry THF (1 mL) and dry *n*-hexane (10 mL) were added and the resulting mixture stirred until complete dissolution of the reactant occurred. When the solution was perfectly homogeneous it was cooled to 0°C with an ice bath and *n*-BuLi (1.6 M in hexane, 0.69 mL, 0.0011 mol) was slowly added dropwise. The solution became dark and after 15 min of stirring at the same temperature, diphenylchlorophosphine (0.4 mL, 0.48 g, 0.0022 mol) was added in one pot with a syringe. The resulting solution became clear and the system was allowed to warm up to room temperature and stirring was continued for 16h. Subsequently the crude reaction mixture was dried under reduced pressure, diluted with dry dichloromethane (10 mL), adsorbed on silica and loaded at the top of a column for flash chromatographic separation using hexane:dichloromethane (9:1) as eluent. The product was isolated as a white oily solid in 42% yield.

^{1}H-NMR (300 MHz, $CDCl_3$): δ 1.86 (s, 3H), 1.99 (s, 3H), 6.87 (s, 1H), 7.22 (bd, J_{H-P}=6.0 Hz, 1H). 7.40-7.31 (m, 10 H).
^{31}P-NMR (122 MHz, $CDCl_3$): δ -18.94.
^{19}F- NMR (283 MHz, $CDCl_3$): δ -109.99 (bs, 2F), -110.14 (bs, 2F), -131.83 (q, J=5.67 Hz, 2F).
MS (ESI) (*m/z*): 587 (M^+).
HRMS calc. for $C_{27}H_{18}ClF_6PS_2$:587.01803, found: 587.02530.

*Synthesis of (4-(3,3,4,4,5,5-hexafluoro-2-(2-methyl-5-phenylthiophen-3-yl)cyclopent-1-en-1-yl)-5-methylthiophen-2-yl)diphenylphosphine (**1b-o**)*

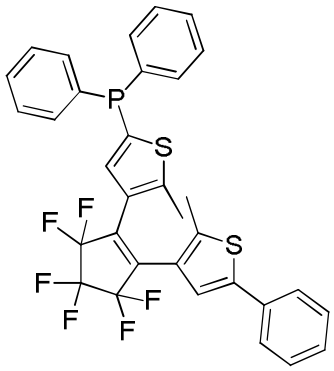

A two necks round bottom flask connected to a vacuum/nitrogen line was flame dried and 3 vacuum/nitrogen cycles were performed. Subsequently **3b** (0.157 g, $3.3\cdot10^{-4}$ mol) and dry diethyl ether (5 mL) were added and the resulting solution cooled at -78°C with acetone/$CO_{2(s)}$ bath. At this temperature *t*-BuLi (1.7 M in pentane, 0.21 mL, $3.6\cdot10^{-4}$ mol) was slowly added dropwise and the solution stirred at the same temperature for 30 min. After that a solution of diphenylchlorophosphine in dry diethyl ether (0.5M, 1.44 mL,$7.2\cdot10^{-4}$ mol) was added via syringe and stirring was continued for 15 min at -78°C and for 16h room temperature. Subsequently the crude reaction mixture was dried under reduced pressure, diluted with dry dichloromethane (10 mL), absorbed on silica and loaded on a flash chromatographic column using hexane:dichloromethane (9:1) as eluent. The product was isolated as a white oily solid in 63% yield.

^{1}H-NMR (300 MHz, $CDCl_3$): δ 1.95 (s, 3H), 1.96 (s, 3H), 7.21 (s, 1H), 7.29 (d, J_{H-P}=7.1 Hz, 1H), 7.31-7.54 (m, 15 H).
^{31}P-NMR (121 MHz, $CDCl_3$): δ -18.92.
^{13}C-NMR(75 MHz, $CDCl_3$): δ 14.58, 14.90, 122.59, 125.74, 128.08, 128.67, 128.77, 129.16, 129.26, 131.73, 131.87, 132.98, 133.24, 133.43, 136.07, 136.47, 136.87, 137.26, 137.37, 141.13, 142.43, 148.62 (not all ^{13}C were detected due to high substitution pattern and to coupling with ^{19}F and ^{31}P; J_{C-P} was detected and reported whenever possible)**.**
^{19}F-NMR (MHz, $CDCl_3$): δ -109.89 (bs, 2F), -109.95 (bs, 2F), -131.18 (q, J=5.6 Hz, 2F).
MS (ESI) (m/z): 629 (M^++ H).
HRMS calc. for $C_{33}H_{23}F_6PS_2$: 628.08830, found: 629.09557.

*Synthesis of (4-(3,3,4,4,5,5-hexafluoro-2-(5-(4-methoxyphenyl)-2-methylthiophen-3-yl)cyclopent-1-en-1-yl)-5-methylthiophen-2-yl)diphenylphosphine (**1c-o**)*

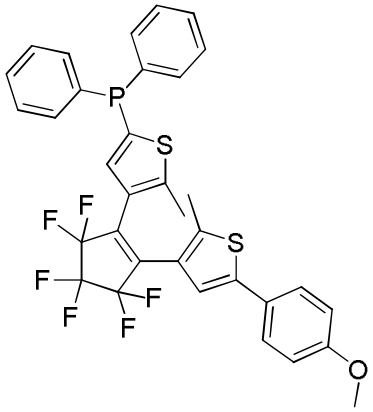

This product was synthesized and isolated following the same procedure used for the preparation of **1b-o** replacing **3b** with **3c**. The product was obtained as a white oily solid in 60% yield.

^{1}H-NMR (300 MHz, $CDCl_3$): δ 1.94 (s, 3H), 1.98 (s, 3H), 3.85 (s, 3H), 6.92 (d, J=8.8 Hz, 2H), 7.10 (s, 1H), 7.28 (d, J_{H-P}=6.2 Hz, 1H), 7.38-7.33 (m, 10 H), 7.45 (d, J=8.8 Hz, 2H).
^{31}P-NMR (121 MHz, $CDCl_3$): δ -18.92.
^{13}C-NMR(75 MHz, $CDCl_3$): δ 14.51, 14.89, 55.53, 114.52, 121.43, 125.78, 126.28, 127.05, 128.66, 128.76, 129.24, 132.96, 133.24, 136.11, 136.49, 136.77, 137.18, 137.28, 137.39, 140.14, 142.35, 148.62, 159.65 (not all ^{13}C were detected due to high substitution pattern and to ^{19}F and ^{31}P coupling; J_{C-P} was detected and reported whenever possible).
^{19}F-NMR (282 MHz, $CDCl_3$): δ -109.83 (bs, 2F), -109.94 (bs, 2F), -131.79 (q, J=5.9 Hz, 2F).
MS (ESI) (m/z): 659 (M^++H).
HRMS calc. for $C_{34}H_{25}F_6OPS_2$: 658.09886, found: 659.10614.

*Synthesis of (4-(2-(5-chloro-2-methylthiophen-3-yl)cyclopent-1-en-1-yl)-5-methylthiophen-2-yl)diphenylphosphine (**2a-o**)*

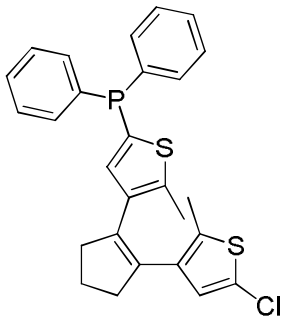

This product was synthesized and purified following the same procedure reported for the preparation of **1a-o** using **6** instead **5**. The product was obtained as a white oily solid in 48% yield.

^{1}H-NMR (300 MHz, $CDCl_3$): δ 1.92 (s, 3H), 2.05 (s, 3H), 2.10-199 (m, 2H), 2.84-2.68 (m, 4H), 6.59 (s, 1H), 6.97 (d, J_{H-P}=6.3 Hz, 1H), 7.43-7.30 (bs, 10H).

^{31}P-NMR (121 MHz, $CDCl_3$): δ -20.94.
^{13}C-NMR(75 MHz, $CDCl_3$): δ 14.12, 14.63, 22.96, 38.22, 38.25, 125.06, 125.97, 126.89, 128.57 (d, J_{C-P}=6.9 Hz), 128.78, 133.00 (d, J_{C-P}=19.4 Hz), 133.58, 134.09, 135.08, 135.21, 136.87 (d, J_{C-P}=7.7 Hz), 137.75 (d, JC-P=26.1 Hz), 130.01(d, JC-P=8.6 Hz), 141.92 (not all ^{13}C were detected due to high substitution pattern and to^{31}P coupling; J_{C-P} was detected and reported whenever possible).

*Synthesis of (5-methyl-4-(2-(2-methyl-5-phenylthiophen-3-yl)cyclopent-1-en-1-yl)thiophen-2-yl)diphenylphosphine (**2b-o**)*

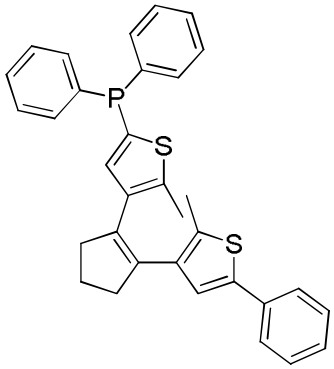

This product was synthesized and purified following the same procedure reported for the preparation of **1b-o** replacing **3b** with **4b**. The product was isolated as a white oily solid in 63% yield.

^{1}H-NMR (MHz, $CDCl_3$): δ 2.00 (s, 3H), 2.01 (s, 3H), 2.12-2.01 (m, 2H), 2.90 -2.70 (m, 4H), 6.96 (s, 1H), 7.01 (d, J_{H-P}=6.6 Hz, 1H), 7.70-7.20 (bs, 15H).
^{31}P-NMR (MHz, $CDCl_3$): δ -20.91.
^{13}C-NMR(MHz, $CDCl_3$): δ 14.50, 14.75, 23.17, 38.40, 38.46, 124.17, 125.44, 127.09, 128. 50 (d, JC-P=6.9 Hz), 128.87 (d, J_{C-P}=7.9 Hz), 133.11 (d, J_{C-P}=19.4 Hz), 134.40, 134.62, 134.64, 135.08, 136.75, 137.26 (d, J_{C-P}=8.0 Hz), 137.91, 138.14, 138.26, 139.82, 142.12 (not all ^{13}C were detected due to high substitution pattern and to^{31}P coupling; J_{C-P} was detected and reported whenever possible.

*Synthesis of (4-(2-(5-(4-methoxyphenyl)-2-methylthiophen-3-yl)cyclopent-1-en-1-yl)-5-methylthiophen-2-yl)diphenylphosphine (**2c-o**)*

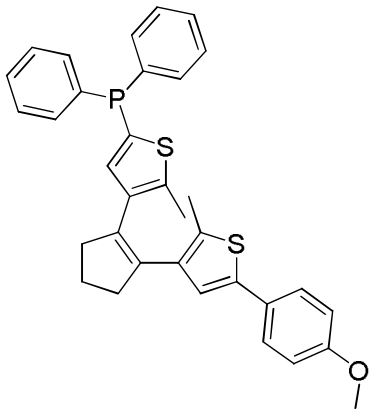

This product was synthesized and purified following the same procedure reported for the preparation of **1c-o** replacing **3c** with **4c**. The product was isolated as a white oily solid in 64% yield.

^{1}H-NMR (MHz, $CDCl_3$): δ 2.20 (s, 3H), 2.21 (s, 3H), 2.25 (q, J=7.2 Hz, 2H), 3.05-2.94 (m, 4H), 4.04 (s, 3H), 7.04 (s, 1H), 7.08 (d, J=8.7 Hz, 2H), 7.22 (d, J_{H-P}=6.3 Hz, 1H), 7.63-7.43 (m, 10H), 7.60 (d, J=8.7 Hz, 2H).
^{31}P-NMR (MHz, $CDCl_3$): δ -20.92.
^{13}C-NMR(MHz, $CDCl_3$): δ 14.29, 14.62, 38.25, 38.33, 55.37, 114.20, 122.97, 126.58, 127.46, 128.31 (d, J_{C-P}=6.9 Hz), 128.67, 132.81, 132.98 (d, J_{C-P}=19.2 Hz), 133.15, 133.20, 134.67 (d, J_{C-P}=19.2 Hz), 136.45, 137.17 (d, J_{C-P}=7.9 Hz), 137.82, 138.02, 138.13, 139.57, 141.96, 158.83.

*Synthesis of (4-(2-(5-chloro-2-methylthiophen-3-yl)-3,3,4,4,5,5-hexafluorocyclopent-1-en-1-yl)-5-methylthiophen-2-yl)diphenylphosphine selenide (**1a-o (Se)**)*

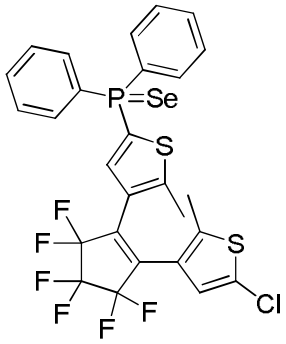

In a two necks round bottom flask equipped with a condenser and connected to a vacuum/nitrogen line, three vacuum/nitrogen cycles were performed and under nitrogen atmosphere **1a-o** (0.050 g, $8.5 \cdot 10^{-5}$ mol), chloroform (ml) and selenium (0.135 g, 0.0017 mol) were added. The mixture was refluxed for 2h; subsequently the reaction crude was allowed to warm up to room temperature and filtered through a silica pad to remove the excess of selenium. The silica pad was eluted with dichloromethane until all the phosphine selenide was collected. After removal of the solvent under reduced pressure, the product was obtained as a white/yellowish solid in quantitative yield.

^{1}H-NMR (MHz, CD_2Cl_2): δ 1.84 (s, 3H), 2.12 (s, 3H), 6.80 (s, 1H), 7.09 (d, JH-P=8.4 Hz, 1 H), 7.57-7.42 (m, 6H), 7.75-7.65 (m, 4H).
^{31}P-NMR (122 MHz, CD_2Cl_2): δ 22.05 (J_{P-Se}=745 Hz).

*Synthesis of (4-(3,3,4,4,5,5-hexafluoro-2-(2-methyl-5-phenylthiophen-3-yl)cyclopent-1-en-1-yl)-5-methylthiophen-2-yl)diphenylphosphine selenide (**1b-o (Se)**)*

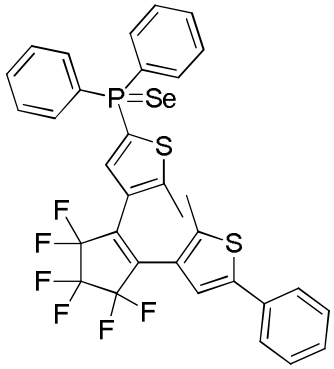

This product was synthesized and purified following the same procedures reported for the preparation of ***1a-o (Se)*** using ***1b-o*** as starting phosphine. The product was isolated as white/yellowish solid in quantitative yield.

^{1}H-NMR (300 MHz, CD_2Cl_2): δ 1.96 (s, 3H), 2.13 (s, 3H), 7.17-7.12 (m, 3H), 7.54-7.30 (m, 11H), 7.76-7.66 (m, 5H).
^{31}P-NMR (121 MHz, CD_2Cl_2): δ 22.08 ($J_{P\text{-}Se}$=744 Hz).

*Synthesis of (4-(3,3,4,4,5,5-hexafluoro-2-(5-(4-methoxyphenyl)-2-methylthiophen-3-yl)cyclopent-1-en-1-yl)-5-methylthiophen-2-yl)diphenylphosphine selenide (**1c-o (Se)**)*

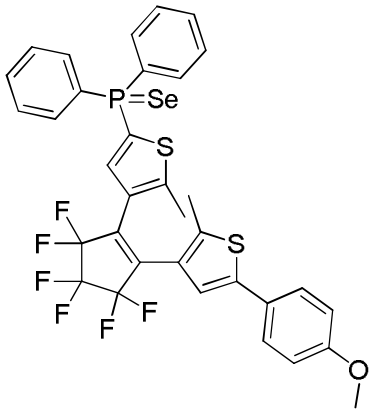

This selenide was synthesized and isolated using the same procedures reported for the preparation of ***1a-o (Se)*** selenide, ***1b-o***. The product was obtained as a white solid in quantitative yield.

^{1}H-NMR (300 MHz, CD_2Cl_2): δ 1.95 (s, 3H), 2.15 (s, 3H), 3.83 (s, 3H), 6.93 (d, J=8.8 Hz, 2H, 7.07 (s, 1H), 7.14 (d, JH-P=8.5 Hz), 7.55-7.38 (m, 7H), 7.75-7.64 (m, 5H).
^{31}P-NMR (121 MHz, CD_2Cl_2): δ 21.95 ($J_{P\text{-}Se}$=743 Hz).

*Synthesis of (4-(2-(5-chloro-2-methylthiophen-3-yl)cyclopent-1-en-1-yl)-5-methylthiophen-2-yl)diphenylphosphine selenide (**2a-o (Se)**)*

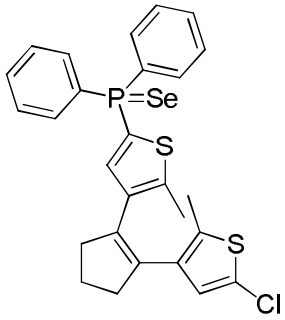

This product was synthesized and purified following the same strategy reported for the preparation of ***1a-o (Se)***, using ***2a-o*** as starting phosphine. The product was obtained as a white/yellowish solid in quantitative yield.

^{1}H-NMR (MHz, CD_2Cl_2): δ 2.08 (s, 3H), 2.21 (q, J=7.2 Hz, 2H), 2.36 (s, 3H), 3.02-2.82 (m, 4H), 6.70 (s, 1H), 7.10 (d, J_{H-P}=9.0 Hz, 1H), 7.72-7.60 (m, 6H), 7.95-7.85 (m, 4H).
^{31}P-NMR (MHz, CD_2Cl_2): δ 20.32 (JP-Se=737 Hz).

*Synthesis of (5-methyl-4-(2-(2-methyl-5-phenylthiophen-3-yl)cyclopent-1-en-1-yl)thiophen-2-yl)diphenylphosphine selenide (**2b-o (Se)**)*

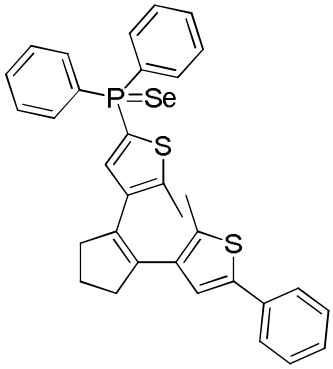

This selenide was synthesized and purified following the same procedures reported for the preparation of ***1a-o (Se)***, using ***2b-o*** as starting phosphine. The product was isolated as yellowish solid in quantitative yield.

^{1}H-NMR (MHz, CD_2Cl_2): δ 2.01 (s, 3H), 2.05 (q, J=7.5 Hz), 2.21 (s, 3H), 2.84-2.62 (m, 4H), , 6.87 (d, J_{H-P}=8.7 Hz), 6.95 (s, 1H), 7.70-7.22 (m, 15H).
^{31}P-NMR (MHz, CD_2Cl_2): δ 20.17 (J_{P-Se}=740 Hz).

*Synthesis of (4-(2-(5-(4-methoxyphenyl)-2-methylthiophen-3-yl)cyclopent-1-en-1-yl)-5-methylthiophen-2-yl)diphenylphosphine selenide (**2c-o (Se)**)*

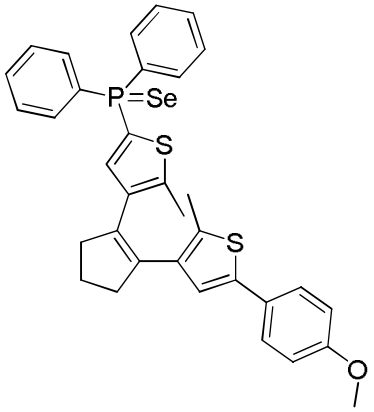

This product was obtained following the same synthetic and purification procedures reported for the preparation of ***1a-o (Se)***, using ***2c-o*** as starting phosphine. The product was obtained as white solid in quantitative yield.

^{1}H-NMR (300.15 MHz, CD_2Cl_2): δ 1.98 (s, 3H), 2.04 (q, J=7.5 Hz), 2.21 (s, 3H), 2.83-2.71 (m, 4H), 3.82 (s, 3H), 6.82 (s, 1H), 6.86 (d, J_{H-P}=8.7 Hz, 1H), 6,89 (d, J=8.7 Hz, 2H), 7.48-7.30 (m, 7H), 7.70-7.58 (m, 4H).
^{31}P-NMR (121.5 MHz, CD_2Cl_2): δ 20.14 (J_{P-Se}=737 Hz).

Synthesis of Rh(I) Vaska type complex bearing (4-(2-(5-chloro-2-methylthiophen-3-yl)-3,3,4,4,5,5-hexafluorocyclopent-1-en-1-yl)-5-methylthiophen-2-yl)diphenylphosphine

***trans*-[Rh(CO)Cl(1a-o)$_2$]**

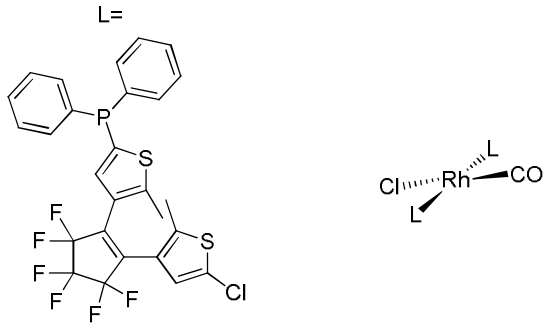

In a two necks round bottom flask connected to a nitrogen/vacuum line three vacuum/nitrogen cycles were performed and subsequently under nitrogen atmosphere dry dichloromethane (5 mL) and $[Rh(CO)_2]_2Cl_2$ (0.0167g, $4.3\cdot10^{-5}$ mol) were added. To the well stirred reaction mixture, at room temperature, a dichloromethane solution of **1a-o** (0.034 M, 5 mL, $1.7\cdot10^{-4}$ mol) was added dropwise with a syringe. During the addition carbon monoxide evolution was observed and after 2h stirring at the same temperature the solvent was removed under vacuum yielding a yellow solid. The product obtained in quantitative yield was not further purified.

^{1}H-NMR (MHz, CD_2Cl_2): δ 1.84 (s, 3H), 2.06 (s, 3H), 6.86 (s, 1H), 7.58-7.38 (m, 6H), 7.75-7.60 (m, 5H).
^{31}P-NMR (121 MHz, CD_2Cl_2): δ 19.30 (J_{P-Rh}=128 Hz).
IR (CH_2Cl_2, cm^{-1}): 1986.

Synthesis of Rh(I) Vaska type complex bearing (4-(3,3,4,4,5,5-hexafluoro-2-(2-methyl-5-phenylthiophen-3-yl)cyclopent-1-en-1-yl)-5-methylthiophen-2-yl)diphenylphosphine

***trans*-[Rh(CO)Cl(1b-o)$_2$]**

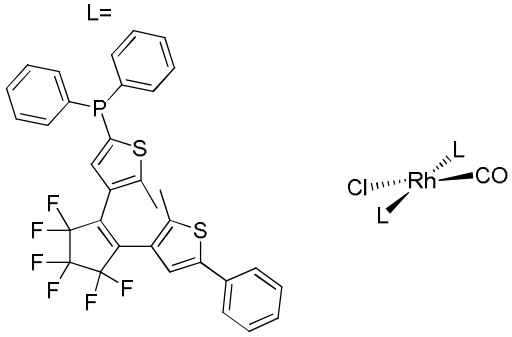

This complex was obtained following the same procedure reported for the preparation of ***trans*-[Rh(CO)Cl(1a-o)$_2$]**, using **1b-o** as starting phosphine. The product was obtained in quantitative yield as a yellow solid.

^{1}H-NMR (MHz, CD_2Cl_2): δ 1.95 (s, 3H), 2.05 (s, 3H), 7.21 (s, 1H), 7.72-7.25 (m, 16H).
^{31}P-NMR (MHz, CD_2Cl_2): δ 19.32 (J_{P-Rh}=129 Hz).
IR (CH_2Cl_2, cm^{-1}): 1983.

Synthesis of *Rh(I) Vaska type complex bearing (4-(3,3,4,4,5,5-hexafluoro-2-(5-(4-methoxyphenyl)-2-methylthiophen-3-yl)cyclopent-1-en-1-yl)-5-methylthiophen-2-yl)diphenylphosphine*

***trans*-[Rh(CO)Cl(1c-o)$_2$]**

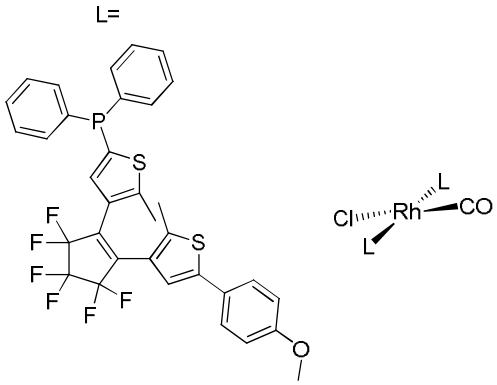

The complex was obtained following the same procedure reported for the preparation of ***trans*-[Rh(CO)Cl(1a-o)$_2$]**, using **1c-o** as starting phosphine. The product was obtained as a yellow solid in quantitative yield.

^{1}H-NMR (MHz, $CDCl_3$): δ 1.96 (s, 3H), 2.05 (s, 3H), 6.92 (d, J=8.6 Hz, 2H), 7.13 (s, 1H), 7.60-7.30 (m, 13H).
^{31}P-NMR (MHz, $CDCl_3$): δ 20 (bs).
IR (CH_2Cl_2, cm^{-1}): 1983.

Synthesis of *Rh(I) Vaska type complex bearing (4-(2-(5-chloro-2-methylthiophen-3-yl)cyclopent-1-en-1-yl)-5-methylthiophen-2-yl)diphenylphosphine*

***trans*-[Rh(CO)Cl(2a-o)$_2$]**

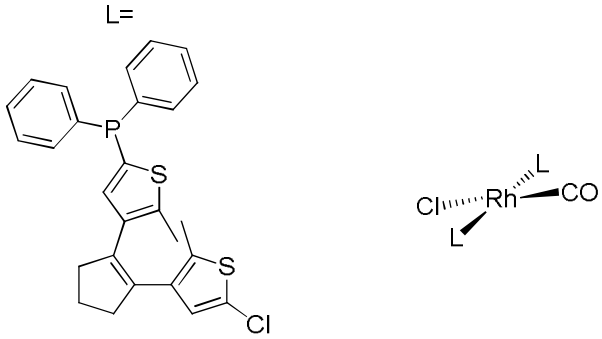

This complex was obtained following the same procedure reported for the preparation of ***trans*-[Rh(CO)Cl(1a-o)$_2$]**, **2a-o** as starting phosphine. The product was obtained as a yellow solid in quantitative yield.

^{1}H-NMR (MHz, CD_2Cl_2): δ 1.88 (s, 3H), 2.02 (q, J=7.5 Hz, 2H), 2.10 (s, 3H), 2.82-2.65 (m, 4H), 6.56 (s, 1H), 7.20 (d, J_{H-P}=6.9 Hz, 1H), 7.52-7.38 (m, 6H), 7.75-7.60 (m, 4H).
^{31}P-NMR (MHz, CD_2Cl_2): δ 16.41 (d, J_{P-Rh}=127 Hz).
IR (CH_2Cl_2, cm^{-1}): 1981.

Synthesis of Rh(I) Vaska type complex bearing (5-methyl-4-(2-(2-methyl-5-phenylthiophen-3-yl)cyclopent-1-en-1-yl)thiophen-2-yl)diphenylphosphine

***trans*-[Rh(CO)Cl(2b-o)$_2$]**

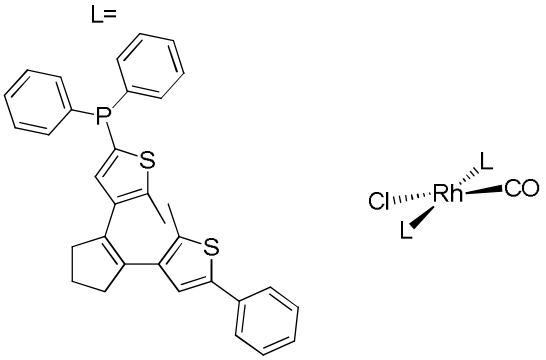

This compound was obtained following the same procedure reported for the preparation of ***trans*-[Rh(CO)Cl(1a-o)$_2$]**, using **2b-o** as starting phosphine. The product was isolated as a yellow solid in quantitative yield.

^{1}H-NMR (MHz, $CDCl_3$): δ 2.01 (s, 3H), 2.10-1.98 (m, 2H), 2.09 (s, 3H), 2.79 (bt, J=7.4 Hz, 4H), 6.96 (s, 1H), 7.50-7.20 (m, 12H), 7.66-7.57 (m, 4H).
^{31}P-NMR (MHz, $CDCl_3$): δ 16.42 ($J_{P\text{-}Rh}$=127 Hz).
IR (CH_2Cl_2, cm^{-1}): 1981.

Synthesis of Rh(I) Vaska type complex bearing (4-(2-(5-(4-methoxyphenyl)-2-methylthiophen-3-yl)cyclopent-1-en-1-yl)-5-methylthiophen-2-yl)diphenylphosphine

***trans*-[Rh(CO)Cl(2c-o)$_2$]**

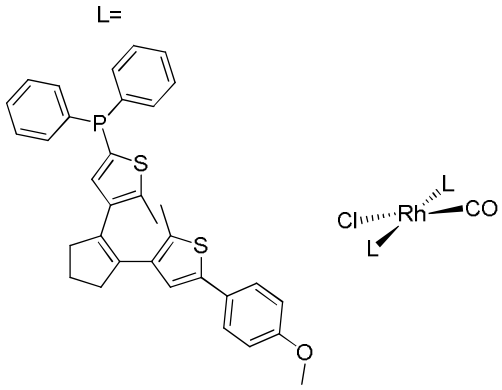

This compound was obtained following the same procedure reported for the preparation of ***trans*-[Rh(CO)Cl(1a-o)$_2$]**, **2c-o** as starting phosphine. The product was obtained as a yellow solid in quantitative yield.

^{1}H-NMR (MHz, CD_2Cl_2): δ 1.99 (s, 3H), 2.04 (q, J=7.5 Hz, 2H), 2.09 (s, 3H), 2.78 (bt, J=7.5 Hz, 4H), 3.79 (s, 3H), 6.90-6.80 (m, 3H), 7.43-7.21 (m, 8H), 7.67-7.56 (m, 4H).
^{31}P-NMR (MHz, CD_2Cl_2): δ 16.40 (d, $J_{P\text{-}Rh}$=126 Hz).
IR (CH_2Cl_2, cm^{-1}): 1981.

PHOTOMODULABLE INHIBITORS FOR SUPRAMOLECULAR CATALYSTS

Supramolecular interactions have been proving to be useful in catalysis when the host directly binds the substrate. Supramolecular hosts are of great interest because of their enzyme-like non-covalent interactions with substrates; one of the best example of supramolecular catalyst is represented by *β*-cyclodextrin while one of the most interesting supramolecular host is the hexamer obtained by the hydrogen bonding self-assembly of six resorcin[4]arene molecules which showed to be able to encapsulate both large organic molecules and metallorganic complexes.

Recently new attentions have been directed to the possibility of merging the photo-modulation properties of certain chromophores with the host-guest ability of *β*-cyclodextrin, allowing the preparation of the supramolecular photo-regulated systems.[149] Many of these systems take advantage from the different ability of *Z* and *E* isomers of an azobenzene moiety to be encapsulated by *β*-cyclodextrin and this combination of host and photo-modulable guest has been widely used in the realization of photomodulable catalytic systems. More precisely the different host guest skills are an expression of the different geometrical shape of the *Z* and *E* isomers of the azobenzene. Diarylethenes molecules are another well-known class of chromophores and their supramolecular interactions with host systems such as cyclodextrin are, to the best of our knowledge, unknown.

Design of the systems

Since we have been interested in the development of photo-modulable catalytic systems, we decided to study the host-guest interactions of dithienylethenes species with two different host systems. The first system considered is constituted by the hexamer (**$3_6 \cdot 8H_2O$**) obtained from the self-assembly of six resorcin[4]arene molecules **3** (equipped with long alkyl chains) in chloroform which is characterized by an internal volume of 1375 $Å^3$, with an internal diameter of 14 Å usually filled by six to eight solvent molecules.[55,56] The second system studied is constituted by the *β*-cyclodextrin (***β*-CD**) which is a 7-membered sugar cyclic molecule with overall conical shape with an internal diameter of 7 Å.

The dithienylethene molecule chosen for this study is equipped with two pyridine moieties in the thiophene rings. Alkylation with methyl trifluoromethanesulfonate yields a *bis*-pyridinium ion **5o** which shows two important features: *i)* a double positive charge, which makes it a good guest for the hexamer; *ii)* water solubility which gives access to its interaction with *β*-cyclodextrin thanks to hydrophobic effect. The chosen *bis*-pyridinium ion was obtained from alkylation of the *bis*-pyridine dithienyl cyclopentene which was synthesized by Suzuki cross coupling between suitable pyridine and diarylethene molecules (Scheme 51).

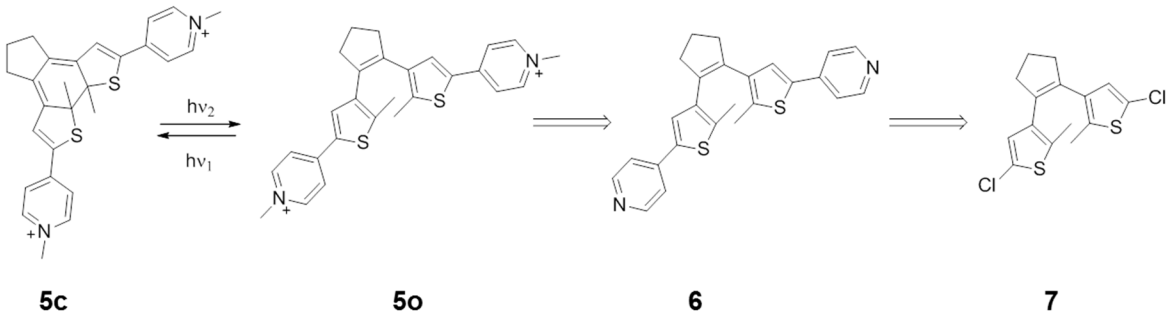

Scheme 51. Retrosynthetic approach for the synthesis of the desired photochromic *bis*-pyridinium cationic guest **5o**. The starting dithienylethene **7** is the same one previously used in the synthesis of diarylethene-based phosphines discussed in the previous chapter.

Geometrical optimization of the *bis*-cation revealed a distance of 16.2 Å between the two pyridinium methyl carbons for **5o**, while 17.4 Å was found for the **5c**. These values are close to the internal diameter of the hexamer and it seems reasonable that the encapsulation could be successful, especially for the less rigid open isomer. Measurement of the maximum width of the molecule revealed 6 to 7 Å width for the open and closed forms, respectively.[n] These values are comparable to the internal diameter of the ***β*-CD** and this supports in principle an *host-guest* interaction between the two.

Scheme 53 reports the expected supramolecular interactions between the hexamer (**$3_6 \cdot 8H_2O$**) and both **5o** and **5c**. Since resorcin[4]arene is known to self-assemble in apolar solvents like chloroform and benzene, and since the inner cavity of the hexamer clearly resembles an enzyme's pocket, the proposed strategy for the control of the electronic and geometric properties of such cavity could be considered at least an allosteric control of supramolecular catalyst operating in organic media.

Conversely the interactions between the photomodulable guest and ***β*-CD** could be considered a useful strategy for the control of supramolecular catalyst in aqueous media (Scheme 52). Indeed ***β*-CD** is known catalyze reactions by formation of inclusion complexes between reactants and its inner cavity. When **5o** and **5**c are used as competitive guests it may be argued that the two photochromic forms will display different affinity for ***β*-CD**'s cavity and, by virtue of this different availability of the supramolecular catalyst should be expected.

n Geometrical optimization at semi empirical PM3 level.

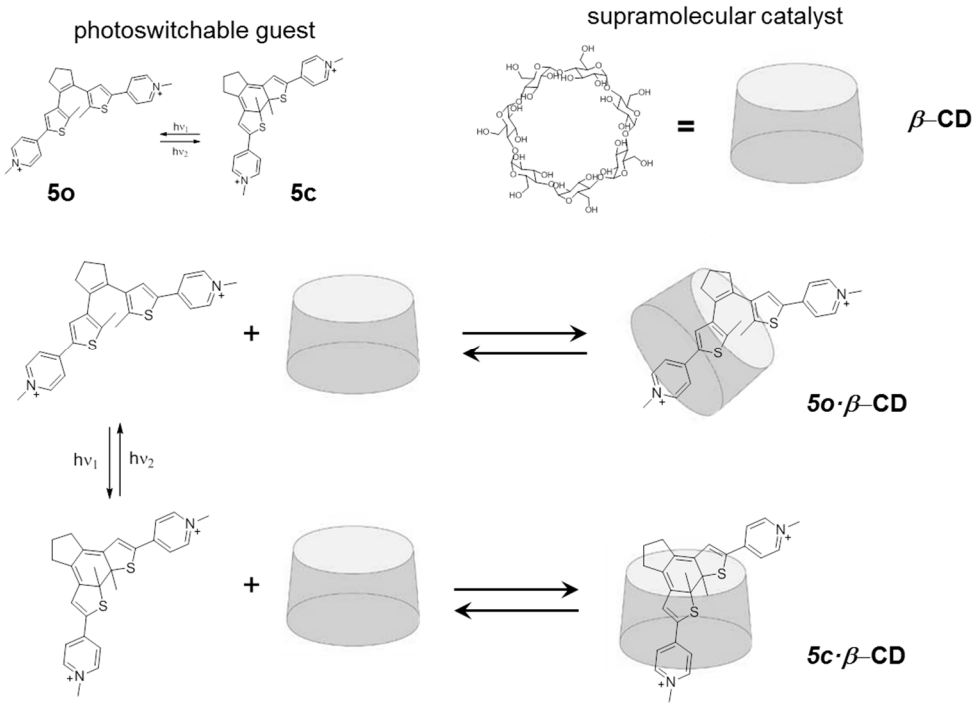

Scheme 52. The two different photochromic forms of the guest molecule **5o** and **5c** hosted within the cavity of ***β*-CD**, yielding two different inclusion complexes.

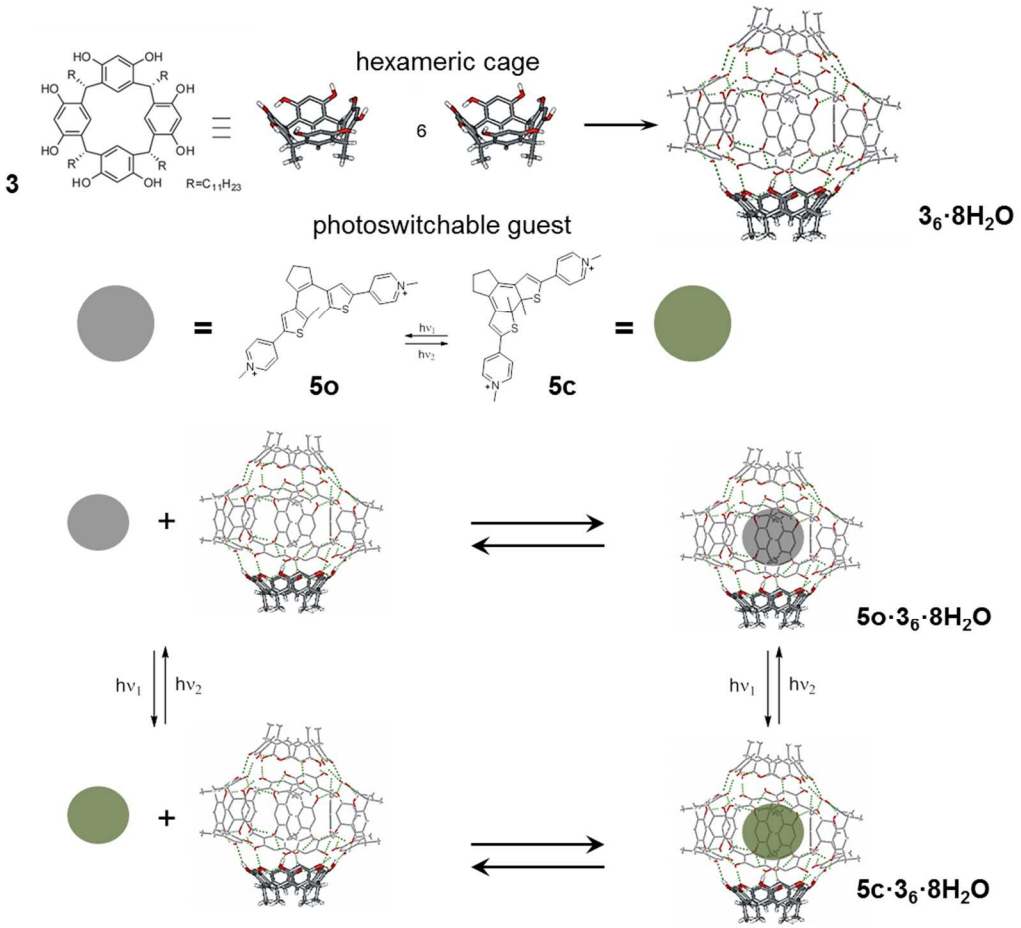

Scheme 53. The two different photochromic forms of the guest molecule **5o** and **5c** hosted within the cavity of the hexameric-cage $\mathbf{3_6 \cdot 8H_2O}$ yielding two geometrically different internal environments.

Synthesis of the Photoswitchable guest

*Synthesis of 1,2-bis(2-methyl-5-(pyridin-4-yl)thiophen-3-yl)cyclopent-1-ene (**6**)*

The *bis*-pyridine-based dithienyl cyclopentene was synthesized using a known and previously used procedure, as reported in Scheme 54.

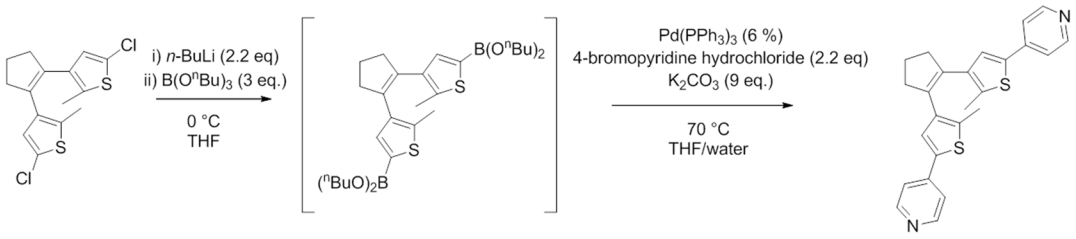

Scheme 54. Synthesis of the dithienyl cyclopentene unit bearing two pyridine moieties in the thiophene rings.

The first part of the synthesis consisted in the preparation of a *bis*-thienyl-borate suitable for the cross coupling reaction. Such product was obtained by two consecutive reactions, firstly chlorine-lithium exchange was performed in dry THF at 0°C and then the *bis*-thienyl-lithium obtained species was reacted with *tris*-*n*-butylborate. In the second part of the reaction, the previously prepared THF solution containing the thienyl-borate was added dropwise with a syringe to a refluxing THF/water solution of potassium carbonate, 4-bromopyridine and Pd(0)*tetrakis*-triphenylphosphine. The bromo-pyridine was added to the reaction mixture as its hydrochloride salt since it is not stable as it is and it needs to be unlocked prior to use by reaction with a base. When the addition was completed, the mixture was refluxed for 16h and product **6** extracted with diethyl ether and isolated by flash chromatography in 62% yield. The yield obtained with this improved procedure is considerably higher (2.7 times higher) than that obtained by other authors for the same product.[150] The product appears as a colorless solid which becomes light-violet in the presence of ambient light irradiation and it was characterized by ^{1}H-NMR and ^{13}C-NMR obtaining data consistent with those reported in the literature.[150]

*Synthesis of 4,4'-(4,4'-(cyclopent-1-ene-1,2-diyl)bis(5-methylthiophene-4,2-diyl))bis(1-methylpyridin-1-ium) bis(trifluoromethanesulfonate) (**5o**)*

The *bis*-pyridinium was synthesized following the known procedure reported in Scheme 55.

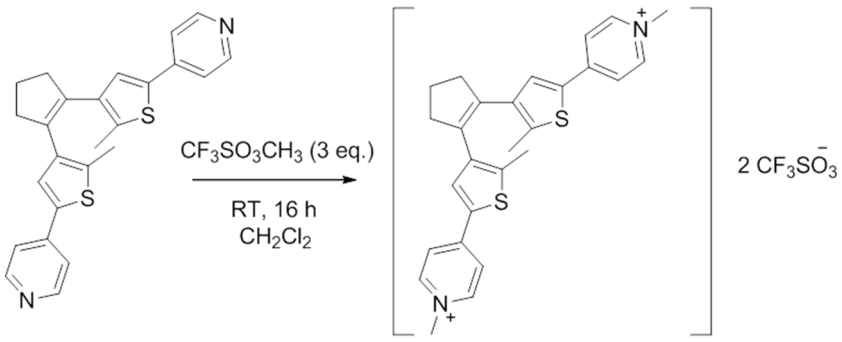

Scheme 55. Alkylation of the *bis*-pyridine molecule with methyl trifluoromethanesulfonate.

The *bis*-pyridine **6** obtained in the previous step was solubilized in dry dichloromethane and reacted with an excess of methyl trifluoromethanesulfonate. During the addition the light-violet solution turned greenish and after stirring for 16h the product was isolated by removing both the solvent and the excess of alkylating agent under reduced pressure. The product was obtained in quantitative yield as a greenish solid that was characterized by ^{1}H-NMR and ^{13}C-NMR analysis.

Photochemical behavior of the photo-modulable bis-cationic inhibitor

The switching between the two photochromic forms of the *bis*-cationic guest was studied in water at different irradiation times. Figure 40 reports the ^{1}H-NMR spectra of a $1 \cdot 10^{-3}$M solution of the photomodulable guest upon different irradiation times at 365 nm. From the latter solution were also obtained more diluted solutions (10^{-5} M), which were used for UV-Vis analysis.

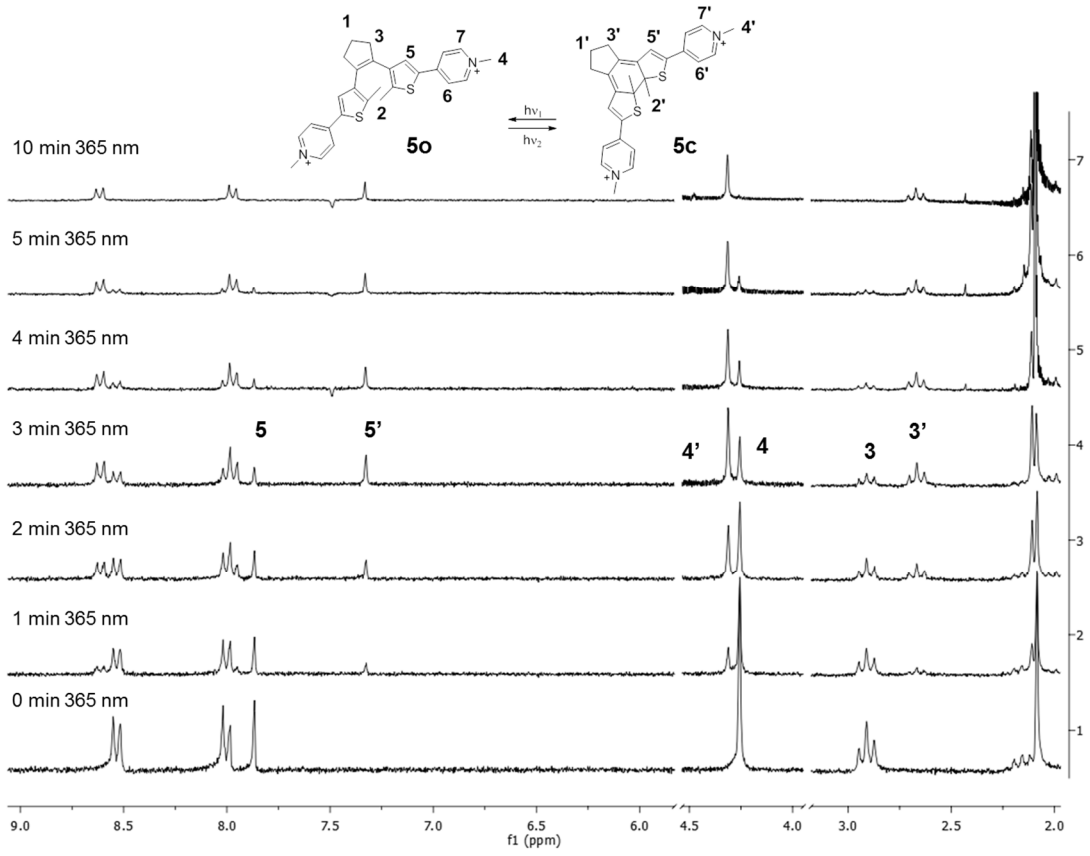

Figure 40. ^{1}H-NMR spectra at different irradiation times for the ring closing reaction of **5o** (10^{-3} M solution in water-d).

As can be easily noticed from the ^{1}H-NMR spectra reported in Figure 40, after 5 min of irradiation more than 80% of **5o** was converted into **5c** and, in order to achieve complete conversion, 10 minutes of irradiation was requested. The ring closing reaction is characterized by the up-field shift of several resonance of the *bis*-cation. As a remarkable example, the proton of the thiophene moiety shifted from 7.70 ppm in the open isomer to 7.19 ppm in the closed one; other protons showing enhanced variation of their chemical shifts were the allylic

protons of the cyclopentene bridging unit which shifted from 2.76 ppm in the open isomer to 2.53 ppm in the closed one. Regarding the UV-Vis properties of the *bis*-pyridinium, it was observed that **5o** adsorbs in the UV region until about 470 nm showing two relative maxima at 385 and 336 nm, while **5c** showed two new maxima, one at 444 nm and one in the visible region at 685 nm together with two isosbestic points for the photochromic forms at 312 and 425 nm. The conversion between the two forms, determined by ^{1}H-NMR spectroscopy, was subsequently correlated with the absorbance at the new determined maximum, revealing an extinction molar coefficient for the closed isomer at 685 nm of about 18350 ($cm^{-1} \cdot M^{-1}$).

Host guest interactions with the resorcin[4]arene hexamer

Both open and closed inhibitors turned out to be suitable guests for the capsule $\mathbf{3_6 \cdot 8H_2O}$ as reported in Figure 41 where it is shown that the resonances of the free cations completely disappeared upon addition of six equivalents of **3** (Figure 41B). For **5o** broad resonances for the encapsulated inhibitor are observed at 6.7 ppm for the aromatic residues and in the region -0.6 ppm for the aliphatic moieties. Cation **5c** cannot be easily generated in chloroform-d by UV irradiation, rather it was obtained in acetonitrile-d upon 1h irradiation with an UV lamp (Figure 41E). The product was only sparingly soluble in chloroform-d as observed from the presence of weak broad resonances in Figure 41C but it was completely dissolved upon addition of **3** (Figure 41D) observing only very broad resonances for the hosted cationic inhibitor. NMR experiments carried out in the range -20°C up to 50°C did not provide more resolved spectra.

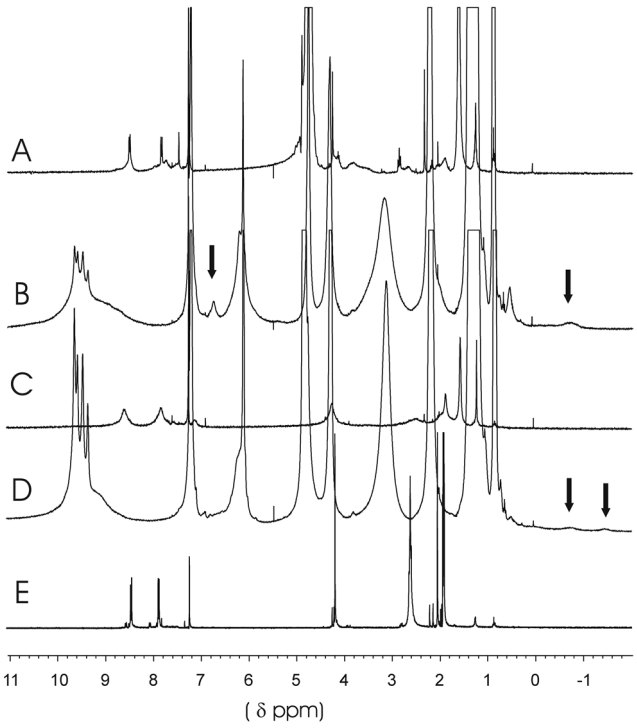

Figure 41.. **A)** free open cation **5o** (6 mM) in water saturated chloroform-d; **B) 5o** open *bis*-cation(6 mM) and **3** (36 mM); **C) 5c** closed *bis*-cation (6 mM); **D) 5c** (6 mM) and **3** (36 mM); **E) 5c** closed *bis*-cation (6 mM in acetonitrile-d_3); ↓ encapsulated inhibitor.

Photochemical behavior with the hexamer

When a chloroform solution containing the open isomer **5o** and resorcin[4]arene **3** in a 1:6 ratio was irradiated at 365 nm, no appreciable coloration of the sample was observed and, as evaluated by ^{1}H-NMR spectroscopy, the formation of the closed isomer **5c** resulted inhibited. Analogous results were obtained using directly **5c** when trying to open it back by irradiation with visible light. This brings to the conclusion that the ring closing reaction results inhibited by the presence of the hexamer.

Since **3** adsorbs light at shorter wavelength with respect to the *bis*-pyridinium it is likely that the hosting species could not shield the guest from the light source; a possible explanation for the inhibition could be imputable to the restricted space available within the hexamer that do not allow the correct rotation of the thiophene rings for effective switching to the closed form. Another possible explanation could be ascribed to possible energy transfers from the excited ***5o** to the hexamer, in other words the hexamer could enhance the relaxation processes of the encapsulated dithienylethene.

Since both **5o** and **5c** showed to be encapsulated within the hexamer of resorcin[4]arene, we decided to test the effect of the two different forms operating in independent experiments on a test reaction for which the hexamer $\mathbf{3_6 \cdot 8H_2O}$ acts as a supramolecular catalyst encapsulating the substrate and favoring its conversion into products.

Hydration of isonitriles within the hexamer

The hydration of isonitriles to the corresponding N-formamide was chosen as test reaction (Scheme 56).

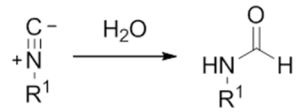

1a-e **2a-e**

R^1=Cy **1a**, *i*Pr **1b**, *t*Bu **1c**, Ph **1d**, 2,6(Me)$_2$Ph **1e**

Scheme 56. Hydration reaction of isonitriles.

Isonitriles[151] are valuable intermediates in organic synthesis that received minor attention mainly because of the limited commercial availability and the extremely repellent odour that discourages manipulation. Isonitriles **1** are neutral molecules where the R-NC moiety can be described with two mesomeric formulas, one switterionic with positive N and negative C, and the other with predominantly carbenic electronic structure yielding overall a linear geometry resulting from the significant energetic stabilization due to nitrogen π lone pair donation.[152] The carbon atom in isocyanides behaves as a nucleophile or an electrophile and this led to the employment of for multi-component reactions (MCRs)[153] like Ugi and Passerini or recent reactions with carboxylic acids.[154,155] Several are also the examples of naturally occurring isonitriles[156] as well as application of isonitriles in total syntheses.[157,158] Recent approaches

for the synthesis of isocyanides make use of alcohols as starting materials,[159] while, more traditionally, they are synthesized by reaction of primary amines with dichlorocarbene or by condensation of an amine with formic acid, yielding a *N*-formamide, and subsequent dehydration.[160] The inverse reaction, isonitrile hydration forming *N*-formylamides **2** is usually carried out, taking care of avoiding polymerization,[151] in strongly acidic aqueous media. Usual catalysts are acetic[161] and trifluoroacetic acid,[162] HCl[163] in H_2O/1,4-dioxane under homogeneous conditions or polymer-supported *p*-toluenesulfonic acid as a highly effective and eco-friendly isocyanide scavenger.[164] In particular, high temperatures and low concentrations favour *N*-formylamides.[155]

We were surprised to observe that addition of ten equivalents of cyclohexyl isonitrile **1a** to a solution of the self-assembled capsule $\mathbf{3_6 \cdot 8H_2O}$ in a water saturated chloroform-d solution led to the encapsulation of the neutral guest as confirmed by the appearance of new up-field shifted broad resonances in the ^{1}H NMR spectrum in the range 0.1- -0.7 ppm (Figure 42B and C) with respect to the free isonitrile in solution (Figure 42A).
The same results were observed employing other aliphatic and aromatic isonitriles characterized by smaller size like isopropyl isonitrile **1b**, *t*-butyl isonitrile **1c** as well as with benzyl isonitrile **1d** and 2,6-dimethylphenyl isonitrile **1e**. In particular aliphatic isonitriles **1b** showed several resonances for the encapsulated substrates in the range -0.3 - -0.7 ppm, while **1c** showed a major single relatively sharp resonance at -0.62 ppm corresponding to a shielding effect of $\Delta\delta$ -2.07 ppm (see experimentals). Benzyl substrate **1d** showed shielded aromatic resonances experiencing $\Delta\delta$ -0.8 - -1.2 ppm and **1e** showed similar behaviour with the corresponding shielded aromatic resonances that appeared upfield with a $\Delta\delta$ of about -1.6 ppm, while for the methyl groups present on **1e** the shielding effect was higher about -2.0 ppm.
The encapsulation of isonitriles within hexameric self-assembled capsule $\mathbf{3_6 \cdot 8H_2O}$ is an unexpected result since isonitriles are neutral molecules with low hydrogen bonding properties and therefore theoretically poor guests for the assembly. As recently described,[152] the electronic distribution of isonitriles has to be considered predominantly carbenic with substantial nitrogen π lone pair donation thus explaining the strong electrophilic character of the C atom. It is likely that the high electron-density provided by the closed aromatic surfaces of $\mathbf{3_6 \cdot 8H_2O}$ provides stabilization of the carbenic-like structure of the substrate.

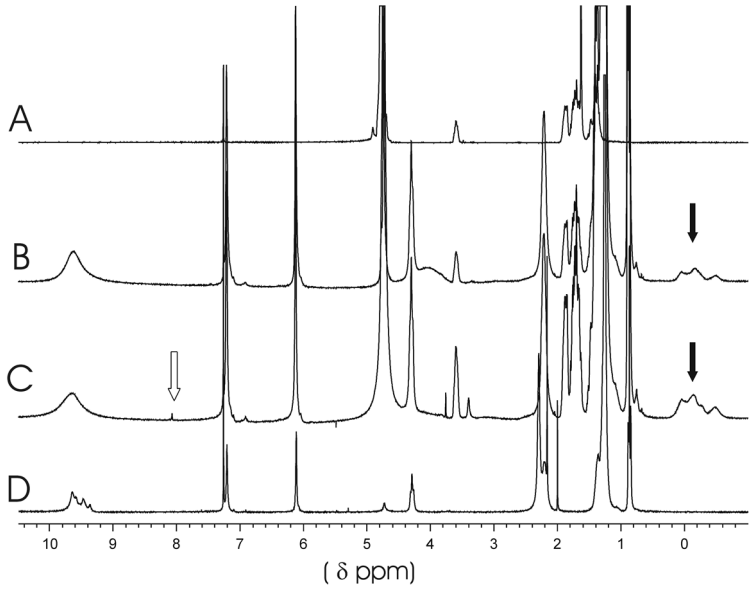

Figure 42. ^{1}H NMR spectra in water saturated chloroform-d: **A) 1a** (60 mM); **B) 1a** (60 mM) and **3** (36 mM); **C) 1a** (120 mM) and **3** (36 mM); **D) 3** (36 mM). ⇓ encapsulated substrate, ⇩ *N*-formylamide product.

While **1a** showed to be stable water saturated chloroform-d at 60°C for >18h (Table 11, entry 1), complete conversion of **1a** under the same experimental conditions into the corresponding *N*-formylamide **2a** was achieved simply adding **3** (36 mM) as a supramolecular catalyst (Table 11, entry 2). The formation of the *N*-formylamide **2a** was confirmed by GC-MS analysis and by the formation of a new resonance at 8.09 ppm attributed to the formyl proton. The accepted mechanism for isonitrile hydration occurs via protonation of the carbenic like C atom followed by water addition to the same C atom.[161-163,165] Therefore it is likely that the catalytic effect imparted by the capsule consists in stabilizing the cationic intermediate by means of interaction with the electron rich concave internal surfaces of the resorcin[4]arene **3** units.

In order to demonstrate that the catalytic activity displayed by the hexameric self-assembled capsule $\mathbf{3_6 \cdot 8H_2O}$ is unambiguously a consequence of the encapsulation of substrate **1a**, we performed control experiments repeating the hydration reaction in the presence of an excess of $(NEt_4)(OTf)$ **4** (60 mM) as a competitive cationic guest for the capsule where three molecules of **4** are concomitantly hosted within the capsule.[166] No product formation was detected indicative of complete inactivation of the hydration reaction (Table 11, entry 3). Similarly, the reaction performed in the absence of **3** but in the presence of resorcinol (*p*Ka>9) as a partially acidic and strongly H-bonding molecule in solution did not provide formation of the *N*-formylamides **2a** expected demonstrating that the reaction is not promoted by the weak Brønsted acidity of the resorcinol residues present in **3**.

Table 11. Catalytic tests for the hydration of 1a mediated by **3**.

#	$\mathbf{3_6 \cdot 8H_2O}$	**4**	**2a (%)**[a]
1	-	-	0
2	+	-	>98

3	+	+	<5
4	-	+	0
5[b]	-	-	<5

Experimental conditions: [**1a**]= 60 mM, [**3**]= 36 mM, [**4**]= 60 mM (10 eq. with respect to the capsule), water saturated chloroform-d (0.5 mL), T=60°C, time 18h. +: presence; -: absence; a) Determined by GC; b) **[resorcinol]** = 144 mM (4 eq. with respect to **3**).

The catalytic activity showed to be highly dependent on the size and electronic nature of the isonitrile substrate **1a-e** as reported in Table 12. In fact, the smaller **1b** bearing an *i*-propyl residue showed only reduced conversion to the corresponding *N*-formylamide **2b**, while the slightly larger *t*-butyl isonitrile **2c** turned out to be poorly reactive (Table 12). Aromatic isonitriles are intrinsically less reactive leading to the corresponding hydration products in about 60% yield even in the case of the sterically demanding substrate **1e**.

Table 12. Catalytic tests for the hydration of 1a-e mediated by $\mathbf{3_6 \cdot 8H_2O}$.

#	Substrate	Product	Yield (%)[a]
1	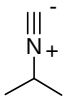	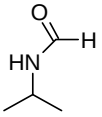	>98[c] 0[b,c] 93[c,d]
2	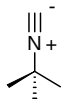	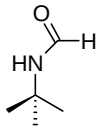	20 0[b] <5[d]
3	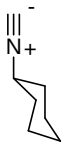	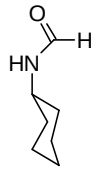	>98 0[b] 85[d]
4	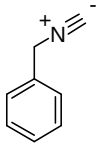	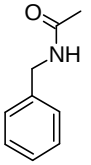	98 0[b] 98[d]
5	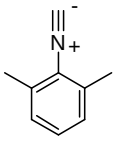	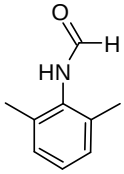	65 0[b] 48[d]

Experimental conditions: [1a-e] = 60 mM, **[3]** = 36 mM, water saturated chloroform-d (0.5 mL), T=60°C, time 18h. a) Determined with GC; b) in the absence of $\mathbf{3_6 \cdot 8H_2O}$; c) determined by ^{1}H NMR. d) **[1a-e]**= 120 mM.

Catalytic isonitrile hydration tests were performed in the presence of 1 equivalent of open **5o** and closed **5c** inhibitor with respect to the hexameric host $\mathbf{3_6 \cdot 8H_2O}$ (Figure 43). It is clearly

evident that the reaction with the open competitive guest **5o** allowed much lower conversion with respect to the reaction carried out in the absence of inhibitor (Figure 43), 10% and 55% yield of **2a** after 3h, respectively). Conversely, in the presence of the **5c** the reaction was not particularly inhibited observing 33% of **2a** after 3h. Initial rates of the reactions were determined and showed that open inhibitor **5o** led to almost a 10 times reduced rate of the reaction with respect to the closed **5c**. After 18h 33% of **2a** was observed with **5o** and 68% with **5c**.

The two isomeric inhibitors have almost identical molecular volume and they provide packing coefficient[167] of 0.24 within the hexamer, similarly to what is known considering encapsulation of three molecules of **4**.[166] This implies that room for some substrate or solvent molecules is available in the remaining space within the cavity to fit the best packing coefficient typical of supramolecular encapsulation phenomena.[167] The higher inhibition provided by the open **5o** isomer with respect to the closed **5c** is likely to be dependent on the higher flexibility of the former species that tend to better occupy the space available within the cavity, while the latter, being more rigid and planar, occupies diametrically the cavity and leaves more space close to the internal aromatic surfaces allowing the substrate to better experience the stabilizing effect of the aromatic surfaces that is responsible for the catalytic effect imparted by the capsule.

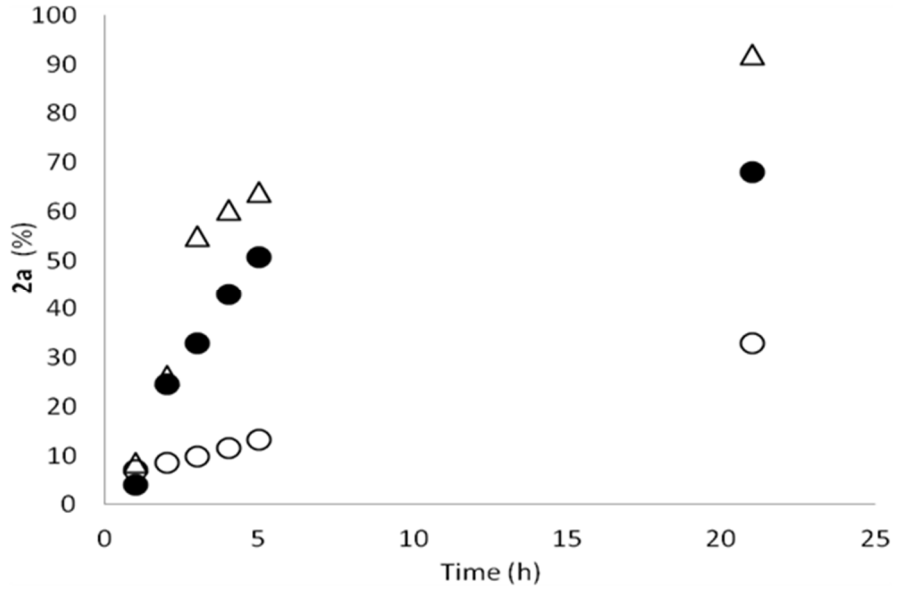

Figure 43. Plot of the time course of the reaction of hydration of **1a** to **2a** in water saturated chloroform-d (0.5 mL) at 60°C in the presence of a) free $\mathbf{3_6 \cdot 8H_2O}$ (Δ); b) $\mathbf{3_6 \cdot 8H_2O}$ with **5o** (o); c) $\mathbf{3_6 \cdot 8H_2O}$ with **5c** (•). **3** (36 mM), **1a** (60 mM) and **5o** or **5c** (6 mM).

Similar inhibition effect was observed with the smaller substrate **1b** that provided the corresponding hydration product **2b** in 15 and 26% yield after 2h with **5o** and **5c**, respectively, and 50 and 59% yield with **5o** and **5c** after 18h (Table 13). The difference in inhibition activity is better evidenced on experiments carried out with **5o** and **5c** at room temperature for seven days observing 38 and 67% yield for **2b**, respectively.

Table 13. Catalytic tests for the hydration of **1a-b** mediated by $\mathbf{3_6 \cdot 8H_2O}$ in the presence of competitive photo-modulable guests **5o** and **5c**.

#	Substrate	Inhibitor	2a (%)[a]
1[b]	**1a**	**5o**	10
2[b]	**1a**	**5c**	33
3	**1a**	**5o**	33
4	**1a**	**5c**	68
5[c]	**1b**	**5o**	15[d]
6[c]	**1b**	**5c**	26[d]
7	**1b**	**5o**	50[d]
			38[d,e]
8	**1b**	**5c**	59[d]
			67[d,e]

Experimental conditions: **[1a-c]** = 60 mM, **[3]** = 36 mM, **[5o or 5c]** = 6 mM, water saturated chloroform-d (0.5 mL), T=60°C repeated at r.t, time 18h. a) Determined by GC; b) reaction time 3h; c) reaction time 2h; d) determined by ^{1}H-NMR. e) Experiments run at room temperature for 7 days.

Unfortunately, as previously described, direct photo-isomerization of the encapsulated **5o** to the corresponding encapsulated **5c** derivative by means of UV irradiation in chloroform-d and the opposite re-opening of the inhibitor did not work. This did not allow direct photo-regulation of the inhibition properties for the supramolecular hydration of isonitriles mediated by the hexameric capsule $\mathbf{3_6 \cdot 8H_2O}$.

Conclusions

In conclusion, herein we described an example of supramolecular catalysis where the hexameric capsule $\mathbf{3_6 \cdot 8H_2O}$ hosts neutral non hydrogen bonding isonitrile substrates and catalyzes their conversion into the corresponding *N*-formylamides in the presence of water under mild experimental conditions. Inhibition by a competitive *bis*-cationic guest whose geometry can be regulated by irradiation with proper wavelength was possible even though the process was not reversible.

G. Bianchini, G. La Sorella, N. Canever, R. A. Michelin, A. Scarso, G. Strukul *Efficient Isonitrile Hydration through Encapsulation within a Hexameric Self Assembled Capsule and Selective Inhibition by a Photo-Modulable Competitive Guest*, manuscript in preparation.

Host-guest interactions with β-cyclodextrin

The evaluation of the supramolecular interactions between the photo-switchable cationic inhibitor **5o** and *β*-CD in water involved a) the study of the specific supramolecular interactions occurring between the two, b) the determination of stoichiometry of the adduct between host and guest species and c) the determination of the binding constants of the species involved.

The presence of any supramolecular interaction between *bis*-pyridinium and the *β*-cyclodextrin in water was evaluated by ^{1}H-NMR analysis since the formation of the host-guest species affects the resonances of the protons of both species and more precisely the signals result more or less shielded as a consequence of the new surrounding environment. The exchange rate between free and bound species for both the host and the guest influences the NMR spectrum. When the rate of exchange is much higher than the NMR timescale, the NMR signals are the weighted average between free and bound species, while when the rate exchange is much slower with respect to the NMR timescale separate signals are found for the free and bound species.

By addition of ***β*-CD** to a water solution of **5o** it was observed that several protons of the latter resulted shifted and the corresponding exchange rate was found to be fast with respect to the NMR timescale. The signals that were more heavily influenced by the presence of the *β*-cyclodextrin cavitand were the vinyl and the methyl protons linked to the thiophene ring and the pyridine protons in *meta* position with respect to the nitrogen atom (Figure 44). In details the methyl protons and the pyridine protons resulted de-shielded while the thiophene proton results shielded. These variations of chemical shift suggests that the thiophene ring resides within the cavity of the cyclodextrin and because of this it experiences a more electron-rich environment while the other protons are found closer to the upper and lower rim of the cyclodextrin causing the de-shielding of the nearby resonances induced by the proximity with the hydroxyl groups.

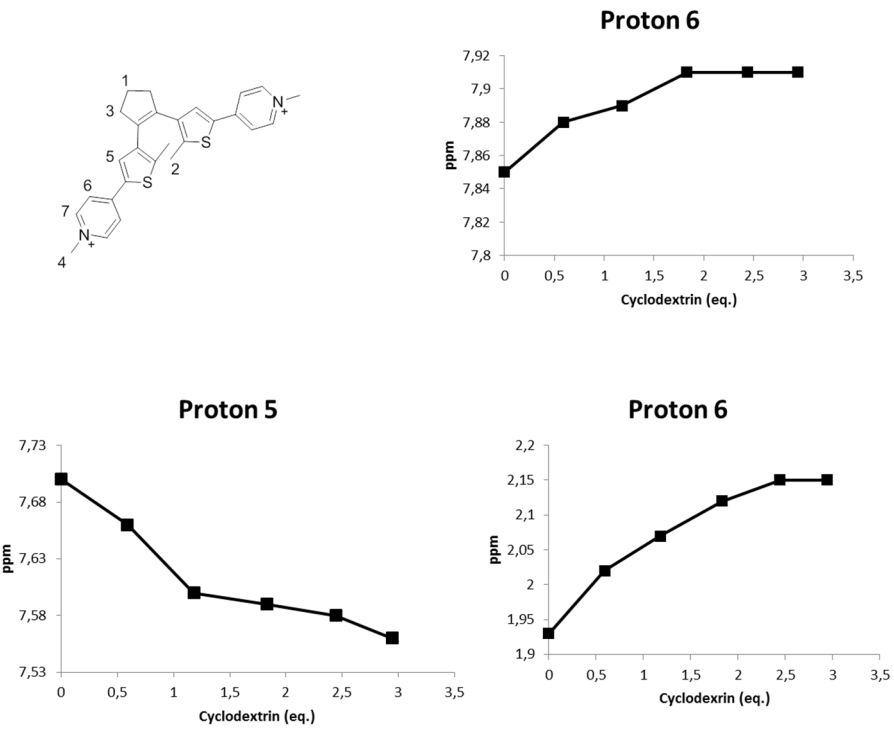

Figure 44. Most significant variation of chemical shift of the resonances of **5o** during the titration with with ***β-CD***.

As long as the closed isomer **5c** is concerned, the same experiments were carried out and it was found that the formed supramolecular adduct showed specific resonances in fast exchange on the NMR timescale but with different shielding effect with respect to the open guest. The vinyl and the methyl protons of the thiophene ring resulted respectively shielded and de-shielded as above, while all the protons of the cyclopentene moiety resulted de-shielded (Figure 45). These observations suggest that the closed isomer threads more deeply in the cyclodextrin and the latter influences the chemical shift of the cyclopentene moiety as well.

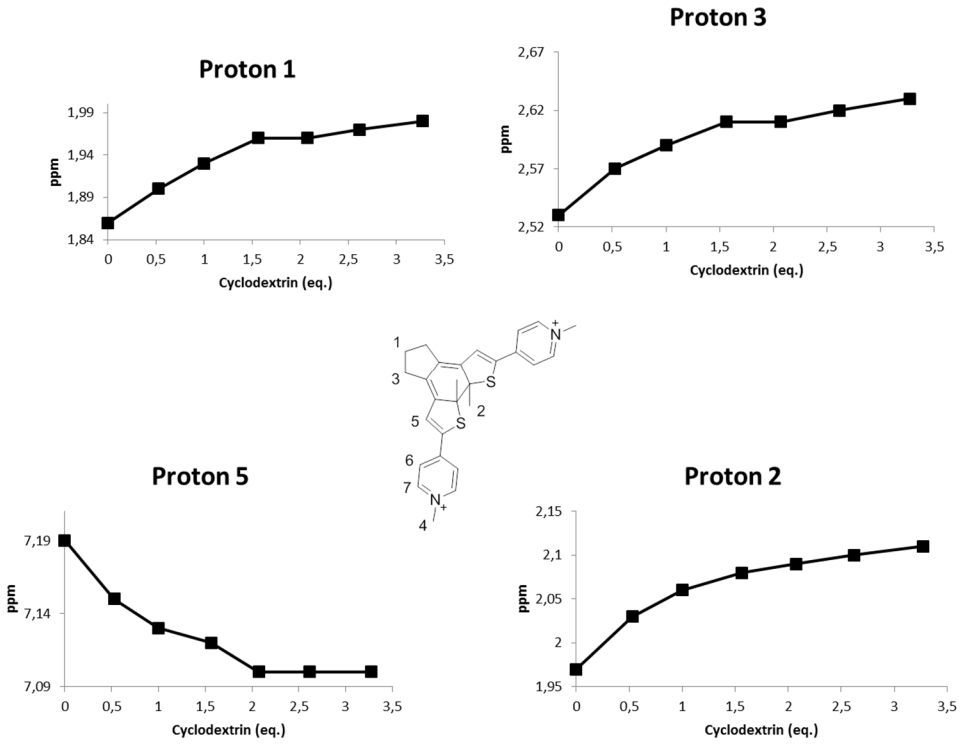

Figure 45. Most significant variation of chemical shift of the resonances of **5c** during the titration with with ***β-CD***.

It is possible to affirm that the switching between the two photochromic forms induces, as expected, a drastic change in the electronic distribution between the two thiophene rings and this causes the shift of the average position occupied by the cyclodextrin towards the middle of the molecule. Since the protons in the methyl bound to the thiophene ring and the protons of the cyclopentene unit are de-shielded, it is likely that they are placed facing the hydroxyl groups on the edges of the cyclodextrin and the deeper penetration of the guest within the cyclodextrin is stopped probably because of steric encumbrance. In Scheme 57 are reported two schematic pictures showing the different positioning of host and guest for the open and closed bis-cationic photochromic guest.

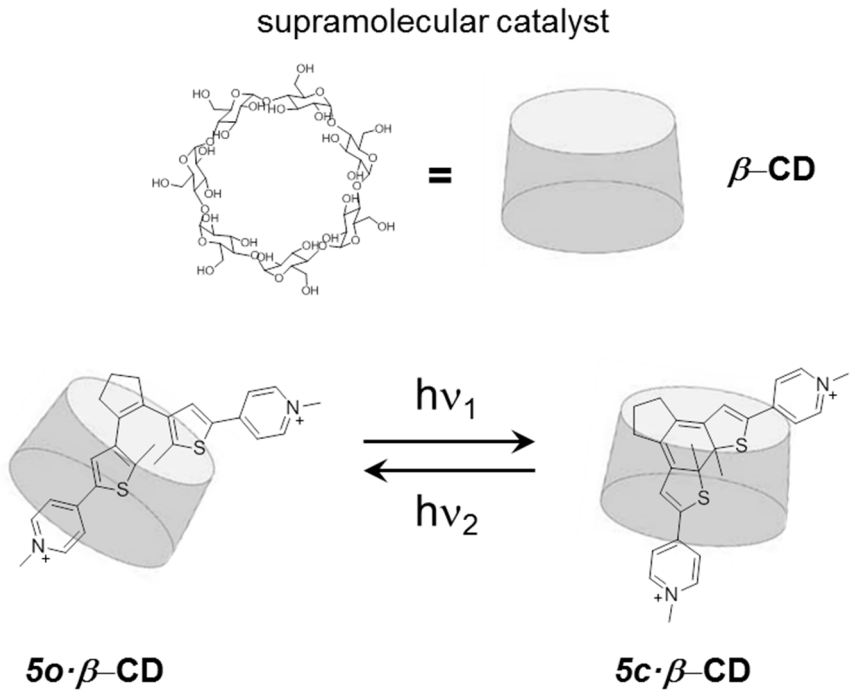

Scheme 57. Supramolecular interactions between *β*-cyclodextrin and the **5o** and **5c**. The switching from the open to the closed isomer of the guest transfer the electronic density from the thiophene rings to the new π-extended formed system. The inner hydrophobic cavity of the ***β*-CD** chases this electronic variation until being stopped for steric reasons. The ***β*-CD** could be considered an electron density probe.

Conversely to what observed for host-guest interactions between the hexamer and the photo-switchable *bis*-pyridinium, in this case the *β*-cyclodextrin does not inhibit the photochemical conversion from the open to the closed isomer and the two photochromic adducts are interconvertible by irradiation with proper wavelength.

Determination of the stoichiometry of the adduct between 5o, 5c and β-CD. Job's plot

The next in the comprehension of the *host-guest* interactions between the *β*-cyclodextrin and the two forms of the dithienylethene-based *bis*-pyridinium is the understanding of the stoichiometry between the two species. We decided to perform a Job plot analysis that consisted in recording different ^{1}H-NMR spectra of different solutions containing both the *bis*-pyridinium ion and *β*-cyclodextrin. The sum of the concentration of the two species was kept constant and different molar fractions (X) from 0 to 1 of one species with respect to the other were tested. Data treatment consisted in plotting the chemical shift variations of a chosen resonance (Δppm) weighed for the effective concentration of the molecular species with the molar fraction (Figure 46). [o] The stoichiometry can be easily determined from the x-coordinate at the maximum in the curve.

o For further details and theoretical please refer to: K. Hirose *Journal of Inclusion Phenomena and Macrocyclic Chemistry* **2001**, *39*, 193-209.

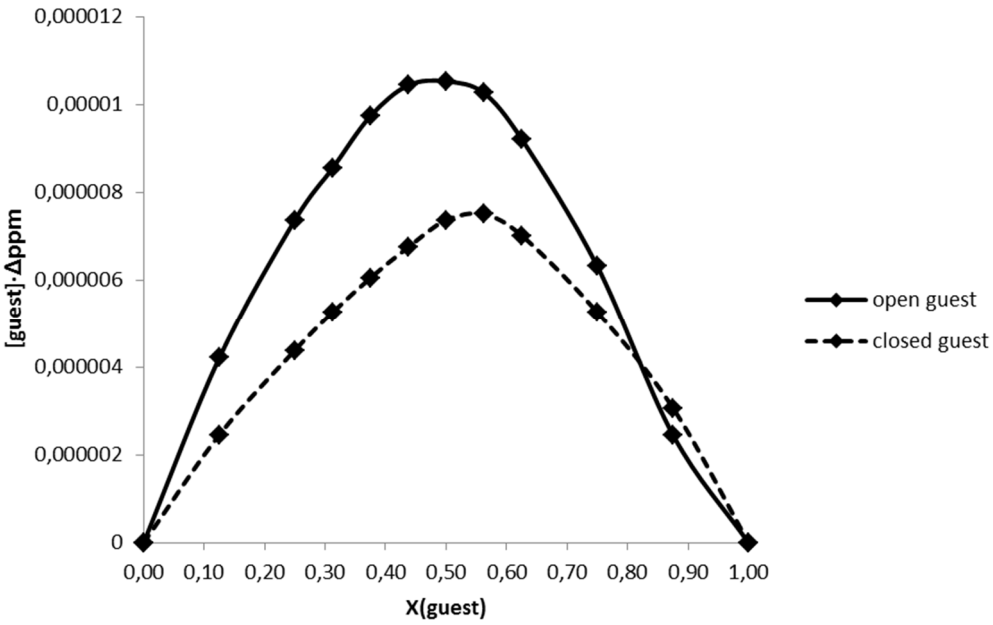

Figure 46. The Job's plots obtained for **5o** and **5c** in the presence of ***β*-CD**. Both curves are centred at X=0.5, suggesting 1:1 as stoichiometric ratio between the ***β*-CD** and the photochromic guests.

The Job plot of the two isomers showed slightly different maxima, at X=0.46 for **5o** and X=0.56 for **5c**. The obtained values are quite similar and could be both approximated to 0.5 corresponding to a 1:1 stoichiometry between cation and cyclodextrin. This value was quite expected considering the previously reported conclusions regarding the reciprocal positioning of the cyclodextrin and *bis*-pyridinium in the inclusion complex. Looking in detail the values reported on the y-axis for the two isomers, it is evident that the open isomer showed higher values than the closed isomer and since the y-axis value in correspondence to the maximum is proportional to the concentration of the *host-guest* adduct, it is possible to conclude that the concentration of the host-guest adduct for the open isomer is larger than that of the closed species. In other words, the supramolecular interactions between *β*-cyclodextrin and the open *bis*-pyridinium species are stronger with respect to the interactions with the closed isomer. Furthermore, for the above mentioned reasons the y-axis values could be used for establishing an approximate value of the ratio between the binding constants between **5o** ($K_{\mathbf{5o}\cdot\boldsymbol{\beta}\text{-}\mathbf{CD}}$), **5c** ($K_{\mathbf{5c}\cdot\boldsymbol{\beta}\text{-}\mathbf{CD}}$) and *β*-CD. From this consideration a value of 1.38 ($K_{\mathbf{5o}\cdot\boldsymbol{\beta}\text{-}\mathbf{CD}}/K_{\mathbf{5c}\cdot\boldsymbol{\beta}\text{-}\mathbf{CD}}$) is expected and this evaluation will be compared with more accurate data obtained from titration experiments.

Determination of the binding constant between open and closed photochromic guests and β-cyclodextrin

Titration tests were realized by adding increasing amounts of ***β*-CD** to a water solution of the **5o** (2.15 mM). The addition of *β*-cyclodextrin was performed until the chemical shift at ^{1}H-NMR for the supramolecular host-guest system resulted constant. The methyl protons of the thiophene ring were chosen as reference by virtue of their high sensitivity towards the addition of CD. The plot of the chemical shift variation against the concentration of ***β*-CD**

yielded the profile reported in Figure 47 which, after non-linear regression yielded a value for the binding constant of 740±50 M^{-1} ($K_{\mathbf{5o}\cdot\boldsymbol{\beta}\text{-CD}}$).

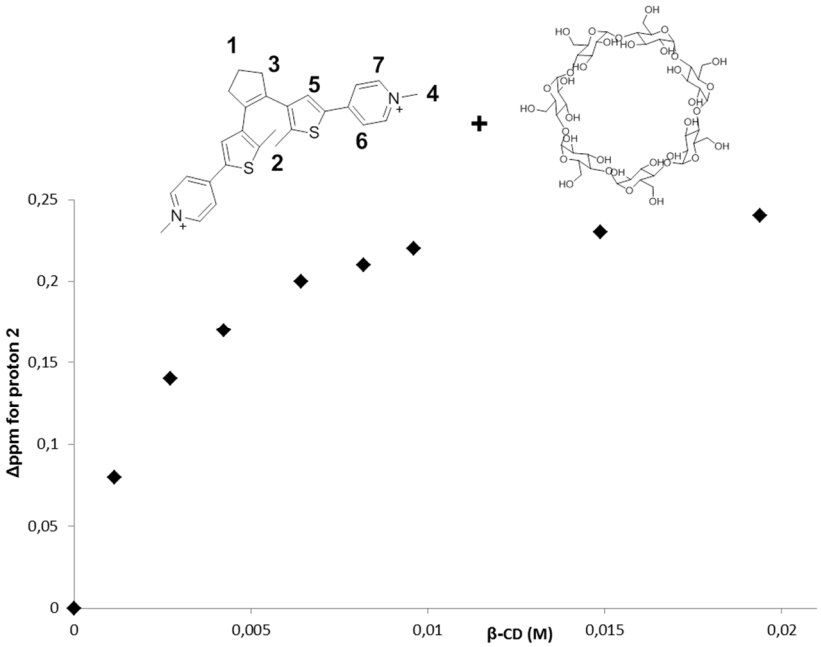

Figure 47. Titration of **5o** (2.15 mM) with ***β*-CD** in water-d_2.

An analogous study was performed for **5c** yielding a value for the binding constant of 530±50 M^{-1} ($K_{\mathbf{5c}\cdot\boldsymbol{\beta}\text{-CD}}$) (Figure 48).

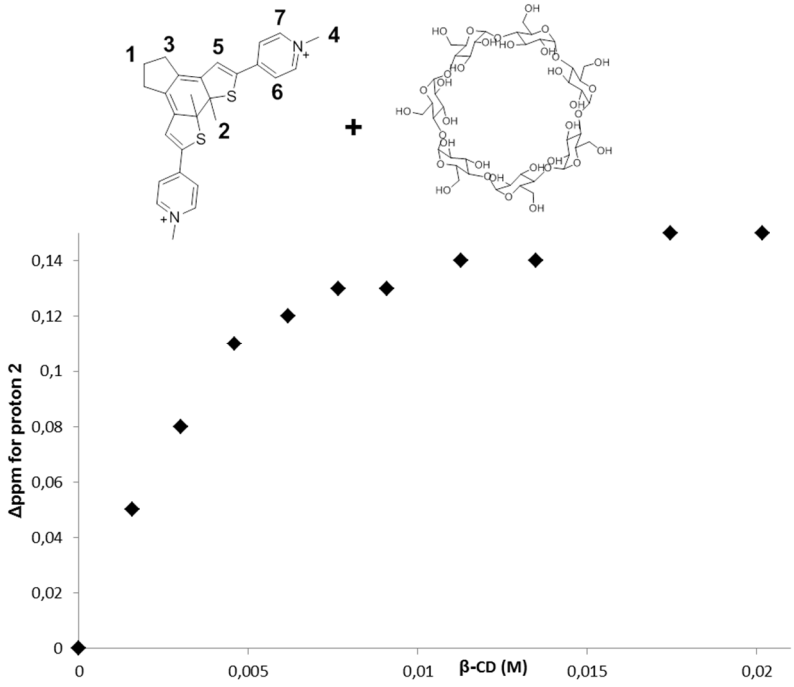

Figure 48. Titration of **5c** (2.15 mM) with ***β*-CD** in water-d_2.

Conclusions

After titration experiments of **5o** and **5c**, the value of the ratio ($K_{\mathbf{5o}\cdot\boldsymbol{\beta}\text{-}\mathbf{CD}}/K_{\mathbf{5c}\cdot\boldsymbol{\beta}\text{-}\mathbf{CD}}$) resulted 1.41, confirming the evaluation previously made on the basis of the Job plot.

The inclusion complex between ***β*-CD** and an eventual reactant is characterized by a binding constant ($K_{\mathbf{R}\cdot\boldsymbol{\beta}\text{-}\mathbf{CD}}$) and its value must be compared to the ones obtained for inhibitors **5o** and **5c**. Three different cases are possible

1. $K_{\mathbf{R}\cdot\boldsymbol{\beta}\text{-}\mathbf{CD}} \ll K_{\mathbf{5o}\cdot\boldsymbol{\beta}\text{-}\mathbf{CD}}$ and $K_{\mathbf{R}\cdot\boldsymbol{\beta}\text{-}\mathbf{CD}} \ll K_{\mathbf{5c}\cdot\boldsymbol{\beta}\text{-}\mathbf{CD}}$; in this case the inclusion complex between reactant and cyclodextrin is always disfavoured. No allosteric control could be performed

2. $K_{\mathbf{R}\cdot\boldsymbol{\beta}\text{-}\mathbf{CD}} \gg K_{\mathbf{5o}\cdot\boldsymbol{\beta}\text{-}\mathbf{CD}}$ and $K_{\mathbf{R}\cdot\boldsymbol{\beta}\text{-}\mathbf{CD}} \gg K_{\mathbf{5c}\cdot\boldsymbol{\beta}\text{-}\mathbf{CD}}$; in this case the inclusion complex between reactant and cyclodextrin is always favoured and also in this case no allosteric control could be performed.

3. $K_{\mathbf{5o}\cdot\boldsymbol{\beta}\text{-}\mathbf{CD}} \approx K_{\mathbf{R}\cdot\boldsymbol{\beta}\text{-}\mathbf{CD}} \approx K_{\mathbf{5c}\cdot\boldsymbol{\beta}\text{-}\mathbf{CD}}$; in this case formation of the inclusion complex with reactant is in competition with the formation of the inclusion complexes of both photochromic forms of inhibitor and allosteric control could be performed. When $K_{\mathbf{5c}\cdot\boldsymbol{\beta}\text{-}\mathbf{CD}}$ and $K_{\mathbf{R}\cdot\boldsymbol{\beta}\text{-}\mathbf{CD}}$ values are close the two species will strongly compete for cyclodextrin's cavity and switching the inhibitor to the open form may slow down the reaction's rate by virtue of its higher binding constant value. Conversely when $K_{\mathbf{5o}\cdot\boldsymbol{\beta}\text{-}\mathbf{CD}}$ and $K_{\mathbf{R}\cdot\boldsymbol{\beta}\text{-}\mathbf{CD}}$ has similar value than switching the inhibitor to the closed form may enhance the reaction's rate. Finally, when $K_{\mathbf{5c}\cdot\boldsymbol{\beta}\text{-}\mathbf{CD}} \leq K_{\mathbf{R}\cdot\boldsymbol{\beta}\text{-}\mathbf{CD}} \leq K_{\mathbf{5o}\cdot\boldsymbol{\beta}\text{-}\mathbf{CD}}$ three inclusion complexes are in equilibrium between each other and switching from the open form to the closed one is expected to enhance reactivity, the contrary when switching is performed from the closed to the open form.

Experimental

^{1}H-NMR, ^{13}C{^{1}H}-NMR and ^{31}P{^{1}H}-NMR were recorded at 298 K with a BRUKER AVANCE spectrometer operating respectively at 300.15, 75 and 121.5 MHz and with a BRUKER AC200 operating at 200, 50 and 80.7 MHz, respectively.

GC analysis were performed on HP SERIES II 5890 equipped with a HP5 column (30 m, I. D. 0.25 m, film 0.25 μm) using He as gas carrier and FID. GC-MS analyses were performed on a GC Trace GC 2000 equipped with a HP5-MS column (30 m, I.D. 0.25 mm, film 0.25 μm) using He gas carrier and coupled with a quadrupole MS Thermo Finnigan Trace MS with *Full Scan* method. Identification of the products was accomplished by reference samples or by comparison with samples obtained as described in literature.

TLC analysis were performed on TLC Polygram ® Sil G/UV254 of 0.25 mm thickness and flash-chromatography separations were performed on silica gel Merk 60, 230-400 mesh as reported by W. C. Still, M. Khan, A. Mitra *J. Org. Chem.* **1978**, *43*, 2923.

Solvents and reactants were used purchased; otherwise they were purified as reported in D. D. Perrin, W. L. F. Armarego *Purification of Laboratory Chemicals*, 3rd Ed., **1988**, Pergamon Press Ltd., Oxford OX3 0BW, England. Compound **7** was synthesized as reported in the chapter *Photoswitching the electronic properties of phosphinic ligands* (compound **6**), resorcin[4]arene **3** was already available in laboratory otherwise it was prepared according to Y. Aoyama. Y. Tanaka, S. Sugahara *J. Am. Chem. Soc.* **1989**, *111*, 5397-5404.

Irradiation at 365 nm was performed with a Wood lamp, omnilux 25 W, irradiance at 365 nm 10 W/m^2 (10 cm) while irradiation at 254 nm was performed with the low pressure Hg lamp commonly used for the visualization of TLC plates (12 W).

*Synthesis of 1,2-bis(2-methyl-5-(pyridin-4-yl)thiophen-3-yl)cyclopent-1-ene (**6**)*

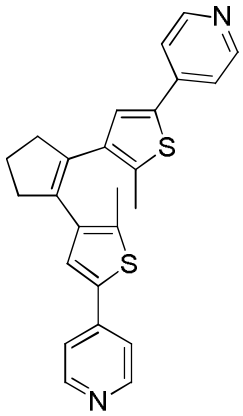

The synthesis of this product is divided in two parts. *Part A* concerns the preparation of THF solution of a thiophene-borate reactant bearing the dithyenilethene moiety suitable for the Suzuki cross coupling. *Part B* reports the cross-coupling reaction.

Part A. A two necks round bottom flask equipped with a rubber septum and connected to a vacuum/nitrogen line was flame dried and 3 vacuum/nitrogen cycles performed. Subsequently

under nitrogen atmosphere **7** (1.88 g, 0.0057 mol) and dry THF (15 mL) were added. The resulting mixture was cooled to 0°C with an ice bath and *n*-BuLi (2.5 M, 5.04 mL, 0.0126 mol) was slowly added with a syringe. During the addition the mixture turned dark grey and upon completion of the addition it was stirred for further 15 min at the same temperature. Subsequently *tris*-*n*-butylborate (3.94 g, 4.62 mL, 0.0171 mol) was added in one portion with a syringe and the resulted orange solution was allowed to warm up to room temperature and stirred for 1h.

Part B. To a two necks round bottom flask equipped with a condenser, THF (20 mL) and $Pd(PPh_3)_4$ (0.370 g, $3.2 \cdot 10^{-4}$ mol) were added and the resulting solution heated at 70°C. After 15 min at this temperature, aqueous K_2CO_3 (2 M, 25 mL, 0.05 mol), ethylene glycol (10 drops), 4-bromopyridine hydrochloride (2.43 g, 0.00125 mol) were added and, to the well stirred solution at the same temperature, the THF solution containing the borate prepared in *Part A* was slowly added with a syringe. The mixture was left at 70°C for 16h further cooled to room temperature followed by addition of water (20 mL) and product extraction with diethyl ether (3x50 mL). The combined organic phases were dried over $MgSO_4$ and concentrated under reduced pressure. The product was obtained as a light violet solid in 62% yield.

^{1}H-NMR (300.15 MHz, $CDCl_3$): δ 2.02 (3, 6H), 2.11 (q, J=7.5 Hz, 2H), 2.85 (t, J=7.5 Hz, 4H), 7.21 (s, 2H), 7.34 (dd, J=4.6 and 1.7 Hz, 4H), 8.53 (dd, J=4.6 and 1.7 Hz, 4H).
^{13}C-NMR (75 MHz, $CDCl_3$): δ 14.64, 22.98, 38.45, 119.24, 126.27, 134.79, 136.65, 137.07, 137.26, 141.27, 150.24.

*Synthesis of 4,4'-(4,4'-(cyclopent-1-ene-1,2-diyl)bis(5-methylthiophene-4,2-diyl))bis(1-methylpyridin-1-ium) bis(trifluoromethanesulfonate) (**5o**)*

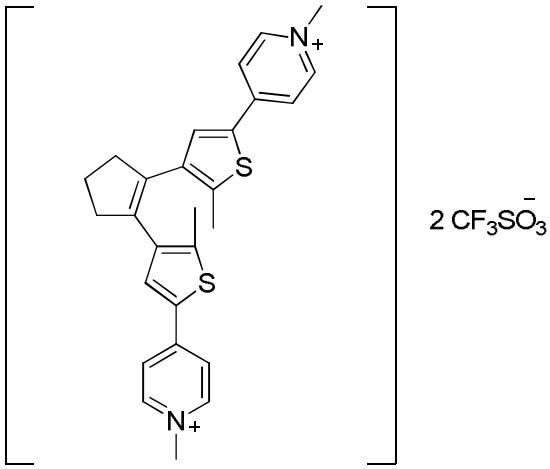

A two necks round bottom flask connected to a vacuum/nitrogen line was flame dried and three vacuum/nitrogen cycles were performed, subsequently under nitrogen atmosphere **6** (0.47 g, 0.0011 mol) and dry dichloromethane (20 mL) were added. To the well stirred solution methyl trifluoromethanesulfonate (0.54 g, 0.37 mL, 0.0033 mol) was then added with a syringe and immediately the light violet solution turned greenish. The mixture was stirred for further 16h. The solvent and the un-reacted methyl triflate were removed under vacuum and the product isolated in quantitative yield was not further purified.

^{1}H-NMR (300.15 MHz, CD_3CN): δ 2.11 (s, 6H), 2.13 (q, J=7.4 Hz, 2H), 2.88 (t, J=7.4 Hz, 4H), 4.17 (s, 6H), 7.78 (s, 2H), 7.94 (d, J=6.8 Hz, 4H), 8.44 (d, J=6.8 Hz, 4H).
^{1}H-NMR (300.15 MHz, D_2O): δ 1.93 (s, 3H), 2.01 (q, J=7.4 Hz, 2H), 2.76 (t, J=7.4 Hz, 4H), 4.11 (s, 6H), 7.70 (s, 2H), 7.84 (d, J=7.1 Hz, 4H), 8.39 (d, J=7.1 Hz, 4H) .
^{13}C-NMR (75 MHz, CD_3CN): δ 13.40, 14.24, 38.07, 47.03, 121.58, 132.94, 132.99, 135.11, 138.91, 144.65, 144.93, 148.49; (12 of 13 found).

*Preparation of ring closed isomer of 4,4'-(4,4'-(cyclopent-1-ene-1,2-diyl)bis(5-methylthiophene-4,2-diyl))bis(1-methylpyridin-1-ium) bis(trifluoromethanesulfonate) (**5c**)*

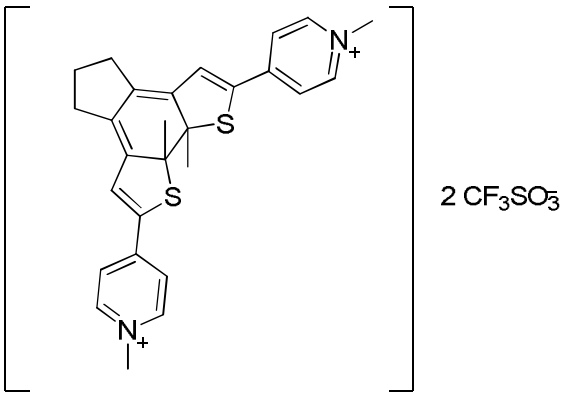

5o (0.003 g, $4.04 \cdot 10^{-6}$ mol) and the desired deuterated solvent (0.65 mL) were loaded in a NMR tube. The resulting solution was irradiated with a Wood lamp until the ring closing reaction was complete (about 5 min) as confirmed by acquisition of the ^{1}H NMR spectrum. During the irradiation the sample became dark green.

^{1}H-NMR (300.15 MHz, D_2O): δ 1.86 (q, J=7.2 Hz, 2H), 1.97 (s, 6H), 2.53 (t, J=7.2 Hz, 4H), 4.18 (s, 6H), 7.19 (s, 2H), 7.83 (d, J=6.2 Hz, 4H), 8.48 (d, J=6.2 Hz, 4H).

*Typical procedure for isonitrile hydration reaction in presence of **5o***

In a 1.2 mL vial were introduced a water saturated chloroform solution of **3** (36 mM, 0.5 mL) and **5o** (1 eq. with respect to $\mathbf{3_6 \cdot 8H_2O}$, 0.003 mmol, 2.3 mg) and the resulted mixture vigorously stirred until completely homogeneous. Subsequently the desired isonitrile was added (10 eq. with respect to $\mathbf{3_6 \cdot 8H_2O}$, 0.030 mmol), the vial sealed and termostatted at 60 °C. Reaction's course was followed by GC or ^{1}H-NMR analyses sampling the reaction's mixture at different times.

*Typical procedure for isonitrile hydration reaction in presence of **5c***

5o (0.003 mmol, 2.3 mg) was photoisomerized to **5c** in an acetonitrile solution as previously described. After solvent removal at reduced pressure, a water saturated chloroform solution of **3** (36 mM, 0.5 mL) was added and the system stirred until completely homogeneous. Subsequently the desired isonitrile was added (10 eq. with respect to $\mathbf{3_6 \cdot 8H_2O}$, 0.030 mmol) and the obtained solution transferred in a 1.2 mL vial which was in turn sealed and termostatted at 60 °C. Reaction's course was followed by GC or ^{1}H-NMR analyses sampling the reaction's mixture at different times.

*Encapsulation of **1b** within $3_6 \cdot 8H_2O$*

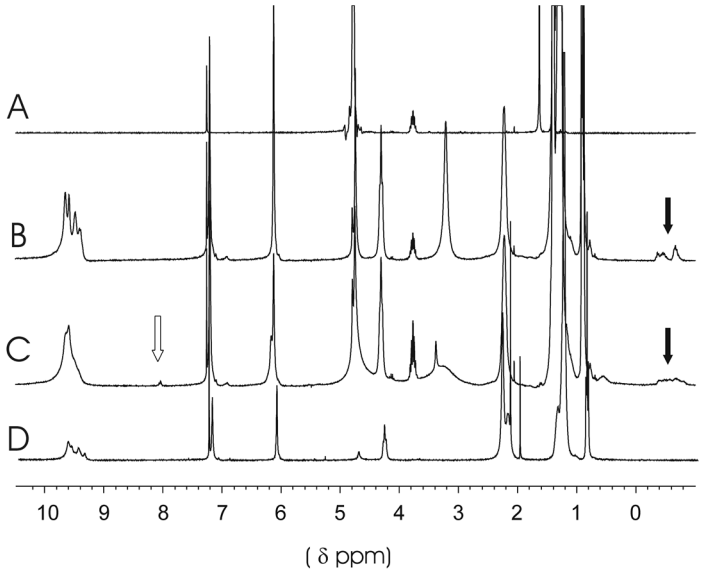

Figure 49. ^{1}H NMR spectra in water saturated chloroform-d: A) **1b** *i*-propylisonitrile (60 mM); B) **1b** (60 mM) and **3** (36 mM); C) **1b** (120 mM) and **3** (36 mM); D) **3** (36 mM). ⇓ encapsulated substrate, ⇩ *N*-formylamide product.

*Encapsulation of **1c** within $3_6 \cdot 8H_2O$*

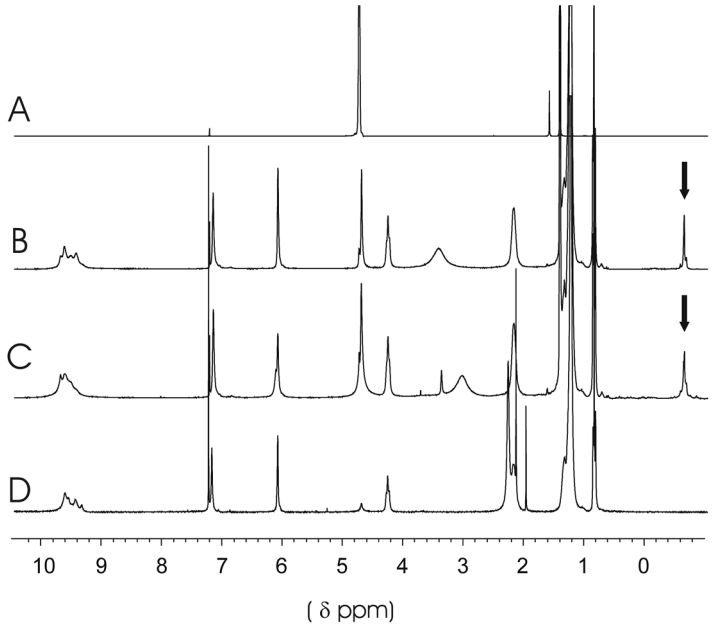

Figure 50. ^{1}H NMR spectra in water saturated chloroform-d: A) **1c** *t*-butylisonitrile (60 mM); B) **1c** (60 mM) and **3** (36 mM); C) **1c** (120 mM) and **3** (36 mM); D) **3** (36 mM). ⇓ encapsulated substrate.

*Encapsulation of **1d** within $3_6 \cdot 8H_2O$*

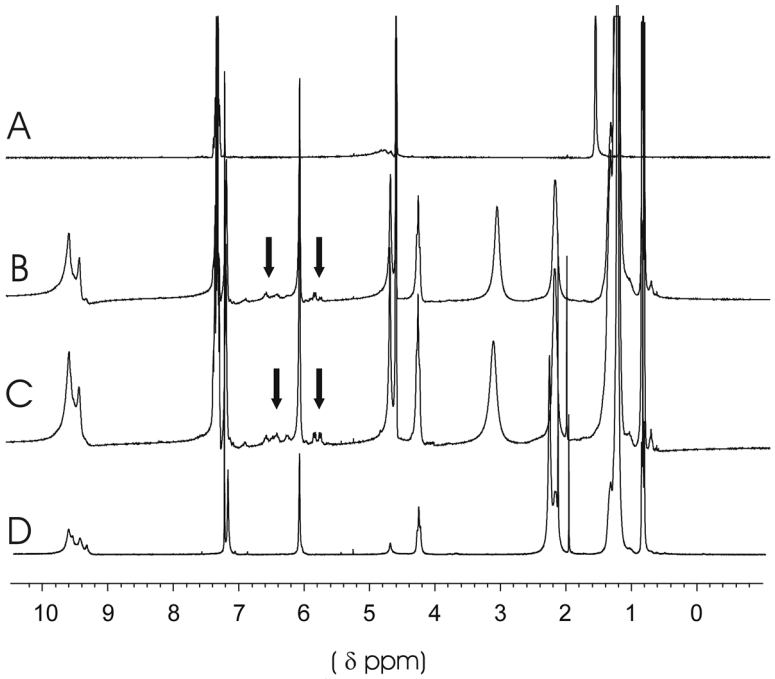

Figure 51. ^{1}H NMR spectra in water saturated chloroform-d: A) **1d** benzylisonitrile (60 mM); B) **1d** (60 mM) and **3** (36 mM); C) **1d** (120 mM) and **3** (36 mM); D) **3** (36 mM). ⬇ encapsulated substrate, ⇩ *N*-formylamide product.

*Encapsulation of **1e** within $3_6 \cdot 8H_2O$*

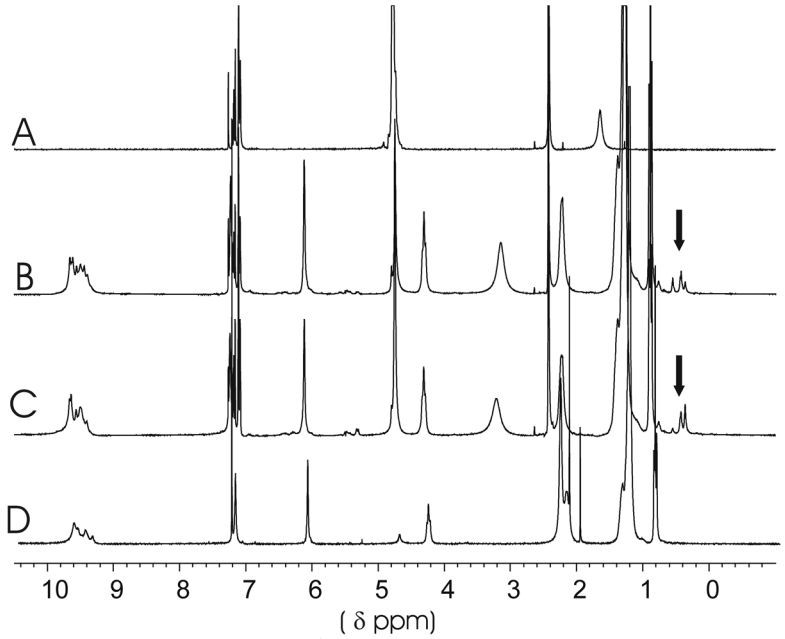

Figure 52. ^{1}H NMR spectra in water saturated chloroform-d: A) **1e** 2,6-dimethyl-phenylisonitrile (60 mM); B) **1e** (60 mM) and **3** (36 mM); C) **1e** (120 mM) and **3** (36 mM); D) **3** (36 mM). ⬇ encapsulated substrate.

Determination of the stoichiometry of the bis-pyridinium/β-Cyclodextrin adduct. Job's plot

Starting from different mother solutions of *β*-cyclodextrin, 5o and 5c in deuterated water, new solutions characterized by sharing the same final total concentration of *host* and *guest* species were prepared. In Table 14 are reported the different solutions prepared and the corresponding

^{1}H-NMR resonances determined for protons 5 of **5o** in presence of *β*-cyclodextrin while Table 15 reports the data obtained for the protons 5 of **5c**. The protons are reported following the legend deducible from the figure reported above the tables.

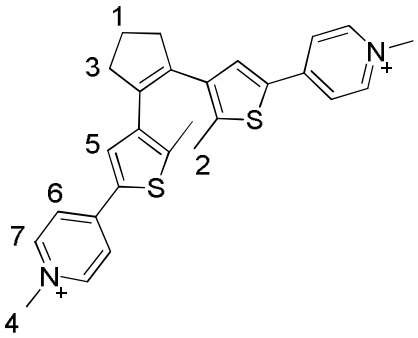

Table 14. Job's plot data for inclusion complex **5o·*β*-CD** formation.

[5o][a]	[*β*-CDX][a]	X[b](5o)	X[b](*β*-CDX)	Proton 5 (δ, ppm)	Δ[c] (ppm)	Δ·[5o]
0	$7.02\cdot10^{-4}$	0.00	1.00	0	0	0
$8.77\cdot10^{-5}$	$6.14\cdot10^{-4}$	0.13	0.88	7.799	0.028	$4.21\cdot10^{-6}$
$1.75\cdot10^{-4}$	$5.26\cdot10^{-4}$	0.25	0.75	7.805	0.025	$7.37\cdot10^{-6}$
$2.19\cdot10^{-4}$	$4.82\cdot10^{-4}$	0.31	0.69	7.808	0.024	$8.55\cdot10^{-6}$
$2.63\cdot10^{-4}$	$4.39\cdot10^{-4}$	0.38	0.63	7.810	0.023	$9.74\cdot10^{-6}$
$3.07\cdot10^{-4}$	$3.95\cdot10^{-4}$	0.44	0.56	7.813	0.022	$1.04\cdot10^{-5}$
$3.51\cdot10^{-4}$	$3.51\cdot10^{-4}$	0.50	0.50	7.817	0.021	$1.05\cdot10^{-5}$
$3.95\cdot10^{-4}$	$3.07\cdot10^{-4}$	0.56	0.44	7.821	0.019	$1.03\cdot10^{-5}$
$4.39\cdot10^{-4}$	$2.63\cdot10^{-4}$	0.63	0.38	7.826	0.016	$9.21\cdot10^{-6}$
$5.26\cdot10^{-4}$	$1.75\cdot10^{-4}$	0.75	0.25	7.835	0.010	$6.32\cdot10^{-6}$
$6.14\cdot10^{-4}$	$8.77\cdot10^{-5}$	0.88	0.13	7.843	0.005	$2.46\cdot10^{-6}$
$7.02\cdot10^{-4}$	0	1.00	0.00	7.847[c]	0	0

a) [M]=mol·l^{-1} in water-d; b) molar fraction; c) reference value for the determination of Δ

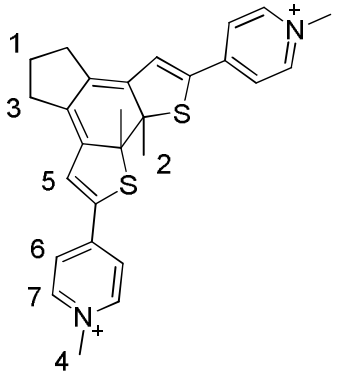

Table 15. Job's plot data for inclusion complex **5c·*β*-CD** formation.

[5c][a]	[*β*-CDX][a]	X[b](5c)	X[b](*β*-CDX)	Proton 5 (δ, ppm)	Δ[c] (ppm)	Δ·[5c]
0	$7.02\cdot10^{-4}$	0.00	1.00	0	0	0
$8.77\cdot10^{-5}$	$6.14\cdot10^{-4}$	0.13	0.88	7.278	0.048	$2.46\cdot10^{-6}$

$1.75\cdot10^{-4}$	$5.26\cdot10^{-4}$	0.25	0.75	7.281	0.042	$4.39\cdot10^{-6}$
$2.19\cdot10^{-4}$	$4.82\cdot10^{-4}$	0.31	0.69	7.282	0.039	$5.26\cdot10^{-6}$
$2.63\cdot10^{-4}$	$4.39\cdot10^{-4}$	0.38	0.63	7.283	0.037	$6.05\cdot10^{-6}$
$3.07\cdot10^{-4}$	$3.95\cdot10^{-4}$	0.44	0.56	7.284	0.034	$6.75\cdot10^{-6}$
$3.51\cdot10^{-4}$	$3.51\cdot10^{-4}$	0.50	0.50	7.285	0.030	$7.37\cdot10^{-6}$
$3.95\cdot10^{-4}$	$3.07\cdot10^{-4}$	0.56	0.44	7.287	0.026	$7.50\cdot10^{-6}$
$4.39\cdot10^{-4}$	$2.63\cdot10^{-4}$	0.63	0.38	7.290	0.021	$7.02\cdot10^{-6}$
$5.26\cdot10^{-4}$	$1.75\cdot10^{-4}$	0.75	0.25	7.296	0.012	$5.26\cdot10^{-6}$
$6.14\cdot10^{-4}$	$8.77\cdot10^{-5}$	0.88	0.13	7.302	0.004	$3.07\cdot10^{-6}$
$7.02\cdot10^{-4}$	0	1.00	0.00	7.306[c]	0	0

a) [M]=mol·l^{-1} in water-d; b) molar fraction; c) reference value for the determination of Δ

Host-guest interaction with β-Cyclodextrin-Tritration

A water-d solution of **5o** (2.15 mM, 0.65 mL) was loaded in a NMR tube and increasing amounts of *β*-cyclodextrin added. The ^{1}H-NMR spectrum were recorded after every addition of cyclodextrin and the ^{1}H-NMR chemical shifts of the *bis*-pyridinium ion were reported as a function of the number of equivalents of *β*-cyclodextrin added. In Table 16 are reported the chemical shift values of proton 5 of **5o** upon addition of increased amounts of *β*-cyclodextrin while Table 17 reports the analogous values obtained for **5c**. The protons are reported following the chart reported above the tables.

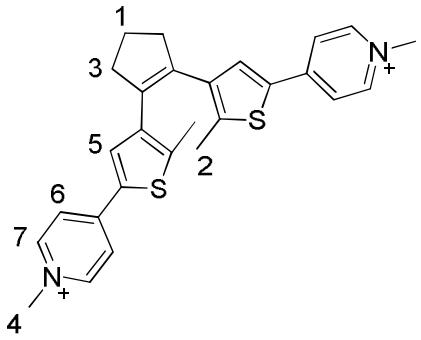

Table 16. Data from titration of **5o** with ***β*-CD** in water.

[β-CD][a]	Proton 5 (δ, ppm)	Δ[b]
0.00000	1.88	0.00
0.001145	1.96	0.08
0.002731	2.02	0.14
0.004229	2.05	0.17
0.006432	2.08	0.20
0.008194	2.09	0.21
0.009603	2.10	0.22
0.014890	2.11	0.23
0.019383	2.12	0.24
0.029427	2.13	0.25

a) [M]=mol·l^{-1} in water-d; b) reference value for the determination of Δ was 1.88.

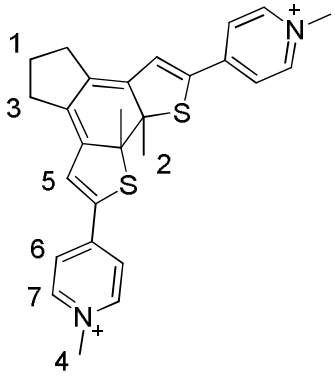

Table 17. Data from titration of **5c** with ***β*-CD** in water.

[β-CD][a]	**Proton 5 (δ, ppm)**	**Δ**[b]
0.00000	1.91	0.oo
0.00159	1.96	0.05
0.00300	1.99	0.08
0.00458	2.02	0.11
0.00617	2.03	0.12
0.00767	2.04	0.13
0.00907	2.04	0.13
0.01128	2.05	0.14
0.01348	2.05	0.14
0.01744	2.06	0.15
0.02018	2.06	0.15

a) [M]=mol·l^{-1} in water-d; b) reference value for the determination of Δ was 1.91 ppm.

SWITCHING THE ACTIVITY OF A PHOTOREDOX-CATALYST THROUGH REVERSIBLE ENCAPSULATION AND RELEASE

As previously reported, the modulation of the solvatation sphere could be effective for the regulation of catalytic performance. Encapsulation of common organometallic catalysts within cavitands proved to be crucial for the regulation of the selectivity while both catalyst activity and selectivity are influenced by encapsulation inside cages.[13,49,58] Since encapsulation can be reversed by addition of competitive *guests* for the *host* systems, this strategy can be suitable for the development of allosterically controlled systems.

Herein we report the modulation of the catalytic activity of a known catalyst based on its reversible encapsulation within the hexameric capsule obtained by self-assembly of six resorcin[4]arene molecules. The system was devised as follows: *i)* sequestration of the catalyst inside the cage must cause rapid and effective separation of the catalyst from the reactants, *ii)* the encapsulated catalyst has not to show any catalytic activity and, *iii)* quantitative expulsion of the catalyst from the cage must be reached as a consequence of the addition of competitive guest, *iv)* after expulsion the catalytic activity must be restored (proof of reversibility).

Design and evaluation of the system

The allosteric catalytic system was constituted by three species: the supramolecular cage, the catalyst and the competitive *guest*. Concerning the supramolecular *host*, resorcin[4]arene with long alkyl chains **2** was chosen by virtue of its known ability to self-assemble in spherical hexameric capsule $\mathbf{2_6 \cdot 8H_2O}$ held together by 60 hydrogen bond and characterized by an internal volume of about 1375 Å^3.[55,56] The catalytic species was constituted by the photoredox complex $[Ru(bpy)_3]^{2+}$ **1**, which is known to be active in visible light photoredox oxidation[168] of thioethers through conversion of O_2 into H_2O_2 as reported by Zen.[169] Since it is known that the hexameric capsule shows good encapsulation abilities towards cationic species, the chloride counterions of the commercially available $[Ru(bpy)_3]_2$, were replaced by less coordinating triflate ions by reaction with an AgOTf acetone solution and by removal of the insoluble silver chloride. We expected that this replacement of ruthenium counterions would enhance the encapsulation of the photoredox species within the hexamer. Finally tetraethyl ammonium triflate **3** and tetrapropyl ammonium triflate were chosen as competitive guests by virtue of the known *host-guest* abilities of the hexameric cage towards these molecular species.[57]

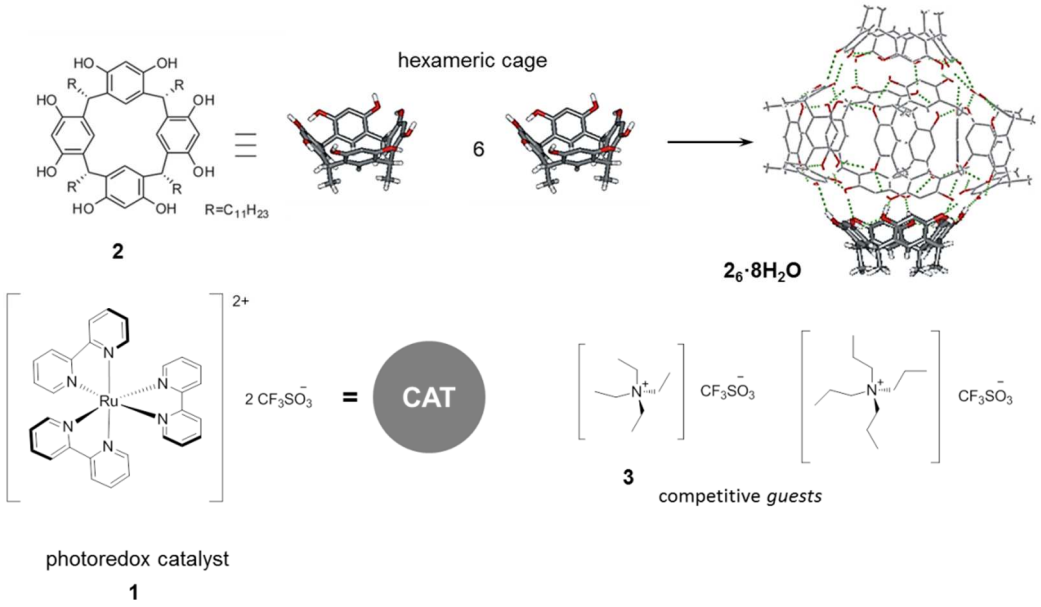

Figure 53. The three basic components chosen for the development of the allosteric catalytic system. $[Ru(bpy)_3](CF_3SO_3)$ **1** represents the catalytic moiety which could be encapsulated within the hexameric cage obtained by six resorcin[4]arene molecules equipped with long alkyl chains **2**. Encapsulation could be reverted by addition of competitive guests such as $[NEt_4](CF_3SO_3)$ **3** and $[NPr_4](CF_3SO_3)$.

The encapsulation process was firstly studied by ^{1}H-NMR spectroscopy using as 2.3 mM deuterated chloroform solution of the Ru(II) catalyst. The spectrum A, reported in Figure 54, clearly shows the resonances of the aromatic protons of $[Ru(bpy)3]^{2+}$ between 7.40 and 8.50 ppm. Upon addition of 6 equivalents of resorcin[4]arene the resonances of **1** completely disappear as a consequence of the encapsulation of the metal species, while new, extremely weak broad resonances emerge at higher field at 6.6 ppm (Figure 54, spectrum B). To proof the reversibility of the encapsulation process, 10 equivalents of tetraethylammonium triflate, which acts as competitive cationic guest, were added to the solution and consequently the typical resonances and coupling constants of **1** were restored (Figure 54, spectrum C). In the latter spectrum the resonances were detected at slightly lower chemical shifts than those reported in spectrum A of Figure 54. This could be due to either weak cationic-π interactions between the Ru(II) complex and the external surface of the aromatic capsule or caused by the increased concentrations of ions present in solution.

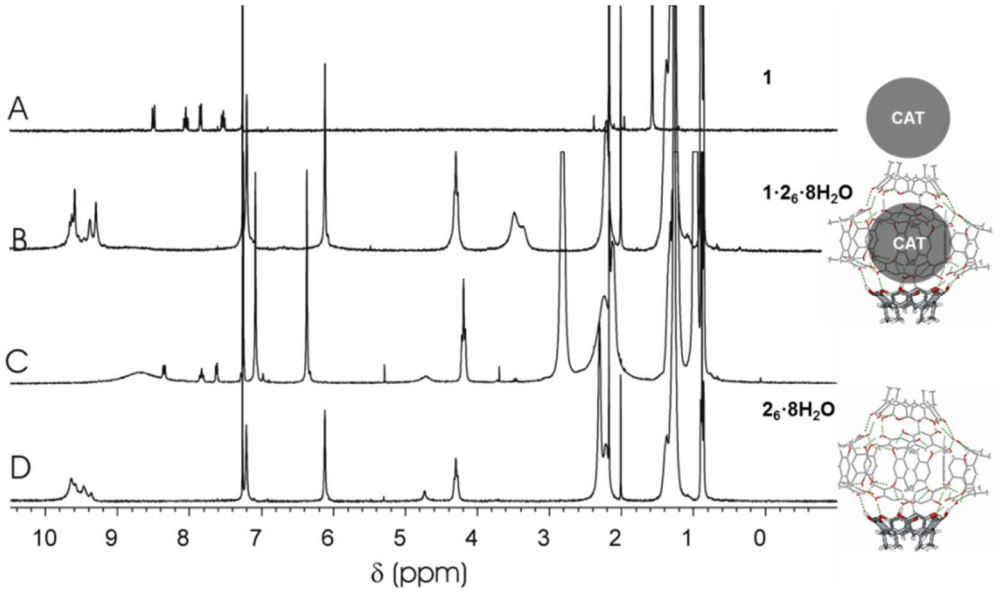

Figure 54. ^{1}H-NMR spectra in chloroform-d: **A) 1** (2.3 mM); **B) 1** (2.3 mM) and **2** (13.8 mM); **C) 1** (2.3 mM) and **2** (13.8 mM) and **3** (22.9 mM); **D**) **2** (13.8 mM)

After having proved the encapsulation and expulsion of the Ru(II) photoredox catalyst, we studied the effects of these operation by UV-Vis spectroscopy. As reported by the red spectrum in Figure 55, **1** shows, in absence of any supramolecular *host* and competitive *guests*, an intense absorption in the visible region with a maximum at 455 nm. Upon addition of 6 equivalents of resorcin[4]arene no particularly relevant variation of colour was observed and the UV-Vis spectrum revealed a shift to higher frequency of the maximum by only 8 nm (yellow spectrum, Figure 55). After expulsion of **1** by addition of 10 equivalents of tetraethylammonium triflate the original maximum at 455 nm was restored as shown in the green spectrum of Figure 55. This behaviour suggests that the encapsulation within the hexameric cage does not drastically affect the absorption properties of the ruthenium photoredox catalyst.

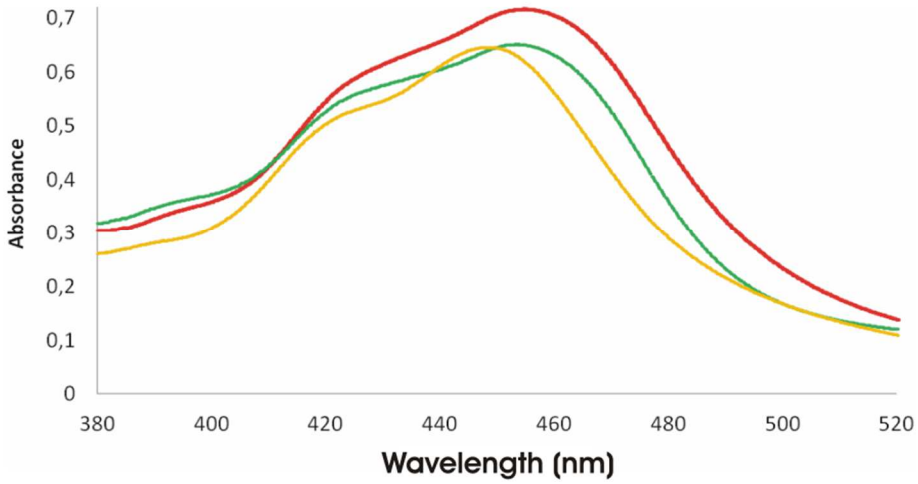

Figure 55. UV-VIS spectra for chloroform-d solutions: RED: **1** (2.3 mM); YELLOW: **1** (2.3 mM) and **2** (13.8 mM); GREEN: **1** (2.3 mM) and **2** (13.8 mM) and **3** (22.9 mM).

Catalytic aerobic oxidation of sulphides

The aerobic oxidation of thioethers was used as test reaction, using as test substrate the electron rich and highly reactive dibutylsulphide **4** (Scheme 58). Several catalytic tests were performed to show the effect of the encapsulation on the catalytic activity of $[Ru(bpy)_3]^{2+}$. The typical reaction procedure involves the addition of 50 equivalent of **4** to a 2.3 mM chloroform-d solution of ruthenium catalyst, purging O_2 through the solution and, after having termostatted the reactor at at 50 °C under 1 atm of O_2, visible light irradiation was performed by a 120 W lamp. The formation of the corresponding dibutyl sulfoxide **5**, dibutylsulfone **6** and dibutyl disulphide **7** was monitored over time by GC analysis. Table 18 reports the conversion's data obtained for the most important oxidation tests.

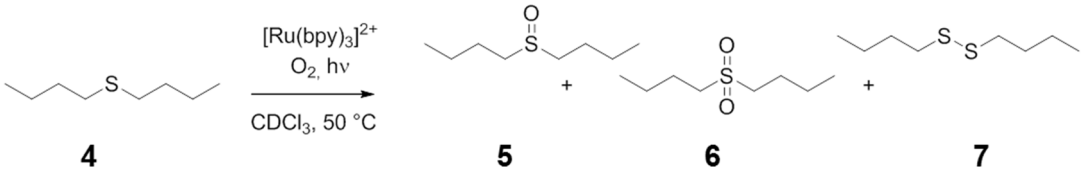

Scheme 58. Aerobic oxidation of sulphide **4** mediated by **1**.

Table 18. Catalytic tests for the aerobic oxidation of sulphide **4** mediated by **1** and regulated by addition of **2_6·8H_2O** and competitive guests.

#	**1**	**2_6·8H_2O**	**O_2**	**hν**	**3**	**5**[a] (%)	**6**[a] (%)	**7**[a] (%)
1	+	-	+	+	-	32	2	5
2	+	+	+	+	-	0	0	0
3	-	-	+	+	-	0	0	0
4	+	-	-	+	-	0	0	0
5	+	-	+	-	-	0	0	0
6	+	-	+	+	+	36	7	4
7	+	+	+	+	+[b]	29	1	1
8	+	+	+	+	+[c]	10	1	1
9	+	+	+	+	+[d]	5	0	0
10	+	+	+	+	+[e]	10	1	1
11	+[f]	-	+	+	-	63	13	8
12	+[g]	-	+	+	-	79	10	11

Experimental conditions: [1] = 2.3 mM, **[2]** = 13.8 mM, **[4]** = 115 mM, chloroform-d 0.5 mL, T=50°C, reaction time 3 h. +: presence, -: absence. A 120-W halogen lamp was used; a) Determined with GC; b) **[3]** = 23 mM (10 eq. with respect **2_6·8H_2O**); c) **[3]** = 11.5 mM, (5 eq. with respect **2_6·8H_2O**); d) **[3]** = 4.6 mM, (2 eq. with respect **2_6·8H_2O**); e) **[(NPr_4)(OTf)]** = 23 mM (10 eq. with respect **2_6·8H_2O**) was used instead of 3; f) **[4]** = 57.5 mM; g) **[4]** = 28.8 mM.

After 3h dibutylsulfoxide was obtained in 32% yield, together with **6** and **7** at 2% and 5% yields, respectively (Table 18, entry 1). A catalytic test was repeated with the addition of 6 equivalents of **2** under identical experimental conditions and omplete inactivity of the catalyst was observed (Table 18, entry 2). Control experiments were carried out under other various contitions (Table 18, entries 3-6) confirming that no oxidation occurred if any of the following species was missing: catalyst, light or O_2. Addition of a competitive guest for the capsule like $[NEt_4](CF_3SO_3)$ (10 equivalents compared to Ru(II) catalyst) in the aerobic oxidation by 1 and $\mathbf{2_6 \cdot 8H_2O}$ led to complete restoration of the catalytic activity (Table 18, entry 7). This was due to the displacement of the ruthenium catalyst from the cavity into solution previously reported. Lower amounts of competitive ammonium guest **3** with respect to the catalyst led to incomplete displacement of **1** from the capsule as confirmed by gradual decrease of the amount of all oxidation products (Table 18, entry 8 and 9). A larger ammonium competitive species such as $[NPr_4](CF_3SO_3)$ proved to be a poor competitive guest for the capsule since it did not completely restore the catalytic activity of the catalyst (Table 18, entry 10). The oxidation reaction can be further accelerated simply decreasing the amount of substrate employed (Table 18, entry 11 and 12). With 4% or 8% mol of catalyst the reaction was complete within 200 or 100 min, respectively.

Additional experiments were undertaken in order to ascertain the real oxidant species. Addition of 2,6-di-*t*-butylphenol did not suppress catalytic oxidation of dibutylsulphide by free $[Ru(bpy)_3]^{2+}$, thus excluding singlet oxygen formation in solution. The reaction in the absence of Ru(II) complex and in the presence of 1 equivalent of H_2O_2 with respect to the substrate showed a kinetic profile comparable to that observed with free O_2 and Ru(II) complex under irradiation, suggesting that H_2O_2 is likely photo-catalytically formed from O_2 by visible light activation of $[Ru(bpy)_3]^{2+}$. Iodometric determination of the presence of H_2O_2 of an irradiated solution of $[Ru(bpy)_3]^{2+}$ with O_2 unfortunately did not provide a clear colour change because of interference by the intrinsic UV-Vis absorption of$[Ru(bpy)_3]^{2+}$. Overall, in agreement with the mechanism proposed by Zen,[169] it is likely that visible light with $[Ru(bpy)_3]^{2+}$ as photosensitizer transforms O_2 in the wet solvent employed into H_2O_2 that directly oxidizes the electron rich substrate dibutylsulphide.
The catalytic system is sensitive to the electron density of the thioether. In fact, after 3h with methyl phenyl sulfide the reaction provides the corresponding sulfoxide in only 5% yield. This again supports the formation of H_2O_2 as true oxidant without direct participation of Ru(II) photoredox complex in the oxygen transfer step.

Allosteric regulation of the photoredox catalyst

The reversible control of the catalytic activity of **1** was demonstrated performing the sulfoxidation experiment described in Figure 56. The reaction was started following the oxidation of **4** with **1** under visible light with O_2. After 100 minutes 6 eq. of **2** were added to the system leading to the encapsulation of $\mathbf{1 \cdot 2_6.(H_2O)_8}$ thus causing a halt of the sulfide consumption and formation of oxidation products. The concentration of the former species remained unchanged until, after 165 minutes from the beginning of the reaction, 10 eq. of **3** were added leading to release the catalyst **1** into solution, formation of $\mathbf{3 \cdot 2_6.(H_2O)_8}$ and

consequent restoration of the catalytic activity (Figure 2). The increased rate of the reaction observed in this second part seems to be related to the presence of an excess of **3** in solution that, as observed in Table 18, entries 1 and 6, slightly promotes oxidation of **4**. A second stopping of the reaction was achieved by addition of a second amount of **2** (33 eq.) after 230 min from the beginning of the reaction. Confinement of the photocatalyst **1** within the supramolecular host $\mathbf{2_6 \cdot 8H_2O}$ does not alter its absorption properties, therefore the lack of catalytic activity in the presence of the capsule is likely due to the interrupted energy transfer from the Ru(II) center to O_2, the latter probably not a suitable co-guest for the cavity of $\mathbf{2_6 \cdot 8H_2O}$, or due to the lack of water within the cavity.[p]

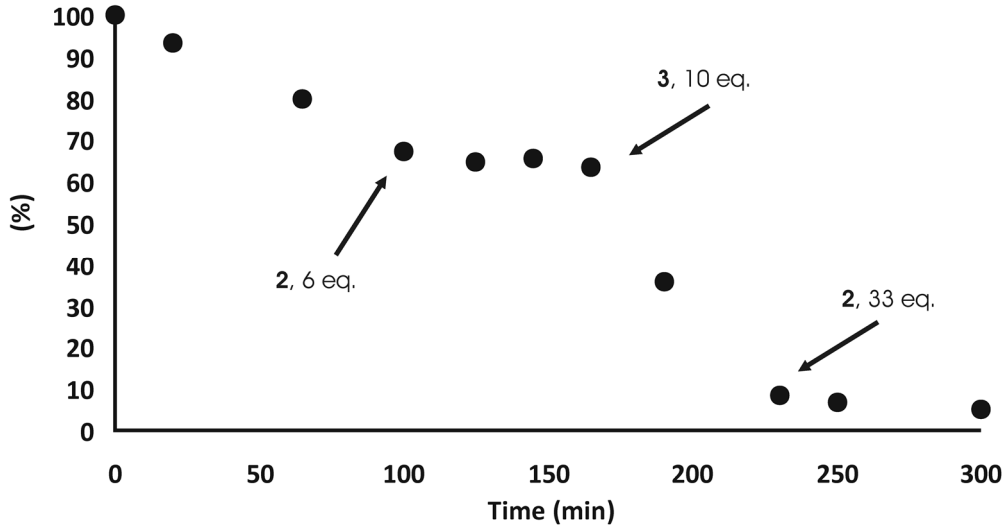

Figure 56. Variation of the residual sulfide **4** during reversible switching of **1** through sequential additions of **2** (6 eq., 100 min), competitive guest **3** (10 eq., 165 min) and **2** (33 eq., 230 min).

Conclusions

In conclusion, herein we described a new supramolecular method for the reversible modulation of the catalytic activity of a photoredox complex through its reversible encapsulation and release. The photocatalyst is in the on-state as long as it operates free in solution, while it is switched off when sequestered in the self-assembled, hydrogen-bonded capsule. The reversibility of the process is achieved through addition of a suitable competitive guest at proper concentrations.

The results reported in this chapter have been recently published in *"Switching the activity of a photoredox catalyst through reversible encapsulation and release"*, G. Bianchini, A. Scarso, G. La Sorella, , G. Strukul *Chem. Commun.* **2012**, *48*, 12082-12084.

p It is known that water is not a suitable guest for the hexamer as observed in the hydration reaction of alkynes mediated by an encapsulated Au(I) catalyst: Cavarzan A.; Scarso A.; Sgarbossa P.; Strukul G.; Reek J.N.H. *J. Am. Chem. Soc.*, **2011**, *133* , 2848.

Experimental

^{1}H-NMR, ^{13}C{^{1}H}-NMR and ^{31}P{^{1}H}-NMR were recorded at 298 K with a BRUKER AVANCE spectrometer operating respectively at 300.15, 75 and 121.5 MHz and with a BRUKER AC200 operating at 200, 50 and 80.7 MHz, respectively.

GC analysis were performed on HP SERIES II 5890 equipped with a HP5 column (30 m, I. D. 0.25 m, film 0.25 μm) using He as gas carrier and FID. GC-MS analyses were performed on a GC Trace GC 2000 equipped with a HP5-MS column (30 m, I.D. 0.25 mm, film 0.25 μm) using He gas carrier and coupled with a quadrupole MS Thermo Finnigan Trace MS with *Full Scan* method. Identification of the products was accomplished by reference samples or by comparison with samples obtained as described in literature.

TLC analysis were performed on TLC Polygram ® Sil G/UV254 of 0.25 mm thickness and flash-chromatography separations were performed on silica gel Merk 60, 230-400 mesh as reported by W. C. Still, M. Khan, A. Mitra *J. Org. Chem.* **1978**, *43*, 2923.

Solvents and reactants were used purchased; otherwise they were purified as reported in D. D. Perrin, W. L. F. Armarego *Purification of Laboratory Chemicals*, 3rd Ed., **1988**, Pergamon Press Ltd., Oxford OX3 0BW, England. Resorcin[4]arene **2** was already available in laboratory otherwise it was prepared according to Y. Aoyama. Y. Tanaka, S. Sugahara *J. Am. Chem. Soc.* **1989**, *111*, 5397-5404.

Irradiation in the visible region was performed with a visible ligh lamp (120 W).

*Synthesis of $[Ru(bpy)_3]\cdot(CF_3SO_3)_2$ (**1**)*

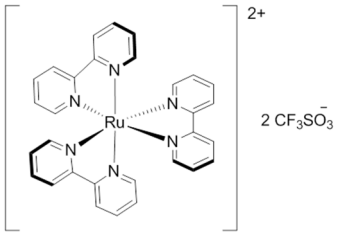

In a round bottom flask were placed $[Ru(bpy)_3]Cl_2\cdot(H_2O)_6$ (0.250 g, $0.334\cdot10^{-3}$ mol) and water (10 mL) and the resulting red solution stirred at room temperature. Subsequently an acetone solution of silver trifluoromethanesulfonate (0.098 M, 6.8 mL, $0.666\cdot10^{-3}$ mol) was added under vigorous stirring. The white precipitate was filtered and the solvents removed at reduced pressure yielding the product in 94 % as orange solid.

^{1}H-NMR (300.15 MHz, $CDCl_3$): δ 7.53 (t, J=6.0 Hz, 2H), 7.86 (d, J=6.0 Hz, 2H), 8.04 (t, J=6.0 Hz, 2H), 8.45 (d, J=6.0 Hz, 2H).
Elemental analysis, calc.: C 39.55 %, H 2.30 %, N 10.64 %, S 8.12 %; found C 39.60 %, H 2.33 %, N 10.74 %, S 8.06 %.

*Synthesis of tetraethylammonium trifluoromethanesulfonate (**3**)*

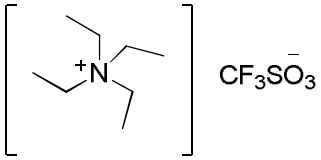

In a round bottom flask protected from light silver were placed trifluoromethanesulfonate (0.775 g, $3.02 \cdot 10^{-3}$mol), tetraethylammonium chloride (0.500 g, $3.02 \cdot 10^{-3}$mol) and dichloromethane (15 mL). The mixture was stirred at room temperature for 3 hours, after which the reaction crude filtered and the precipitated silver chloride washed with dichlomethane (3x15 mL). The combined organic phases were concentrated at reduced pressure leading the product in 82 % yield as fluffy white solid.

^{1}H-NMR (300.15 MHz, CD_3OD): δ 1.29 (tt, J=7.31 and 1.83 Hz, 12 H), 3.30 (q, J=7.31 Hz, 8 H).
13C-NMR (75.6 MHz, CD_3OD): δ 7.59, 53.27.
Elemental analysis, calc.: C 38.60 %, H 7.22%, N 5.01%, S 11.48%; found: C 38.51 %, H 7.18 %, N 5.11 %, S 11.52 %.

Synthesis of tetra-n-propylammonium trifluoromethanesulfonate

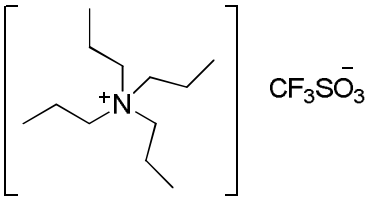

In a round bottom flask protected from light silver were placed trifluoromethanesulfonate (0.410 g, $1.59 \cdot 10^{-3}$mol), tetra-*n*-propylammonium iodide (0.500 g, $1.59 \cdot 10^{-3}$mol) and dichloromethane (15 mL). The mixture was stirred at room temperature for 3 hours, after which the reaction crude filtered and the precipitated silver chloride washed with dichlomethane (3x15 mL). The combined organic phases were concentrated at reduced pressure leading the product in 85 % yield as grey solid.

^{1}H-NMR (300.15 MHz, CD_3OD): δ 1.01 (t, J=7.3 Hz, 12 H), 1.71 (m, 8H), 3.19 (m, 8H).
^{13}C-NMR (75.6 MHz, CD_3OD): δ 10.89, 16.37, 61.36.
Elemental analysis calc.: C 46.55 %, H 8.41 %, N 4.18 %, S 9.56 %; found: C 46.44 %, H 8.37 %, N 4.15 %, S 9.61 %.

Typical experimental procedure for the on-off catalytic oxidation experiment

In a 3 mL vial were introduced a water saturated chloroform solution of **1** ($2.3 \cdot 10^{-3}$ M, 2 mL, $4.6 \cdot 10^{-6}$ mol). The solution was purged three times with oxygen and the vial termostatted at 50 °C under oxygen atmosphere. Subsequently dibutylsulfide **4** (40.3 μL, g, mol) was added and the vial exposed to a 120 W visible lamp. The progress of the oxidation reaction was monitored by sampling the solution followed by GC analysis. After 100 min, a water saturated chloroform solution of resorcin[4]arene **2** (0.112 M, 0.255 mL, $2.86 \cdot 10^{-5}$ mol) was

added observing the stop of catalytic activity. After 165 min, a solution of **3** (0.38 M, 0.120 mL, $4.56 \cdot 10^{-5}$ mol) was added to the system observing restoration of the catalytic activity. After 230 min, a water saturated chloroform solution of **2** (0.112 M, 1.400 mL, $1.57 \cdot 10^{-4}$ mol) was added observing a second stop of the catalytic activity.

GENERAL CONCLUSIONS

In this thesis the control of the activity in homogeneous catalysis was considered under different points of view. In the first approach the variation of the geometric environment surrounding a catalytic metal center was successfully modulated by means of intramolecular photodimerization of a coumarin-based phosphine coordinated to the metal center. In this approach light was used as effector and switching from the monodentate phosphines to the bidentate chelating bisphosphine showed to be effective for regulating the availability of the catalytic sites by virtue of the particular design of both chosen ligand and complex. The developed strategy represents a general approach for the regulation of those reactions where the catalytic activity and selectivity are in great part affected by the topicity of the ligands, like hydroformylation and hydrogenation reactions.

Light was used also to switch the electronic properties of common P ligands by means of introduction of the dithyenyl moiety within the molecular structure. In this study particular relevance was given to the substitution pattern of the dithienylethene moiety, more precisely one thiophene ring was equipped with the phosphine moiety while the other one was functionalised with substituents showing different electronic properties. It was found that significant enhancement of the σ-donation ability could be obtained switching the diarylethene fragment from the open form to the closed one. The difference of σ-donation ability between the two photochromic forms of the ligand resulted in first place dependent by the electronic nature of the chosen bridging unit between the two thiophene rings while the electronic nature of the substituents in the second thiophene ring were found less important. The synthesis of monophosphines containing the dithienylethene moiety is unprecedent and, after this preliminary study, new complexes equipped with these ligands could be developed for catalytic pourposes with a better knownledge of the effects induced by the photoisomerization reaction.

Another strategy faced in this work of thesis was the regulation of the availability of catalyst. For this pourpose supramolecular catalysts were chosen while a photomodulable dithienyl-based molecule was used as inhibitor. This study considered two different reaction media; in organic medium the hexameric capsule obtained by self-assembly of six resorcin[4]arene molecule was used as supramolecular catalyst in the hydration reaction of isonitriles, finding that the catalyst activity was strongly dependent by the photochromic form of the inhibitor. It was also observed that the presence of the hexameric capsule prevents the light promoted interconversion between the two photochromic forms of the chosen inhibitor and consequently the inhibiting effect could not be triggered by means of irradiation with light at the proper wavelength.

The same inhibitor was tested also in aqueous reaction medium. In this study the supramolecular catalyst was constituted by *β*-cyclodextrin and a complete study of the *host-guest* interactions between these components was carried out, establishing the basis for the development of new photomodulable supramolecular catalysts operating in water.

Finally the modulation of the coordination sphere surrounding a known organometallic catalyst was studied as possible effector for the regulationof of the catalystic activity. The model was designed using a $Ru(II)^{2+}$ photoredox complex as catalyst while the above mentioned hexameric capsule was used as effector. The availability of the catalyst in the bulk

solution was remotely controlled by encapsulation within the hexameric capsule that was reversibly performed by addition of competitive guests for the cavity. When the photocatlytic aerobic oxidation of sulphides was used as test reaction, it was found that the encapsulated Ru(II) complex was completely inactive at variance with the activity shown when it was free in solution. Thanks to the addition of competitive guests, like ammonium salts, and fresh hexameric capsule the activity of the catalyst could be switched instantaneously.

In conclusion the development of new strategies to induce allosteric behavior in man-made catalysts requires the crossing of different chemistry fields: organic and metallorganic synthesis, design and evaluation of ligands, synthesis of photochromic molecules, photochemistry, supramolecular chemistry and of course homogeneous catalysis.

REFERENCES

1 Catalyst and Catalysis

2 D. Voet, J. G. Voet *Biochimica,* Zanichelli, **1993**, Bologna; translation of: *Biochemistry* (with 1991-1992 *Supplements to Biochemistry*), 1990, John Wiley & Sons, Inc.

3 M. J. Wiester, P. A. Ulmann, C. A. Mirkin *Angew. Chem. Int. Ed*. **2011**, *50*, 114-137.

4 For reviews see: a) M. Fujita, K. Ogura *Coord. Chem. Rev.* **1996**, *148*, 249-264; b) S. J. Dalgarno, N. P. Power, J. L. Atwood *Coord. Chem. Rev*. **2008**, *252*, 825-841; c) F. A. Cotton, C. Lin, C. A. Murillo *Acc. Chem. Res.* **2001**, *34*, 759-771; d) S. R. Seidel, P. J. Stang *Acc. Chem. Res.* **2002**, *35*, 972-983; e) M. Fujita, M. Tominaga, A. Hori, B. Therrien *Acc. Chem. Res.* **2005**, *38*, 371-380; f) S. Leininger, B. Olenyuk, P. J. Stang *Chem. Rev*. **2000**, *100*, 853-908; g) F. Würthner, C.-C. You, C. R. Saha- Möller *Chem. Soc. Rev*. **2004**, *33*, 133-146; h) B. H. Northrop, Y. –R. Zheng, K. –W. Chi, P. J. Stang *Acc. Chem. Res*. **2009**, *42*, 1554-1563.

5 D. L. Caulder, K. N. Raymond *Acc. Chem. Res.* **1999**, *32*, 975-982.

6 a) J. R. Farrell, C. A. Mirkin, I. A. Guzei, L. M. Liable-Sands, A. L. Rheingold *Angew. Chem. Int. Ed.* **1998**, *37*, 465-467; b) B. J. Holliday, C. A. Mirkin Angew. Chem. Int. Ed. 2001, 40, 2022-2043; c) N. C. Gianneschi, M. S. Masar III, C. A. Mirkin *Acc. Chem. Res.* **2005**, *38*, 825-837.

7 G. A. Morris, S. T. Nguyen, J. T. Hupp, *J. Mol. Catal. A* **2001**, *113*, 4239-4242.

8 M. L. Merlau, M. del Pilar Mejia, S. T. Nguyen, J.T. Hupp *Angew. Chem. Int. Ed.* **2001**, *40*, 4239-4242.

9 S. J. Lee, S. –H. Cho, K. L. Mulfort, D. M. Tiede, J. T. Hupp, S. T. Nguyen *J. Am. Chem. Soc*. **2008**, *130*, 16828-16829.

10 D. L. Caulder, R. E. Powers, T. N. Parac, K. N. Raymond *Angew. Chem. Int. Ed* **1998**, *37*, 1840-1843.

11 A. Davis, D. Fiedler, M. Ziegler, A. Terpin, K. N. Raymond *J. Am. Chem. Soc.* **2007**, *129*, 2746-2747.

12 D. H. Leung, D. Fielder, R. G. Bergman, K. N. Raymond *Angew. Chem. Int. Ed.* **2004**, *43*, 963-966.

13 D. H. Leung, R. G. Bergman, K. N. Raymond *J. Am.Chem. Soc.* **2007**, *129*, 2746-2747.

14 a) D. Fielder, R. G. Bergman, K. N. Raymond *Angew. Chem. Int. Ed.* **2004**, *43*, 6748-6751; b) D. Fielder, H. van Halbeek, R. G. Bergman, K. N. Raymond *J. Am. Chem. Soc* **2006**, *128*, 10240-10252.

15 M. D. Pluth, R. G. Bergman, K. N. Raymond *Angew. Chem. Int. Ed.* **2007**, *46*, 8587-8589.

16 a) M. D. Pluth, R. G. Bergman, K. N. Raymond *Science*, **2007**, *316*, 85-88; b) M. D. Pluth, R. G. Bergman, K. N. Raymond *J. Am. Chem. Soc.* **2008**, *130*, 11423-11429.

17 C.J. Hastings, M.D. Pluth, R.G. Bergman, K.N. Raymond, *J. Am. Chem. Soc*., **2010**, *132*, 6938–6940.

18 a) M. Fujita, D. Oguro, M. Miyazawa, H. Oka, K. Yamaguchi, K. Ogura *Nature*, **1995**, *378*, 469-471; b) M. Fujita, M. Tominaga, A. Hori, B. Therrien *Acc. Chem. Res.* **2005**, *38*, 369-378; c) S. –Y. Yu, T. Kusukawa, K. Biradha, M. Fujita *J. Am. Chem. Soc.* **2000**, *122*, 2665-2666; d) K. Suzuki, J. Iida, S. Sato, M. Kawano, M. Fujita *Angew. Chem. Int. Ed.* **2008**, *47*,5780-5782; e) K. Suzuki, M. Tominaga, M. Kawano, M. Fujita *Chem. Comm.* **2009**, 1638-1640;

19 H. Ito, T. Kusukawa, M. Fujita *Chem. Lett.* **2000**, *29*, 598-599.

20 T. Kusukawa, T. Nakai, T. Okano, M. Fujita *Chem. Lett*. **2003**, *32*, 284-285.

21 Y. Nishioka, T. Yamaguchi, M. Kawano, M. Fujita *J. Am. Chem. Soc.* **2008**, *130*, 8160-8161.

22 M. Yoshizawa, M. Tamura, M. Fujita *Science*, **2006**, *312*, 251-254.

23 a) R. Bellini, J. N. H. Reek *Chem. Eur. J.* **2012**, *18*, 13510-13519; b) V. F. Slagt, P. Kaiser, A. Berkessel, M. Kuil, A. M. Kluwer, P. W. N. M. van Leeuwen, J. N. H. Reek *Eur. J. Inorg. Chem.* **2007**, 4653-4662.

24 For reviews see: a) M. J. Wilkinson, P. W. N. M. van Leeuwen, J. N. H. Reek *Org. Biomol. Chem.* **2005**, *3*, 2371; b) B. Breit *Angew. Chem. Int. Ed.* **2005**, *44*, 6816; c) A. J. Sandee, J. N. H. Reek *Dalton Trans.* **2006**, 3385.

25 a) V. F. Slagt, P.W. N. M. van Leeuwen, J. N. H. Reek *Angew. Chem. Int. Ed.* **2003**, *42*, 5619-5623; b) V. F. Slagt, P. W. N. M. van Leeuwen, J. N. H. Reek *Chem. Comm.* **2003**, 2474-2475.

26 a) J. C. Poulin, T. P. Dang and H. B. Kagan *J. Organomet. Chem.*, **1972**, 92; b) R. Selke and H. Pracejus *J. Mol. Catal.* **1986**, *37*, 213.

27 P. W. N. M. van Leeuwen, P. C. J. Kamer, J. N. H. Reek and P. Dierkes *Chem. Rev.* **2000**, *100*, 2741.

28 a)V. F. Slagt, M. Röder, P. C. J. Kamer, P.W. N. M. van Leeuwen, J. N. H. Reek *J. Am. Chem. Soc.* **2003**, *126*, 4056-4057; b) X.-B. Jiang, L. Lefort, P. E. Goudriaan, A. H. M. de Vries, P. W. N. M. van Leeuwen, J. G. de Vries, J. N. H. Reek *Angew. Chem. Int. Ed.* **2006**, *45*, 1223-1227; c) V. F. Slagt, P. Kaiser, A. Berkessel, M. Kuil, A. M. Kluwer, P. W. N. M. van Leeuwen, J. N. H. Reek *Eur. J. Inorg. Chem.* **2007**, 4653-4662.

29 I. O. Fritsky, R. Ott, R. Krämer *Angew. Chem. Int. Ed.* **2000**, *39*, 3255-3258.

30 L. Kovbasyuk, H. Pritzkow, R. Krämer, I. O. Fritsky *Chem. Comm.* **2004**, 880-881.

31 A. Scarso, U. Scheffer, M. Göbel, Q. B. Broxterman, B. Kaptein, F. Formaggio, C. Toniolo, P. Scrimin *Proc. Natl. Acad. Sci. USA* **2002**, *99*, 5144-5149.

32 A. Scarso, G. Zaupa, F. Bodar Houillon, L. J. Prins, P. Scrimin *J. Org. Chem.* **2007**, *72*, 376-385.

33 N. C. Gianneschi, S. T. Nguyen, C. A. Mirkin *J. Am. Chem. Soc.* **2005**, *127*, 1644-1645.

34 H. J. Yoon, J. Kuwabara, J-Hyun Kim, C. A. Mirkin *Science*, **2010**, 330, 66-69.

35 For review see: a) R. Breslow, S. D. Dong *Chem. Rev.* **1998**, *98*, 1997-2011; b) K. Takahashi *Chem. Rev.* **1998**, *98*, 2013-2033.

36 R. L. van Etten, G. A. Clowes, J. F. Sebastian, M. L. Bender *J. Am. Chem. Soc.* **1967**, *89*, 3253.

37 R. Breslow, G. Trainor, A. Ueno *J. Am. Chem. Soc.* **1983**, *105*, 2739.

38 a) R. Breslow, P. Campbell *J. Am. Chem. Soc.* **1969**, *91*, 3085; b) R. Breslow, P. Campbell *Bioorg. Chem.* **1971**, *1*, 140; c) R. Breslow, H. Kohn, B. Siegel *Tetrahedron Lett.* **1976**, 1645.

39 a) D. Rideout,.R. Breslow *J. Am. Chem. Soc.* **1980**, *102*, 7812; b) H. -J Schneider,N. K. Sangwan. *Angew. Chem.* **1987**, *99*, 924; c) H.-J, Schneider, N. K. Sangwan *J. Chem. Soc., Chem. Commun.***1986**, 1787; d) T. Hudlicky,G. Butora, S. P. Fearnley, A. G. Gum, P. J. III, M. R. Stabile; J. S. Merola *J. Chem. Soc., Perkin Trans.* **1995**, *1*, 2393-2398.

40 S. P. Kim, A. G. Leach, K. N. Houk *J. Org. Chem.***2002**, *67*, 4250-4260.

41 a) J. N. H. Reek, P. W. N. M. Van Leeuwen *Supramolecular Catalysis*; Ed.; Wiley, VCH: Weinheim, **2008**; pp 199-234. (b) Hapiot, F.;Tilloy, S.; Monflier, E. *Chem. Rev.* **2006**, *106*, 767–781.

42 a)E. Monflier, G. Fremy, Y. Castanet, A. Mortreux *Angew. Chem. Int. Ed.* **1995**, *34*, 2269-2271; b) M. Dessoudeix, M. Urrutigoïty, P. Kalck *Eur. J. Inorg. Chem.***2001**, *7*, 1797-1800.

43 E. Monflier, H. Bricout, F. Hapiot, S. Tilloy, A. Aghmiz, A. M. Masdeo-Bultó *Adv. Synth. Catal.***2004**, *346*, 425-431.

44 L. Leclercq, A. R. Schimitzer *Organometallics*, **2010**, *29*, 3442-3449.

45 A. R. Khan, P. Forgo, J. S. Keith, V. T. D'Souza *Chem. Rev.* **1998**, *98*, 1977-1996.

46 S. Richeter, J. Rebek Jr *J. Am. Chem. Soc.* **2004**, *126*, 16280-16281.

47 R. J. Hooley, J. Rebek Jr *Org. Biomol. Chem.* **2007**, *5*, 3631-3636.

48 M. A. Sarmentero, P. Ballester *Org. Biomol. Chem.* **2007**, *5*, 3046-3054.

49 M. A. Sarmentero, H. Fernández-Pérez, E. Zuidema, C. Bo, A. Vidal-Ferran, P. Ballester *Angew. Chem. Int. Ed.* **2010**, *49*, 7489-7492.

50 For review see: a) M. M. Conn, J. Rebek Jr *Chem. Rev.* **1997**, *97*, 1647-1668.

51 C. Valdes, U. P. Spitz, L. M. Toledo, S. W. Kubik, J. Rebek Jr *J. Am. Chem. Soc.* **1995**, *117*, 12733-12745.

52 Y. Tokunaga, J. Rebek Jr *J. Am. Chem. Soc.* **1998**, *120*, 66-69.

53 J. Kang, J. Rebek Jr *Nature*, **1997**, *385*, 50-52.

54 J. Kang, J. Santamaría, G. Hilmersson, J. Rebek Jr *J. Am. Chem. Soc.* **1998**, *120*, 7389-7390.

55 L. R. McGillivray, J. L. Atwood *Nature*, **1997**, *389*, 469-472.

56 Y. Cohen, L. Avram *Org. Lett.* **2002**, *4*, 4365-4368.

57 a) Y. Cohen, L. Avram *J. Am. Chem. Soc.* **2004**, *126*, 11556-11563; b) J. Rebek Jr *Angew. Chem. Int. Ed.* **2005**, *44*, 2068-2078; c) A. Shivanyuk, J. Rebek Jr *PNAS USA* **2001**, *98*, 7662-7665; d) L. Avram, Y Cohen *Organic Letters*, **2008**, *10*, 1505-1508.

58 A. Cavarzan, A. Scarso, P. Sgarbossa, G. Strukul, J. N. H. Reek *J.Am. Chem. Soc.* **2011**, *133*, 2848-2851.

59 J. W. Hastings *J. Mol. Evol.* **1983**, 309-321.

60 R. S. Stoll, S. Hecht *Angew. Chem. Int. Ed.* **2010**, *49*, 5054-5075; and reference therein.

61 a) S. Funyu, T. Isobe, S. Akagi, D. A. Tryk, H. Inoue *J. Am. Chem. Soc.* **2003**, *125*, 5734; b) H. Inoue, T. Okamoto, Y. Kameo, M. Sumitani, A. Fujiwara, D. Ishibashi, M. Hida *J. Chem. Soc., Perkin Trans. 1* **1994**, 105.

62 a) R. Miyatani, Y. Amao *J. Mol. Catal. B* **2004**, *27*, 121; b) J. Grodkowski, D. Behar, P. Neta *J. Phy* s. *Chem. A* **1997**, *101*, 248.

63 H. Inoue, S. Funyu, Y. Shimada, S. Takagi *Pure Appl. Chem.* **2005**, *77*, 1019.

64 a) J. G. Vos, J. M. Kelly *Dalton Trans.***2006**, 4869; b) J. P. Paris, W. W. Brandt *J. Am. Chem. Soc.* **1959**, *81*, 5001.

65 a) M. A. Ischay, Z. Lu, T. P. Yoon *J. Am. Chem. Soc.***2010**, *132*, 8572-8574; b) J. Du, T. P. Yoon *J. Am. Chem. Soc.* **2009**, *131*, 14604-14605.

66 A. Inagaki, M. Akita *Coord. Chem. Rev.* **2010**, *254*, 1220-1239.

67 K. P. C. Vollhardt *Angew. Chem. Int. Ed.* **1984**, *23*, 539-556.

68 a) L. Delaude, A. Demonceau, A. F. Noels *Chem. Commun.* **2001**, 986-987; b) L. Delaude, M. Szypa, A. Demonceau, A. F. Noels *Adv. Synth. Catal.* **2002**, *344*, 749-756.

69 X. Sun, J. P. Gao, Z. Y. Wang *J. Am. Chem. Soc.* **2008**, *130*, 8130-8131.

70 K. K. Benjamin, R. H. Grubbs *J. Am. Chem. Soc.* **2009**, *131*, 2038-2039; and references therein.

71 http://en.wikipedia.org/wiki/Photochromismhttp://en.wikipedia.org/wiki/Photochromism

72 M. B. Smith, J. March *March's Advanced Organic Chemistry*, John Wiley & Sons, 6th Ed., **2007**, Hoboken, New Jersey.

73 P. E. Sonnet *Tetrahedron* **1980**, *36*, 557-604; and references therein.

74 E. Merino, M. Ribagorda, *Beilnstein J. Org. Chem.* **2012**, *8*, 1071-1090; and reference therein.

75 A. Ueno, K. Takahashi, T. Osa *J. Chem. Soc. Chem. Commun.* **1980**, 837-838.

76 W. –S. Lee, A. Ueno *Macromol. Rapid. Commun.* **2001**, *22*, 448-450.

77 F. Würthner, J. Rebek Jr *Angew. Chem. Int. Ed.* **1995**, *34*, 446-448.

78 R. Cacciapaglia, S. Di Stefano, L. Mandolini *J. Am. Chem. Soc.* **2003**, *125*, 2224-2227.

79 H. Sugimoto, T. Kimura, S. Inoue *J. Am. Chem. Soc.* **1999**, *121*, 2325-2326.

80 M. V. Peters, R. S. Stoll, A. Kühn, S. Hecht *Angew. Chem. Int. Ed.* **2008**, *47*, 5968-5972.

81 R. Stoll, M. V. Peters, A. Kühn, S. Heiles, R. Goddard, M. Bühl, C. M. Thiele, S. Hecht *J. Am. Chem. Soc.* **2009**, *131*, 357-367.

82 a) R. Anet *Can. J. Chem.* **1962**, *40*, 1249; b) G. O. Schenck, I. von Wilucki, C. H. Krauch *Chem. Ber.* **1962**, *95*, 1409; c) G. S. Hammond, C. A. Stout, A. A. Lamola *J. Am. Chem. Soc.* **1964**, *86*, 3103; d) H. Morrison, H. Curtis, T. McDowell *J. Am. Chem. Soc.* **1966**, 5415-5419; e) R. Hoffman, P. Wells, H. Morrison *J. Org. Chem.* **1971**, 102-108.

83 N. Hoffmann *Chem. Rev.* **2008**, *108*, 1052-1103.

84 a) Q. Jin, F. Mitschang, S. Agarwal *Biomacromolecules,* **2011**, *12*, 3684-3691; b) N. K. Mal, M. Fujiwara, Y. Tanaka, T. Taguchi, M. Matsukata *Chem. Mater.* **2003**, *15*, 3385-3394.

85 Y. Zhao *Macromolecules,* **2012**, *45*, 3647-3657.

86 K. Ilioupuolos, O. Krupka, D. Gindre, M. Sallé *J. Am. Chem. Soc.* **2010**, *132*, 14343-14345.

87 a) D. Kehrlösser, J. Träger, H.-C. Kim, N. Hampp *Langmuir*, **2010**, *26*, 3878-3882; b) Y. Zhao, J. Bertrand, X. Tong, Y. Zhao *Langmuir*, **2009**, *25*, 13151-13157; c) J. He, X. Tong, Y. Zhao *Macromolecules,* **2009**, *42*, 4845-4852; d) X. Jiang, R. Wang, Y. Ren, J. Yin *Langmuir*, **2009**, *25*, 9629-9632.

88 T. Nozaki, M. Maeda, Y. Maeda, H. Kitano *J. Chem. Soc., Perkin Trans. 2* **1997**, 1217-1220.

89 For computational study on spirooxazines/merocyanine interconversion mechanism see: P. J. Castro, I. Gómez, M. Cossi, M. Reguero *J. Phys. Chem. A* **2012**, *116*, 8148-8158.

90 G. Berkovic, V. Krongauz, V. Weiss *Chem. Rev.* **2000**, *100*, 1741-1753.

91 A. V. Metelitsa, J. C. Micheau, N. A. Voloshin, E. N. Voloshina, V. I. Mikin *J. Phys. Chem. A* **2001**, *105*, 8417-8422.

92 T. P. I. Saragi, T. Spehr, A. Siebert, T. Fuhrmann-Lieker, J. Salbeck *Chem. Rev.* **2007**, *107*, 1011-1065.

93 a) K. Szacilowski *Chem. Rev.* **2008**, *108*, 3481-3548; b) G. Berkovic, V. Krongauz, V. Weiss *Chem. Rev.* **2000**, *100*, 1741-1753.

94 B.-H. Tan, M. Yoshio, T. Ichikawa, T. Mukai, H. Ohno, T. Kato *Chem. Commun.* **2006**, 4703-4705.

95 a) L. Florea, D. Diamond, F. Benito-Lopez *Macromol. Mater. Eng*. **2012**, *297*, 1148-1159; b) R. Klajn, J. F. Stoddart, B. A. Grzybowski *Chem. Soc. Rev*. **2010**, *39*, 2203-2237.

96 a) Y. P. Strokach, T. M. Valova, V. A. Barachevskii, A. I. Shienok, V. S. Marevtsev *Russ. Chem. Bull*., Int. Ed. **2005**, *54*, 1477-1480; b) M. M. Paquette, B. O. Patrick, N. L. Frank *J. Am. Chem. Soc*. **2011**, *133*, 10081-10093; c) X.-C. Zhang, Z.-M. Huo, T.-T. Wang, H.-P. Zeng *J. Phys. Org. Chem.* **2012**, *25*, 754-759; d) S. V. Paramonov, V. Lokshin, O. A. Fedorova *Journal of Photochemistry and Photobiology C: Photochemistry Reviews*, **2011**, *12*, 209-236; e) M. Querol, B. Bozic, N. Salluce, P. Belser *Polyhedron* , **2003**, *22*, 655-664.

97 G. Liu, J. Wang *Angew. Chem. Int. Ed.* **2010**, *49*, 4425-4429.

98 M. Irie, K. Uchida *Bull. Chem. Soc. Jpn.* **1998**, *71*, 985-996.

99 S. Nakamura, M. Irie *J. Org. Chem.* **1988**, *53*, 6136.

100 M. Irie, K. Sakemura, M. Okinaka, K. Uchida *J. Org. Chem.* **1995**, *60*, 8305-8309.

101 J. M. Lehn et al. *Chem. Eur. J.* **1995**, 275-284.

102 S. Kawauchi, H. Yoshida, N. Yamashina, M. Ohira, S. Saeda, M. Irie *Bull. Chem. Soc. Jpn.* **1990**, *63*, 267.

103 J. R. Gispert *Coordination Chemistry*, WILEY-VCH Verlag GmbH Co. KGaA, **2008**, Weinheim.

104 O. S. Wenger, *Chem. Soc. Rev.* **2012**, *41*, 3772-3779.

105 U. Al-Atar, R. Fernandes, B. Johnsen, D. Baillie, N. R. Branda *J. Am. Chem. Soc.* **2009**, *131*, 15966-15967.

106 A. J. Myles, N. R. Branda *Adv. Funct. Mater.* **2002**, *12*, 167-173.

107 Z. Arno, I. Yildiz, B. Gorodetsky, F. M. Raymo, N. R. Branda *Photochem. Photobiol. Sci.* **2010**, *9*, 249-253.

108 a) V. Lemieux, M. D. Spantulescu, K. K. Baldridge, N. R. Branda *Angew. Chem. Int. Ed.* **2008**, *47*, 5034-5037; b) D. Wilson, N. R. Branda *Angew. Chem. Int. Ed.* **2012**, *5431-5434;* c) Z. Erno, A. M. Asadirad, V. Lemieux, N. R. Branda *Org. Biomol. Chem.* **2012**, *10*, 2787-2792; d) H. D. Samachetty, V. Lemieux, N. R. Branda *Tetrahedron*, **2008**, *64*, 8292-8300.

109 F. Nourmohammadian, T. Wu, N. R. Branda *Chem. Commun.* **2011**, *47*, 10954-10956.

110 B. M. Neilson, V. M. Lynch, C. W. Bielawski *Angew. Chem. Int. Ed.* **2011**, *50*, 10322-10326.

111 B. M. Neilson, C. W. Bielawski *J. Am. Chem. Soc.* **2012**, *134*, 12693-12699.

112 G. A. Grasa, T. Güveli, R. Singh, S. P. Nolan *J. Org. Chem.* **2003**, *68*, 2812-2819.

113 D. Sud, R. McDonald, N. R. Branda *Inorganic Chemistry*, **2005**, *44*, 5960-5962.

114 D. Sud, T. B. Norsten, N. R. Branda *Angew. Chem. Int. Ed.* **2005**, *44*, 2019-2021.

115 a) H. Valizadeh, A. Shockravi *Tetrahedron Letters*, **2005**, *46*, 3501-3503; b) M. K. Potdar, S. S. Mohile, M. M. Salunkhe *Tetrahedron Letters*, **2001**, *42*, 9285-9287; c) S. K. De, R. A. Gibbs *Synthesis*, **2005**, 1231-1233; and references therein.

116 C. E. Song, D. –U. Jung, S. Y. Choung, E. J. Roh, S. -G. Lee *Angew. Chem. Int. Ed.* **2004**, 6183-6185.

117 a) B. C. Ranu, R. Jana *Eur. J. Org. Chem.* **2006**, 3767-3770; b) C. Su, Z. –C. Chen, Q. –G. Zhen *Synthesis*, **2003**, 555-559.

118 Y. Yamamoto, N. Kirai *Org. Lett.* **2008**, *10*, 5513-5516.

119 T. N. Van, S. Debenedetti, N. D. Kimpe *Tetrahedron Letters*, **2003**, 4199-4201.

120 H. Valizadeh, A. Shockravi *Synthetic Communications*, **2009**, 4341-4349.

121 a) A. Shockravi, H. Valizadeh, M. M. Heravi *Phosphorous, Sulfur and Silicon and the Related Elements*, **2003**, 501-504; b) H. Valizadeh, A. Shockravi, M. M. Heravi, H. B. Ghadim *Journal of Chemical Research Synopses*, **2003**, 718-720.

122 a) G. Annibale, P. Bergamini, M. Cattabriga *Inorg. Chim. ACTA* **2001**, *316*, 25-32; b) T. G. Appleton, H. C. Clark, L. E. Manzer *Coord. Chem. Rev*. **1973**, *10*, 335-422.

123 L. Moggi, A. Juris, M. T. Gandolfi *Quaderni di Fotochimica-Manuale del Fotochimico*, **2006**, Bononia University Press, Bologna, p 38.

124 a) K. Gnanaguru, N. Ramasubbu, K. Venkatesan, V. Ramamurthy *J. Org. Chem.* **1985**, *50*, 2337; b) J. N. Moorthy, K. Venkatesan, R. G. Weiss *J. Org. Chem.* **1992**, *57*, 3292; c) K. Vishnumurthy, T. N. G. Row, K. Venkatesan *Tetrahedron*, **1998**, *54*, 11235.

125 D. M. Roundhill *Modern Inorganic Chemistry-Photochemistry and Photophysics of Metal Complexes*, **1994**, Plenum Press, New York.

126 Gary Wulfesbergm *Inorganic Chemistry*, University Science Book, **2000**, Sausalito CA (USA).

127 a) R. Romeo, D. Minnita, M. Trozzi, *Inorg. Chem.* **1976**, *15*, 1134; b) W. J. Louw, R. van Eldik, H. Kelm *Inorg. Chem.* **1980**, *19*, 2878-2880.

128 A. Scarso, M. Colladon, P. Sgarbossa, C. Santo, R. A. Michelin, G. Strukul *Organometallics,* **2010**, *29*, 1487-1497.

129 R. A. Michelin, P. Sgarbossa, A. Scarso, G. Strukul, *Coord. Chem. Rev*. **2010**, *254*, 646-660.

130 a) E. Pizzo, R. A. Michelin, A. Scarso, P. Sgarbossa, M. Mozzon, G. Strukul, A. Tassan, F. Benetollo, *J. Organomet. Chem.* **2006**, *691*, 3259-3666. b) G. Strukul *Top. Catal.* **2002**, *19*, 33-42.

131 L. N. Lucas, J. J. D. de Jong, R. M. Kellog, J. H. van Esch, B. L. Feringa *Eur. J. Org. Chem.* **2003**, 155-166.

132 S. Hermes, G. Dassa, G. Toso, A. Bianco, C. Bertarelli, G. Zerbi **2009**, 1614-1617.

133 Y. Yokoyama, N. Hosoda, Y. T. Osano, C. Sasaki *Chemistry Letters* **1998**, 1093-1094.

134 S. Gronovitz, A. –B. Hörnfeldt *Thiophenes*, Elsevier, **2004**, Oxford.

135 J. J. D. de Jong, L. N. Lucas, R. M. Kellog, B. L. Feringa, J. H. van Esch *Eur. J. Org. Chem.* **2003**, 1887-1893.

136 W. R. Browne, J. J. D. de Jong, T. Kudernac, M. Walko, L. N. Lucas, K. Uchida, J. H. van Esch, B. L. Feringa *Chem. Eur. J.* **2005**, *11*, 6430-6441.

137 M. Moreno-Manas, M. Perez, R. Pleixats *J. Org. Chem.* **1996**, *61*, 2346-2351.

138 J. Areephong, W. R. Browne, B. L. Feringa *Org. Biomol. Chem.* **2007**, *5*, 1170-1174.

139 V. A. Migulin, M. M. Krayushkin, V. A. Barachevsky, O. I. Kobeleva, T. M. Valova, K. A. Lyssenko *J. Org. Chem.* **2012**, *77*, 332-340.

140 A. G. Orpen, N. G. Connelly *Organometallics*, **1990**, *9*, 1206-1210.

141 a) S. –X. Xiao, W. C. Trogler, D. E. Ellis, Z. Berkovitch-Yellin *J. Am. Chem. Soc.* **1983**, *105*, 7033-7037; b) D. S. Marynick *J. Am. Chem. Soc*. **1984**, *106*, 4064-4065.

142 M. Wrighton *Chem. Rev.* **1974**, 401; and references therein.

143 O. Kühl *Coord. Chem Rev.* **2005**, 693-704.

144 C. A. Tolman *Chem. Rev.* **1977**, 313.

145 a) D. W. Allen, B. F. Taylor *J. Chem. Soc. Dalton Trans.* **1982**, 51-54; b) D. W. Allen, I. W. Nowell, B. F. Taylor *J. Chem. Soc. Dalton Trans.* **1985**, 2505-2508.

146 S. C. Van der Slot, J. Duran, J. Luten, P. C. J. Kamer, P. W. N. M. van Leeuwen *Organometallics*, **2002**, *21*, 3873-3883.

147 A. Roodt, S. Otto, G. Steyl *Coord. Chem Rev.* **2003**, *245*, 121-137.

148 a) K. Motoyama, H. F. Li, K. M. Hatakeyama, S. Yokojima, S. Nakamura, M. Akita *J. Chem. Soc. Dalton Trans.* **2011**, *40*, 10643; b) R. T. F. Jukes, V. Adamo, F. Hartl, P. Belser, L. De Cola *Inorg. Chem.* **2004**, *43*, 2779.

149 a) L. Zhu, H. Yan, C. Y. Ang, K. T. Nguyen, M. Li, Y. Zhao *Chem. Eur. J.* **2012**, 13979-13983; b) C. Gao, X. Ma, Q. Zhang, Q. Wang, D. Qu, H. Tian *Org. Biomol. Chem.* **2011**, *9*, 1126-1132.

150 B. Qin, R. Yao, X. Zhao, h. Tian *Org. Biomol. Chem.* **2003**, *1*, 2187-2191.

151 G. Gokel, G. Ltidke, I. Ugi, In *Isonitrile Chemistry*; I. Ugi Ed.; Academic Press: New York, **1971**; 145-199.

152 R. Ramozzi, N. Chéron, B. Braïda, P.C. Hiberty, P. Fleurat-Lessard *New J. Chem.*, **2012**, *36*, 1137-1140.

153 (a) A.Dömling, I. Ugi *Angew. Chem., Int Ed.* **2000**, *39*, 3168-3210. (b) J. Zhu *Eur. J. Org. Chem.* 2003, 1133–1144. (c) J. D. Sunderhaus, S.F. Martin *Chem. Eur. J.* **2009**, *15*, 1300-1308; (d) J. Zhu, H. Bienaymé *Multicomponent Reactions*, Ed. Wiley-VCH: Weinheim, Germany, **2005**, pp 1-468. (e) A. Dömling *Chem. Rev*. **2006**, *106*, 17–89; (f) L. Banfi, R.Riva, *The Passerini Reaction In Organic Reactions*, L. Overman Ed., Wiley: Hoboken, NJ, **2005**; Vol. *65*, pp 1-140.

154 X. Li, S.J. Danishefsky *J. Am. Chem. Soc*. **2008**, *130*, 5446-5448.

155 J.G. Polisar, J.R. Norton *Tetrahedron*, **2012**, ***68***, 10236-10240.

156 P.J. Scheuer *Acc. Chem. Res.*, **1992**, *25*, 433–439.

157 T. Wang, S.J. Danishefsky *J. Am. Chem. Soc*. **2012**, *134*, 13244-13247.

158 T.-h. Fu, W.T. McElroy, M. Shamszad, S.F. Martin *Org. Lett***. 2012**, *14*, 3834-3837.

159 (a) Y. Kitano, K. Chiba, M. Tada *Tetrahedron Lett*. **1998**, *39*, 1911-1912; (b) Y. Kitano, K. Chiba, M. Tada *Synthesis* **2001**, 437-443; (c) I. Okada, Y. Kitano *Synthesis*, **2011**, *24*, 3997-4002.

160 A. Porcheddu, G. Giacomelli, M. Salaris *J. Org. Chem.* **2005**, *70*, 2361-2363 and references therein.

161 (a) H. Prawat, C. Mahidol, S. Wittayalai, P. Intachote, T. Kanchanapoom, S. Ruchirawat *Tetrahedron*, **2011**, *67*, 5651-5655; (b) J.S. Simpson, M.J. Garson, *Org. Biomol. Chem*. **2004**, *2*, 939-948.

162 D. Zhang, X. Xu, J. Tan, Q. Liu *Synlett*, **2010**, *6*, 917-920.

163 A. Alimardanov, A. Nikitenko, T.J. Connolly, G. Feigelson, A.W. Chan, Z. Ding, M. Ghosh, X. Shi, J. Ren, E. Hansen, R. Farr, M. MacEwan, S. Tadayon, D.M. Springer, A.F. Kreft, D.M. Ho, J.R. Potoski *Org. Proc. Res. Dev*. **2009,** *13*, 1161-1168.

164 J. Azuaje, A. Coelho, A. El Maatougui, J.M. Blanco, E. Sotelo *ACS Comb. Sci.* **2011**, *13*, 89–95.

165 Isonitrile hydratase mechanism involves protonation on the carbenic like C atom followed by cysteine nucleophilic attack on the same C atom: a) M. Lakshminarasimhan, P. Madzelan, R. Nan, N.M. Milkovic, M.A. Wilson *J. Biol. Chem.* **2010**, *285*, 29651-29661; b) M. Goda, Y. Hashimoto, M. Takase, S. Herai, Y. Iwahara, H. Higashibata, M. Kobayashi *J. Biol. Chem.* **2002**, *277*, 45860-45865 c) Iron containing enzymes that catalyze isonitrile hydration operates via C coordination of the substrate to the metal and subsequent water attack on same carbon atom, K. Hashimoto, H. Suzuki, K. Taniguchi, T. Noguchi, M. Yohda, M. Odaka *J. Biol. Chem*. **2008**, *283*, 36617-36623.

166 L.C. Palmer, A. Shivanyuk, M. Yamanaka, J. Rebek Jr. *Chem. Commun*. **2005**, 857.

167 S. Mecozzi, J. Rebek Jr. *Chem. Eur. J.* **1998**, *4*, 1016-1022.

168 Narayanam, J.M. R.; Stephenson, C.R.J. *Chem. Soc. Rev*. **2011**, *40*, 102.

169 Zen, J.-M.; Liou, S.-L.; Senthil Kumar, A ; Hsia, M.-S. *Angew. Chem. Int. Ed.* **2003**, *42*, 577.

Estratto per riassunto della tesi di dottorato

Studente: GIULIO BIANCHINI matricola: 796184

Dottorato: SCIENZE CHIMICHE

Ciclo: XXV

Titolo della tesi[169] : *New Directions on Photochemical and Supramolecular Control of Homogeneous Catalysis*

Abstract: Mimicking the allosteric control typical of enzymatic catalysis is a long lasting goal for chemists. The present thesis deals with the development of new strategies to control the performance and hopefully switch ON and OFF homogeneous catalysts by implementing photochemical and supramolecular devices. As long as the photochemical approach is concerned, a new phosphine ligand endowed with a coumarin moiety, known to be a typical photo-dimerizable molecule, was prepared and employed for the preparation of Pt(II) metal complexes. The ligand topicity on the complex could be switched from monodentate to bidentate upon irradiation and coumarin dimerization. This feature was investigated in different solvents and exploited in three different catalytic reactions such as alkene isomerization and dimerization as well as Diels-Alder cycloaddition. In all cases the photo-dimerized catalyst bearing the bidentate ligand showed clearly a different behaviour with respect to the original catalyst bearing two monophosphines. Another approach consisted in the synthesis and study of the coordination properties of new phosphine ligands incorporating a dithienyl moiety which is known to be an excellent reversible photochromic unit characterized by geometric and electronic variations between two isomeric forms. The electronic properties of the ligands were studied in detail by synthesis of the corresponding selenides and Rh(I)carbonyl Vaska type complexes. Dithienyl derivatives bearing pyridine moieties were also prepared to be transformed by alkylation into the corresponding bis-cations and these were employed as competitive inhibitors for supramolecular catalysts. In particular, they were tested both in organic medium in the reaction of hydration of isonitriles catalyzed by a self-assembled hexameric capsule based on resorcin[4]arene units and in aqueous medium in the Diels Alder cycloaddition reaction between standard dienes and dienophiles catalyzed by β-cyclodextrin. In former case the two photogenerated isomeric dithienyl cations led to different inhibition activity as a consequence of their different geometry that results in modified host-guest interactions with the supramolecular catalysts employed. The above mentioned hexamer has been successfully exploited as an allosteric reversible supramolecular effector able to modulate the photo-catalytic activity of $[Ru(bpy)_3](OTf)_2$ in the sulfoxidation of thioethers in organic medium in the presence of molecular oxygen. The catalytic activity was reversibly turned off when the Ru(II) catalyst was hosted within the hexameric capsule, and was turned on by addition of a competitive guest for the hexamer such as tetraethylammonium triflate. This approach demonstrates that simply changing the solvation sphere of a catalyst form the bulk solvent into a more static supramolecular assembly it is possible to completely control the performance of a catalyst. Overall, the present PhD dissertation introduced innovative photochemical and supramolecular approaches to modulate the homogeneous catalytic activity of a catalyst opening the road to further developments and possible applications.

La mimesi delle proprietà allosteriche proprie degli enzimi è da sempre una delle sfide più stimolanti per i chimici. In questo lavoro di tesi sono state prese in considerazione diverse strategie per modulare le prestazioni di catalizzatori omogenei, dagli approcci supramolecolari all'incorporazione di residui fotochimici all'interno del sistema catalitico stesso. In un primo approccio il residuo cumarinico, noto per le reazioni di fotocicloaddizione, è stato incorporato all'interno di un legante fosfinico che è stato a sua volta impiegato nella sintesi di bisfosfino complessi di Pt(II). La dimerizzazione del residuo cumarinico ha permesso il passaggio del sistema legante da monodentato a bidentato e i conseguenti complessi fotoreagito e non, sono stati testati nelle reazioni di isomerizzazione e dimerizzazione di alcheni e nelle reazioni di Diels Alder. In tutti i casi sono state osservate apprezzabili variazioni di attività tra le due forme, in particolar modo nelle reazioni di Diels Alder. Un secondo studio ha previsto l'incorporazione del residuo ditieniletene all'interno di leganti di tipo fosfinico, allo scopo di verificare come il passaggio dalla forma aperta a quella ciclizzata del diariletene influenzi le proprietà elettroniche del legante stesso. Lo studio delle proprietà è stato realizzato tramite la sintesi dei corrispondenti complessi di Rh(I) di tipo Vaska e dei seleniuri delle fosfine; in particolare questi ultimi hanno permesso di valutare le differenti capacità σ-donatrici per gli isomeri aperti e chiusi. Il residuo diariletene è stato quindi studiato nell'ottica di inibitore fotomodulabile nei confronti di specie catalitiche supramolecolari. In un primo approccio in mezzo organico è stato osservato che le due forme isomeriche di un piridinio, incorporante il residuo ditieniletene, mostrano diversa abilità nella reazione di idratazione di isonitrili mediate dal complesso esamerico ottenuto a partire dal resorcin[4]arene. Entrambe le forme dell'inibitore foto modulabile sono state successivamente studiate in soluzione acquosa in presenza di β-ciclodestrina e le interazioni *host-guest* tra i due componenti sviscerate. Dagli studi effettuati si è dedotto che, anche in questo le due forme fotocromiche del piridinio possano determinare un diverso effetto inibitore in reazioni test quali cicloaddizioni catalizzate da β-ciclodestrina. L'esamero sopracitato è stato infine impiegato quale effettore supramolecolare nei confronti del complesso $[Ru(bpy)_3]^{2+}$, nella foto-ossidazione aerobica di tioeteri. L'esamero ha dimostrato totale capacità di inibizione della reazione in virtù della sua capacità di incapsulare il catalizzatore inoltre, il completo controllo allosterico è stato ottenuto ripristinando l'attività catalitica tramita aggiunta di un competitor per la capsula esamerica.

In conclusione il presente lavoro di tesi ha affrontato diversi aspetti del controllo allosterico proponendo nuove strategie per il controllo di sistemi catalitici omogenei e aprendo la strada per futuri sviluppi e applicazioni.

Firma dello studente